PREDICTION OF FREEZING AND THAWING
TIMES FOR FOODS

A thesis presented in partial fulfilment of the
requirements for the degree of Doctor of
Philosophy in Biotechnology at
Massey University

DONALD JOHN CLELAND

1985

ABSTRACT

A study of methods to predict the freezing and thawing times of both regular and irregular shaped foods was made.

Experimental thawing data for foods found in the literature, were limited in value because the experimental conditions were not sufficiently accurately measured, described and controlled to allow meaningful testing of thawing time prediction methods to be made. A comprehensive set of 182 experimental measurements of thawing time were made over a wide range of conditions using regular shapes made of Tylose, a food analogue, and of minced lean beef. Freezing and thawing experiments for irregular shapes were also carried out because of the paucity of published experimental data. Using twelve different two- and three-dimensional irregular shaped objects 115 experimental freezing and thawing runs were conducted. Combining experimental results with reliable published experimental data for freezing, a data set comprising 593 experiments was established against which prediction methods were tested.

The partial differential equations that model the actual physical process of heat conduction during freezing and thawing can be solved by the finite difference and finite element methods. Testing of the finite element method has not been extensive, particularly for three-dimensional shapes. Therefore a general formulation of the finite element method for one-, two- and three-dimensional shapes was made and implemented. Both numerical methods accurately predicted freezing and thawing times for regular shapes. Sufficiently small spatial and time step intervals could be used so that errors arising from the implementation of the methods were negligible compared with experimental and thermal property data uncertainties. Guidelines were established to choose space and time grids in application of the finite element method for irregular shapes. Adherence to these guidelines ensured that prediction method error was insignificant. A simplified finite element method was formulated and implemented. It had lower computation costs but was less accurate than the general formulation.

No accurate, general, but simple method for predicting thawing times
was found in the literature. Four possible approaches for a generally
applicable, empirical prediction formula were investigated. Each could
be used to predict experimental data for simple shapes to within ±11.0%
at the 95% level of confidence. This accuracy was equivalent to that
displayed by similar formulae for freezing time prediction, and was
only slightly inferior to the accuracy of the best numerical methods.
All four methods are recommended as accurate predictors.

For multi-dimensional shapes there were two existing geometric factors
used to modify slab prediction methods - the equivalent heat transfer
dimensionality (EHTD) and the mean conducting path length (MCP). New
empirical expressions to calculate these factors for regular shapes
were developed that were both more accurate and more widely applicable
than the previous versions. Principles by which EHTD and MCP could be
determined accurately for any two- or three-dimensional shapes were
established. The effect of the first and second dimension were
accurately predicted but lack of sufficient data (due to high data
collection costs) prevented accurate modelling of the effect of the
third dimension for some irregular shapes.

<u>ACKNOWLEDGEMENTS</u>

TABLE OF CONTENTS

        2.4.4 Numerical Methods...................................24

    2.5 THE EFFECT OF GEOMETRY ON FREEZING AND THAWING

         TIME PREDICTIONS...27

    2.6 PHYSICAL PARAMETERS REQUIRED FOR CALCULATION OF PHASE

         CHANGE IN FOODS..29

        2.6.1 Thermal Property Data...............................29

        2.6.2 Surface Heat Transfer Coefficients..................30

    2.7 SUMMARY...31

3 RESEARCH OBJECTIVES...33

4 NUMERICAL METHOD FORMULATIONS...................................37

    4.1 INTRODUCTION..37

    4.2 THE FINITE ELEMENT METHOD.................................38

        4.2.1 Finite Element Method Formulation...................39

        4.2.2 Computer Implementation.............................42

        4.2.3 Finite Element Method Testing.......................45

    4.3 THE FINITE DIFFERENCE METHOD..............................51

        4.3.1 Finite Cylinder Finite Difference Scheme Formulation..52

        4.3.2 Computer Implementation and Testing.................54

5 EXPERIMENTAL PROCEDURE AND DATA COLLECTION......................57

    5.1 EXPERIMENTAL ERROR..57

    5.2 CHOICE OF PHASE CHANGE MATERIALS..........................58

    5.3 TEMPERATURE MEASUREMENT AND CONTROL.......................60

    5.4 THAWING OF SLABS..65

        5.4.1 The Equipment.......................................65

        5.4.2 Thickness Control and Measurement...................66

        5.4.3 Measurement and Control of Surface Heat

               Transfer Coefficients...............................66

        5.4.4 Analysis of Heat Transfer in Slabs..................72

    5.5 THAWING OF INFINITE CYLINDERS.............................78

        5.5.1 The Equipment.......................................78

        5.5.2 Diameter Control and Measurement....................79

APPENDICES D and E are included on microfiche at the end of APPENDIX C.

LIST OF TABLES

LIST OF FIGURES

1   INTRODUCTION

Low temperature is one of the most important and common means of food
preservation. For New Zealand, whose economy is based on primary
industries and export of perishable products to distant markets, this
is especially true. Freezing, cold storage and subsequent thawing are
all operations on the frozen food chain in which losses of food quality
can be significant. Important roles for the food engineer are
therefore to design, operate and control equipment that maintains
product quality whilst keeping processing costs low.

Low temperature preservation can, at best, only maintain food quality
levels so there has been extensive research into factors affecting food
quality during freezing, cold storage and thawing. The physical,
chemical and biological changes that occur during these processes have
been related to the temperature history of the food and the process
conditions used. For some foods, data suggesting optimal sets of
conditions and equipment to minimise damage to the food product have
been found. To design and optimise equipment for low temperature
preservation of food the food engineer must be able to predict freezing
and thawing rates for these conditions. Both operating and capital
costs can be reduced if simple and accurate methods to do this are
available.

In the past, freezing has been more important commercially than thawing
as thawing has been predominately a domestic practice. Extensive
research into the physical aspects of freezing has produced methods to
predict freezing times that are satisfactory for many practical
situations. However, in general, these methods are either specific to
individual food products or apply only to simple regular geometries.
Many frozen foodstuffs are irregular in shape so further research is
warranted to develop, test and validate a general method that predicts
freezing times for a wide variety of shapes.

Recently, with greater quantities of goods being frozen and greater
emphasis on further processing of frozen products, thawing has become
an important industrial process. A simplistic approach is to treat

thawing as the reverse of freezing, but the validity of this approach is questionable as it has not been proven that accurate thawing predictions will be obtained. As for freezing, much of the research into thawing rate and time prediction has been for individual products. There remains the need for research to find a general method for prediction of thawing times. Ideally, the method would be similar to those used to predict freezing times. It may incorporate the same techniques to account for product geometry. This would allow the entire area of prediction of phase change in foods to be considered as a whole.

If accurate prediction of freezing and thawing under a wide range of conditions and geometries can be achieved this would enable more efficient process equipment design within the cold chain and hence would reduce costs. Therefore the present research into prediction of thawing times and into the effect of product shape on both freezing and thawing rates is clearly needed.

2 LITERATURE REVIEW

Phase change in foods is a complex process. Most research into methods
for prediction of rates of phase change has used simplified model
systems for analysis. It is therefore convenient to consider the
literature sub-divided according to the type of simplification made.
Initially the process of phase change in foods is examined and
described and the phase change problem formulated.

2.1 PHASE CHANGE IN FOODS

Foodstuffs are a complex system of water, solutes and macromolecules
but are often considered for engineering purposes as two fractions; an
aqueous solution and a solid component. Phase change in foods involves
intricate interactions between the aqueous and solid fractions. In
many so-called "high moisture" solid foods (for example - meat,
vegetables and fish) the water is bound in a solid matrix and there is
almost negligible migration of water during freezing or thawing. Phase
change involves mainly the aqueous part changing from ice to water or
vice versa, with the solid being relatively inert. The interactions in
the food cause continuous freezing point depression as ice separates
from the aqueous phase, so latent heat is released or absorbed over a
range of temperatures during phase change (Rolfe 1968 p.184, Dickerson
1977).

The thermal conductivity and specific heat capacity of water vary by a
factor of about three from those of ice. Latent heat is released or
absorbed as water changes phase, whilst the solid fraction is
essentially unchanged. Therefore the thermal properties of food are
highly dependant on the fraction of ice in the food (Mellor & Seppings
1976, Heldman 1982). The latent heat can be "lumped" together with the
sensible heat to give an "apparent" (effective) specific heat capacity
(Comini & Bonacina 1974). For a typical solid high moisture food the
relationship between ice fraction, thermal conductivity, apparent
specific heat capacity and enthalpy as a function of temperature are
shown in Figs. 2.1 to 2.4 (Mellor 1978). The area under the peak in
the specific heat capacity curve, excluding the sensible heat
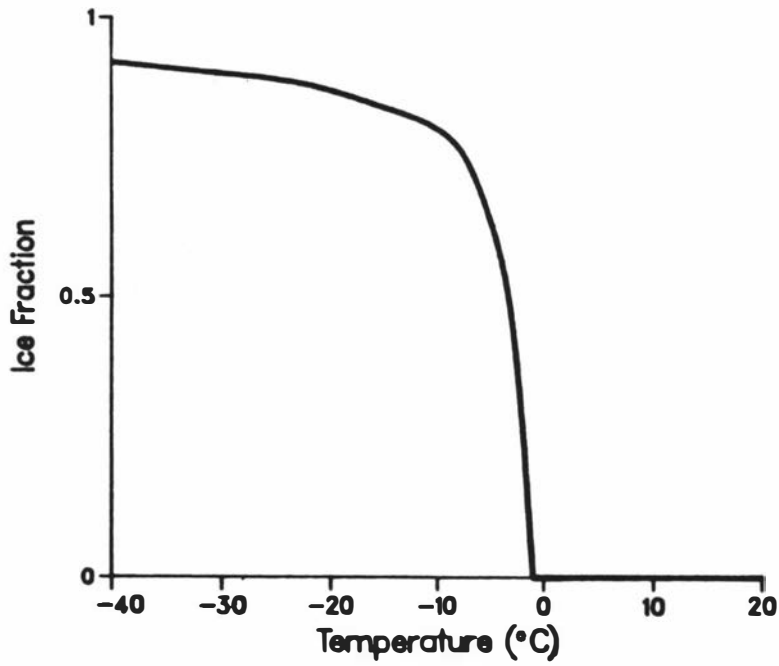
Fig. 2.1 Ice Fraction of Freezable Water Data For a Typical Foodstuff.
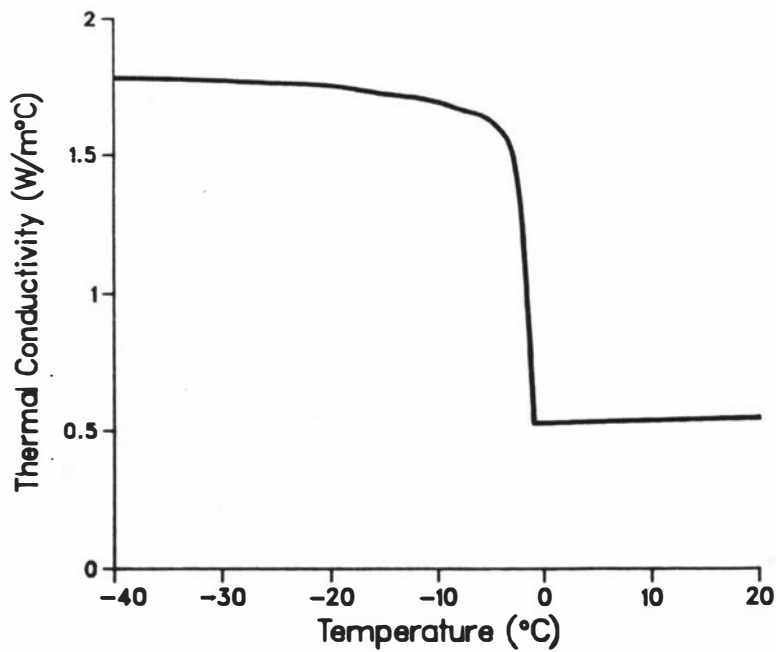
Fig. 2.2 Thermal Conductivity Data For a Typical Foodstuff.
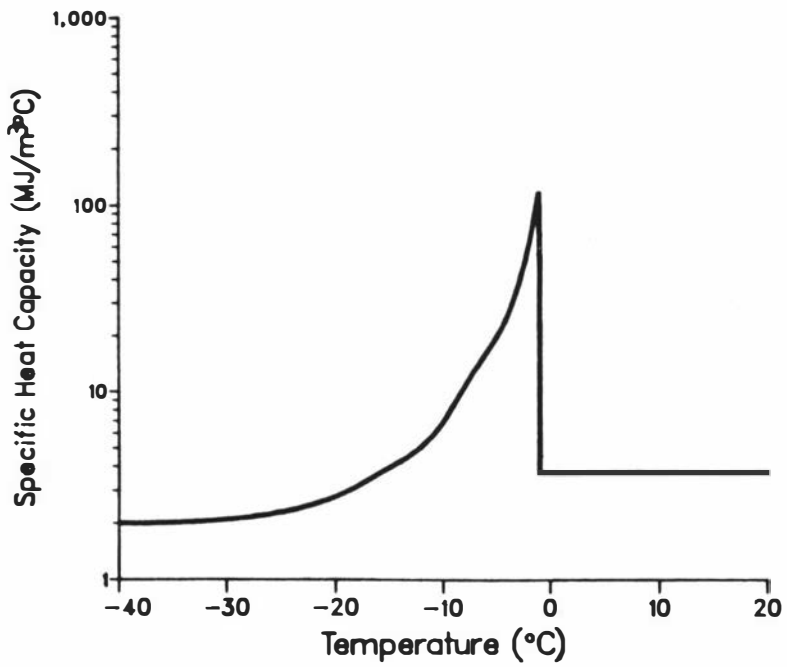
Fig. 2.3 Apparent Volumetric Specific Heat Capacity Data For a Typical
Foodstuff.
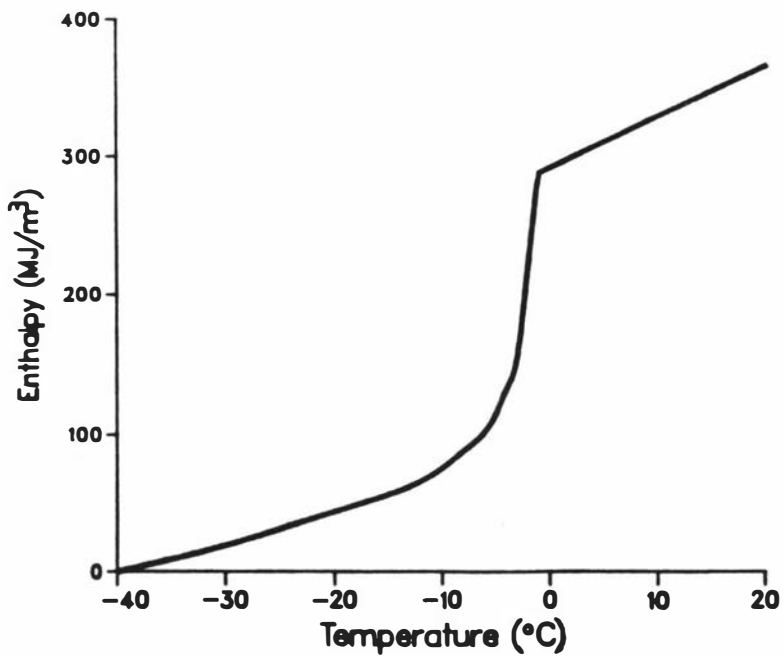
Fig. 2.4 Enthalpy Data For a Typical Foodstuff.
Datum: $H = 0.0$ J m^{-3} at $-40.0 °C$.

contribution, is the latent heat component.

Freezing and thawing processes differ considerably. In freezing of food there is a quite distinct initial freezing temperature (T_{if}), at which ice first starts to form. Above this temperature thermal properties are relatively constant and below this temperature rapid changes occur as the ice fraction increases. These changes in properties decline as less liquid water remains, until only "bound" water is left (Moran 1930, Riedel 1961, Rolfe 1968 p.186, Comini & Bonacina 1974). At lower temperatures further ice formation is limited and properties are relatively constant at the so called frozen phase values. In thawing the temperature region where phase change occurs is entered slowly and thermal properties change gradually. As more latent heat is absorbed and more ice melts, freezing point depression is reduced so T_{if} is approached. The majority of latent heat is absorbed at temperatures just below T_{if} giving a final rapid change in thermal properties. This effect is indicated by the height and slope of the apparent specific heat capacity and enthalpy curves for typical foods (Figs. 2.3 and 2.4).

In freezing some non-equilibrium behaviour has been observed (Cleland et al 1982). Supercooling of the food below T_{if} prior to initial ice crystal nucleation has probably occurred. This type of effect is unlikely in thawing as there is no equivalent nucleation process and the latent heat is gradually absorbed initially, over a large temperature range.

2.2 PHASE CHANGE FORMULATION

2.2.1 Governing Partial Differential Equations

Physically, phase change in foods is defined as heat conduction in a solid. This is governed in a three-dimensional volume, **V, by the** partial differential equation:

$$C \frac{\partial T}{\partial t} = \frac{\partial}{\partial x} \left[k \frac{\partial T}{\partial x} \right] + \frac{\partial}{\partial y} \left[k \frac{\partial T}{\partial y} \right] + \frac{\partial}{\partial z} \left[k \frac{\partial T}{\partial z} \right] + Q \qquad (2.1)$$

where C   = volumetric specific heat capacity $(J\ m^{-3}\ {}^{\circ}C^{-1})$

            $= f_1(T,material)$

    T   = temperature $({}^{\circ}C\ or\ K)$

    t   = time (s)

    k   = thermal conductivity $(W\ m^{-1}\ {}^{\circ}C^{-1})$

            $= f_2(T,material)$

x,y,z = distance in the three axial directions (m)

    Q   = internal heat generation $(W\ m^{-3})$

            $= f_3(T,material)$

Non-linearity arises from the temperature variable thermal properties and the complex nature of the boundary conditions applied. Approximate methods must therefore be used, or simplifying assumptions made, to enable an analytical solution to be found. One such assumption is that the latent heat is transferred at a unique temperature (T_{if}) and thermal properties undergo a step change in values at this temperature (Carslaw & Jaeger 1955, p.282). The formulation becomes that of a moving boundary (Stefan) problem and the position of the phase change front (boundary) is determined by Eq. (2.1) subject to:

$$L\ \frac{\partial V_1}{\partial t} = k^+ \left[\partial y\ \partial z\ \frac{\partial T}{\partial x}\ l_x + \partial x\ \partial z\ \frac{\partial T}{\partial y}\ l_y + \partial x\ \partial y\ \frac{\partial T}{\partial z}\ l_z \right] \Bigg|_{V_1^+}$$

$$- k^- \left[\partial y\ \partial z\ \frac{\partial T}{\partial x}\ l_x + \partial x\ \partial z\ \frac{\partial T}{\partial y}\ l_y + \partial x\ \partial y\ \frac{\partial T}{\partial z}\ l_z \right] \Bigg|_{V_1^-} \qquad (2.2)$$

at the boundary between the solid and liquid phases

where L   = latent heat $(J\ m^{-3})$

    V_1 = volume of material in unfrozen state (m^3)

    l   = directional cosine to outward normal

Although this assumption of a unique phase change temperature is true in some common phase change situations such as ice formation and melting, freezing and thawing of pure liquids and pure metal casting, it is not true for phase change in most solid, high moisture foods. The possibility of deriving simple prediction methods by using this assumption has been explored extensively. However the methods derived can only be approximate for phase change in food.

2.2.2 Initial and Surface Boundary Conditions

In freezing and thawing of foods a variety of initial and surface boundary conditions can apply. Mathematically, Eq. (2.1) is subject to the first kind of boundary condition (prescribed surface temperature):

$$T = T_a \qquad \text{on surface, } S_1, \text{ for } t > 0 \quad (2.3)$$

the second kind of boundary condition (prescribed surface heat flux):

$$k \left[\frac{\partial T}{\partial x} l_x + \frac{\partial T}{\partial y} l_y + \frac{\partial T}{\partial z} l_z \right] = \phi \qquad \text{on surface, } S_2, \text{ for } t > 0 \quad (2.4)$$

the third kind of boundary condition (convective and radiative cooling or heating):

$$k \left[\frac{\partial T}{\partial x} l_x + \frac{\partial T}{\partial y} l_y + \frac{\partial T}{\partial z} l_z \right] = \phi_{con} + \phi_{rad} \text{ on surface, } S_3, \text{ for } t > 0 \quad (2.5)$$

the fourth kind of boundary condition (arbitrary surface temperature):

$$T = T_w \qquad \text{on surface, } S_4, \text{ for } t > 0 \quad (2.6)$$

and the initial condition:

$$T = T_{in} \qquad \text{in volume, } V, \text{ for } t = 0 \quad (2.7)$$

where T_a = ambient medium temperature   (°C)

   ϕ = prescribed heat flux   (W m^{-2})

       = f_4(t,position)

   ϕ_{con} = convective heat flux   (W m^{-2})

       = $h_{con}(T_{ac} - T)$

   ϕ_{rad} = radiative heat flux   (W m^{-2})

       = $h_{rad}(T_{ar} - T)$

   h_{con} = convective heat transfer coefficient   (W m^{-2} °C^{-1})

       = f_5(t,position)

   T_{ac} = convective ambient temperature   (°C)

       = f_6(t,position)

   h_{rad} = radiative heat transfer coefficient   (W m^{-2} °C^{-1})

       = $\sigma \varepsilon (T_{ar}^2 + T^2)(T_{ar} + T)$

   T_{ar} = radiative ambient temperature   (°C or K)

       = f_7(t,position)

   ε = radiation emissivity

       = f_8(material)

   T_w = surface temperature   (°C)

       = f_9(t,position)

   T_{in} = initial temperature   (°C)

$$= f_{10}(\text{position})$$

2.2.2.1 <u>Applicability of Boundary Conditions</u> The first and fourth kind of boundary conditions can be considered as a special case of the third where $h_{con} \to \infty$ and $T_{ac}=T_w$ or $T_{ac}=T_a$. In practice because some surface resistance to heat transfer always exists, h_{con} is not infinitely large so the first and fourth boundary conditions are seldom the best boundary descriptions possible. In most food freezing or thawing situations radiation is not a major means of heat transfer so it is conveniently grouped with convection in the third kind of boundary condition. The second kind of boundary condition infrequently occurs and is seldom used even under highly controlled and accurately measured experimental conditions. The third kind of boundary condition is the most physically realistic boundary condition in food phase change processes.

2.2.2.2 <u>Initial Conditions</u> Both uniform and non-uniform initial temperature conditions occur in practice. To derive a simple analytical type of solution a uniform initial temperature distribution must usually be assumed. Numerical solutions can handle either uniform or non-uniform initial conditions. Use of a mean bulk temperature (Loeffen et al 1981) allows the effect of a non-uniform initial temperature distribution on a freezing or thawing time to be approximated, if a simple method using a uniform initial temperature is used for calculations.

The release of latent heat over a range of temperature presents problems in defining the onset of thawing. The initial thawing point unlike the initial freezing point, T_{if}, is not well defined for food. Choice of initial temperatures (T_{in}) of less than -10°C throughout the material to be thawed, will ensure that the process includes all significant latent heat transfer for common foods. For freezing the equivalent restraint is that T_{in} must be greater than or equal to T_{if}. Because of the aqueous nature of food and freezing point depression, T_{if} will always be less than or equal to 0°C. Significant superheating above T_{if} for freezing or subcooling below -10°C for thawing, is normal in commercial practice because of prior processing or storage conditions so these conditions are seldom limiting.

2.2.3 Completion of Phase Change

To complete the definition of freezing and thawing processes an end
point must be defined (Cowell 1974). If the assumption of a moving
boundary is made the end point is clearly when the phase change front
reaches the thermodynamic centre of the object.

The non-distinct phase change region for foods precludes this
definition. The best alternative is to consider the process complete
when the thermodynamic centre reaches a certain temperature, or when a
certain mass average temperature is reached (Purwadaria & Heldman
1983). The disadvantage of using a mass average temperature end point
is that the mean bulk temperature is difficult to measure or estimate
in practice without extensive temperature data (Khatchaturov 1958). In
contrast using a specified final thermodynamic centre temperature as
the end point means:
- the phase change operation is generally conservatively designed as
  the mass average temperature is less limiting than the thermodynamic
  centre temperature
- a choice of final centre temperature can be made to approximate any
  desired equilibration temperature
- unless the thermodynamic centre moves (Fleming 1970) there is no
  doubt that phase change is complete throughout the material when the
  centre reaches the endpoint temperature
- this means of determining the end point is the most common and easy
  to use.
For these reasons it was used in the present work.

For freezing, a number of final centre temperatures have been used ;
-5°C (Rolfe 1968 p.197, Cowell 1974, James et al 1976), -10°C
(Khatchaturov 1958, I.I.R. 1972 p.36, Cleland 1977, de Michelis &
Calvelo 1983) and -18°C (Moleeratanond et al 1982, de Michelis &
Calvelo 1983, Hung & Thompson 1983). The process time obviously
lengthens as the final thermodynamic centre temperature is lowered. A
freezing time prediction method would ideally take account of these
changes. Methods with this capability are available (Cleland & Earle
1984b). The best choice of the final thermodynamic centre temperature
is made to ensure that all significant latent heat release takes place

above it, and that it is commensurate with the subsequent storage temperature. The endpoint temperature of -10°C was chosen for the present work as it meets these requirements and the bulk of published freezing data are for this temperature (Cleland & Earle 1984a).

For thawing, an obvious choice for the final centre temperature is 0°C. Large non-equilibrium effects are unlikely to occur so phase change must be complete at this temperature, even if the food behaves closely to pure water, as T_{if} is always less than or equal to 0°C. Further, in most thawing situations thawing throughout the material is demanded (for example, so the material can be divided or used immediately in further processes), yet the lowest mass average temperature is desired to minimise post-thawing quality losses (James et al 1976). A temperature of 0°C meets both these criteria. Above 0°C only sensible heat effects need to be considered. If predictions to other final centre temperatures are required, then similar methods to those available to adjust freezing time predictions for different final temperatures can probably be used.

2.2.4 Symmetry Conditions

In geometric shapes where there is an axis of rotational symmetry the formulation can be restated axisymmetrically. Equations (2.1),(2.4) and (2.5) become:

$$r^a \, C \, \frac{\partial T}{\partial t} = \frac{\partial}{\partial r} \left[r^a \, k \, \frac{\partial T}{\partial r} \right] + \frac{\partial}{\partial y} \left[r^a \, k \, \frac{\partial T}{\partial y} \right] + r^a \, Q \qquad (2.8)$$

$$r^a \, k \, \left[\frac{\partial T}{\partial r} \, l_r + \frac{\partial T}{\partial y} \, l_y \right] = r^a \, \phi \qquad (2.9)$$

and

$$r^a \, k \, \left[\frac{\partial T}{\partial r} \, l_r + \frac{\partial T}{\partial y} \, l_y \right] = r^a \, \left[\phi_{con} + \phi_{rad} \right] \qquad (2.10)$$

where r   = radial distance from axis of rotation   (m)

    a   = 1 for cylindrical co-ordinates

        = 2 and terms in y are deleted for spherical
            co-ordinates.

At all boundaries with no other boundary condition defined the symmetry (no net heat transfer) boundary condition is assumed to apply:

$$k \left[\frac{\partial T}{\partial x} l_x + \frac{\partial T}{\partial y} l_y + \frac{\partial T}{\partial z} l_z \right] = 0 \qquad \text{on surface, } S_5, \text{ for } t>0 \quad (2.11)$$

2.3 SOLUTIONS USING THE ASSUMPTION OF A UNIQUE PHASE CHANGE TEMPERATURE

To attempt analytical solution of phase change problems it is usual to assume that phase change occurs at a unique temperature (T_{if}) and that thermal properties undergo a step change at this temperature, from constant frozen values to constant, but different, unfrozen values (or vice versa). Even with this moving boundary assumption the phase change problem is still mathematically non-linear and no general analytical solution has been found.

To facilitate analysis further physical assumptions and limitations are necessary arising both from the mathematics and from the physical properties of foods. Generally the density difference between the phases is ignored and a uniform initial temperature distribution is assumed. Only simple geometric shapes (slabs, infinite cylinders, spheres, infinite rods and rectangular bricks) are considered. Also analysis is often restricted to the simpler first and second boundary conditions and the initial condition that the material is at the phase change temperature (no superheating for freezing or subcooling for thawing). Variation of boundary conditions with time is generally not examined except by numerical methods or some form of time-averaging technique. All of these assumptions reduce the range of applicability of the resulting solution. Many of the solutions are not appropriate for food freezing or thawing processes, although they may be in other phase change situations such as pure metal casting, or melting and solidification of pure substances. In addition some analytically derived solutions may require numerical evaluation by computer so there are both physical assumptions and numerical truncation or rounding errors in these cases. In contrast, finite difference and finite element numerical methods require no physical assumptions although they introduce numerical errors. The lack of physical assumptions make the latter group the preferred methods if numerical solution is required.

The common assumption of phase change at a unique temperature and a step change in thermal properties leads to methods that have been shown to poorly predict freezing processes in foods (Cleland 1977). Bankoff (1964), Muehlbauer and Sunderland (1965), Bakal and Hayakawa (1973), Ockenden and Hodgkins (1975), Cleland (1977), Hayakawa (1977), Wilson et al (1978) and Crank (1981) all review solutions making use of this assumption.

2.3.1 Exact Solutions

Exact solutions for phase change assuming a unique phase change temperature are summarised in Table A.1. The semi-infinite slab geometry description and the boundary conditions used in all of these solutions virtually never occur in practical food phase change situations, so these exact solutions are of little practical value (Cleland 1977). All other solutions to phase change problems involve the use of mathematical techniques and approximations as well as simplifying physical assumptions.

2.3.2 Approximate Solutions for Slabs

For slabs the approximate analytical solutions can be classed into three groups: heat balance integral and variational techniques, perturbation and series solutions, and other analytical approaches. These are summarised in Table A.2.

2.3.2.1 Heat Balance Integral and Variational Techniques The heat balance integral (integral profile) technique of Goodman (1964) and the variational technique of Biot (1957) reduce the set of partial differential equations defining the problem into a set of simpler ordinary integro-differential equations. In both methods an approximation to the temperature profile in each phase is assumed. The method is sensitive to choice of the appropriate temperature profile (Goodman 1961). It is difficult to predict the accuracy achieved by a particular profile (Langford 1973). Bell (1978) subdivides the region and solves for each section simultaneously, while Albin et al (1976) study six stages in the phase change process, in attempts to increase the accuracy of the method. Most solutions are restricted as they

consider only the first or second kind of boundary condition and the semi-infinite rather than the finite slab, they require numerical evaluation, or they apply only where the initial temperature is equal to the phase change temperature. The only solutions for the third kind of boundary condition that do not require numerical integration are those due to Goodman (1958), for a semi-infinite slab where initial superheating or subcooling are ignored, and Hrycak (1963, 1967) who extends this to the case with superheating or subcooling for both a homogeneous and stratified semi-infinite material. Hrycak applies the quasi-steady state assumption (linear temperature profile between the surface and the internal moving phase change boundary) and assumes that the movement of the phase change front and the heat penetration front are proportional.

2.3.2.2 Perturbation and Series Solutions The basis of this group of solutions is to assume a series solution and fit the terms to the initial and boundary conditions. The more complex boundary condition of the third kind is analysed but numerical integration or computer calculation are required because these analytical solutions are tedious to use due to their complexity. Alternatively, a less accurate solution is obtained when only the first few terms in the series are taken. To apply these methods to food freezing and thawing the assumption that initial temperature is equal to the phase change temperature must be made which is a major disadvantage.

2.3.2.3 Other Analytical Approaches A number of mathematical techniques such as embedding, integral transformations, analytical integration and simplifying assumptions such as assuming the solution to be of the form that the distance the phase change front has moved is proportional to the square root of time, have been used to arrive at simple formulae or sets of ordinary differential equations requiring numerical integration. These are approximate solutions to the phase change problem. Ozisik (1978) describes the formulation of the phase change problem as a heat conduction problem with a moving heat source and the use of Green's functions to solve it. Some other solutions given in Table A.2 use a co-ordinate transformation due to Landau (1950) that immobilises the phase change front. Plank (1913) and London & Seban (1943) make the quasi-steady state heat conduction

assumption, that sensible heat capacity in the phase between the outer surface and the phase change front is negligible. The temperature profile in this region is therefore linear and a simple analytical solution is obtained for the third kind of boundary condition but with the material initially at the phase change temperature. Both these assumptions will tend to yield low predictions of phase change times. Rutov (1936) considered the sensible heat capacity of the phase change material after phase change and derives a correction factor to account for it. Cochran (1955) and Kreith & Romie (1955) both considered the sensible heat capacity lumped at a mid-point in the slab, but were unable to arrive at a simple solution except for unduly restrictive boundary conditions. Kern (1977) and Glasser & Kern (1978) derive bounds for the solution by considering the effect of the quasi-steady state assumption and approximating the integration, by assuming different temperature profiles between the surface and the moving boundary.

2.3.3 Approximate Solutions for Radial Geometry

Many of the approximate techniques used to get solutions for slabs have been extended to the case of radial heat flow in infinite cylinders and spheres, but retain the same problems when applied to food phase change. These solutions are listed in Table A.3. For a boundary condition of the third kind with no initial superheating or subcooling Plank (1913), London & Seban (1943), Koromi & Hirai (1970), Shih & Chou (1971), Shih & Tsay (1971), Tien (1980), Seeniraj & Bose (1982) and Hill & Kucera (1983) have derived solutions. Chuang & Szekely (1972) solve for fusion of infinite cylinders with the initial temperature not equal to the phase change temperature and the third kind of boundary condition, but the method requires numerical integration of the resulting ordinary differential equation.

2.3.4 Approximate Solutions for Multi-Dimensional Shapes

Where the geometry is complex so that heat transfer is in more than one direction, development of even approximate analytical solutions is very difficult. Solutions have been limited to dealing with objects of regular geometric configurations. These solutions are mostly of

limited practical importance because of the initial and boundary conditions used. Table A.4 summarises available methods.

Solutions of practical importance for foods are those due to Plank (1941), Tanaka & Nishimoto (1959, 1960, 1964) and Shamsundar (1982). All use the quasi-steady state assumption and assume that the surface of the object is isothermal. The general approach is to find geometric factors that modify solutions for slabs. Plank finds appropriate factors for phase change in infinite rod and rectangular brick shapes subject to the third kind of boundary condition and the initial temperature equal to the phase change temperature, by assuming that the moving boundary remains parallel to the outer surface. Tanaka & Nishimoto extend this analysis for conical shapes, finite cylinders and trapezoidal bodies. Shamsundar employs a similar approach for the same problem but allows different configurations of the phase change front to be considered. Using mathematically defined geometries, conduction shape factors suggest simple analytic solutions similar to those of Plank. Hahne & Grigull (1975) tabulate the conduction shape factors for a wide range of regular shapes and assumed interface geometries.

However for most multi-dimensional shapes the temperature is not the same over the surface at any time, and the shape of the interface will change as phase change progresses, so the accuracy of the derived geometric factors is subject to doubt.

2.3.5 Empirical Approaches

This group of solutions have resulted from recognition that even with major simplifying assumptions analytical solution of phase change heat transfer is sufficiently difficult that alternative approaches are worthwhile. The approaches are varied in nature, and are described in Table A.5.

Charm & Slavin (1962) modify Neumann's solution for the first kind of boundary condition to make it applicable to the third kind of boundary condition by adding a fictitious thickness to the object to account for surface resistance to heat transfer. Churchill & Gupta (1977) define an effective specific heat capacity value so standard exact analytical

solutions for heat conduction without change of phase will approximate melting or solidification.   Baxter (1962), for slabs and infinite cylinders and Tao (1968), for slabs, infinite cylinders and spheres, studied freezing subject to the third kind of boundary condition but with no superheating or subcooling using finite differences.   Their results are displayed as regression equations and charts. Baxter's solution is similar in form to Plank's equation.   Shamsundar & Scrivisan (1979) and Shamsundar (1981) derive a similarity rule so numerical results can be applied over a wide range of conditions without additional computations.

None of these solutions apply where latent heat is not released or absorbed at a unique temperature as is the case for foods.

2.3.6   Use of Analogues and Graphical Methods

Before the use of versatile digital computers became common and powerful numerical methods were available, analogue and graphical solutions for phase change were used.   Using electrical analogues London & Seban (1943), Cochran (1955), Kreith & Romie (1955) and Horvay (1960) investigated sensible heat effects neglected by the quasi-steady state assumption using a lumped heat capacity method. Liebman (1956) and Stephan (1969) also worked with electrical analogues for phase change heat transfer while Hashemi & Sliepcevich (1967b) developed a diffusion analogue. Some graphical methods for phase change are due to Ede (1949), Keller & Ballard (1956), Heiss (1958), Longwell (1958), Sunderland & Grosh (1961) and Sokulski (1972b).

Graphical and analogue methods for solving freezing and thawing processes are no longer important because of the relative ease and accuracy of using numerical methods on digital computers.

2.3.7   Numerical Solutions

Mathematical approximations to Eqs. (2.1) to (2.11) can be made using the finite difference method (Dusinberre 1945) or the finite element method (Turner et al 1956). The third kind of boundary condition and initial superheating or subcooling are easily modelled, though many

solutions consider only simpler conditions.

A number of methods to determine the position of the phase change front have been used. Fox (1975) and Crank (1981) review these methods and describe the principles behind the techniques. Briefly, they can be divided into six groups.

(a) Normal finite difference or finite element approximations to Eq. (2.1) are used throughout the object except for the section which has just reached the phase change temperature. The nodes representing these regions are artifically held at the phase change temperature until the calculated accumulation or removal of heat is equivalent to the latent heat. Then the phase change front moves into the next section and normal approximations using the thermal properties of the new phase are reinstigated. Researchers who used the finite difference method include Dusinberre (1949), Tao (1967), Charm (1971), Charm et al (1972), Roshan et al (1974) and Tarnawski (1976). Zienkiewicz et al (1973) and Rolphe & Bathe (1982) used the finite element method. A refinement of this method where the position of the phase change front within each region is predicted and temperatures near the front are estimated by interpolation gives more accurate temperature profiles with less oscillatory behaviour (Murray & Landis 1959, Seider & Churchill 1965, Teller & Churchill 1965, Padmanabhan & Subba Raji 1975, Forgac et al 1979, Cichy et al 1981).

(b) A co-ordinate transformation (Landau 1950) is employed to give a variable space grid that fixes the boundary (phase change front) at one node. The movement of the front is calculated while normal approximations are used in each phase. Iterative solution is often necessary to fit all the specified conditions. Murray & Landis (1959), Lotkin (1960), Heitz & Westwater (1970), Kroeger & Ostrach (1974), Duda et al (1975), Saitoh (1978), Hsu et al (1981), Heurtault et al (1982) and Moore & Bayazitoglu (1982) used finite differences while Bonnerot & Jamet (1974) and Lynch & O'Neill (1981) employed finite elements. This method gives more accurate estimate of the front position than (a) but less accurate temperature profiles (Murray & Landis 1959).

(c) A variable time stepping scheme is used with a fixed space grid so
    that the phase change front jumps a full nodal division with each
    time step. An iterative approach is required to approximate the
    boundary conditions with heat balances and temperature profiles
    defined by Eq. (2.2) (Douglas & Gallie 1955, Goodling & Khader
    1974, Goodling & Khader 1975, Sparrow et al 1976, Gupta & Kumar
    1980, Yuen & Kleinmann 1980, Gupta & Kumar 1981).

(d) The enthalpy transformation of Eyres et al (1946) is used to remove
    the non-linearity due to the moving boundary so that Eq. (2.1)
    becomes:

$$\frac{\partial H}{\partial t} = \frac{\partial}{\partial x}\left[k \frac{\partial T}{\partial x} \right] + \frac{\partial}{\partial y}\left[k \frac{\partial T}{\partial y} \right] + \frac{\partial}{\partial z}\left[k \frac{\partial T}{\partial z} \right] + Q \qquad (2.12)$$

where H   = enthalpy $(J\ m^{-3})$

$$= \int_0^T C\ dT$$

$$= f_{11}(T, position)$$

Normal finite difference approximations to Eq. (2.12) can be used
throughout the region (Price & Slack 1954, Baxter 1962, Lockwood
1966, Shamsundar & Sparrow 1975). The method has been refined by
using interpolation to determine the temperature distribution and
interface position more accurately between space grid points
(Shamsundar & Sparrow 1976, Voller & Cross 1981a, 1981b, 1983, Bell
1982). Ichikawa & Kikuchi (1979) and Kikuchi & Ichikawa (1979)
used the similar method of variational inequalities.

(e) The isotherm migration method transforms the problem from that of
    determining the dependent variable, temperature, as a function of
    position and time to that of determining the dependent variable,
    position, as a function of time and temperature (Crank & Gupta
    1975, Talmon & Davis 1981, Talmon et al 1981, Talmon et al 1983,
    Gupta & Kumar 1984).

(f) A variety of different schemes are used near the phase change front
    to account for latent heat effects and the moving boundary
    condition (Ehrlich 1958, Lazaridus 1970, Morrison 1970, Goodrich
    1978, Ramakrishna & Sastri 1984). Wellford & Ayer (1977), Rubinsky
    & Cravahlo (1981) and Raymond & Rubinsky (1983) use the finite

element method and include special elements or nodes at the phase
change front that approximate the latent heat effect by a heat
source or sink distributed over the element. Allen & Severn (1962)
use a relaxation method and model latent heat release as moving
heat generation.

Except for the enthalpy transformation few solutions for food freezing
and thawing are based on these methods, as phase change in foods
departs substantially from the basic assumption of a unique phase
change temperature.   Other numerical methods can approximate latent
heat release or absorption over a range of temperature more closely and
have been used in preference.

2.4   SOLUTIONS FOR PHASE CHANGE OVER A RANGE OF TEMPERATURES

The second way that phase change in food can be taken into account is
by making mathematical allowance for phase change over a range of
temperatures.   Phase change over a range of temperatures is the actual
situation occurring in food freezing and thawing. The most general
approach would take account of any variation in apparent volumetric
specific heat capacity, C, and the thermal conductivity, k, in
Eq. (2.1) meaning that no physical assumptions about the phase change
process need be made. For foods the apparent volumetric specific heat
capacity is defined at any temperature as:

$$C = \frac{dH}{dt} \tag{2.13}$$

Simpler semi-analytical and empirical approaches have also been taken.

Metal alloy solidification is a similar phase change process.   It is
usually modelled by a two-phase zone of solid and liquid between two
phase change fronts moving through the material.   This approach is
closer to the true physical situation during phase change in foods,
than the assumption of a unique phase change temperature, but is still
only approximate because it requires assumptions about the distribution
of latent heat across the phase change region.

2.4.1 Approximate Analytical Solutions for Alloy Solidification

Approximate analytical solutions for alloy solidification are summarised in Table A.6. In alloy solidification it is normally assumed that latent heat is released uniformly over an extended temperature range. Error will occur in using these solutions for phase change in food because foods do not have constant latent heat release with respect to change in temperature.

Muelbauer et al (1973) and Hayakawa & Bakal (1973) consider the third kind of boundary condition but both solutions, though analytical in nature, are complex and impractical to use.

2.4.2 Semi-Analytical Solutions

Many attempts have been made to modify existing analytical solutions to take account of their limitations and give them less dependence on assumptions made in their theoretical development. Plank's (1913) equation for a finite slab not initially superheated or subcooled is often used as a base for these modifications because of its simple form, its application to a range of regular shapes (Plank 1941) and because it is for the boundary condition of the third kind. Plank's equation can be written as:

$$t = \frac{\Delta H}{|T_a - T_{if}|} \left[P\,\frac{D}{h} + R\,\frac{D^2}{k} \right] \qquad (2.14)$$

or in dimensionless form (Tchigeov 1958):

$$Fo = \frac{P}{Bi\ Ste} + \frac{R}{Ste} \qquad (2.15)$$

where ΔH = change in enthalpy during the process $(J\ m^{-3})$

T_a = ambient temperature   (°C)

T_{if} = initial freezing temperature   (°C)

P,R = geometric factors depending on object shape

D = full thickness or diameter   (m)

h = surface heat transfer coefficient $(W\ m^{-2}\ °C^{-1})$

Fo = Fourier number

= $\alpha t / D^2$

Bi = Biot number

= hD/k

Ste   = Stefan number

   = $C \; |T_a - T_{if}| / \Delta H$

α = thermal diffusivity $(m^2 \; s^{-1})$

   = k/C

Various approximate methods have been employed to account for non-constant thermal properties, sensible heat effects both above and below the phase change temperature range and the non-isothermal latent heat release or absorption. Some fit experimental data while others attempt corrections based on theoretical grounds. Although sometimes derived for a specific product or condition many of the methods can be made to apply to a wider range of problems. Kinder & Lamb (1974) and Cleland (1979) review the relative merits of these formulae for food freezing.

Cowell (1967), Lotz (1974), Mascheroni & Calvelo (1982), De Michelis & Calvelo (1983) and Pham (1984a) all divide the freezing process into separate precooling, phase change and tempering periods. For the phase change period versions of Plank's equation are used, whilst for the other periods a variety of different techniques are used to calculate the heat conduction without change of phase. Pham (1984a) writes Plank's equation in a form analogous to Newton's law of cooling and uses this for all three periods. For precooling and tempering, this is the same as the lumped capacity method of Cochran (1955) and London & Seban (1943) except that the position of the lumped heat within the object is determined by the Biot number. For all these methods thermal properties are chosen or calculated by averaging techniques to model more accurately the true heat transfer conditions during each period. For similar reasons Mott (1964), Fleming (1967), Sokulski (1972a), Albin et al (1979) and Pham (1984a, 1984b) all suggested the use of a weighted average freezing temperature or temperature difference in solutions based on a unique phase change temperature, when phase change is over a range of temperatures such as in food freezing and thawing. Levy (1983b, 1983c, 1984) also considered the freezing and thawing processes in three stages and defined effective heat capacities and thermal conductivities for each stage for use in solutions for heat conduction without phase change.

Nagaoka et al (1955), Eddie & Pearson (1958), Levy (1958), Earle & Freeman (1966), Fleming (1967), Frazerhurst et al (1972), Slatter & Jones (1974) and Mellor & Seppings (1976) for freezing and Walker (1970), Vanichseni (1971) and Vanichseni et al (1972) for thawing, all propose modifications to Plank's equation in the form of multiplicative factors. These generally aim to account for sensible heat effects that Plank assumed negligible.

Khatchaturov (1958) and Golovkin et al (1974) give formulae based both on fitting experimental data and analytical considerations. Schwartzberg et al (1977) examines temperature profiles during phase change for infinite and zero Biot numbers. Modifications at intermediate values of Biot number are used to predict phase change times. Sastry (1984) used an enthalpy transformation and Goodman's (1964) heat balance integral technique to approximate and solve the change in enthalpy profiles with time during partial freezing and thawing in slabs. Teider (1963), de Michelis & Calvelo (1982) and Mascheroni et al (1982) developed methods to account for different surface boundary conditions on each face during freezing of slabs.

2.4.3 Empirical Solutions

The difficulty in deriving a general solution to phase change that has wide applicability, even with only a partial analytical basis, has meant that many empirical approaches have been proposed. Some of these are relatively general in their application, whilst others are very specific to the food product and/or phase change conditions to which they apply. These latter solutions may only interpolate experimental data.

For freezing slabs, infinite cylinders, spheres and rectangular bricks to a final temperature of -10°C Cleland (1977) and Cleland & Earle (1976b, 1977a, 1979a, 1979b, 1982b) empirically modified the geometric factors in Plank's equation by regression analysis of experimental data. By a similar analysis of slab freezing data to a final temperature of -18°C Hung & Thompson (1983) found different modifications.

Calvelo (1981) for thawing of slabs, Creed & James (1981) for thawing of beef slabs, Hayakawa et al (1983a, 1983b) for freezing of finite cylinder and infinite rod shapes and Succar & Hayakawa (1984) for freezing of slabs give regression equations calculated from results predicted by numerical methods.

Pham (1984c) used a similar approach to Pham (1984a) but empirically defines the average phase change temperature as a function of the final thermodynamic centre temperature and the ambient temperature.

Differential forms of empirically developed versions of Plank's equation allow Loeffen et al (1981) and Cleland & Earle (1982c) to consider time variable boundary conditions by simple numerical methods. A non-uniform initial temperature distribution was handled by calculation with a mean initial temperature.

The empirical solutions are summarised in Table A.7.

For a range of regular shapes two recent studies (Cleland & Earle 1984a, Pham 1984c) have shown the methods to predict freezing times due to Pham (1983, 1984a, 1984b, 1984c) and Cleland & Earle (1982b) to be accurate by comparison with a large composite freezing data set.

2.4.4 Numerical Methods

Direct numerical approximation of Eq. (2.1) is an approach requiring no assumptions about the physical processes of freezing and thawing. Errors may arise from imprecise thermal data, and from numerical truncation and rounding errors. A wide range of numerical methods have been used.

Those using the finite difference method include: simple explicit schemes where k and C are combined and thermal diffusivity, α, is taken as a function of temperature (Earle & Earl 1966, Cullwick & Earle 1971, Bailey & James 1974, Heldman 1974a, Heldman & Gorby 1974, Chattopadhay 1975, James et al 1977, James & Creed 1980, Creed & James 1981b, Heldman 1983), explicit solutions where k and C are taken as separate functions of temperature (James et al 1979, James & Bailey 1980,

Mascheroni & Calvelo 1980, de Michelis & Calvelo 1982, Mascheroni & Calvelo 1982, Mascheroni et al 1982), explicit difference formulae based on the enthalpy transformation (Eyres et al 1946, Price & Slack 1954, Albasiny 1956, Lockwood 1966, Cordell & Webb 1972, Joshi & Tao 1974, Shamsundar & Sparrow 1975, 1976), fully implicit and two time level implicit schemes (Crank & Nicholson 1947, Albasiny 1960, Hashemi & Sliepcevich 1967a, Fleming 1971c, Steinhagen & Myers 1983, Succar & Hayakawa 1984) and three time level implicit solutions (Bonacina & Comini 1971, Bonacina et al 1973, Comini & Bonacina 1974, Cleland & Earle 1977b, 1979a).

Bonacina & Comini (1971) and Cleland & Earle (1984a) considered the different finite difference schemes and concluded that the implicit three time level scheme due to Lees (1966) is superior in terms of accuracy. It is also stable and convergent. The three time level scheme predicted freezing data to within about ±10% for slabs, infinite cylinders, spheres and rectangular brick shapes (Cleland et al 1982).

Methods for the infinite cylinder and sphere geometries are based on the scheme proposed by Albasiny (1960). Where implicit methods are used for two- and three-dimensional geometry a number of alternating direction implicit schemes have been used (Douglas 1955, Peaceman & Rachford 1955, Douglas & Rachford 1956, Brian 1961, Fairweather & Mitchell 1965, Allada & Quan 1966, Fleming 1970, McKee & Mitchell 1971, Bonacina & Comini 1973, Cleland & Earle 1979b). All the above schemes are limited to shapes with regular configuration. Finite difference schemes to model irregular geometry in two dimensions (Fleming 1971a, Brisson-Lopes & Domingos 1979, Koskelainen 1979) and non-homogeneous materials (Fleming 1971b) have been developed but are complex.

The finite element method has been widely used for problems with phase change (Comini et al 1974b, Comini & Del Guidice 1976, Comini & Lewis 1976, Lewis & Bass 1976, Rebellato et al 1978, Frivik & Thorbergson 1981, Frivik & Comini 1982, Hayakawa et al 1983b, Purwadaria & Heldman 1983). The major advantages of the finite element method over the finite difference method are that it is able to cope easily with irregular geometries and heterogeneous materials (Arce et al 1983). Complex boundary conditions are incorporated simply (Comini & Bonacina

1974) and higher order (quadratic or cubic rather than linear) approximations to temperature profiles can be used (Emery & Carson, 1971). Disadvantages of the finite element method are that the time step is neccessarily shorter for stability and non-oscillation (Myers 1978, Bald 1981) and that the computer storage requirements and processing time are greater (Yalamanchilli & Chu 1973) than for finite differences.

Testing of the finite element method has demonstrated good accuracy of prediction against experimental data for two-dimensional problems considering freezing of roads (Frivik et al 1977), freezing of ice (Hsu & Pizey 1981), freezing of food (Purwadaria 1980), thawing of fish (Miki et al 1978) and freezing of fish (Miki et al 1982).

Finite elements are commonly employed to discretise in space, but both the finite element method (Bruch & Zyroloski 1974, Chung 1981) and finite difference schemes have been used in time (Donea 1974, Wood & Lewis 1975). Using finite elements means higher order time approximations can be used but significantly increases the size of the computing problem. Where thermal properties are changing rapidly the linear, centrally balanced, three time level Lees' scheme has been found to be stable and convergent (Comini et al 1974b).

In numerical methods the calculated heat flow through the object surface should equal the internal enthalpy change over the whole phase change process. Close agreement (referred to as a heat balance) must be achieved for a numerical method to be considered both accurate and valid. To ensure a heat balance, a number of different methods to calculate the thermal properties (especially in the latent heat peak temperature range) have been proposed (Comini et al 1974b, Comini & Del Guidice 1976, Lemmon 1979). Morgan et al (1978) suggest they may not give benefits over direct evaluation. Cleland et al (1982), studying numerical prediction of freezing, discovered that the better finite difference and finite element methods are probably more limited by thermal data uncertainty than numerical approximations. Both the finite element method and the finite difference method for continuously variable thermal properties can model a unique phase change temperature by appropriate choice of the thermal property functions (Bonacina et al

1973).

The boundary element method, which is similar to the finite element method, has been proposed for non-linear transient heat conduction with variable properties (Brebbia & Walker 1980). It has the advantage of reducing the dimensionality of the problem and therefore the computing requirements (Wrobel & Brebbia 1981), but will only be accurate for shapes with large surface area-to-volume ratios (Wrobel & Brebbia 1979). It has not been used for heat transfer with phase change as it has no proven advantages over the finite element method for this type of problem.

2.5 THE EFFECT OF GEOMETRY ON FREEZING AND THAWING TIME PREDICTIONS

Apart from some finite difference methods and finite element schemes, methods for freezing or thawing time prediction are nearly all restricted to regular geometric configurations such as slabs, infinite cylinders, spheres, infinite rods and rectangular bricks. Many food products are not regular in shape so methods are required to take account of irregular geometry.

By assuming (a) a geometrical description for the phase change front, (b) that the surface temperature is constant but still time variable over the surface and (c) that the quasi-steady state assumption is applicable in the phase between the surface and the phase change front, Plank (1941), Tanaka & Nishimoto (1959, 1960, 1964) and recently Shamsundar (1982) derived geometric factors to account for the object configuration for many regular shapes. Where the second assumption is true and the phase change front is parallel to the surface, the factors depend directly on the surface area times thickness-to-volume (AD/2V) ratio. Rutov (1936) and Mott (1964) both extended the idea to using the ratio of product surface area times thickness-to-volume as an index of the shape in calculations for all geometries. This approach is accurate for slabs, infinite cylinders and spheres with the third kind of boundary condition as the surface is always isothermal, irrespective of Biot number. Cleland & Earle (1982a, 1982b) show it is not accurate for other shapes when the Biot number is non-zero. Pham (1984b) used the same general approach but includes a correction to the Biot number

based on the "mean heat conducting path" (MCP) from the centre to the surface of the object. A method to calculate the mean conducting path length is given for freezing of rectangular brick shapes based on fit to experimental data. Sokulski (1972a) uses the AD/2V ratio but only considers a section of the object near the thermodynamic centre.

Cleland & Earle (1982b) define EHTD (equivalent heat transfer dimensionality) as the ratio of the freezing time for a slab of equivalent thickness to the freezing time of the shape in question, under the same initial and boundary conditions. The value of EHTD is calculated from the ratios of dimensions for rectangular brick shapes or from experimental data but is, like Pham's method, essentially equivalent to the area times thickness-to-volume ratio with a correction for Biot numbers greater than zero.

Both the EHTD and MCP concepts gave accurate predictions of experimental data for freezing of rectangular bricks when applied in conjunction with an accurate prediction method for freezing of the simple slab shape. Neither method has a totally theoretical basis, but both consider the limiting cases of Bi→0 and Bi→∞. Goodness of fit to experimental data was also used in their derivation. Both EHTD and MCP have been postulated as suitable for irregular shapes, but this has not been verified.

A common method to account for geometry in phase change of irregularly shaped foods has been to approximate the shape by the closest simple shape (slab, infinite cylinder, sphere) and define an equivalent diameter or thickness. This method is of limited use as the appropriate correlation for equivalent diameter is specific for each product type and requires experimental data to determine it accurately. Often the equivalent diameter is chosen to include correction for errors in the prediction method used, as well as the effect of shape on heat transfer. A general model to account for geometric effects within a calculation method is superior to an experimental correlation for a particular product, as it is not restricted by product type. Table A.8 lists researchers who use equivalent diameters for irregular shapes.

For heat conduction without phase change, Smith et al (1967), Smith et al (1968), Clary et al (1968), Smith & Nelson (1969) and Clary et al (1971) defined a geometry index for irregular shapes calculated from an ellipsoidal model shape that has equal orthogonal cross-sectional areas to the anomalous shape that it replaces. This index has not been tested for phase change problems.

2.6 PHYSICAL PARAMETERS REQUIRED FOR CALCULATION OF PHASE CHANGE IN FOODS

2.6.1 Thermal Property Data

The thermal properties required to predict phase change in food include thermal conductivity, k, volumetric specific heat capacity, C, latent heat content, L, phase change temperature, T_{if}, and specific heat generation, Q. No method to predict freezing or thawing times for foodstuffs can be accurate if the food thermal properties required by the method cannot be obtained accurately, or are not representative of the whole product. There has been a great deal of research, reviewed by Woolrich (1966), Woodams & Nowry (1968), Morley (1972), Mellor (1976, 1978, 1979, 1980), Polley et al (1980) and Meffert (1984), into thermal property data required to calculate phase change for foods. A complied set of data for meat (Morley 1972) demonstrates some inconsistencies in the thermal property data. Similar inconsistencies in data could be expected for other foods.

Collection of thermal property data is tedious and expensive because of the variability of foodstuffs in composition and structure and the wide range of temperature for which data is required. Data for frozen food are especially difficult to determine because it is difficult to maintain the appropriate experimental conditions.

Because of these difficulties, numerous attempts have been made to mathematically model food properties and hence derive calculation methods for the thermal properties. Data that can be determined simply, cheaply and accurately such as initial freezing temperature, composition, average unfrozen thermal conductivity and specific heat capacity and the bound water fraction are used as input data for these

models. The simplest models sum the effect of the solid and liquid component parts (Comini et al 1974a, Lamb 1976, Dickerson 1977, Lentz & Van Den Berg 1977, Mascheroni et al 1977, Levy 1981, Levy 1982a). An alternative is to predict the water and ice fraction from freezing point depression equations and relate this to the changes in properties from unfrozen values (Heldman 1974b, Heldman & Gorby 1975, Schwartzberg 1976, Schwartzberg 1977, Mascheroni & Calvelo 1980, Heldman 1981, Heldman 1982, Mascheroni & Calvelo 1982, Larkin et al 1984). A third approach is to use empirical or regression equations to fit the data (Levy 1979, Chang & Tao 1981, Ramaswamy & Tung 1981, Levy 1982b, 1982c, 1983a). All three approaches are claimed to lead to data of similar accuracy to that obtainable by direct measurement.

Numerical methods based on approximating Eq. (2.1) need extensive thermal data over the full temperature range whereas many simple methods do not. Complete thermal property tables, simplified linear approximations to the actual data (Bonacina et al 1974, Comini et al 1974a, Bonacina & Comini 1976, Tao 1975) and systems based on the above property prediction methods have all been used in numerical methods with good reported accuracy.

Meffert (1984) and Hsieh et al (1977) investigated the error in thermal property data and its effect on prediction accuracy. Considering that error on individual values of any property can be as high as 40% the error can be substantial in any subsequent predictions of freezing and thawing.

2.6.2 Surface Heat Transfer Coefficients

One of the most difficult parameters to determine independently in food freezing and thawing processes that involve the third kind of boundary condition is the surface heat transfer coefficient between the ambient medium and the product surface. Arce & Sweat (1980) review techniques to estimate, and give data for, surface heat transfer coefficients in many food heat transfer situations.

There are many correlations (McAdams 1954) but these tend to be medium, product, and situation specific, and of doubtful accuracy. Measurement

in situ is a better proposal as the actual heat transfer conditions are more closely represented and any variation due to equipment will be taken into account. Some transient methods are discussed by Cleland & Earle (1976a) and Earle & Cleland (1979). Some researches have used metal transducers (Fleming 1967, Kopelman et al 1970, Earle 1971, Cowell & Namor 1974). Users of such devices cannot be sure of the correlation between the surface heat transfer coefficient measured for the transducer and those for the actual foodstuff or material. Others workers have used the actual food under similar experimental conditions and have chosen the surface heat transfer coefficient to fit solutions for heat transfer without phase change (Charm 1963, Baker & Charm 1969), or to give the best fit of surface and centre temperature predictions using finite difference methods (Beck 1969, Bonacina & Comini 1972, Chavarria & Heldman 1984). Comini (1972) shows that surface temperatures are most sensitive to change in the surface heat transfer coefficient and hence advocates their use in an optimal experimental design. For measuring surface heat transfer coefficients to irregular shapes only metal transducers are can be used without the need for complex trial and error computer analysis by the finite element method. For similar reasons in situ transient determinations are limited to regular geometric shapes. Variation of the surface heat transfer coefficient over the surface is common with variable geometric configurations and in conditions such as air flow (Purwadaria 1980). Local variations of the surface heat transfer coefficient can be significant but are very difficult to measure. Often an average value must be determined or estimated.

2.7 SUMMARY

There are a large number of solutions to the problem of heat conduction with phase change for regular geometric shapes. Most analytical and some numerical solutions are based on the assumption that phase change occurs at a unique temperature. None of these have been proven accurate for food where phase change is over a range of temperatures. Other common limitations of methods are that they do not consider the most common and useful third kind of boundary condition, do not account for initial temperature not being at the phase change temperature, and are derived for semi-infinite rather than finite geometric shapes.

Modified analytical and empirical solutions retain the simple analytical form, have less detailed thermal data requirements than more rigorous methods, but tend to be product or situation specific. Within this group, those formulae of a general nature have been tested against experimental freezing data and some have shown acceptable accuracy. There has been no extensive testing of simple prediction methods for thawing.

The finite difference numerical method is of proven accuracy for freezing of regular shapes. The finite element method has been formulated and shown to be superior to the finite difference method for predicting phase change in two-dimensional irregular shapes. Neither numerical method has been tested extensively for thawing of food in regular shapes or for freezing or thawing of foods of irregular geometry due to the lack of suitable experimental data.

Simple analytical methods to allow calculations for irregular shapes have been proposed, but no significant testing or refinement against experimental or numerically calculated data over a range of conditions has been carried out.

3 RESEARCH OBJECTIVES

Ultimately, verification of the accuracy of any method to predict freezing and thawing times must be made by comparison with accurate experimental freezing and thawing data (Heldman 1983, Cleland & Earle 1984a). The most useful data set would be large and diverse in order to differentiate between error due to imprecise knowledge and control of the phase change conditions (experimental error), error due to uncertainty in thermal property data (data error) and inaccuracy arising from assumptions or approximations made in the derivation of the prediction method (prediction error).

For freezing of regular shapes such as slabs, cylinders, spheres and rectangular bricks Linge (1973), Cleland (1977), de Michelis & Calvelo (1983), Hayakawa et al (1983a), Hung & Thompson (1983) and Succar & Hayakawa (1984) have published major data sets for a variety of foodstuffs and food analogues, frozen under a range of conditions. Cleland & Earle (1984a) and Pham (1984c) used an amalgamated data set from these sources to test freezing time prediction methods for regular shapes. This study showed that accurate freezing time prediction methods existed for these shapes.

Data given for irregular shaped objects tend to be product specific. In virtually all cases published in the literature, detailed geometrical descriptions have not been given and consistency in size and shape during experiments was not controlled. For example, in the freezing and thawing of mutton carcasses the size and shape information is often limited to the relevant weight range (Earle & Fleming 1967, Vanichseni et al 1972). This information is generally not sufficiently detailed to test prediction methods other than product specific empirical formulae.

The restricted nature of published data led to the formulation of the first two aims of the present research:
(1) to collect thawing data for the basic slab, infinite cylinder, sphere and rectangular brick shapes
(2) to collect freezing and thawing data for other (irregular) shapes.

This expansion of the data base was necessary to facilitate testing of thawing time prediction methods for simple shapes and prediction methods applicable to irregular geometries for both freezing and thawing.

Table 3.1 gives the desirable attributes of any method for food freezing and thawing time prediction discussed by Slatter & Jones (1972), Cleland (1977) and Cleland & Earle (1977a). The methods available are conveniently divided into two broad groups for further study:

Group (I): Formulae requiring only hand calculation

Group(II): Numerical methods requiring computer calculation.

These groups differ slightly from those used in Sec. 2.3 and 2.4. Many engineers do not have the specialised knowledge to implement numerical methods. They will not use Group II methods unless they are available as computer packages. Such people therefore must often rely on the simple formulae (Group I). The greater sophistication of numerical methods may justify their use if complex conditions are to studied and more detailed design information is required. Often imprecise knowledge of the phase change conditions and uncertainty in thermal data mean that the more complex numerical methods are no more accurate in practice than Group I methods.

Conditions usually imposed in the derivation of Group I methods are listed in Table 3.2. If any of these conditions are violated Group I methods can only be applied to practical problems by taking appropriate averages for the phase change process. In contrast Group II methods are applicable whether these assumptions are made or not.

Provided the eight assumptions in Table 3.2 are met, freezing or thawing times are influenced by the seven major factors listed in Table 3.3. The accuracy and usefulness of any experimental data collected is dependent on the ability to measure these parameters, to control accurately the experimental environment and to meet the conditions in Table 3.2. The data sets collected were designed so that all important parameters could be examined. These data enabled the third, fourth and fifth aims of the current study to be considered. These were to:

(3) assess the accuracy of both Group I and Group II methods for

prediction of thawing times for regular shapes

(4) assess the accuracy of Group II methods for prediction of freezing and thawing times for irregular shapes and

(5) investigate the possibility of developing a Group I method to predict freezing and thawing times for irregular shapes.

A decision was made to limit the current study to situations where the eight conditions listed in Table 3.2 apply. This decision was made because of time and resource limitations. Despite this restriction a wide range of practically important problems can still be covered. Future work may investigate situations not limited by these assumptions.

Table 3.1 Desirable Attributes of Freezing and Thawing Time Prediction Methods

(a) Sufficient accuracy over a wide range of conditions

(b) Simple and cheaply processed calculations

(c) Applicability to a wide range of biological materials of various sizes and shapes

(d) Applicability to the practically important third kind of boundary condition in situations where there is superheating or subcooling

(e) Minimal need for detailed thermal property data

(f) Prediction of heat flow and temperature profiles as functions of time

(g) Use of a unified approach for both freezing and thawing.

(h) Applicability where boundary conditions are time and position variable

Table 3.2 <u>Conditions Required For Derivation of Simple Freezing and</u>
          <u>Thawing Time Prediction Formulae</u>

(a) That the boundary and initial conditions are constant with time
    and/or position
(b) Homogeneous materials
(c) That the third boundary condition describes the heat transfer at
    the boundary adequately and that radiation effects are
    insignificant
(d) No internal heat generation
(e) Isotropic materials
(f) Negligible density change during phase change
(g) Internal heat transfer by conduction only
(h) No mass transfer, such as evaporation, at the surface
(i) That the object retains its physical integrity during the phase
    change process.

Table 3.3 <u>Factors Affecting Freezing and Thawing Times</u>

(a) Thermal properties of the material
(b) Size of the object
(c) Initial temperature of the material
(d) The ambient heating or cooling temperature
(e) The surface resistance to heat transfer as defined by the surface
    heat transfer coefficient
(f) The geometric configuration of the object
(g) The final temperature at the thermodynamic centre at the completion
    of the phase change process.

4 NUMERICAL METHOD FORMULATIONS

It was neccessary to develop some numerical freezing and thawing time prediction methods beyond what has been reported in the literature in order to meet the fourth research objective defined in Chap. 3.

4.1 INTRODUCTION

Numerical methods to predict rates of phase change processes in foods can be divided into three groups:

(a) the finite element method

(b) the finite difference method

(c) the approximate analytical methods that require numerical integration or are too complex for hand calculation.

The latter group have few advantages over the other two and have the major disadvantage that usually severely limiting physical approximations are made. Therefore this group of numerical methods was not considered further. Only numerical methods that account for phase change by considering continuously temperature variable thermal properties were considered as they are physically the most realistic. The alternative numerical methods treating phase change as a moving boundary problem by assuming a unique phase change temperature do not approximate phase change in foods very closely and are therefore inferior (Cleland 1977).

Advances in computing technology have meant that costs for computer computation power and data storage are now relatively low so numerical methods become attractive compared with simple analytical methods. The availability of comprehensive programs is increasing so detailed knowledge of computer programming and of the numerical techniques are not neccessarily required to use these methods.

Numerical methods have been advocated as a standard method for prediction of phase change against which all other prediction methods should be compared, because numerical methods are the closest to an "exact" prediction method that exists (Heldman 1983). Comparisons with numerical methods should only complement, not replace, comparisons with

actual experimental freezing and thawing data (Cleland & Earle 1984a).
A numerical method can only be accurate if it has been correctly
formulated and, implemented and if reliable data are used. Comparisons
with experiments are necessary to assess these factors. The finite
difference method is limited by practical constraints to use for
regular shaped objects such as slabs, infinite cylinders, spheres,
infinite rods and rectangular bricks. For these shapes fixed regular
grids can be used for the finite difference approximations and
comparatively simple schemes developed. For irregular shapes more
complex finite difference schemes and irregularly spaced grids can be
used (Fleming 1971c). These are more complex to implement on computers
than finite element methods.

Numerical methods require no physical assumptions about the phase
change process but make numerical approximations. For complex boundary
conditions, irregular shapes, non-homogeneous materials and where
temperature profiles change rapidly with position, the finite element
method is able to make more exact approximations than the finite
difference method. For these reasons only the finite element method
has been used extensively for irregular shapes (Comini et al 1978).

4.2 THE FINITE ELEMENT METHOD

Although the finite element method has been widely used for phase
change (Comini et al 1978) none of the published applications of the
finite element method to phase change considered three-dimensional
problems, and only limited testing of some two-dimensional finite
element codes against experimental data has been carried out
(Sec. 2.4.4). A simple problem specific program was available for
three-dimensional heat transfer (Lim 1975) but a general finite element
program was not. Therefore a general formulation for heat conduction
in three-dimensional geometry was developed and programmed (Cleland et
al 1984).

4.2.1 Finite Element Method Formulation

The finite element method can be formulated for heat transfer with change of phase in a three-dimensional object by using the Galerkin weighted residual method for spacewise discretization of Eqs. (2.1) and (2.8) (Zienkiewicz 1971, Segerlind 1976). Incorporating the boundary conditions (Eqs. (2.3) to (2.6) and (2.9) to (2.11)) using Green's theorem, yeilds the n simultaneous differential equations to be solved implicitly for the temperatures at the n nodal points defined throughout the region. Written in matrix form the solution becomes (Zienkiewicz & Parekh 1970, Comini et al 1974b):

$$\mathbf{K}\ \underline{T}(t) + \mathbf{C}\ \dot{\underline{T}}(t) = \underline{F} \tag{4.1}$$

where $\mathbf{K}$ = thermal conductance matrix

     $\underline{T}$ = vector of nodal temperatures as a function of time

     $\mathbf{C}$ = thermal capacitance matrix

     $\underline{F}$ = thermal forcing vector

The typical matrix elements are:

$$K_{ij} = \Sigma \int_{V_e} k \left[\frac{\partial N_i}{\partial x} \frac{\partial N_j}{\partial x} + \frac{\partial N_i}{\partial y} \frac{\partial N_j}{\partial y} + \frac{\partial N_i}{\partial z} \frac{\partial N_j}{\partial z} \right] W\ dV$$

$$+ \Sigma \int_{S_{3e}} \left(h_{con} + h_{rad} \right) N_i\ N_j\ W\ dS_3 \tag{4.2}$$

$$C_{ij} = \Sigma \int_{V_e} C\ N_i\ N_j\ W\ dV \tag{4.3}$$

$$F_i = \Sigma \int_{V_e} Q\ N_i\ W\ dV + \Sigma \int_{S_{2e}} \phi\ N_i\ W\ dS_2$$

$$+ \Sigma \int_{S_{3e}} \left(h_{con} T_{ac} + h_{rad} T_{ar} \right) N_i\ W\ dS_3 \tag{4.4}$$

where W   = $2\pi r$ for cylindrical co-ordinates

     = $4\pi r^2$ for spherical co-ordinates

     = 1 otherwise

   N_i, N_j = shape functions for the ith or jth node in the element or surface undergoing integration.

Equation (4.1) can be approximated by finite differences or finite elements and solved for future times given the appropriate initial condition. Using finite elements in the fourth (time) dimension greatly increases the size of the problem for computer implementation but does allow non-linear estimation in the time domain. Use of finite differences in the time domain is more common. The three time level, linear, finite difference scheme proposed by Lees (1966) is well proven

for phase change problems (Comini & Bonacina 1974):

$$c^i \frac{\mathbf{T}^{i+1} - \mathbf{T}^{i-1}}{2\Delta t} + \frac{\mathbf{K}^i}{3} \left[\mathbf{T}^{i-1} + \mathbf{T}^i + \mathbf{T}^{i+1} \right] = \mathbf{F}^i \tag{4.5}$$

It has the advantage over other finite difference schemes that it is centrally balanced so only central time values of the $\mathbf{K}$ and $\mathbf{C}$ matrices and $\mathbf{F}$ vector are required. Therefore iterative time stepping algorithms are not needed to incorporate correct values of the temperature and time dependent thermal properties, and the boundary conditions. The Lees' scheme has been shown to be unconditionally stable and convergent in the context of finite element analysis (Comini et al 1974b).

By using the temperature-dependent apparent specific heat capacity and thermal conductivity (such as Figs. 2.2 to 2.3) this numerical method will closely model the true physical process during phase change if data are accurate. To account for both changes in thermal properties over each element volume with time and the possible time dependence of the boundary conditions, the integrations shown in Eqs. (4.2) to (4.4) must be repeated for each time step, and $\mathbf{K}$, $\mathbf{C}$ and $\mathbf{F}$ re-evaluated. In Eqs. (4.2) to (4.4) the summations are taken for each element, V_e, in the element region, and for each element surface, S_{2e} or S_{3e}, on which Eq. (2.3) or (2.4) is specified. The spatial arrangement is chosen so that within each element or on each surface the variables k, C, Q, ϕ, h_{con}, ε, T_{ac} and T_{ar} are no longer dependent on position. In physical terms, this means that no element covers a region made up of more than one material type, and that boundary surfaces are chosen so that boundary variables ϕ, h_{con}, ε, T_{ac} and T_{ar} can be assumed constant for that surface, but not neccessarily the same as for other boundary surfaces. Knowledge of these variables is often subject to significant uncertainty. Therefore from a practical viewpoint the above limitations should not be restrictive. The dependence on temperature of k, C, Q, h_{rad}, and on time of h_{con}, ϕ, T_{ac} and T_{ar} at each of the surfaces, remains.

The full numerical integration of Eqs. (4.2) to (4.4) requires a large computation effort at each time step. Therefore a simpler formulation is also proposed in which Eqs. (4.2) to (4.4) become:

$$K_{ij} = \Sigma \, k_e \int_{V_e} \left[\frac{\partial N_i}{\partial x} \frac{\partial N_j}{\partial x} + \frac{\partial N_i}{\partial y} \frac{\partial N_j}{\partial y} + \frac{\partial N_i}{\partial z} \frac{\partial N_j}{\partial z} \right] W \, dV$$

$$+ \Sigma \, (h_{con} + h_{rad})_e \int_{S_{3e}} N_i \, N_j \, W \, dS_3 \qquad (4.6)$$

$$C_{ij} = \Sigma \, C_e \int_{V_e} N_i \, N_j \, W \, dV \qquad (4.7)$$

$$F_i = \Sigma \, Q_e \int_{V_e} N_i \, W \, dV + \Sigma \, \phi_e \int_{S_{2e}} N_i \, W \, dS_2$$

$$+ \Sigma \, (h_{con}T_{ac} + h_{rad}T_{ar})_e \int_{S_{3e}} N_i \, W \, dS_3 \qquad (4.8)$$

This requires the further assumptions that within each of the elements or across each of the element surfaces for which the summations are made, that the properties k, C, Q and h_{rad} are constant with respect to temperature, but that these values can change from one time step to the next. Even though this is not physically accurate, if a value of these properties that is representative of the whole element or element surface can be determined, and if the elements are not large this approach may be sufficiently accurate for many purposes. Given that the time step is controlled so that temperature changes per time step are small, the major disadvantage of this simpler formulation is that the properties are not re-evaluated at each integration point. In the full formulation evaluation at each integration point helps account for property variation over the element region so that oscillatory behaviour, especially near the phase change temperatures where thermal properties change rapidly, is less likely (Cleland et al 1984). The advantage of the simpler formulation is that the integrations shown in Eq. (4.6) to (4.8) need only to be calculated for the first time step. Thereafter the constant values resulting from the integration can be stored and multiplied element by element (and surface by surface) by the appropriate properties, and the summation completed. This requires far less computation time and computer memory than for the full formulation.

The choice of formulation must take into account the trade-off between loss in accuracy and savings in computation costs. As computation costs are usually far less than the cost of data preparation (Segerlind 1976), the savings may be quite small. Also uncertainties in thermal properties and boundary condition data are substantial (Sec. 2.6). Provided numerical errors are small compared with physical uncertainties no worthwhile increase in prediction accuracy will occur

by making the method more sophisticated. The simplified method uses this fact and possibly increases numerical error, but may not lead to significantly poorer predictions of experimental values. If there was a significant increase in error it would be expected to be a maximum when the temperature gradients across the elements were largest in the temperature range where phase change occurs. In thawing, this corresponds to high surface heat transfer coefficients, initial temperatures close to the phase change temperatures and ambient temperatures greatly different from the phase change temperatures (Cleland et al 1982).

4.2.2 Computer Implementation

Both the formulations given by Eqs. (4.1) to (4.8) were programmed in Fortran 77. The full codes are given in App. D which also includes data preparation notes. The programs use numerical integration of the element matrices and a Gaussian elimination algorithm for symmetric, positive definite, banded matrices with back substitution as the equation solver. Most of the computer process time to run these programs is due to estimation of thermal properties and numerical integration of the element matrices. Therefore use of a more sophisticated and efficient technique to solve the system of equations is not justified. Computer memory requirements are high but can be minimised by matching array dimensions closely to the problem size or by using peripheral storage devices. The special features described below are included in the programs.

The Lees' scheme makes a linear approximation by finite differences in the interval $(t-\Delta t)$ to $(t+\Delta t)$. For a linear variation in temperature the radiation heat transfer coefficient was accurately approximated by the method of Comini et al (1974b):

$$h_{rad} = \varepsilon\sigma\left[\left(T^i+T^i_{ar}\right)\left((T^i)^2+(T^i_{ar})^2\right)+\tfrac{1}{4}\left(T^{i+1}_{ar}-T^{i-1}_{ar}\right)^2\left(T^i_{ar}+T^i-\tfrac{2}{3}T^{i-1}\right)\right.$$
$$\left. + \tfrac{1}{3}\left(T^{i+1}_{ar}-T^{i-1}_{ar}\right)\left(T^i-T^{i-1}\right)\left(T^{i-1}+T^{i-1}_{ar}\right)+\left(T^i-T^{i-1}\right)^2\left(T^i+\tfrac{1}{2}T^{i+1}_{ar}-\tfrac{1}{6}T^{i-1}_{ar}\right)\right] \quad (4.9)$$

in which only known values of temperature are used. This allows central values of Γ to be used with good accuracy and an iterative procedure (Frivik et al 1977) to solve Eq. (4.5) is not required. As radiation is not a major form of heat transfer during food phase change processes this method should be sufficiently accurate for most

purposes.

In finite element analysis stable oscillations frequently occur (Yalamanchilli & Chu 1973, Myers 1978). They can be accentuated when using central values of $\mathbf{\underline{k}}$ (Comini & Lewis 1976). Updating temperatures at the end of each time step using the averaging procedure (Wood & Lewis 1975):

$$T^{i-1} = \tfrac{1}{3}(T^{i-1} + T^i + T^{i+1}) \qquad\qquad (4.10)$$

or reducing the time step (Segerlind 1976) will reduce these oscillations. Too small a time step is undesirable as computation times are increased and computer rounding errors can become significant.

The accuracy of Eq. (4.1) will be best if the variation of k, C, Q, h_{rad}, h_{con}, ϕ, T_{ac} and T_{ar} with time over each time step is small or is reasonably linear. For most problems h_{con}, ϕ, T_{ac} and T_{ar} are essentially constant with time, so that temperature dependence of k, C, Q and h_{rad} will be the larger contribution to inaccuracy.

A number of techniques have been used to find values of k, C and Q that are representative when rates of change of these quantities with space are large, such as near the phase change temperatures (Sec. 2.4.4). These approaches may lead to erroneous results (Morgan et al 1978) so direct evaluation of these properties as functions of temperatures is used. Control of the time step, so that excessive temperature changes over each time step cannot occur, is the ultimate strategy to give accuracy. The time step control ensures proper heat balances across elements and boundaries, helps reduce numerical oscillation and therefore increases precision in the solution. Small temperature changes per time step reduce the error in assuming that there is linear variation in k, C, Q and h_{rad} in the interval $(t-\Delta t)$ to $(t+\Delta t)$. Therefore the use of values for $\mathbf{K}$, $\mathbf{C}$ and $\mathbf{\underline{F}}$ at the central time value, t, will be an accurate approximation. An automatic time step adjustment (Comini et al 1974b) is useful to keep temperature changes per time step low without greatly increasing computation time. This is achieved by appropriate choice of values for the parameters ΔT_{min} and ΔT_{max}, which are the maximum and minimum nodal temperature changes per time step and are used to decide when to adjust the time step. The

most appropriate sizes of ΔT_{min} and ΔT_{max} are governed by the width of the peaks in the profiles of k, C and Q versus temperature (Morgan et al 1978).

The accuracy of thermal property approximations and the numerical method approximations can be checked by calculating the heat balance:

$$\frac{\text{apparent internal enthalpy change}}{\text{heat flow in through + internal heat the surface generation}} = \frac{\left[\int_V H\ dV\right]\Big|_{t_1}^{t_2}}{\int_{t_1}^{t_2}\left[\int_{S_2}\phi\ dS_2 + \int_{S_3}(\phi_{con} + \phi_{rad})\ dS_3 + \int_V Q\ dV\right] dt}$$

$$= 1.0 \text{ for balance} \tag{4.11}$$

A heat balance does not occur if property approximations are insufficiently accurate, time step or spatial intervals are too large or the numerical approximations used are not valid. For example, a heat balance greater than 1.0 generally indicates that "jumping" of the latent heat peak has occurred (Cleland & Earle 1977b) and that time steps should be shortened by reducing both ΔT_{min} and ΔT_{max}. Similarly, a heat balance less than 1.0 generally indicates that temperatures at for some elements have "stayed on" the latent heat peak too long, and that time steps and/or space intervals should be reduced. The first case of "jumping" of the latent heat peak in the apparent specfic heat capacity profile is a problem in freezing calculations because as the temperatures drop below T_{if} the peak is suddenly encountered, whereas the second case occurs most frequently in thawing calculations because the latent heat peak suddenly disappears as temperatures rise above T_{if}.

The programs can be used for heat transfer problems involving objects of one, two or three-dimensions. The axisymmetric feature can be used to simplify problems where one or more axes of rotational symmetry exist. The elements used are based on the rectangular "Serendipity" family (Zienkiewicz 1971). Linear or quadratic isoparametric and superparametric elements are available. The high order elements reduce the total number of elements necessary and allow curved element boundaries to be used to model irregular geometries. The only specific use of subparametric elements would be for regular shapes where a quadratic temperature profile is required. As quadratic isoparametric elements are capable of handling this case just as well, without

significant increases in computation times, subparametric elements are
not included in the programs.

All the boundary conditions given in the formulation (Sec. 4.2.1) can
be used, and any initial temperature distribution may be specified.

4.2.3 Finite Element Method Testing

Testing of the finite element codes was made against experimental
freezing data and analytical solutions for simplified phase change
problems (Cleland et al 1984). The number of nodes and elements used
was a compromise between the higher accuracy and less frequent
occurrence or smaller amplitude of oscillations achieved with a larger
number of nodes, and practical limitations on the computation time and
computer memory storage requirements (Segerlind 1976). Similarly, the
number of integration points used in the numerical integration of
element matrices was a balance between accuracy and computation time.
The use of three integration points in each direction was found to give
adequate accuracy in most cases. For the full formulation the
combination of number of nodes and type of elements (linear or
quadratic) was found to be less important as long as about eleven nodes
(and consequently either ten linear elements or five quadratic
elements) were used in each direction (Cleland et al 1984). For the
simpler formulation the number of elements is more critical as the
assumption of constant k, C and Q over each element becomes less
accurate for a few large quadratic elements rather than with more,
smaller linear elements. The benefit of being able to use a lower
number of quadratic elements is therefore lessened because the time
step must be decreased to maintain heat balances. Increasing the
number of nodes or elements for the full formulation or the number of
integration points for both formulations, above these suggested values,
gave only minor changes in predictions. Quadratic elements should be
used if the product surface is curved or irregular.

The exact solution due to Neumann (Carslaw & Jaeger 1959, p.282) for a
specified temperature boundary condition, the analytical solution for a
specified surface heat flux (Carslaw & Jaeger 1959, p.75) and a
numerical solution for the radiation boundary condition (Haji-Sheikh &

Sparrow 1967) were used to test the programs for the range of boundary conditions incorporated. Similar accuracy to that shown for other finite element codes (Comini et al 1974b) was demonstrated (Tables 4.1 to 4.3). Both finite element formulations gave comparable temperature/time profiles with those given by the finite difference method for the same problems. For heat conduction in solids with the third kind of boundary condition the only solution for three-dimensional geometry is due to Newman (1936). Finite element predictions using a coarse 6x6x6 node grid (Table 4.4) gave similar prediction accuracy to a finite difference program for the identical problem (Cleland & Earle 1979b). The thermal properties are constant in this last problem and it is not difficult to solve the problem numerically. Therefore this problem is more a check that the method has been implemented correctly on the computer, rather than a check that the method is accurate in general.

Comprehensive experimental data available for heat conduction with phase change were limited to freezing of the regular shapes namely: slabs (Cleland & Earle 1977a), infinite cylinders and spheres (Cleland & Earle 1979a) and rectangular bricks (Cleland & Earle 1979b), subject to the boundary condition of the third kind. Although the full formulation could not be run on all the rectangular brick data due to excessive computation times, the overall prediction accuracy compared favourably with the finite difference prediction of this data (Cleland et al 1984).

In all testing the simplified formulation gave similar results to the full formulation though often smaller time steps were required to achieve heat balances for quadratic elements. Computation times for the three-dimensional problems with 216 nodes in a 6x6x6 grid of 125 evenly sized, linear isoparametric elements over 250 time steps were about 15 000 sec. and 3 000 sec. for the two formulations respectively on a Prime 750 computer. By comparison, the three-dimensional, Lees' scheme, finite difference method program with a 6x6x6 node grid used about 300 sec. computer process time for 250 time steps on a Prime 750 computer.

Table 4.1 <u>Comparison of Results From the Finite Element Method Programs</u>
<u>With Neumann's Solution[1] For Thawing of a Slab Subject to the</u>
<u>First Kind of Boundary Condition</u>

$D = 1.0$ m, $k_s = k_l = 1.0$ W m^{-1} °C^{-1}, $C_s = C_l = 1.0$ MJ m^{-3} °C^{-1},
$L = 75.0$ MJ m^{-3}, $T_a = 15$°C, $T_{in} = -15$°C.

Interface Position (m)	t_{neum}[2] (sec)	t_{femf}[2] (sec)	t_{fems}[2] (sec)
0.05	10400	10800	9700
0.10	42500	42700	38600
0.15	93400	95900	88900
0.20	166000	170800	162800
0.25	259300	264700	258000

[1] Carslaw & Jaeger (1959, p.282)

[2] t_{neum} = time calculated from Neumann's solution[1], t_{femf} = time calculated from the full finite element formulation (Eqs. (4.2) to (4.5)) and t_{fems} = time calculated from the simpler finite element formulation (Eqs. (4.5) to (4.8)). Latent heat was evenly distributed over the temperature range from -0.25°C to 0.25°C, 21 nodes and 20 linear isoparametric elements were used in the finite element programs.

Table 4.2 Comparison of Results From the Finite Element Method Programs
         With a Known Analytical Solution[1] For Cooling of a Slab
         Subject to the Second Kind of Boundary Condition

$D = 1.0$ m, $k = 1.0$ W m^{-1} $^{\circ}$C^{-1}, $C = 1.0$ MJ m^{-3} $^{\circ}$C^{-1}, $\phi = 100$ W m^{-2},
$T_{in} = 100\,^{\circ}$C.   Values of temperature ($^{\circ}$C) are tabulated.

Time (sec)	Slab Surface		At 0.1m From Slab Surface	
	Analytical	Numerical[2]	Analytical	Numerical[2]
20	84.04	83.83	92.09	92.90
40	77.43	77.28	86.04	85.90
60	72.36	72.24	81.22	81.10
80	68.09	67.98	77.09	76.99
100	64.32	64.22	73.43	73.34

[1] Carslaw & Jaeger (1959, p.75)

[2] Both the full formulation (Eqs. (4.2) to (4.5)) and the simplified
   formulation (Eqs. (4.5) to (4.8)) gave identical results, 21 nodes
   and 20 linear isoparametric elements were used in the finite element
   programs.

Table 4.3 Comparison of Results From the Finite Element Method Programs
          With a Numerical Solution[1] For Cooling of a Slab Subject to
          the Third Kind of Boundary Condition Including Radiation

$D = 1.0$ m, $k = 1.0$ W m^{-1} °C^{-1}, $C = 1.0$ MJ m^{-3} °C^{-1}, $h = 1.0$ W m^{-2} °C^{-1},
$\epsilon = 1.0$, $T_{ac} = 0$ K, $T_{ar} = 0$ K.   Values of Y are tabulated.

	Slab Surface		Slab Centre	
Fo	Numerical[1]	FEM[2]	Numerical[1]	FEM[2]
		$\epsilon\sigma T_{in}^3 D/k = 1$		
0.02	0.80	0.79	1.00	1.00
0.06	0.70	0.70	1.00	1.00
0.20	0.58	0.58	0.94	0.93
0.40	0.50	0.50	0.80	0.80
1.00	0.33	0.32	0.50	0.50
2.00	0.16	0.15	0.23	0.23
		$\epsilon\sigma T_{in}^3 D/k = 4$		
0.02	0.70	0.69	1.00	1.00
0.06	0.61	0.61	1.00	1.00
0.20	0.51	0.51	0.91	0.91
0.40	0.43	0.43	0.76	0.76
1.00	0.29	0.28	0.44	0.45
2.00	0.13	0.14	0.20	0.21

[1] Haji-Sheikh & Sparrow (1967)

[2] FEM = calculated from the element method, both the full formulation
(Eqs. (4.2) to (4.5)) and the simplified formulation (Eqs. (4.5) to
(4.8)) gave identical results.

Table 4.4 Comparison of Results From the Finite Element Method Programs
         With a Known Analytical Solution[1] For Cooling of a Cube
         Subject to the Third Kind of Boundary Condition

Bi = 4.0. Values of Y are tabulated.

	Centre of Face		Centre of Cube	
Fo	Analytical[1]	Numerical[2]	Analytical[1]	Numerical[2]
0.04	0.489	0.495	0.999	1.001
0.08	0.387	0.392	0.974	0.985
0.12	0.318	0.319	0.897	0.912
0.16	0.261	0.265	0.790	0.804
0.20	0.215	0.218	0.677	0.688
0.24	0.177	0.180	0.570	0.580

[1] Newman (1936)

[2] Both the full formulation (Eqs. (4.2) to (4.5)) and the simplified
   formulation (Eqs. (4.5) to (4.8)) gave identical results, a 216
   (6x6x6) node grid and 125 linear isoparametric elements were used in
   the finite element programs.

The ability of the code to deal with curved irregular geometry in two dimensions was confirmed by modelling the cylindrical shape with the grid given in Fig. 5.15. Prediction accuracy was similar to that obtained using regular one-dimensional axisymmetric elements. Although the finite element code has not been proven for a truely irregular shape, there is no reason why similar prediction accuracy cannot be achieved if sufficiently detailed nodal grids are used, as the finite element method does not treat regular shaped elements any differently from irregularly shaped ones.

The two finite element programs were therefore considered to be accurately formulated and correctly implemented. Hence they were available as prediction methods that would be expected to give accurate predictions of phase change in objects of irregular geometry. Disagreement with experimental data is more likely to be due to imprecise thermal and experimental data than to inadequacies in the formulation or program. If prediction method error arises it is more likely to be because practical limits on memory and computer process time have meant that coarse space and time grids have been used.

4.3 THE FINITE DIFFERENCE METHOD

Development of the finite element method has meant that the finite difference method is mainly used for prediction of heat transfer in regularly shaped objects. For problems with regular shapes, finite differences require less detailed program preparation and have lower computation times. Bonacina & Comini (1971), Cleland (1977) and Cleland & Earle (1977a) studied finite difference methods and found the three time level implicit Lee's scheme to be the best for modelling freezing of food. Computer programs using the Lee's scheme for infinite slabs (Cleland & Earle 1977b), infinite cylinders and spheres (Cleland & Earle 1979a), rectangular rods (Cleland 1977) and rectangular brick (Cleland & Earle 1979b) shapes are available and were subsequently used. These programs have been shown to be accurate to within about ±10% compared with experimental slab, infinite cylinder, sphere and rectangular brick freezing data (Cleland et al 1982). They also meet analytical checks. There is no reason why similar prediction accuracy cannot be expected using these programs for thawing of food.

The equivalent scheme for the finite cylinder geometry has not been published and is therefore described here.

4.3.1 Finite Cylinder Finite Difference Scheme Formulation

For the finite cylinder geometry the general heat conduction equation is:

$$C \frac{\partial T}{\partial t} = \frac{\partial}{\partial r}\left[k \frac{\partial T}{\partial r}\right] + \frac{k}{r}\frac{\partial T}{\partial r} + \frac{\partial}{\partial y}\left[k \frac{\partial T}{\partial y}\right] \tag{4.12}$$

Although the finite cylinder is three-dimensional, because it has an axis of rotational symmetry, it can be considered as two-dimensional. Bonacina & Comini (1973) have shown how the Lee's scheme can be applied to problems in two dimensions by using standard alternating direction implicit procedures. Equation (4.12) can be approximated by a Lees' scheme:

$$
\begin{aligned}
C_{mj}^i \frac{T_{mj}^{i+1}-T_{mj}^{i-1}}{2\Delta t} &= \frac{1}{3(\Delta r)^2}\Big[k_{m+\frac{1}{2}j}^i(T_{m+1j}^{i+1}-T_{mj}^{i+1}+T_{m+1j}^i-T_{mj}^i+T_{m+1j}^{i-1}-T_{mj}^{i-1}) \\
&\quad - k_{m-\frac{1}{2}j}^i(T_{mj}^{i+1}-T_{m-1j}^{i+1}+T_{mj}^i-T_{m-1j}^i+T_{mj}^{i-1}-T_{m-1j}^{i-1}) \\
&\quad + \frac{k_{mj}^i}{2m}(T_{m+1j}^{i+1}-T_{m-1j}^{i+1}+T_{m+1j}^i-T_{m-1j}^i+T_{m+1j}^{i-1}-T_{m-1j}^{i-1})\Big] \\
&\quad + \frac{1}{3(\Delta y)^2}\Big[k_{mj+\frac{1}{2}}^i(T_{mj+1}^{i+1}-T_{mj}^{i+1}+T_{mj+1}^i-T_{mj}^i+T_{mj+1}^{i-1}-T_{mj}^{i-1}) \\
&\quad + k_{mj-\frac{1}{2}}^i(T_{mj}^{i+1}-T_{mj-1}^{i+1}+T_{mj}^i-T_{mj-1}^i+T_{mj}^{i-1}-T_{mj-1}^{i-1})\Big] \tag{4.13}
\end{aligned}
$$

Taking the radial direction first, the two sweeps of the alternating direction implicit method are:

First sweep (in r direction):

$$
T_{m-1j}^{i+1*}\left[X\left(\frac{k_{mj}^i}{2m}-k_{m-\frac{1}{2}j}^i\right)\right] + T_{mj}^{i+1*}\left[C_{mj}^i+X(k_{m+\frac{1}{2}j}^i+k_{m-\frac{1}{2}j}^i)\right] - T_{m+1j}^{i+1*}\left[X\left(k_{m+\frac{1}{2}j}^i+\frac{k_{mj}^i}{2m}\right)\right]
$$

$$
\begin{aligned}
&= C_{mj}^i T_{mj}^{i-1} + X\Big[k_{m+\frac{1}{2}j}^i(T_{m+1j}^i-T_{mj}^i+T_{m+1j}^{i-1}-T_{mj}^{i-1})-k_{m-\frac{1}{2}j}^i(T_{mj}^i-T_{m-1j}^i+T_{mj}^{i-1}-T_{m-1j}^{i-1}) \\
&\quad + \frac{k_{mj}^i}{2m}(T_{m+1j}^i-T_{m-1j}^i+T_{m+1j}^{i-1}-T_{m-1j}^{i-1})\Big]
\end{aligned}
$$

$$
+ Y\left[k_{mj+\frac{1}{2}}^i(T_{mj+1}^i-T_{mj}^i+2T_{mj+1}^{i-1}-2T_{mj}^{i-1})-k_{mj-\frac{1}{2}}^i(T_{mj}^i-T_{mj-1}^i+2T_{mj}^{i-1}-2T_{mj-1}^{i-1})\right] \tag{4.14}
$$

Second sweep (in y direction):

$$-T_{mj-1}^{i+1}\left[Y\ k_{mj-\frac{1}{2}}^{i}\right] + T_{mj}^{i+1}\left[C_{mj}^{i}+Y(k_{mj+\frac{1}{2}}^{i}+k_{mj-\frac{1}{2}}^{i})\right] - T_{mj+1}^{i+1}\left[Y\ k_{mj+\frac{1}{2}}^{i}\right]$$

$$= C_{mj}^{i}T_{mj}^{i+1*} - Y\left[k_{mj+\frac{1}{2}}^{i}(T_{mj+1}^{i-1}-T_{mj}^{i-1})-k_{mj-\frac{1}{2}}^{i}(T_{mj}^{i-1}-T_{mj-1}^{i-1})\right] \quad (4.15)$$

where $X = \dfrac{2\Delta t}{3(\Delta r)^2}$, $Y = \dfrac{2\Delta t}{3(\Delta y)^2}$ and T^* are intermediate temperatures

calculated by the alternating direction scheme that have no physical significance.

Because of the symmetry only a quadrant of the axisymmetrical two-dimensional grid needs be considered, with a space grid of $(M+1)$ x $(J+1)$ nodes, where $M\Delta r = R$ and $J\Delta y = D_y/2$. The third kind of boundary condition is taken into account in a similar manner to that shown by Cleland & Earle (1977b) for slabs and Cleland & Earle (1979a) for radial geometry.

At the radial centre (m=0) the method of Albasiny (1960):

$$\lim_{r\to 0}\frac{1}{r}\frac{\partial T}{\partial r} \to \frac{\partial^2 T}{\partial r^2} \quad (4.16)$$

was used to avoid the singularity. The first sweep (Eq. (4.14)) becomes:

$$T_{m-1j}^{i+1*}\left[-2X\ k_{m+\frac{1}{2}j}^{i}\right] + T_{mj}^{i+1*}\left[C_{mj}^{i}+4X\ k_{m+\frac{1}{2}j}^{i}\right] - T_{m+1j}^{i+1*}\left[2X\ k_{m+\frac{1}{2}j}^{i}\right]$$

$$= C_{mj}^{i}T_{mj}^{i-1} + 2X\left[k_{m+\frac{1}{2}j}^{i}(T_{m+1j}^{i}-2T_{mj}^{i}+T_{m-1j}^{i}+T_{m+1j}^{i-1}-2T_{mj}^{i-1}+T_{m-1j}^{i-1})\right]$$

$$+ Y\left[k_{mj+\frac{1}{2}}^{i}(T_{mj+1}^{i}-T_{mj}^{i}+2T_{mj+1}^{i-1}-2T_{mj}^{i-1})-k_{mj-\frac{1}{2}}^{i}(T_{mj}^{i}-T_{mj-1}^{i}+2T_{mj}^{i-1}-2T_{mj-1}^{i-1})\right] \quad (4.17)$$

setting $k_{m-\frac{1}{2}j}^{i}=k_{m+\frac{1}{2}j}^{i}$ and $T_{m-1j}=T_{m+1j}$ at all time levels. The second sweep is unaltered from Eq. (4.15).

At the radial surface (m=M):

$$h(T_a-T_w) = k\ \frac{\partial T}{\partial r} \quad (4.18)$$

and the first sweep (Eq. (4.14)) becomes:

$$T_{m-1j}^{i+1*}\left[-X\ k_{m-\frac{1}{2}j}^{i}\right] + T_{mj}^{i+1*}\left[C_{mj}^{i}+X\left(k_{m-\frac{1}{2}j}^{i}+h\Delta r\right)\right]$$

$$= C_{mj}^{i}T_{mj}^{i-1} + X\left[k_{m-\frac{1}{2}j}^{i}\left(T_{m-1j}^{i}-T_{mj}^{i}+T_{m-1j}^{i-1}-T_{mj}^{i-1}\right)\right] + X\ h\Delta r\left(3T_a-T_{mj}^{i}-T_{mj}^{i-1}\right)$$

$$+ Y\left[k_{mj+\frac{1}{2}}^{i}\left(T_{mj+1}^{i}-T_{mj}^{i}+2T_{mj+1}^{i-1}-2T_{mj}^{i-1}\right)-k_{mj-\frac{1}{2}}^{i}\left(T_{mj}^{i}-T_{mj-1}^{i}+2T_{mj}^{i-1}-2T_{mj-1}^{i-1}\right)\right] \quad (4.19)$$

while the second sweep is unaltered from Eq. (4.15). For both sweeps the following corrections to the thermal conductivities along the surface must be made, due to the reduced area for conduction:

$$k_{mj\pm\frac{1}{2}}^{i} = \frac{M-\frac{1}{4}}{2M}\ k_{mj\pm\frac{1}{2}}^{i}. \quad \text{Also}\ k_{m-\frac{1}{2}j}^{i} = \frac{M-\frac{1}{2}}{M}\ k_{m+\frac{1}{2}j}^{i}\ \text{and}\ C_{mj}^{i} = \frac{M-\frac{1}{4}}{2M}\ C_{mj}^{i}.$$

At the surface in the y direction (j=J):

$$h\left(T_a-T_w\right) = k\ \frac{\partial T}{\partial y} \quad\quad\quad\quad\quad\quad\quad\quad\quad (4.20)$$

The first sweep is Eq. (4.14) and the second sweep is unaltered from Eq. (4.14) except for making $C_{mj}^{i}=C_{mj}^{i}/2$, $k_{m+\frac{1}{2}j}^{i}=k_{m+\frac{1}{2}j}^{i}/2$, $k_{m-\frac{1}{2}j}^{i}=k_{m-\frac{1}{2}j}^{i}/2$, because only half of the normal volume is associated with each surface node, and setting $k_{mj+\frac{1}{2}}^{i}=h\Delta y$ and $T_{mj+1}^{i+1}=T_{mj+1}^{i}=T_{mj+1}^{i-1}=T_a$.
At corners on the grid a combination of both of the appropriate changes to the scheme given above are used.

4.3.2 Computer Implementation and Testing

The finite cylinder finite difference program was checked against the known analytical solution for the third kind of boundary condition and constant thermal properties (Newman 1936). Table 4.5 shows that the agreement of temperatures for a 10x10 grid is good. Although no data for phase change in finite cylinders were available, freezing data for infinite slabs (Cleland & Earle 1977a) and infinite cylinders (Cleland & Earle 1979a) were used to test the program. Making either the cylinder length dimension (for infinite cylinders) or the radial dimension (for infinite slabs) very large in comparison with the other dimension, heat transfer in these extended directions becomes insignificant at the centre of the grid and the simpler geometry was closely approximated. The experimental infinite slab freezing data was predicted with a mean error of 0.8% and 95% confidence bounds of ±12.2% and the infinite cylinder experimental freezing data with a mean of

-3.6% and 95% bounds of ±9.6% using the thermal data given in Table 5.1. Individual predictions were identical to the results for the specialised slab and infinite cylinder finite difference programs using the same thermal data. It was concluded that this finite difference scheme for a finite cylinder was as accurate as equivalent schemes for other regular shapes.

In the above scheme it was chosen to do the first sweep in the radial direction. The alternative with the first sweep in the y direction was also derived. It has the same truncation errors as the scheme with the radial sweep first and was found to not give significantly different results over the range of problems and different cylinder radius to length ratios used. Consequently the first scheme was retained because the radial dimension is the more important in most problems, although both are equally appropriate.

The program includes the heat balance and temperature updating techniques discussed in Sec. 4.2.2 for finite element methods, in order to prevent oscillation and to detect latent heat peak "jumping" problems. To prevent oscillation during calculation of phase change for infinite cylinders Cleland & Earle (1979a) defined:

$$k^i_{mj} = \tfrac{1}{2}\left(k^i_{m+\frac{1}{2}j} + k^i_{m-\frac{1}{2}j}\right) \tag{4.21}$$

The same method was used in the finite cylinder program.

For eleven nodes in each direction and 1000 time steps a typical computation time for this scheme written in Fortran 77 was 250 sec. on a Prime 750 computer. By comparison, the full finite element formulation (Eqs. (4.2) to (4.5)), using the same grid size, gave computation times of about 1000 sec. for 1000 time steps.

Table 4.5 <u>Comparison of Results From the Finite Cylinder Finite Difference Method Program With a Known Analytical Solution[1] For Cooling of a Finite Cylinder Subject to the Third Kind of Boundary Condition</u>

D_r = 0.02 m, D_y = 0.02 m, k = 0.617 W m^{-1} °C^{-1}, C = 3.69 MJ m^{-3} °C^{-1}. An 11x11 node grid was used. Values of Y are tabulated.

Time (sec)	Edge of Finite Cylinder		Centre of Finite Cylinder	
	Analytical[1]	Numerical	Analytical[1]	Numerical
h = 30.0 W m^{-2} °C^{-1}				
100	0.625	0.624	0.936	0.934
300	0.398	0.397	0.626	0.625
500	0.260	0.259	0.409	0.407
700	0.169	0.169	0.266	0.265
900	0.110	0.110	0.174	0.173
h = 1000.0 W m^{-2} °C^{-1}				
15	0.038	0.037	0.959	1.000
45	0.012	0.014	0.904	0.934
75	0.007	0.006	0.718	0.741
105	0.004	0.004	0.524	0.541
135	0.003	0.003	0.370	0.383

[1] Newman (1936)

5   EXPERIMENTAL PROCEDURE AND DATA COLLECTION

5.1   EXPERIMENTAL ERROR

Whenever any freezing or thawing time prediction method is compared with experimental freezing and thawing data, some lack of agreement is inevitable. This imprecision may arise from one of three sources:

(a) uncertainty in thermal property data for the material being frozen or thawed (data error)

(b) imprecise knowledge and control of the freezing or thawing conditions (experimental error) and

(c) inaccuracy arising from assumptions or approximations made in the derivation of the prediction method (prediction method error).

Thermal property data uncertainty depends on the material used for the experiments and is discussed in Sec. 5.2. To assess in isolation as far as is possible the magnitude of the third source of inaccuracy, the aim of any experimental procedure or technique is to keep experimental errors randomly distributed and small in size.

The first of two sources of experimental error is the error arising from imperfect control of experimental conditions. Many variables are controlled to pre-set values. There is control error within each run as well as control problems in attaining the same pre-set value in all similar runs. The ability to reduce the control error can be measured from the variability of replicate runs for the same set of nominal experimental conditions.

Secondly, there is the error arising from imprecise knowledge of the experimental conditions. Having controlled the experimental conditions during each run the mean values must be measured. Uncertainty can arise as a difference between the measured value of a parameter and the unknown true value.   The uncertainty can be reduced by replicate determinations, but measurements are suspectible to systematic errors which replicate determinations will not discern.   Systematic error cannot be easily quantified and can only be minimised by ensuring that the measurement techniques used are valid and accurate.   Sources of systematic error include;   unwanted edge heat transfer, instrument

calibration errors and inhomogeneities in the phase change material due to the presence of air voids or thermocouple wire.

Cleland & Earle (1984a) discuss the different sources of error commonly encountered in phase change experimentation and give a check list that enables the most probable sources of differences between experiments and predictions other than the prediction method error to be assessed. Experimental data are most useful if systematic error is negligible compared with random errors, and the latter are minimised.

5.2   CHOICE OF PHASE CHANGE MATERIALS

The materials used for phase change experimentation must meet the conditions listed in Table 3.2, be cheap and easy to use, give reproducible results and should have accurately known thermal properties. Food materials are rarely homogeneous, each sample can only be used experimentally once or twice, and they tend to have a wide variation in composition. Consequently thermal property data are often imprecise. For these reasons analogues have commonly been used (Riedel 1960a, Lentz 1961, Frazerhurst et al 1972, Geuze et al 1972, Badari Narayana & Krishna Murthy 1975, Albin et al 1979). "Karlsruhe test substance" developed by Riedel (1960a) is probably the most successful and widely used (Fleming 1967, Bonacina & Comini 1971, Bonacina & Comini 1972, Bonacina et al 1974, Comini et al 1974a, Gorenflo & Mertz 1975, Cleland 1977, Hayakawa et al 1983b). Commonly known and referred to as "Tylose", it is a 23% methyl-cellulose gel. Tylose is easily moulded into different shapes and is homogeneous once equilibration has occurred. It can be used repetitively for experiments without deterioration, its density does not alter significantly as phase change occurs, and it has well characterised thermal properties similar to those of many high moisture foods (Cleland 1977). For these reasons most of the experimental work was done with Tylose. The particular Tylose used was MH1000, a product marketed in New Zealand by Hoechst New Zealand Limited.

On mixing of the powdered material with water, rapid hydration of the gel meant that initially it was non-homogeneous and some air entrainment occurred in the final moulds. The water content of the gel

equilibrated over a period of several days leading to a homogeneous material. Air pockets within the gel tended to be very small (less than 1 mm in diameter) and evenly distributed. By a visual examination of the final gel, the voids volume was estimated as less than 0.5%, whilst breaking the join of the Tylose with flat metal and plastic surfaces showed an almost complete and even contact. The possible effects on heat transfer of imperfect contact are discussed in Sec. 5.4.3. It would be expected that other reseachers using Tylose have had similar problems with air entrainment, yet no deviations from the reported thermal properties have been noted. Therefore it was considered that the uncertainty in thermal properties for Tylose was not significantly increased by the presence of the air bubbles.

Errors in measuring components led to a moisture content of 77.0 ± 0.2% in the gel. Direct measurement of the moisture in the gel after experimental work showed that except where liquid ingress occurred during freezing or thawing by liquid immersion (discussed in later sections for shapes where this was a problem), the final moisture was within 0.5% of the original value.

Cleland & Earle (1984a) give the thermal conductivity and apparent volumetric specific heat capacity versus temperature data for Tylose based on the data of Riedel (1960a) and Comini et al (1974a). Other versions of the thermal property data have been used. Cleland & Earle (1979b) used a "flattened" version which enabled substantial savings in computation times for numerical prediction methods, at a slight cost in terms of loss of accuracy as large time steps could be used without "jumping" of the latent heat peak. Cleland et al (1982) tested a hypothetical volumetric specific heat capacity curve which had some supercooling effects incorporated into it. The Tylose thermal property data used in Group II (numerical) methods in the present work are given in Table 5.1. Comparisons with the original data from Riedel (1960a) and data for minced lean beef are shown in Fig. 5.1 and 5.2. Values in Table 5.1 were chosen to be an accurate representation of Riedel's data, but the shape of the volumetric specific heat capacity curve was altered so that when incorporated into the finite difference method and finite element method programs, "jumping" of the latent heat peak was less likely and large time steps still gave good heat balances. Most

simple freezing and thawing time prediction methods need values of the
thermal property data for only the parts of the overall temperature
range where the change in thermal properties with temperature is small.
The thermal property data for Tylose used by Cleland (1977) were
adopted for Group I (simple) methods. These are given in Table 5.2 and
are consistent with Table 5.1.

To show whether experimental results obtained using Tylose were typical
of the freezing and thawing of real foods, experiments were also
conducted with minced lean beef.   Multiple fat   and   moisture
determinations gave the composition of the minced lean beef as 74.9±
1.9% water and 3.1± 1.1% fat. Meat as a material is less homogeneous
than Tylose, so published thermal property data vary significantly and
are not consistent with each other (Morley 1972). The thermal property
data used were derived from Riedel (1957), Morley (1972) and from the
composition factors of Comini et al (1974a) by Cleland & Earle (1982a).
These are shown in Tables 5.1 and 5.2 and Figs. 5.1 and 5.2. They are
probably less precise than the Tylose data.

5.3   TEMPERATURE MEASUREMENT AND CONTROL

All temperature measurements were made with 24 Standard Wire Gauge
(SWG) copper/constantan thermocouples (0.5 mm wire diameter, 0.9 mm
diameter including plastic insulation) connected to either a 12 point
Taylor Instruments "Multi-Scan Recorder" potentiometer operating on a
60 second print cycle or a 12 point   Honeywell-Brown   recording
potentiometer operating on a 100 second print cycle with an optional
intermittent 15 minute delay between cycles. Both of these machines
were calibrated with the above thermocouple wire to within 0.3°C in the
range -50°C to 50°C.

Prior to thawing or freezing the objects of Tylose or minced lean beef
were kept in temperature controlled rooms for long enough to attain a
uniform temperature throughout. To reduce the variation in initial
temperature during the time from removal of objects from the constant
temperature areas to the start of the freezing or thawing process, the
objects were insulated.   Except for the slab shapes where sheets of
0.05 m thick polystyrene foam board were used, the objects were wrapped

Table 5.1 Thermal Property Data Used In Calculations By Numerical Methods[1]

T (°C)	k (W m^{-1} °C^{-1})	T (°C)	C (MJ m^{-3} °C^{-1})	H[2] (MJ m^{-3})
		Tylose		
-40.0	1.67	-40.0	1.88	0.0
-30.0	1.67	-30.0	1.92	19.0
-20.0	1.66	-20.0	1.95	38.3
-15.0	1.64	-18.0	2.00	42.3
-10.0	1.63	-16.0	2.20	46.5
-9.0	1.61	-14.0	2.30	51.0
-8.0	1.60	-12.0	2.80	56.1
-7.0	1.58	-10.0	3.70	62.6
-6.0	1.56	-9.0	4.20	66.6
-5.0	1.52	-8.0	5.00	71.2
-4.0	1.46	-7.0	5.90	76.6
-3.0	1.35	-6.0	7.20	83.2
-2.5	1.28	-5.0	11.00	92.3
-2.0	1.18	-4.0	17.00	106.3
-1.5	1.04	-3.0	25.00	127.3
-1.0	0.82	-2.5	33.00	141.8
-0.8	0.66	-2.0	45.00	161.3
-0.7	0.55	-1.5	70.00	190.1
-0.6	0.49	-1.3	100.00	207.1
0.0	0.49	-0.6	100.00	277.1
20.0	0.56	-0.5	19.93	283.1
40.0	0.62	0.0	3.71	289.0
100.0	0.62	100.0	3.71	660.0
		Minced Lean Beef		
-40.0	1.58	-40.0	1.89	0.0
-24.0	1.53	-30.0	1.91	19.0
-12.0	1.48	-25.0	2.02	28.8
-8.0	1.40	-20.0	2.70	40.6
-4.0	1.28	-15.0	3.58	56.3
-2.0	0.98	-10.0	4.55	76.7
-1.0	0.48	-8.0	5.26	86.5
0.0	0.49	-6.0	7.71	99.4
100.0	0.50	-5.0	10.40	108.5
		-4.0	15.70	121.5
		-3.0	31.20	145.0
		-2.0	53.10	187.1
		-1.5	73.70	218.8
		-1.3	255.00	251.7
		-1.2	255.00	277.2
		-1.0	3.65	303.1
		100.0	3.65	671.7

[1] Linear interpolation was used.

[2] Datum: H = 0.0 at -40.0°C.

Table 5.2 <u>Thermal Property Data Used In Calculations By Simple Formulae</u>

Property		Tylose	Minced Lean Beef
k_s	$(W\ m^{-1}\ °C^{-1})$	1.65	1.55
k_l	$(W\ m^{-1}\ °C^{-1})$	0.55	0.50
C_s	$(MJ\ m^{-3}\ °C^{-1})$	1.90	1.90
C_l	$(MJ\ m^{-3}\ °C^{-1})$	3.71	3.65
L	$(MJ\ m^{-3})$	209.0	209.0
ΔH	$(MJ\ m^{-3})$	226.0	230.0
T_{if}	$(°C)$	-0.6	-1.0
T_{ifave}	$(°C)$	-2.1	-2.5
k_{ave}	$(W\ m^{-1}\ °C^{-1})$	1.2_f	
		1.0_t	

[1] ΔH = enthalpy difference between 0 °C and -10 °C, k_{ave} = average thermal conductivity during the phase change process, T_{ifave} = mean freezing or thawing temperature.
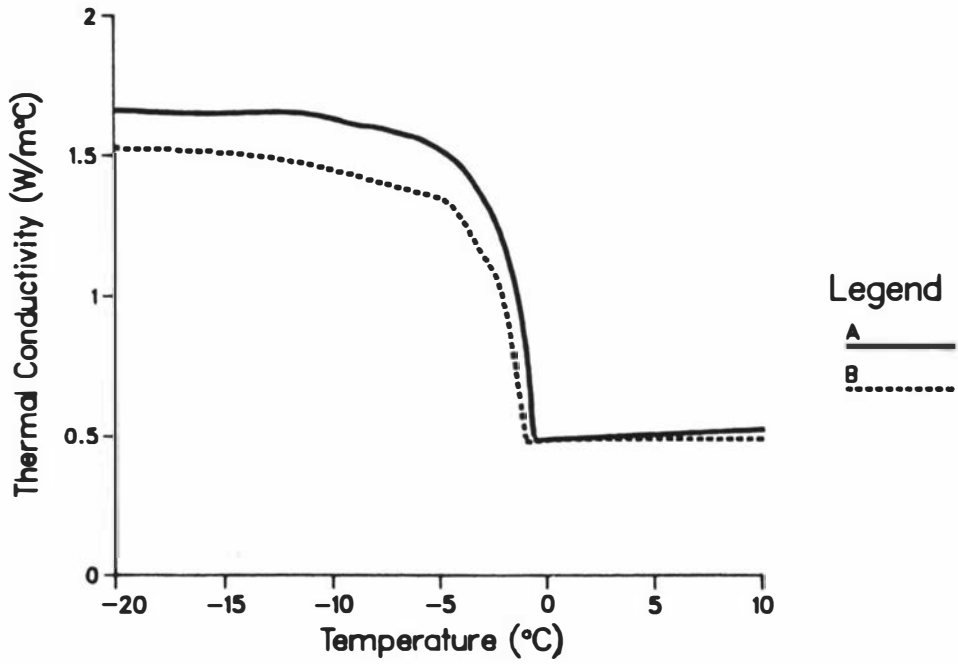
Fig. 5.1 Thermal Conductivity Data For Tylose (A) and Minced Lean
        Beef(B).
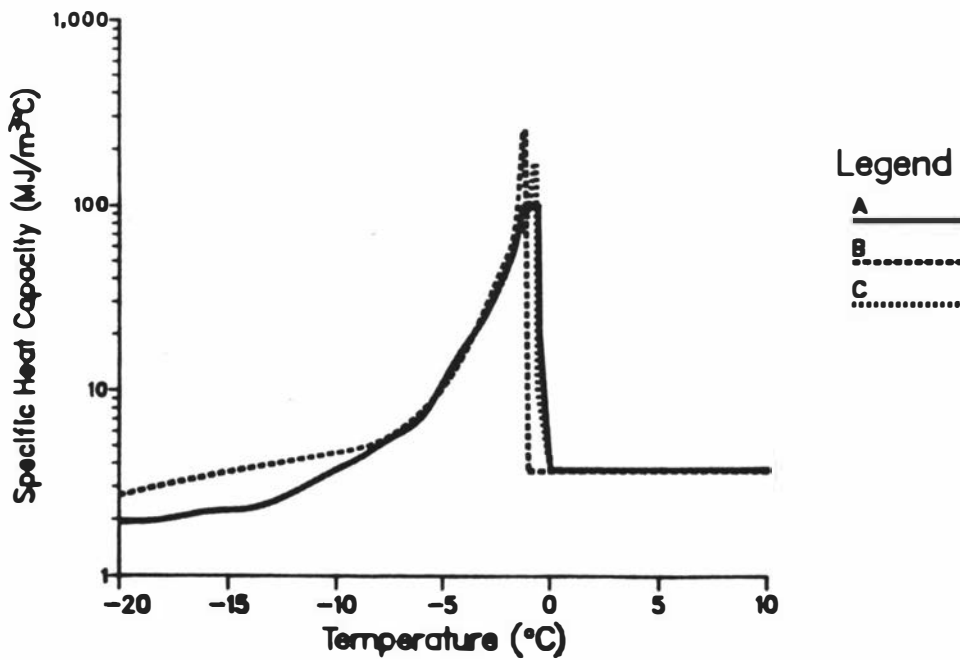
Fig. 5.2 Apparent Volumetric Specific Heat Capacity Data For Tylose
        (A, C) and Minced Lean Beef (B).
        A, B - data from Table 5.1, C - data from Riedel (1960a).

in insulation material and transported in containers lined with 0.02 m
thick polystyrene foam. Though the delays were as long as 10 minutes,
using this method the maximum measured difference in the initial
temperature of the objects from the mean value was found to be 2.0°C.
For slabs, because the insulation could be applied and held more
directly onto the surfaces, the temperature variations were only ±0.5°C
about the mean value.

For variations in temperature of up to 10°C on either side of a mean
initial temperature the difference in predicted freezing time for slabs
was found to be less than 0.5% (Cleland 1977). Whilst this analysis
was carried out using finite difference simulation very similar results
would be expected if an experimental investigation was carried out, as
finite differences provide a sufficiently accurate simulation of the
freezing process. Errors of similar magnitude would be expected for
shapes other than slabs. For thawing the error due to initial
temperature non-uniformity would be expected to be smaller because the
enthalpy change for a 1°C variation in initial temperature is a lower
percentage of the total enthalpy change, compared with that for a 1°C
variation in initial temperature in freezing. The need to use a mean
initial temperature to represent a non-uniform initial temperature
therefore introduced negligible error.

The ambient heating or cooling medium was either water or 29% calcium
chloride brine held in a 1 m^3 insulated tank (Fig. 5.8). The medium
temperature was measured by two thermocouples; one prior to and one
after the experimental section. External circulation of the medium was
used for slab thawing experiments, in which case an additional
thermocouple was located in the return stream to the tank. In all
experiments there was no measurable difference in temperature between
the thermocouples because the circulation rate of the medium within the
piping and around the tank was sufficiently high.

The tank temperature was controlled by a RKC PN-41 "Blind Controller"
activating both refrigeration and heating systems. The thermal
capacity of the tank contents was large compared with the heat loss or
gain from the environment and from the object being frozen or thawed.

This meant that the medium temperature would change only slowly with time if left uncontrolled during the experiment. The control system was sufficiently precise that no variation of the temperature during experiments was detectable with the recorders used.

Taking recorder calibration error into account, the overall error in temperature measurement and control was estimated at less than ±0.5°C.

5.4 THAWING OF SLABS

5.4.1 The Equipment

One-dimensional heat transfer in an infinite slab undergoing freezing can be approximated by an insulated finite-sized slab in a plate freezer (Cleland 1977). A similar arrangement shown in Fig. 5.3 was used for thawing of slabs. Two plates were heated in series by water pumped at a rate of approximately 1 kg s^{-1} from the well mixed temperature controlled tank (Fig. 5.8). Any thickness of slab could be accommodated. Thermal contact between the slab surface and the plates was kept the same for all experimental runs by compressing the plates with pressure provided by 100 kg of weight over the plate area of 0.16 m^2.

For each slab thickness a mould was made by cutting a 0.22 m diameter hole in the centre of a 0.4 m x 0.4 m piece of polystyrene foam board of the appropriate thickness. Two sheets of aluminium foil with one of brown paper between were used to cover one side of the mould, and then it was filled with Tylose or minced lean beef from the opposite side taking care to avoid air entrainment. Copper/constantan thermocouples were inserted, two at different positions on each surface, and three at different positions at the centre thickness of the slab. All thermocouples were run through isothermal regions (parallel to the slab surfaces). Junctions were located near the middle of the 0.22 m diameter material section to minimise errors due to heat conduction along the wires and edge heat transfer effects. Two layers of aluminium foil with one of brown paper between were then fixed to the upper face to give a filled mould as shown in Fig. 5.4. The wrapping added a small heat transfer resistance but prevented dehydration of the

surface of the material. The brown paper, placed between the two
layers of aluminium foil so that it remained dry, provided structural
strength to the wrapping. The material was filled slightly above the
level of the polystyrene insulation to ensure the insulation would not
hinder contact between the plates and the surface of the slab.

5.4.2 Thickness Control and Measurement

The slab thickness was measured after equilibration over several days,
in both the frozen and unfrozen states. Prior to thawing experiments
the slabs were frozen in a plate freezer to ensure a flat surface for
good contact with the thawing plates, even when solid and inflexible,
and to give the required thickness. The thickness of the Tylose slabs
was found to vary by up to 0.5 mm across each slab. There was no
difference between the frozen and unfrozen measurements for Tylose as
the density did not change appreciably. Though the density change for
minced lean beef is of the order of 4% some of the variation in volume
caused the polystyrene surrounding the slab to compress and did not
affect the thickness to this full extent. The values taken in the
frozen and unfrozen states were found to differ by less than 0.5 mm
from the mean for meat. As the smallest slab thickness with minced
lean beef was 0.024 m the error associated with this measurement is
less than 2%. Because all thermocouples were placed towards the centre
of the 0.22 m diameter slab to avoid edge effects in heat transfer,
more emphasis was put on thickness measurements in this region.

5.4.3 Measurement and Control of Surface Heat Transfer Coefficients

In the plate thawing system used the resistance to heat transfer
between the slab surface and the heating medium was small, there were
no significant radiation or mass transfer effects, and so the boundary
condition was adequately described by the third kind of boundary
condition. To alter the surface heat transfer coefficient (h) varying
numbers (0 to 10) of 1.5 mm thick, black "Insertion" rubber sheets were
placed on either side of the test slab between the plates shown in
Fig. 5.3. Different surface heat transfer coefficients were obtained
by altering the number of sheets of rubber.

Four methods were used to measure h: (a) a finite difference approximation method, (b) a heat balance method, (c) the Goodman plot and (d) an analytical method. Details of the first three of these are given by Cleland & Earle (1976a). Because surface temperature is most sensitive to changes in the surface heat transfer coefficient (Comini 1972), these three methods are based on measurement of slab surface temperature as it varies with time. The fourth method used the analytical solution for heat conduction subject to the third boundary condition, for constant thermal properties where there is no change of phase (Carslaw & Jaeger 1959). The procedure involved calculating values of the surface heat transfer coefficient that fitted experimental values of the surface temperature as it changed with time.

The thermal diffusivity of frozen material (α_s) is high so the preheating time prior to phase change occurring during a thawing run is too short to obtain accurate estimation of h by two of the four methods. Also the majority of the heat transfer during thawing will be with the surface of the slab thawed. In the short time the slab surface was still frozen the rigid nature of the slab may have resulted in imperfect contact with the plate surfaces giving effectively lower surface heat transfer coefficients. For these reasons, separate experiments conducted at temperatures greater than the initial freezing point of Tylose were used to determine the surface heat transfer coefficient rather than relying on preheating data. Above 0 °C thermal properties can be considered constant and all four methods could be applied equally well.

A total of 33 runs using a variety of Tylose slab thicknesses, and ambient and initial temperatures were used to determine h. If each of the rubber sheets was incompressible and provided equal resistance to heat transfer a linear variation of the resistance to heat transfer (1/h) with the number of rubber sheets should occur (Cowell & Namor 1974). The maximum number of rubber sheets used was ten and the plate to plate pressure was kept constant at a low value, so it is unlikely that significant variation in resistance either between the sheets or due to the compression of the rubber occurred. The heat capacity of the rubber itself may also affect experiments. By preheating the rubber on the plates the amount of heat transfer required to change the

rubber temperature was kept minimal compared with that needed to heat the actual slab material in both thawing experiments and runs to determine h. If the heating of the rubber was significant, the estimated h values would be lower than those actually occurring and would appear to vary with time. The later trend was not apparent for any of the methods so this effect was considered negligible.

There was no significant differences between values of h calculated from the four methods at the 95% level of confidence. Also the difference in values was insignificant comparing experiments where the slabs were cooled with those where they were heated. There was no correlation of h with the slab thickneses or the ambient and initial temperatures that were used in these runs. Figure 5.5 gives the least squares regression line relating external heat transfer resistance (1/h) to the number of sheets of rubber. Variation in the individually measured h values showed that the error in the average estimates of h for particular numbers of rubber sheets was ±2.2%.

Because of the preparation of slabs by pre-freezing and the use of a constant pressure, the variation in surface heat transfer coefficient between regions on the surface of the slab was considered negligible. Evidence to this effect was found from replicate surface thermocouples. Variation in recorded temperature was less than 1.0°C in any thawing run.

It is possible that surface heat transfer coefficients determined from the separate experiments are not representative of h during thawing runs. However the heat transfer conditions during the separate experiments were similar to those during each thawing run, except for the initial stages in the thawing runs where the slab surface was still frozen. The slabs were initially frozen in a plate freezer and the rubber sheets mounted between the plates and the slab itself had some flexibility. Therefore the contact between the plates and the slab surface was considered constant throughout the thawing experimental runs. Further, predictions of surface temperature by numerical methods were as good initially as they were later in the experimental runs. This confirms that these estimates of h were representative of the actual values throughout thawing. Using a number of separate runs
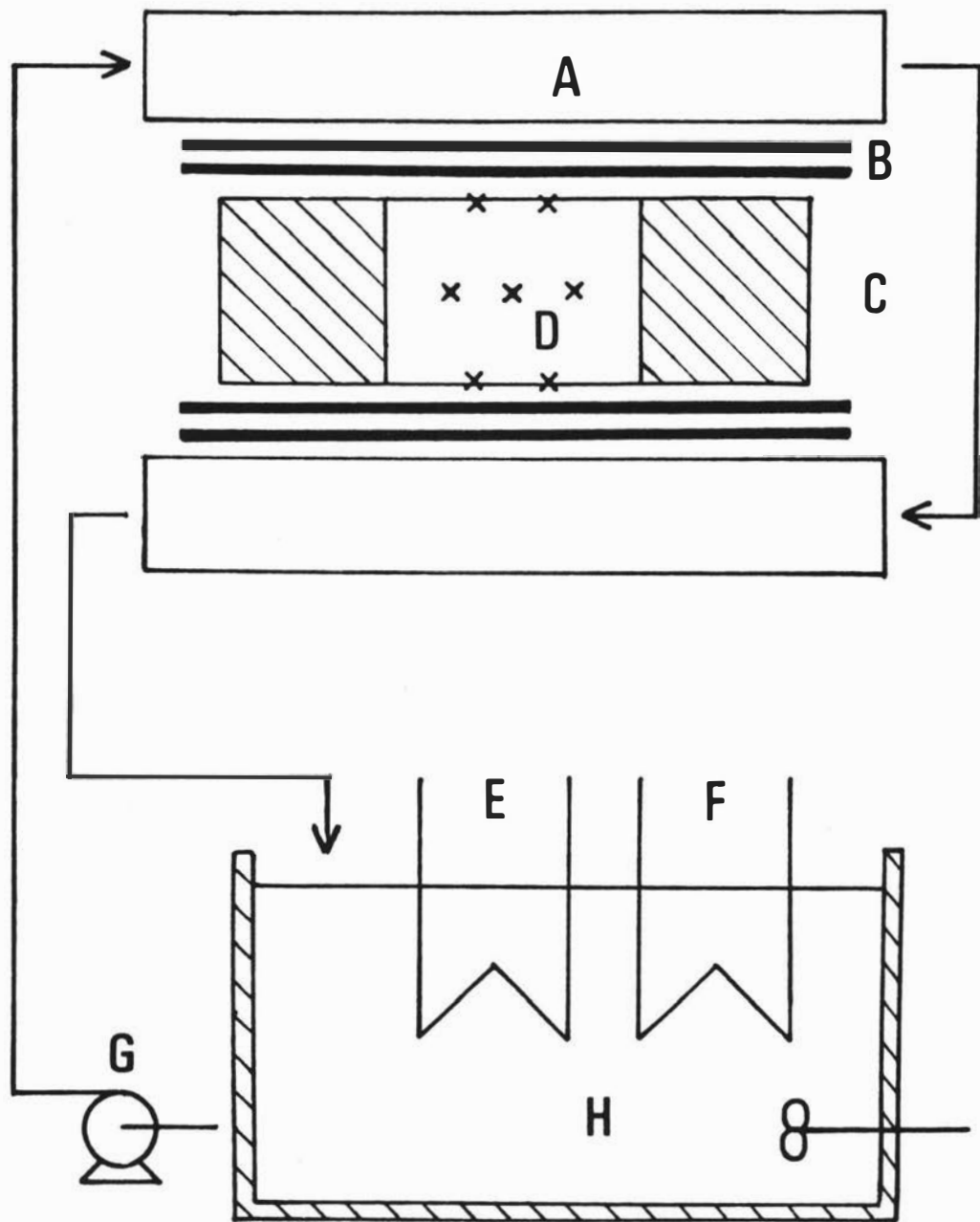
Fig. 5.3 Schematic Diagram of the Experimental Slab Thawing Equipment.
Not to scale. A - heating plates, B - rubber sheets, C -
insulated test slab, D - thermocouples, E - cooling plates, F
- heating elements, G - circulation pump, H - insulated,
agitated, temperature controlled tank.
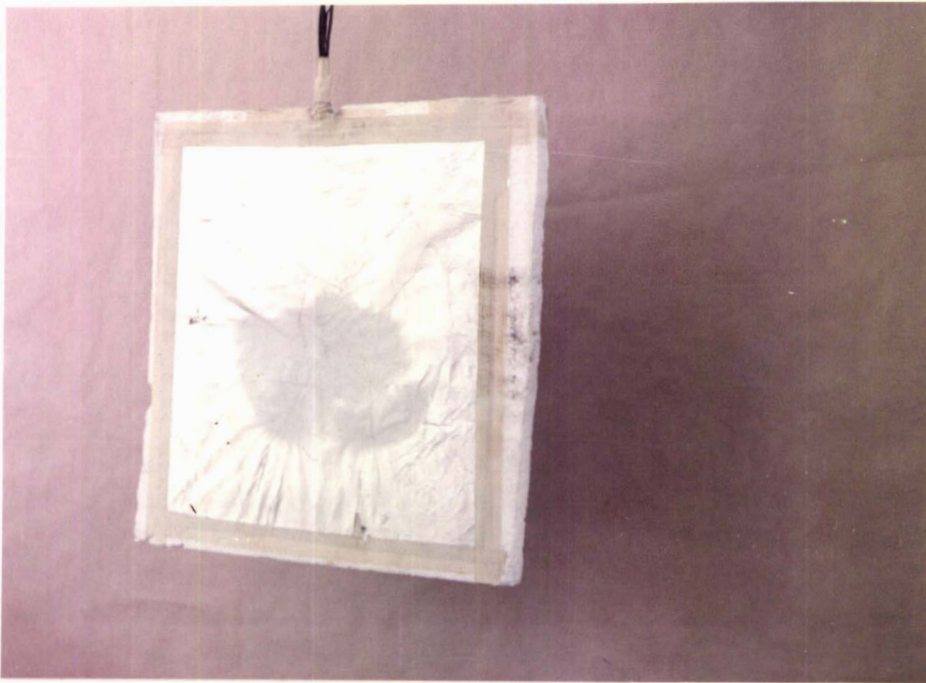
a

b

Fig. 5.4 Construction of Test Slabs.

     (a) a completed slab

     (b) a slab with insulation removed.
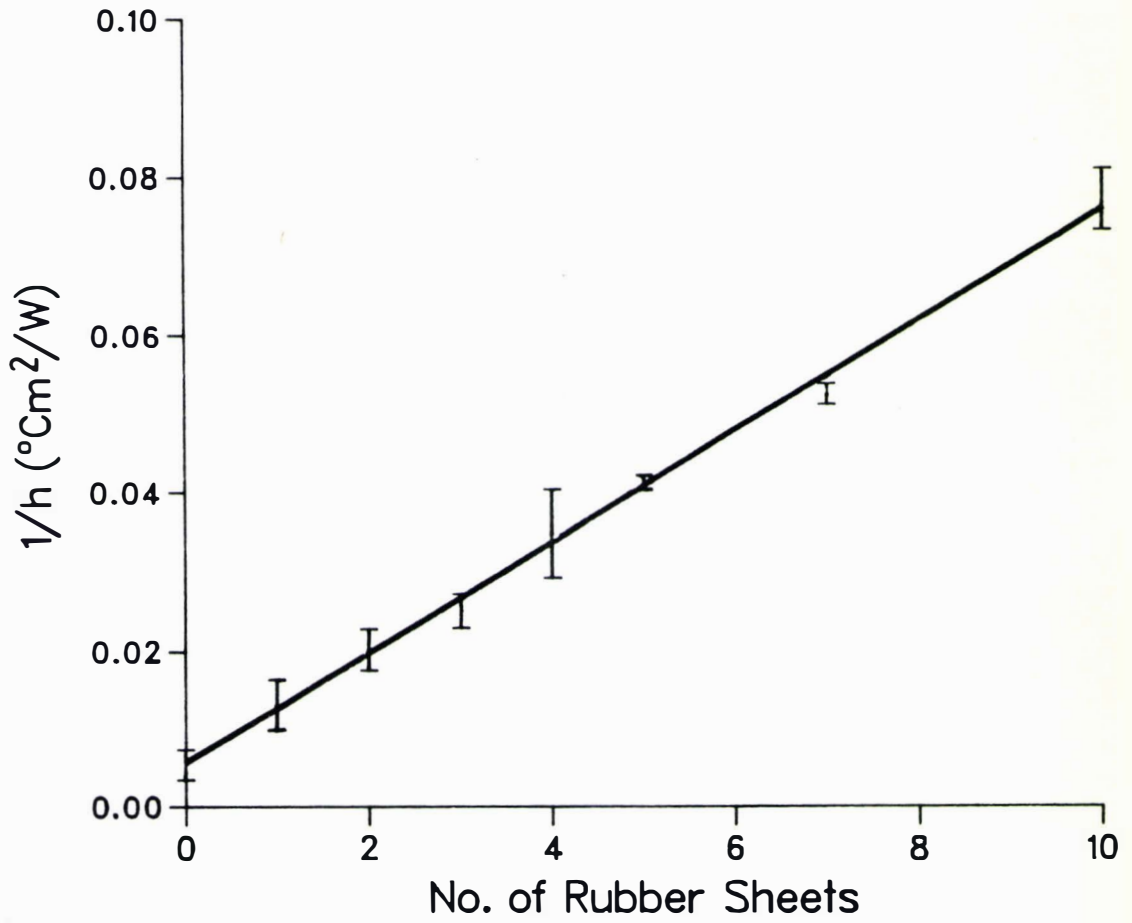
Fig. 5.5 Prediction of Surface Heat Transfer Coefficients For Slab
Thawing Experiments.

meant that h was determined accurately, yet as independently as possible of the thawing time experiments.

To confirm that h values estimated in the separate experiments were representative of values during thawing, some analysis during actual thawing runs was done using all the methods discussed previously. There was no difference in these results compared with the separate experiments.

For the thawing of the minced lean beef slabs the surface heat transfer was assumed to be the same as for the Tylose slabs. There was no reason to suspect that h would be different because most of the resistance to heat transfer was supplied by the rubber sheets, the same slab construction was used and the weighting of the slabs ensured good thermal contact for both materials.

5.4.4 Analysis of Heat Transfer in Slabs

In a true one-dimensional slab there is no heat transfer in the other two dimensions. In practice this is impossible to achieve. To reduce heat transfer in the other two directions three techniques were employed:

(a) the other two dimensions were made larger than the slab thickness, which is the critical dimension by at least a factor of 2.1:1

(b) each slab was surrounded on the edges by at least 0.09m of polystyrene foam insulation, and

(c) the thermocouples were placed near the centre of each 0.22m diameter slab.

For the worst case of a large slab being thawed slowly the effect of edge effects due to heat transfer through the insulation are shown by the analysis in App. B to decrease thawing time by 4.6%. This analysis took the most pessimistic view of the situation. For a more typical case the effect of edge heat transfer on thawing times was less than 1.0%. The slow nature of thawing means that edge heat transfer cannot be avoided, so when data are interpreted it must be remembered that some experiments with slabs were not truly one-dimensional. In only 6 out of 35 slab experiments was the effect on thawing times of heat transfer through the edges, found to be more than 1.0%.

Air entrainment and the resultant less than perfect thermal contact were mentioned in Sec. 5.2. The latter problem did not occur in experimental work with slabs because the weighting of the plates to hold the slabs tightly in place ensured good contact. Pre-freezing the slabs in a plate freezer meant that the protective layer of aluminium foil was always tightly and completely bound to the frozen material. Because air voids in the Tylose gel were small and uniformly distributed their effect is only important if they affect the overall heat transfer behaviour of a slab. Good prediction of experimental surface and centre temperature profiles were obtained by numerical methods for freezing (Cleland & Earle 1977b) and for thawing (Sec. 7.2). These results indicate that thermal properties used were representative of the Tylose material including voids, thus implying that the effect of the voids is negligibly small.

There are also errors consequent on the thermocouple placement within each slab. All thermocouples were inserted parallel to the heat transfer surface through supposedly isothermal regions. Therefore, the only temperature gradient for conduction along the thermocouple wires was due to heat transfer from edge effects, which has been shown above to be generally small. Also the wire cross-sectional area is less than 0.1% of the area available for heat transfer due to side effects, so overall the effect of the conduction along the wires was insignificant.

Of the total area normal to the direction of heat flow at each surface, and at the centre, only 0.5% to 1.0% was covered by thermocouple wire and their plastic insulation. As the greater resistance to heat transfer provided by the plastic insulation against that of Tylose only applies for this limited area the thermocouples did not affect heat flow significantly. The thermocouple leads occupied less than 0.05% of the gel volume so the heat capacity of the slab was not significantly affected by their presence.

Temperature measurements were taken at the two most important places; the surface and the centre of the slabs. The former is sensitive to changes in the external heat transfer conditions and so was used in estimation of the surface heat transfer coefficient. The latter was needed to measure the thawing time. Accurate placement of the

thermocouples at the surface and centre while making the slabs is difficult and migration of the thermocouples within the gel after construction is possible. For these reasons more than one thermocouple was used to measure each temperature.

It was impossible for a thermocouple to be above the slab surface because of the plate configuration. Provided heat transfer is homogeneous across the surface, the fastest heating thermocouple will be the best estimate of the surface temperature. A true estimate of surface temperature would be given by a thermocouple just touching the layer of aluminium foil, so any slower heating thermocouple is likely to be below the surface. However in thawing there is no definitive criterion to distinguish between differences in temperature due to inhomogeneity and those due to thermocouple placement, such as the supercooling behaviour observed in freezing by Cleland (1977). The only other criterion that can be used is whether the surface temperature profiles flatten noticably (plateau) in the latent heat temperature range or not. Because the surface is the first region to thaw and the temperature change can not be slowed by the presence of latent heat addition in regions outside the surface, any thermocouples right at the surface will tend to "slide" through the latent heat temperature range rather than show the typical plateau effect characterised by more central positions. Unfortunately, the speed that the surface temperature passes through this temperature range is dependent on the overall rate of heat transfer. As ambient temperatures close to the thawing temperatures were often used it was difficult to find a clear distinction between good and bad thermocouple positioning. For other ambient conditions some differentiation could be made. Figure 5.6 shows typical temperature profiles for different thermocouples near the surface. Curve A is typical of a well placed surface thermocouple. Its profile is barely affected by latent heat release in the thawing temperature range, but has a plateau at a temperature between this and the ambient temperature. Curve B is for a less precisely positioned thermocouple. The temperature profile flattens considerably due to latent heat before rising because the thermocouple is below the surface. Curve C is for the very bad case where the thermocouple is well below the surface and the rate of temperature change with time is slowed markedly by the absorption of

latent heat.

Clearly, this criterion does not completely distinguish between good and bad surface thermocouple placements, especially where overall rates of heat transfer are low. After deleting obvious badly placed thermocouples it was found that individual thermocouples gave measurements of the surface temperature of the slab that varied by less than 1.0°C around their mean value. Typically one or two out of four surface thermocouples were found to be poorly placed and were not used. After experimentation placement was checked by dismantling the slabs. The observed thermocouple positions compared well with those suggested by the above analysis and in all cases at least one thermocouple was well placed.

Heat transfer conditions on both faces of the slab were as equivalent as possible so the geometric and thermodynamic centres should coincide. Any thermocouple not exactly at the centre will change in temperature more quickly than one at the centre. Provided heat transfer is homogeneous across the slab surface and within the slab, the last thermocouple to reach 0°C will give the best estimate of the slab centre temperature and the most accurate estimate of the thawing time.

When food thaws most of the latent heat is absorbed at temperatures just below the initial freezing temperature (T_{if}). An abrupt change in thermal properties occur at T_{if}, resulting in a sudden increase in temperature. Consider a slightly misplaced centre thermocouple. Thawing will not be completed throughout the slab when this thermocouple reaches T_{if}. Hence a rapid change in the temperature will not occur as heat transfer is still required to supply latent heat to more central regions. The measured temperature tends to remain relatively constant at some temperature just above T_{if} depending on how far it is from the centre. When the last regions of the object thaw, all the temperatures (even at the surface though the effect there is less apparent) undergo a second increase in rate of temperature change with time. This is because heat transfer is now required only for sensible heating. The further from the centre the smaller this second "break" in the temperature profile will be. A similar effect occurs in freezing but is less noticable because the change from latent heat to

sensible heat absorption is less distinct than that in thawing.   James et al (1976) used this principle to predict phase change times by only measuring surface temperature. It can also be used to improve the estimate of thawing times from thermocouples not placed accurately at the centre. Where the slowest heating thermocouple did not "break" away from the latent heat temperature range and immediately head asymptotically for the ambient temperature, this method was used to estimate the thawing time.   Tangential extensions to the temperature profile immediately prior to and immediately after the second "break" point were drawn and the thawing time taken at the time indicated by their intersection as shown in Fig. 5.7.

The error in estimating the thawing time by this breakpoint analysis was investigated in two ways. Firstly, using experimental data where one well placed centre thermocouple could be compared with another centre thermocouple in the same slab. The time predicted using this analysis on the second thermocouple was compared with the time for the well placed thermocouple to reach 0°C.   In all cases studied the difference was less than 0.5% of the total time although the exact distance the second thermocouple was from the actual thermodynamic centre was unknown (dismantling of the slabs showed that all centre thermocouples were within 5% of the total thickness from the geometric centre of the slab). Secondly, finite element and finite difference methods were used so the effect of the error in the position of the thermocouples could be studied quantitatively.   The same effect was shown.   Using this method the predicted freezing times for a thermocouple displaced 10% of the distance from the centre to the surface were within 0.5% of the true values of 0°C at the thermodynamic centre for the wide range of conditions studied. The effect of centre temperature thermocouple placement was therefore not significant in estimates of thawing time but must be considered when comparing predicted temperture profiles. Only experimental runs that had good centre and surface thermocouple positioning were used for temperature profile comparison.

For objects with more than one dimension this same breakpoint analysis will also apply.   In fact, because for these objects less than 5% of the volume is enclosed within a distance 5% from the thermodynamic
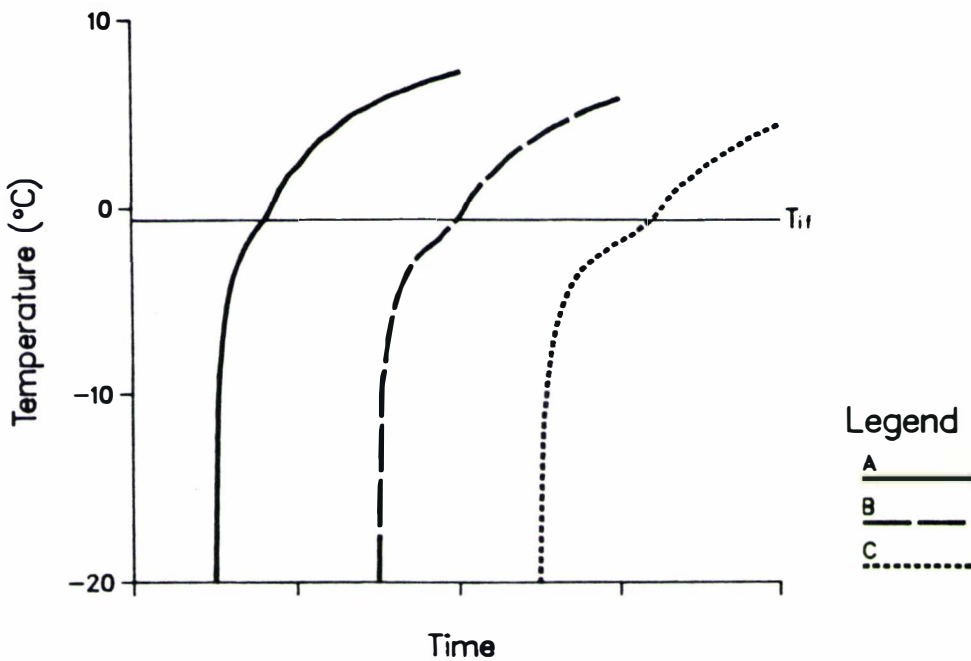
Fig. 5.6 Typical Temperature Profiles For Thermocouples Positioned At
Or Near the Surface of a Thawing Slab. A - at the surface, B
- 0.0025 m below the surface, C - 0.005 m below the surface.
$D = 0.1$ m, $h = 50.0$ W m^{-2} °C^{-1}, $T_a = 13.0$ °C, $T_{in} = -20.0$ °C,
$T_{if} = -0.6$ °C.
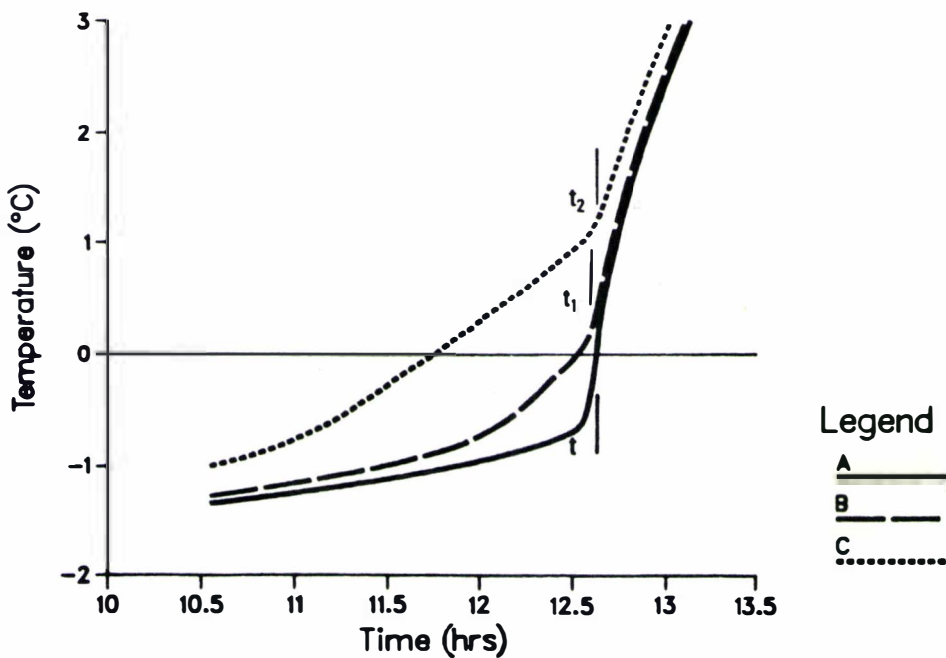
Fig. 5.7 Breakpoint Analysis to Estimate Thawing Times From
Thermocouples Not Positioned Exactly at the Thermodynamic
Centre. A - a thermocouple at the thermodynamic centre, B - a
thermocouple 0.005 m from the thermodynamic centre, C - a
thermocouple 0.01 m from the thermodynamic centre. $D = 0.1$ m,
$h = 50.0$ W m^{-2} °C^{-1}, $T_a = 13.0$ °C, $T_{in} = -20.0$ °C, $T_{if} = -0.6$ °C,
t = estimated thawing time from A, t_1 = estimated thawing
time from B, t_2 = estimated thawing time from C.

centre the break effect will be magnified. Cleland (1977) showed that a thermocouple placed 10% of a spheres radius in error, the measured freezing time would be 0.6% in error even if the above analysis was not used. Any error in placement of the centre thermocouple was highly damped in its effect on freezing time, and did not significantly increase the overall error. For slab thawing, the error for a 10% displacement was found to increase as (T_a-T_{if}) increased but by using the breakpoint method of analysis was only 0.1% for T_a=13°C. The breakpoint analysis was therefore used for all shapes investigated where centre thermocouples were shown to be not accurately placed at the thermodynamic centre.

An estimate of the experimental error arising from imprecise control of experimental conditions for the slab experiments was determined from replicate thawing runs. As far as possible, the replicates were independent of each other including the construction of new slabs for each run. After normalisation of the replicates the variability showed that the experimental error arising from poor control corresponded to 95% confidence bounds of ±5.2%. The total experimental error will be higher than this due to uncertainty in measurement of the experimental conditions and sources of systematic error.

5.5   THAWING OF INFINITE CYLINDERS

5.5.1   The Equipment

To obtain uniform heat transfer conditions at the surface for shapes other than slabs a liquid immersion thawing system was used. Liquid immersion gives much less variation of the surface heat transfer coefficient and ambient temperature around an object than the air thawing system which is also commonly used. A schematic diagram of the liquid immersion tank is shown in Fig. 5.8.

The impeller circulated the thawing medium, water, around the 2.1 m x 0.7 m x 0.7 m insulated tank. The liquid passed over refrigeration plates and then heating elements before flowing through the experimental section (0.8 m x 0.5 m x 0.7 m) and back to the impeller. Two mesh screens (aperature size 1 mm x 1 mm) provided

sufficient head loss to equalise any unevenness in the liquid flow. The circulation was sufficiently high that the tank acts as if it was a perfectly mixed system.   The temperature was controlled to within ±0.3°C in the range 0°C to 50°C for thawing experiments (Sec. 5.3).

Though the variation in surface heat transfer conditions should be small in the liquid system, the test samples were oscillated throughout the experiments to ensure that object orientation within the flow stream did not affect uniformity of surface conditions.   The objects were turned through an angle of 300° every 30 seconds. The sample oscillator is shown in Figs. 5.9, 5.10 and 5.12.

In order to approximate infinitely long cylinders, five different lengths of cylindrical pipe 0.45 m to 0.50 m long were used. Steel pipes of 0.1 m and 0.15 m nominal diameter and polyvinyl chloride (PVC) plastic pipes of 0.05 m, 0.1 m and 0.15 m nominal diameter gave different heat transfer resistances due to the different wall materials and thicknesses.

The cylinders were packed with Tylose and thermocouples introduced at the centre and surface positions from each end through isothermal regions. Two thermocouples at the centre and four at the surface were used for each cylinder.   To reduce end heat transfer effects, polystyrene foam insulation caps of at least 0.05 m thickness were put on the end of each cylinder and the cylinder clamped in the sample holder for oscillation as shown in Figs. 5.9, 5.10 and 5.11.   The thermocouple entry points and the polystyrene caps were sealed to prevent liquid contact with the Tylose.

5.5.2 Diameter Control and Measurement

There was no significant difference in diameter measurements between the frozen and unfrozen states for the cylinders. Any density change that occurred has a longitudinal effect that was absorbed by compression of the polystyrene foam caps. The diameter was measured to an accuracy of ±0.5 mm.
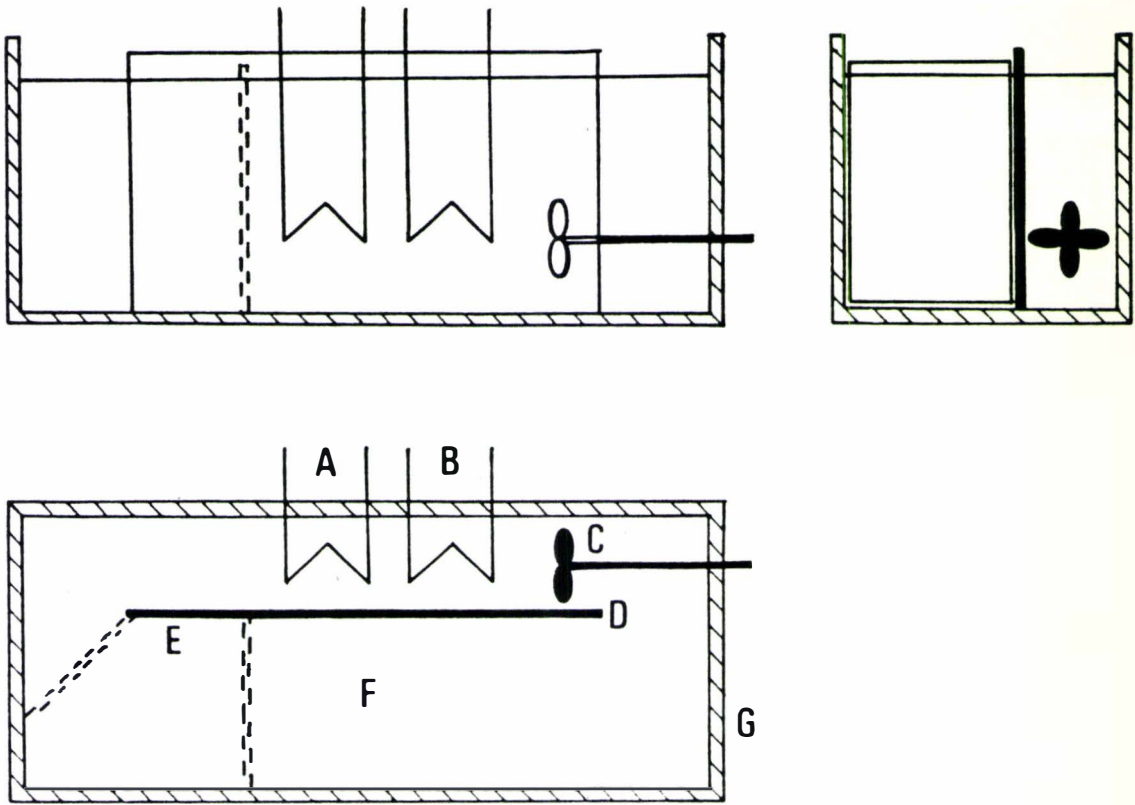
Fig. 5.8 Schematic Diagram of the Liquid Immersion Tank. Approximate scale 1:15. A - heating elements, B - cooling plates, C - impellor for circulation, D - baffle plate, E - mesh screens, F - experimental section, G - insulated tank.
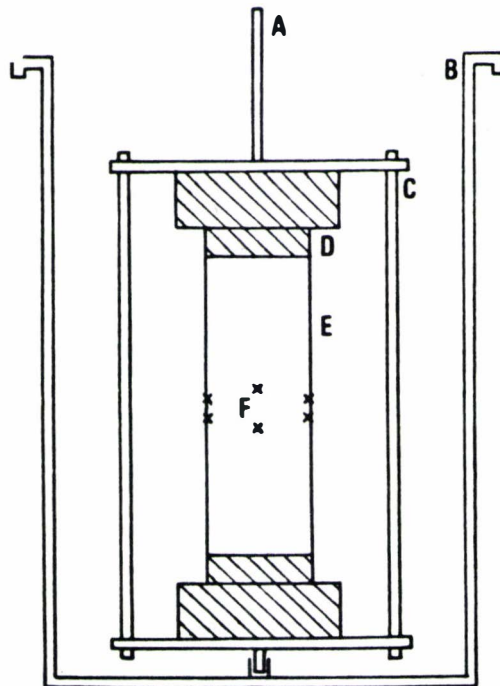
Fig. 5.9 Schematic Diagram of the System Used To Hold and Oscillate the Infinite Cylinders and Two-Dimensional Irregular Shapes in the Liquid Immersion Tank. Approximate scale 1:5.
A - attachment to the sample oscillator, B - stand attached to the immersion tank, C - clamp to hold the test object, D - insulated caps, E - the test object, F - thermocouples.
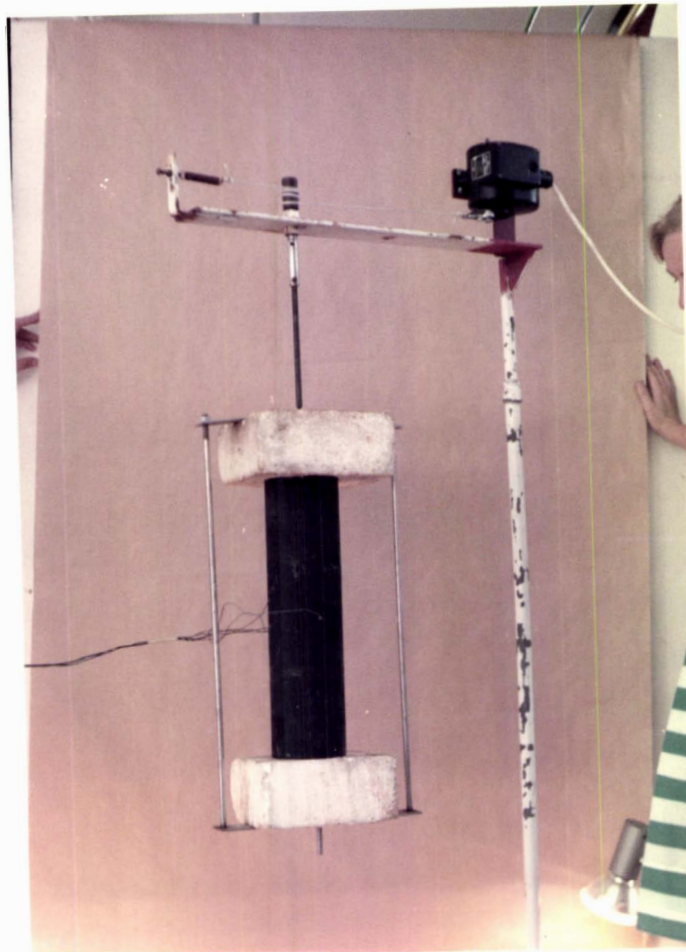
Fig. 5.10 The Sample Oscillator and Infinite Cylinder Thawing Equipment
Used in the Liquid Immersion Tank.
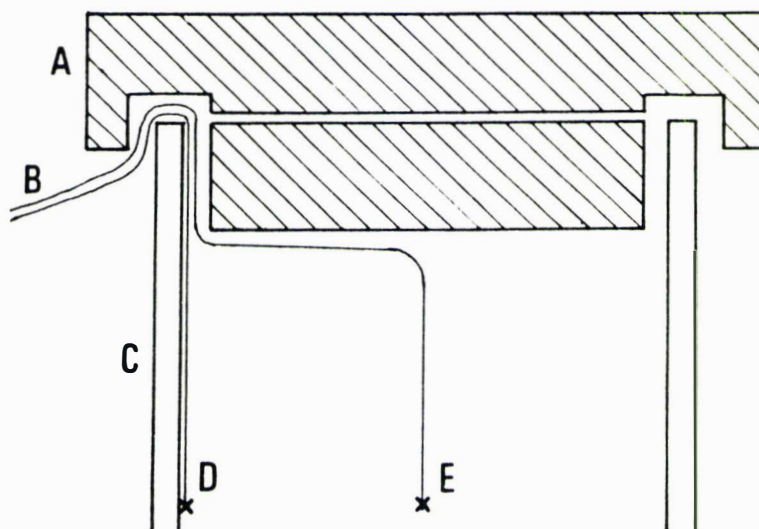
Fig. 5.11 Schematic Diagram Showing the Arrangement of the Polystyrene
Foam Caps and Thermocouples Leads For Infinite Cylinder
Experiments.   Not to scale.
A - polystyrene foam caps, B - thermocouple leads, C - pipe
wall, D - surface thermocouples, E - centre thermocouples.

5.5.3 Measurement and Control of Surface Heat Transfer Coefficients

The difference in cylinder wall material and thickness gave some variation in the surface heat transfer coefficient. To give greater variation of h, and to reduce the surface heat transfer coefficient to values more commonly encountered in air thawing systems, zero to four sheets of rubber were glued to the outside of each cylinder. The rubber used was the same as that used to alter h in the slab thawing experiments. The same linear relationship between heat transfer resistance and the number of rubber sheets used for slabs could not be applied because of the curvature of the cylinder surface area and the need for glue to permanantly attach the rubber. Consequently separate estimates of the surface heat transfer coefficient were made for each combination of pipe material, wall thickness and number of rubber sheets.

For the same reasons as those outlined in Sec. 5.4.3 for slabs, separate heating or cooling experiments without phase change were necessary to accurately estimate h. To determine h for the ten different combinations outlined above, a total of 29 runs were made. Initially the three methods used by Cleland & Earle (1979a) were applied. Similar to the methods used to determine h for slabs, these methods all depended on the measurement of surface temperature as it varied with time. It was found that the results were highly variable and inconsistent. This was thought to be due the effect of imperfect contact of the Tylose to the inside surface of the cylinder walls. Imperfect contact was not a major problem in freezing experiments using the same equipment (Cleland 1977) as the slight expansion of the Tylose and contraction of the pipe wall material during freezing filled any voids. In thawing, slight shrinking of the Tylose and expansion of the pipe wall material occurred and this created voids.

Dismantling of the cylinders after experimentation showed that thermal contact was better than 80%. Where perfect contact did not occur a small gap was present between the pipe wall and the Tylose. These voids were randomly distributed and ill-defined in size so it was impossible to evaluate their individual effect directly. The best way

to account for them was to use an average h value for the whole surface. The mode of heat transfer across these voids would be natural convection. If heat transfer across the gaps was by conduction only then a 0.5 mm void would lead to a significant resistance of $0.025 \ m^2 \ ^{\circ}C \ W^{-1}$. The actual heat transfer resistance due to natural convection would be less than this, but how much less can not be easily predicted.

Individual surface thermocouples would be affected by their proximity to these voids. Hence the value of h estimated from surface temperature measurements would be affected and may not be representative of the true average value. Because there was no criterion to chose which thermocouple most closely resembled the average surface conditions the methods based on surface temperature could not be relied on to give good estimates of h.

A method that considered the centre temperature was therefore used. By using the centre temperature the effect of any variation in heat transfer conditions at the surface was effectively averaged and the h value was more representative of the true value. Localised variation in h is not important if it is relatively small in magnitude and is randomly distributed over the surface. This was probably the case with the surface voids and imperfect contact.

The method used to estimate the surface heat transfer coefficient was the heat penetration method (Arce & Sweat 1980). For long times the analytical solution for heat transfer with constant thermal properties and the third kind of boundary condition (Carslaw & Jaeger 1959) is closely approximated by taking only the first term in the series solution. The surface heat transfer coefficient can be calculated from the slope of a plot of $\ln Y_c$ versus time (Charm 1963, Baker & Charm 1969, Kopelman et al 1970). An advantage of this method is that it is independent of the exact position of the thermocouple within the cylinder. If the centre thermocouple is not precisely located on the central axis, this does not affect the estimation of h by this method.

An indication that the presence of voids was affecting surface temperature readings was that the reading closest to the ambient medium

temperature did not corrospond to the same thermocouple throughout the run. The best estimate of the centre temperature was taken as the thermocouple recording the temperature that was slowest to change towards the ambient temperature. The two central thermocouples tended to show temperature profiles consistently different from each other, indicating that inhomogeneity was largely a surface problem and that any effects of non-uniformity at the surface were highly damped in their effect on heat transfer near the centre.

The rubber sheets gave a constant additional resistance to heat transfer over the whole cylinder surface except for the joint necessary down the length of the cylinder. The rubber was cut accurately so that this joint was always less than 0.5 mm in width. For the smallest cylinder this affected 0.3% of the surface area, which is insignificant. Where multiple layers of rubber were glued on, the joints were not overlapped so the change in surface conditions caused by the joints were not compounded at one section of the cylinder surface. The contact adhesive used gave extremely good contact between rubber layers and the pipe walls with no air spaces so heat transfer through the rubber layers was uniform.

Thawing experiments were carried out with the ambient medium temperature in the range: 5.0°C to 45.0°C. Although the liquid velocity around the tank was constant, some variation of the transport properties of water and therefore the film heat transfer coefficient may occur with temperature. In the temperature range used the changes in liquid properties were small, and the bulk of the resistance to heat transfer was in the pipe wall and sheets of rubber anyway. Hence there was no statistical ly significant correlation of h with ambient temperature.

Centre temperature profiles change less than surface temperatures for a given change in h so there was a loss of measurement sensitivity.   The result was that individual h values differed by up to 20% from the mean value in sets of replicate runs for the same cylinder and rubber thicknesses. The uncertainty in the mean estimates of h were therefore about ±7.0% at the 95% level of confidence.

5.5.4 Analysis of Heat Transfer in Infinite Cylinders

Some of the problems encountered in cylinder experiments were similar to those found for slabs. The lengths of the test cylinders were always greater than the diameter by a factor of at least three, and insulating caps were used to minimise the effect of heat transfer along the length of the cylinders. Using a similar analysis to that for slabs (Sec. 5.4.4 and App. B) the end-effect heat transfer was found to be negligibly small (0.2% decrease in thawing time) for the worst situation used in thawing runs. The test cylinders therefore approximated infinite cylinders very closely.

Apart from the problems at the surface, air voids that occurred in the material were no larger or more common than those found for slabs, so their effect would not be expected to be any more significant than the effect of the internal voids for slabs. This was discussed in Sec. 5.4.4. Voids at the surface of the cylinders and imperfect contact predominantly affected the surface heat transfer and were accounted for by the method discussed in Sec. 5.5.3. A consequence was that the geometric and thermodynamic centre of the cylinder may not have coincided. As surface voidage was evenly distributed across the cylinder surfaces, averaging effects mean that the central axis of the cylinders should coincide closely with the thermodynamic centre. It will be shown below that even if the thermodynamic centre was misplaced slightly, the thawing time is only minimally altered.

Errors due to inhomogeneity created by the presence of thermocouple wires and heat conduction along these wires were of similar magnitude to those found for slabs, and were similarly insignificant. Errors in placement of centre thermocouples were assessed by the same methods used for slabs. Centre thermocouple placement was more difficult than for slabs so a greater variation in temperature was observed between thermocouples. As shown in Sec. 5.4.4 quite large errors in thermocouple placement can occur without significantly affecting prediction of thawing time or centre temperature profiles. Placement of thermocouples near the thermodynamic centre was therefore easily assessed and did not significantly increase the overall error. The breakpoint analysis outlined in Sec. 5.4.4 was used to increase the

precision of thawing time predictions where centre thermocouples were
poorly positioned.   For reasons discussed in Sec. 5.5.3 the fastest
changing individual surface temperature measurement did not necessarily
represent the average heat transfer conditions, and slower changes
could be due to placement below the surface as well as lower h values
in particular regions.   Hence applications of the techniques   of
Sec. 5.5.3 probably led to experimentally measured surface temperatures
nearer to the ambient temperature than those representing the average
heat transfer conditions. Predicted surface temperatures using the
average h value would therefore be expected to lie further from the
ambient medium temperature than the measured data.

The effect of the heat capacity of the rubber insulation and also of
the pipe wall material was greater than that discussed in Sec. 5.4.3
for slabs, because the rubber and pipe wall material could not be
preheated to the ambient thawing temperature due to it being
permanently attached to or part of each cylinder. The heat taken up by
the rubber and wall material was less than 3.0% of the total heat
transfer to each cylinder. Further, the estimate of the surface heat
transfer coefficient to the Tylose surface was determined in such a way
that only heat transferred through the insulating layers was taken into
account. Hence the main effect of heat taken up by the rubber and pipe
wall material would be to distort to some extent the measured Tylose
surface temperature early in the thawing process when the rubber and
wall temperatures were changing most.

No replicate runs were conducted for cylinder thawing due to
limitations in time, so direct measurement of the experimental error
was not made. The errors for cylinder thawing were of the same order
of magnitude as in the slab experiments, except for measurement and
control of the surface heat transfer coefficient.   The experimental
error was therefore expected to be slightly greater than for slabs.

5.6   THAWING OF SPHERES

5.6.1   The Equipment

Hollow metal balls were used to model spherical geometry.   The three
sizes used were approximately 0.05 m, 0.1 m and 0.125 m in diameter.
The metals were stainless steel, copper and mild steel respectively.
Each of the spheres was made from two hemispheres for ease of
construction.   Each hemisphere was packed with Tylose and two surface
thermocouples were inserted along isothermal paths around the
circumference.   The two halves were then welded or soldered together
with a single thermocouple in the centre position.   The disruption to
the surface of each sphere caused by the joint between the two
hemispheres affected 3.5% to 4.0% of the surface area. However the
joints were of similar thermal resistance to other parts of the
surface.   The disruptions and problems caused by voids and imperfect
contact are only important because of their effect on the heat transfer
behaviour of the spheres and are discussed in Secs. 5.6.3 and 5.6.4.

A bolt was soldered or welded to the surface of each ball to enable a
connection to be made to the sample holder and oscillator. Because
both the bolt and the spheres were metal and only 0.04% to 0.2% of the
total surface area was affected, the effect on heat transfer was
considered negligible. A finished sphere and the sample holder are
shown in Fig. 5.12.

The same immersion thawing tank (Fig. 5.8) used for infinite cylinder
experiments was used for spheres. Oscillations of the samples was used
for the reasons outlined in Sec. 5.5.1.

Sealing the outside of each sphere along the joint between the
hemispheres to prevent liquid ingress was a problem, especially where
the thermocouple wires entered the metal shells. Slight water ingress
led to changes in the Tylose near the leak, and often resulted in
density changes and hence splitting of the spheres on freezing.   To
prevent this problem and to give variations in surface heat transfer
coefficients (Sec. 5.6.3) layers of silicone rubber (Dow Corning 3110
RTV) were used to coat the spheres after construction.   The rubber was
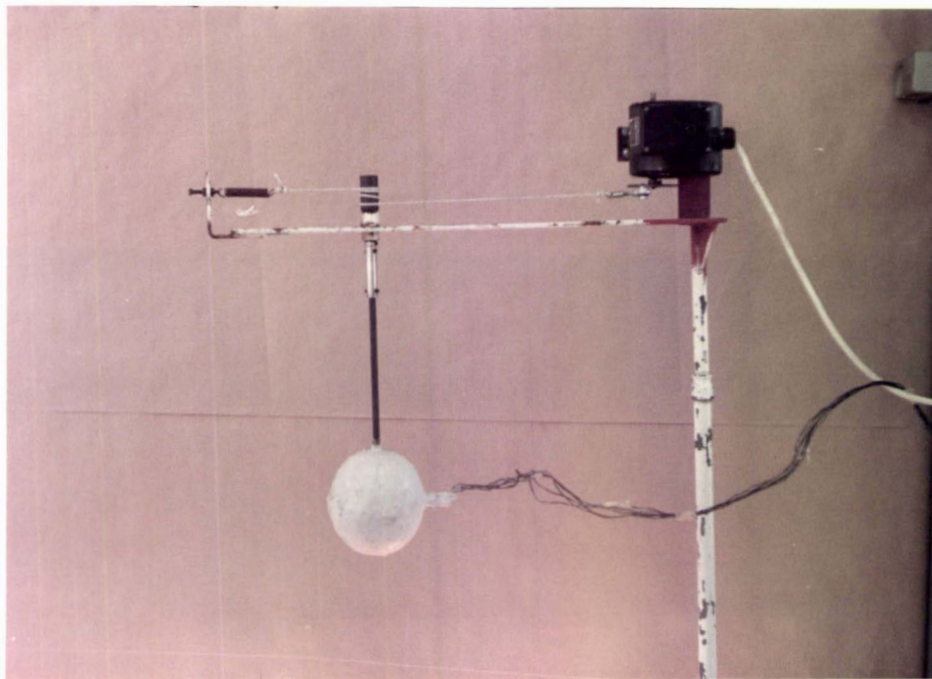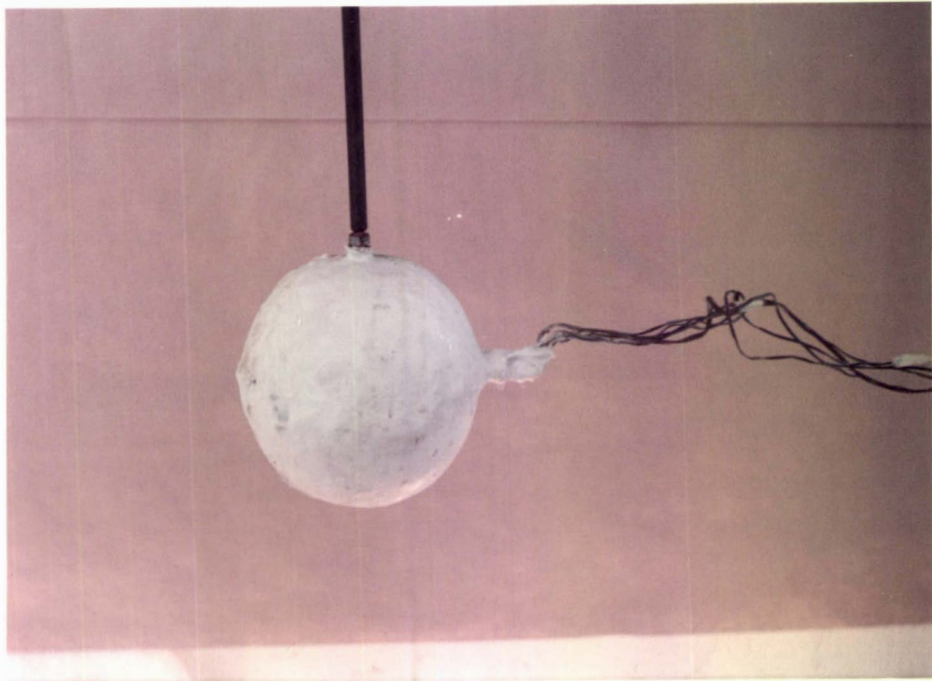
Fig. 5.12 The Sample Oscillator and Sphere Shapes Used in the Liquid Immersion Tank.

applied in a liquid form and the spheres were rotated until the rubber had cured to minimise variations in the rubber thickness. In spite of theis precaution someome localised variation of rubber thickness did occur. By applying multiple layers of rubber this variation was not large and was randomly distributed. The effect on the surface heat transfer coefficient is discussed in Sec. 5.6.3.

5.6.2 Diameter Control and Measurement

The construction of the spheres in two halves, the flexibility of the hollow metal shells used and the distortion in shapes due to water ingress and the consequent density change, meant that the spheres were not constant in diameter. Some variation in diameter occurred with both position around the sphere and whether the spheres were in the frozen or unfrozen state. Measured variations in diameter about the mean value were ±1.0 mm (1.8%) for the smallest sphere, ±3.0 mm (2.7%) for the medium sized sphere and ±2.0 mm (1.6%) for the large sphere. The sphere volume was measured by displacement of liquid and confirmed that the average values were accurate.

5.6.3 Measurement and Control of Surface Heat Transfer Coefficients

The metal balls had low resistance to heat transfer, so most of the change in h was due to the layers of silicone rubber used to coat and seal the surface. Some variation was achieved by varying the number of layers of rubber added.

The same problems with thermal contact and voids that were observed with infinite cylinders (Sec. 5.5.3) occurred for spheres. In addition, exact control of the rubber coating thickness was not possible and irregularities in the metal joint between the sphere halves affected heat transfer. Therefore some variation in the surface heat transfer coefficient over the surface was expected. Estimates of h based on surface temperature measurement and the methods for radial geometry of Cleland & Earle (1979a) did not provide consistent and reliable results. For these reasons, the heat penetration method (Charm 1963) was used to measure h using the centre temperature profiles from independent heating and cooling experiments that involved

no change of phase. As discussed for the infinite cylinder geometry in Sec. 5.5.3 this method averages any random surface variation in h. The only possible source of systematic variation was the joint between hemispheres. The joining material was metallic in nature and therefore had negligible additional resistance to heat transfer compared with the other parts of the metal surface.

However, there were more sources of error in measuring and controlling the surface heat transfer coefficient for spheres than for infinite cylinders. A total of 32 runs were used to estimate the ten different h values used in thawing experiments. Variations of measured h values between relicate runs indicated that the measurement uncertainty in the mean values of h was about ±11.0%.

5.6.4   Analysis of Heat Transfer in Spheres

For spherical geometry there are of course no problems with end heat transfer effects. There were errors due to inhomogeneities on the sphere surface at the joint between hemispheres, unevenness in the rubber coating, attachment of the bolt to allow connection to the sample oscillator and those due to air voids and imperfect contact. The extent to which these factors affected temperatures recorded by the surface and centre thermocouples could not be easily assessed but would be similar to that for infinite cylinders. The major effect was on measured surface temperatures which was discussed in Sec. 5.6.3.   The position of the actual thermodynamic centre was probably not greatly affected by non-homogeneity of surface conditions if they were randomly distributed. Therefore the measured centre temperature and thawing time were only slightly decreased in accuracy by these effects.

For spheres, the thermodynamic centre and the geometric centre coincide at a single point so that only one thermocouple could be placed at this position. Errors due to the inhomogeneity created by presence of thermocouple wire and placement of thermocouples were similar to those found for infinite cylinders, and similarly had insignificant effect on prediction of thawing times. However, in spheres it was not possible for the centre thermocouple to be inserted along isothermal regions. Heat conduction will only be significant along the wire, not along the

insulation. As the cross-sectional area of the wire (3.6×10^{-7} m^2) is only 0.004% of the total surface area of the smaller sphere and the thermal conductivity of the wire is about 200 times that of Tylose, then up to 0.8% of the total heat flow may occur through the wires. Overall, the effect of heat conduction along the central thermocouple wire on thawing time was considered to be small.

Assessment of surface and centre thermocouple placements and estimation of thawing time from experimental runs was made in the same way as that used for infinite cylinders (Sec. 5.5.4). The coating of rubber used on the spheres was far less than that used for infinite cylinders, so the effect of the heat taken up by the rubber and metal shells on the overall heat transfer was insignificant. The volume of water that was able to penetrate each sphere around the thermocouple leads was extremely small and only affected the Tylose in the immediate vicinity of the leak. The major result was some localised expansion when the Tylose was frozen. This affected the dimensions and physical integrity of the joints. An average diameter value for the spheres based on both frozen and unfrozen states was used. Spheres in which the joints became visibly damaged were remade before further use.

Overall, experimental error for spheres was of a similar magnitude to that for thawing of infinite cylinders.

5.7   THAWING OF RECTANGULAR BRICKS

5.7.1   The Equipment

The liquid immersion thawing tank was used. Both metal and polypropylene boxes were constructed (Fig. 5.13). All boxes had a bolt attached to the lid to hold them onto the sample oscillator in the same way as that used for spheres. The face of each box furthest from the geometric centre was chosen to be the lid. This surface has the least effect on heat transfer in the rectangular brick and the bolt affected less than 0.1% of the total surface area, so in all cases the effect of the bolt was insignificant.

Construction of the metal boxes, from sheets of 1.2 mm thick mild steel, required some overlapping of the metal to allow attachment of the lid by screws as shown in Fig. 5.14d. For metal boxes the major resistance to heat transfer at the surfaces is the liquid film heat transfer coefficient. Also the overlapping occurred for less than 25% of the lid area. Therefore the double metal layers at any overlaps resulted in negligible additional heat transfer resistance. By welding and bending corners, all edges of the metal boxes (Fig. 5.14b) closely approximated a sharp cornered brick shape (Fig. 5.14a) except for the lid.

The other boxes were made from polypropylene plastic sheet (5.0 mm thick) with all the joints screwed together (Fig. 5.14c). The presence of the screws altered the heat transfer resistance of less than 0.4% of the surface area depending on the box. The effect of this was insignificant and the corners approximated closely to the ideal type of joint shown in Fig. 5.14a.

Thermocouples were positioned at the geometric centre of each brick and at four to six different places on the surface. Where possible, surface thermocouples were positioned at the centre of the brick faces.

5.7.2 Dimensional Measurement and Control

The dimensions of each rectangular brick were measured in both the frozen and unfrozen states. Water ingress around the thermocouple leads entry point in the lid of some boxes resulted in some local density changes and hence dimensional variability. Density change during phase change was a slight problem for the minced lean beef bricks. Allowing for these factors, plus box construction and measurement imprecision, the dimensions were accurate to ±1.0 mm for all the Tylose and minced lean beef rectangular bricks. The effect of water ingress on heat transfer is discussed in Sec. 5.7.4.

5.7.3   Measurement and Control of Surface Heat Transfer Coefficients

The metal and polypropylene bricks gave two different surface heat transfer coefficient values. To further alter the surface heat transfer coefficient, rubber sheets were glued to each face of the rectangular bricks in a similar manner to that used for infinite cylinders. One layer of rubber was put on the metal boxes and two layers on the polypropylene boxes. In this way four different values of h were obtained for the rectangular brick geometry.

In a rectangular brick shaped object heat transfer at any point on the surface can be treated as one-dimensional until the time that the heat penetration fronts from one or both of the other two dimensions reaches the point. This means that the methods used for the measurement of h in slabs can be applied at some places on the surfaces of rectangular bricks for short times. In Sec. 5.4.3 it was shown that the four methods used for slabs were equally accurate. Therefore the most convenient of these methods to use for short times, that based on Goodman's heat balance integral technique (Cleland & Earle 1976a), was the first method chosen to determine h.

The analytical product solution for heat conduction in three dimensions with the third kind of boundary condition and constant thermal properties (Newman 1936) was the second method used. A similar computer program to that used to estimate h from surface temperature profiles for radial geometry (Cleland & Earle 1979a) was used. The program took values of time, surface temperature and positional coordinates for the position of the thermocouple where the measurements were made, and used an iterative loop to predict the surface heat transfer coefficient needed to attain that temperature, at that time, and in that position.

Both methods are only applicable for times before the onset of phase change. As this time is very short for thawing experiments, separate heating and cooling runs were carried out with each rectangular brick in the unfrozen state. There was no significant variation in estimated h values between bricks of the same wall materials, between analyses using different thermocouples in each brick, or as ambient medium

temperature changed. The disagreement of the two methods was statistically insignificant at the 95% level of significance. Consequently, average values of h for each of the four combinations of wall material and number of rubber sheets used, were calculated from the replicate estimations.

Errors due to inconsistencies in heat transfer on each of the surfaces of each rectangular brick were made negligible by using the liquid immersion tank, oscillating the samples, and using the rubber sheets to alter the surface heat transfer resistance. The mean predicted h value for polypropylene boxes had 95% confidence bounds of $\pm 1.5\%$ (no rubber) and $\pm 2.1\%$ (with two sheets of rubber). For the metal boxes the results were less accurate than those for the polypropylene boxes because the surface heat transfer coefficients were larger and consequently the time for each heating or cooling experiment was shorter than for the polypropylene bricks. The values of h were therefore based on less data. The 95% confidence bounds for the mean values of $\pm 7.5\%$ (no rubber) and $\pm 4.4\%$ (with one rubber sheet) for the metal bricks, reflect this trend.

As for the slab experiments, the h values for runs with minced lean beef were assumed to be the same as those measured for the Tylose bricks. Mince lean beef undergoes significant density changes during phase change and has a fibrous moist nature compared with the dry gel-like nature of Tylose. Therefore air voids within the minced lean beef were less likely and it was possible that the contact resistance was different for the two materials. Hence the assumption of equal h values may introduce some extra uncertainty for the mince lean beef experiments.

5.7.4 Analysis of Heat Transfer in Rectangular Bricks

Errors in experiments for rectangular bricks arose from similar sources to those for other shapes. Voids and ingress of water occurred to the same extent as in spheres and would not be expected to be any more significant for rectangular brick shapes than the radial case. Similarly, any inhomogeneity caused by the presence of thermocouple wires would have a negligible effect.

Problems had been found with imperfect thermal contact for infinite cylinders and spheres. Similar behaviour was not observed for the rectangular bricks. Therefore surface temperatures and surface heat transfer could be analysed in a similar manner to that used for slabs without additional error.

Suitable isothermal regions for thermocouple lead location do not occur in rectangular brick shaped objects. Thermocouples were introduced through regions as near to isothermal as possible to minimise conduction along the wires. Heat fluxes along the wires were therefore similar to those that occurred for spheres. The volume of the brick shapes used were much larger than the smallest sphere so the effect of heat transfer along wires was insignificant.

Errors in placement of thermocouples were assessed in the same way as for other shapes. Because surface heat transfer conditions were equivalent on each face, the geometric and thermodynamic centres of the rectangular bricks coincide at a single point and, similarly to a sphere, only one thermocouple could be placed there. As shown for other shapes (Sec. 5.4.4) the error in placement of the centre thermocouple could be easily assessed by the breakpoint analysis and does not significantly affect the accuracy with which thawing times could be measured.

As was the case for spheres, the volume of the rubber coating and box wall material for the rectangular bricks was sufficiently small compared with the volume of the Tylose brick itself to make the effect of the heat absorbed by the rubber and wall material unimportant.

For thawing of rectangular bricks the overall experimental error was smaller than for thawing of infinite cylinders and spheres (because h could be measured more accurately), and about the same as that for slabs.
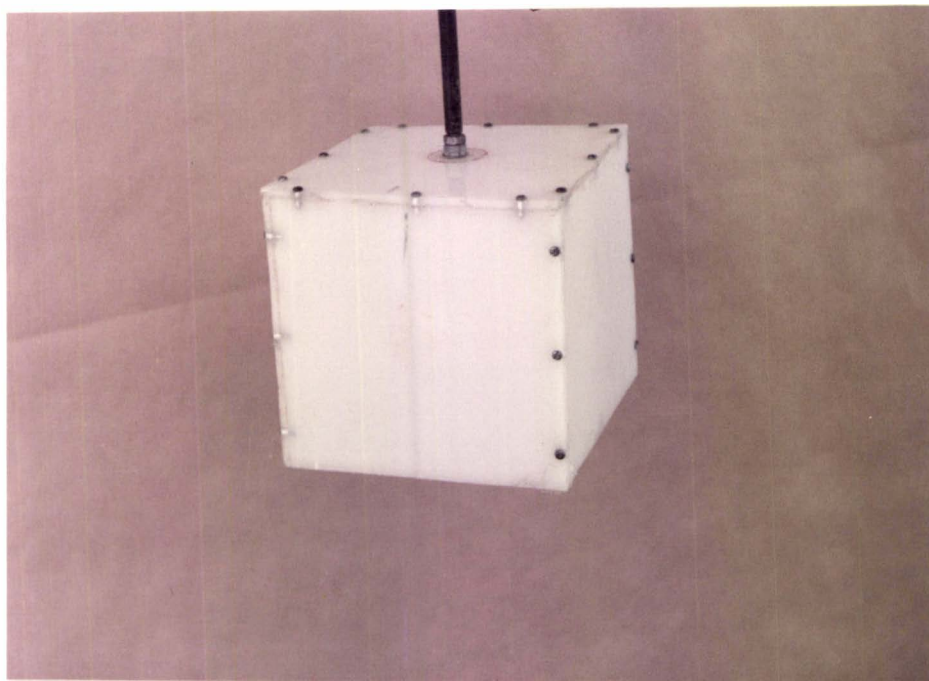
a
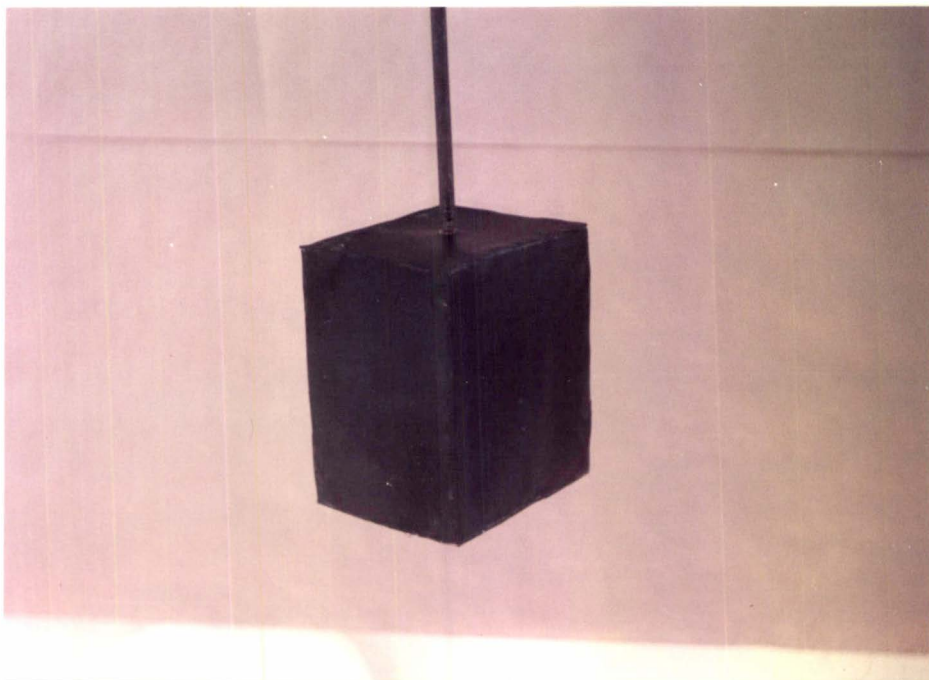
b

Fig. 5.13 Typical Rectangular Brick Shapes.

       (a) polypropylene box

       (b) metal box with one layer of rubber

       (c) polypropylene box on the sample oscillator (p. 97).
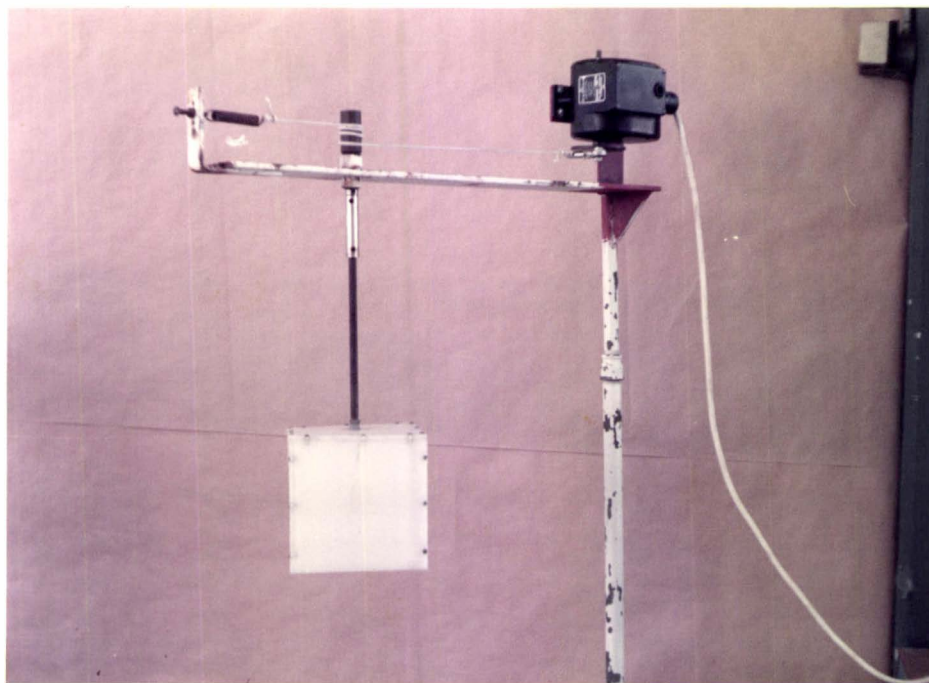
C

Fig. 5.13 Typical Rectangular Brick Shapes.

       (a) polypropylene box (p. 96)

       (b) metal box with one layer of rubber (p. 96)

       (c) polypropylene box on the sample oscillator
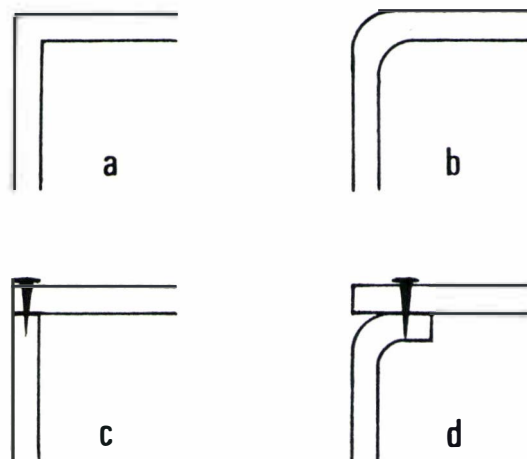
Fig. 5.14 Schematic Diagrams of Box Corner Types.

       (a) ideal corner, (b) metal box corner

       (c) polypropylene box corner, (d) metal box corner with lid.

5.8 HEAT TRANSFER IN TWO-DIMENSIONAL IRREGULAR SHAPES

5.8.1 The Equipment

An infinite number of two-dimensional irregular shapes are possible. The main concerns in choosing experimental shapes were to be able to (a) accurately control and describe the shape, (b) control and measure the surface heat transfer conditions and (c) prevent heat transfer in the third dimension. It was considered that these could be best achieved by using experimental techniques similar to those used for thawing of infinite cylinders (Sec. 5.5).

The shapes were constructed from 0.45 m to 0.50 m lengths of 0.1 m and 0.15 m nominal diameter polyvinyl chloride (PVC) plastic pipes. These pipes were heated until the walls became soft and pliable. They were then moulded lengthwise around smaller diameter pipes and allowed to cool. The new shape had, as closely as was possible, a consistent cross-sectional shape along the length of the pipe. The cross-sections of the various shapes produced are given in Fig. 5.15 to 5.21.

Heat transfer along the length of each object was minimised in a similar manner to that used for infinite cylinders.

The irregular shaped objects were filled with Tylose or minced lean beef from one end to a mid-point of their height. Thermocouples were positioned at five or six locations throughout the objects at this central level. This was done by drilling small holes in the PVC pipe wall just large enough for a single thermocouple lead. By inserting the copper and constantan leads through separate holes and reconnecting and tensioning them within the object as shown in Fig. 5.22, the thermocouple junction was accurately positioned. The thermocouple leads were held in place and the holes in the pipe walls were sealed with a small amount of epoxy resin. Packing of the object with Tylose was then completed and the polystyrene foam end caps were placed in position. The locations of the thermocouples for each shape are indicated on Fig. 5.15 to 5.21. A filled test sample is shown in Fig. 5.23.

ONE–DIMENSIONAL GRID

TWO–DIMENSIONAL GRID
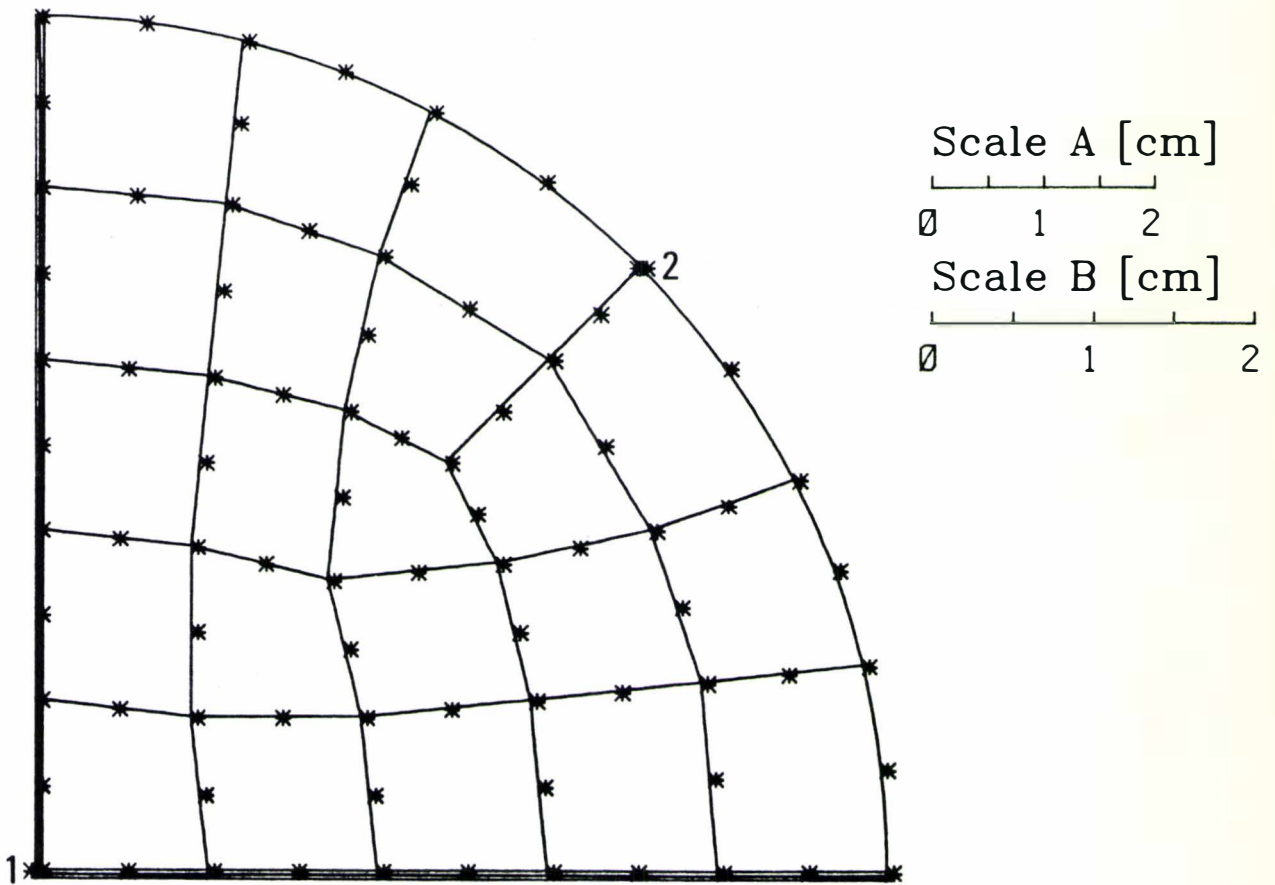
Fig. 5.15 Cross-section and Finite Element Method Grids For the
       Two-Dimensional Irregular Shapes Numbers One and Five.
       Scale A applies for Shape No. 1. Scale B applies for Shape
       No. 5. * - nodes, ** - nodes corrosponding to thermocouples
       positions, _ - element boundaries, ■ - planes of symmetry.
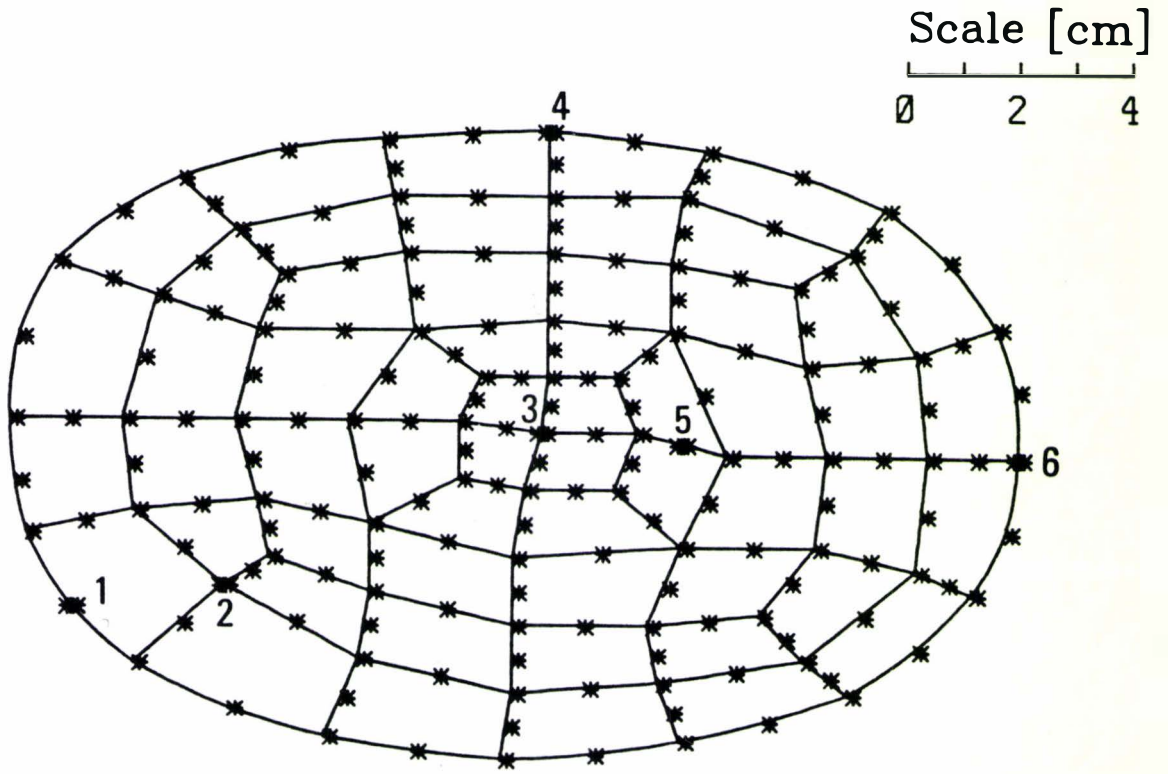
Fig. 5.16 Cross-section and Finite Element Method Grid For the
Two-Dimensional Irregular Shape Number Two.
* - nodes, ** - nodes corrosponding to thermocouples
positions, _ - element boundaries.
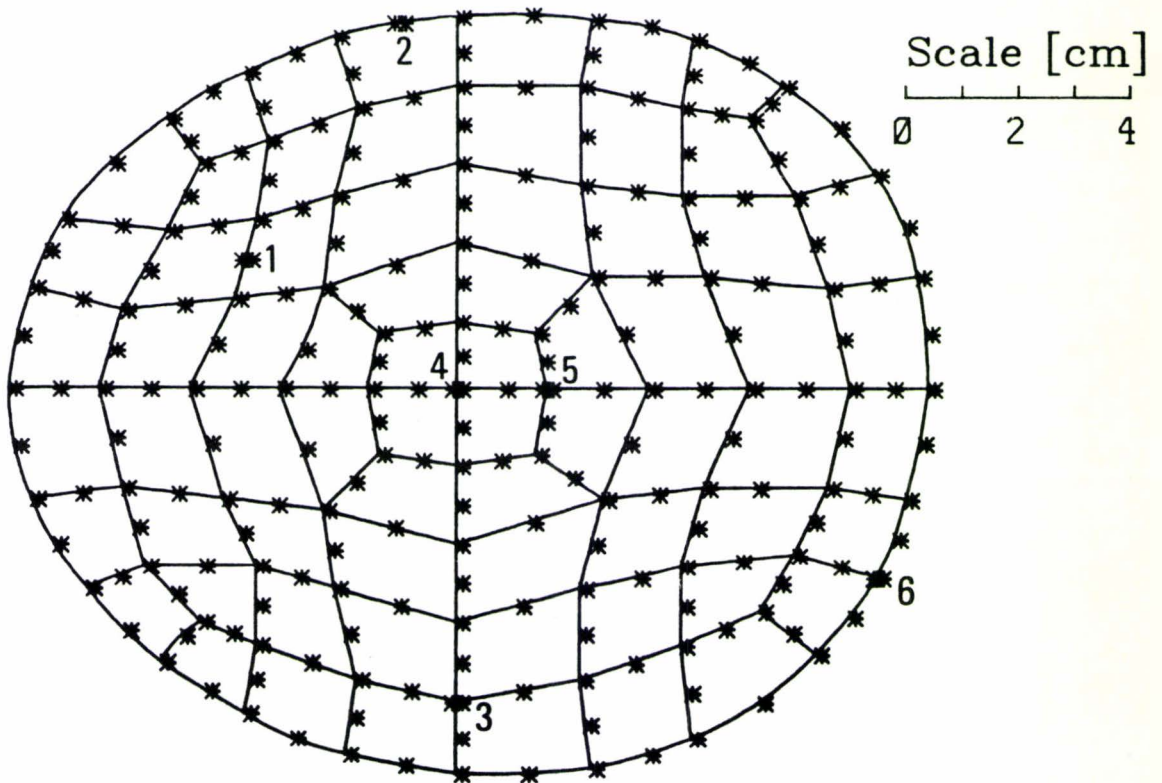
Fig. 5.17 Cross-section and Finite Element Method Grid For the
Two-Dimensional Irregular Shape Number Three.
* - nodes, ** - nodes corrosponding to thermocouples
positions, _ - element boundaries.

Scale [cm]
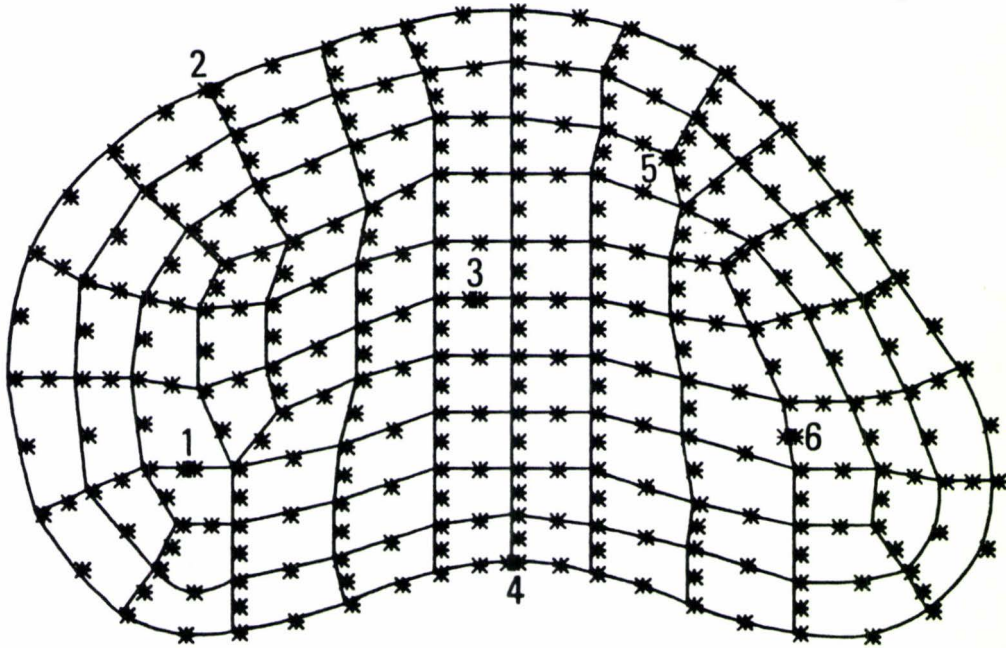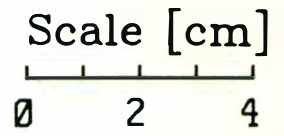
Fig. 5.18 Cross-section and Finite Element Method Grid For the
Two-Dimensional Irregular Shape Number Four.
* - nodes, ** - nodes corrosponding to thermocouples
positions, _ - element boundaries.

Scale [cm]
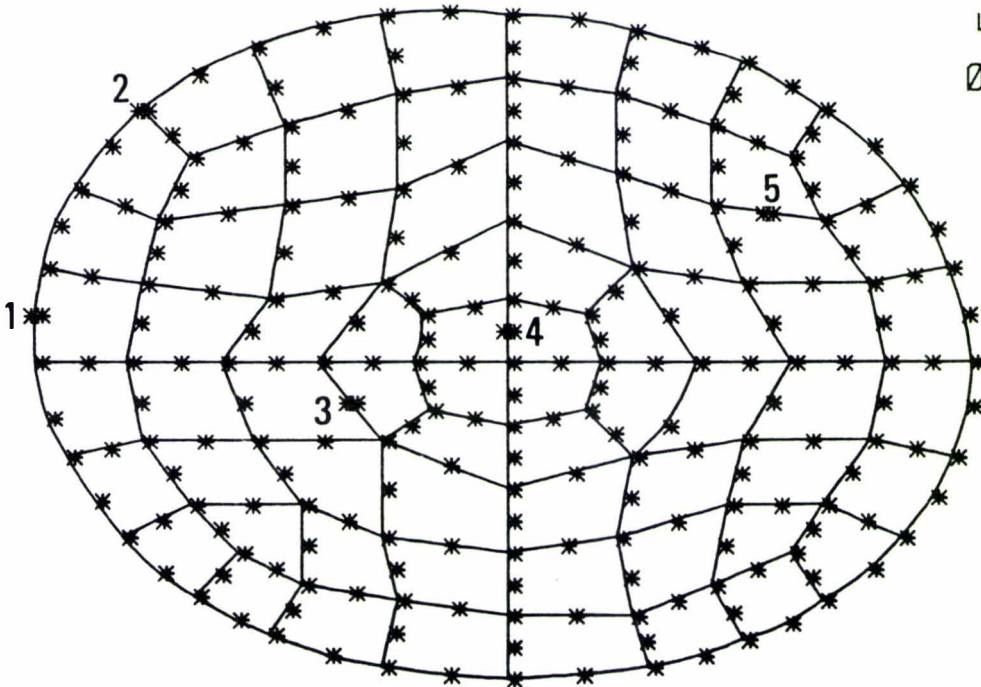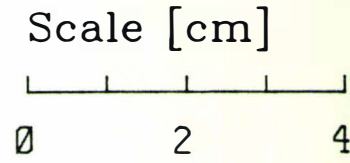
Fig. 5.19 Cross-section and Finite Element Method Grid For the
Two-Dimensional Irregular Shape Number Six.
* - nodes, ** - nodes corrosponding to thermocouples
positions, _ - element boundaries.
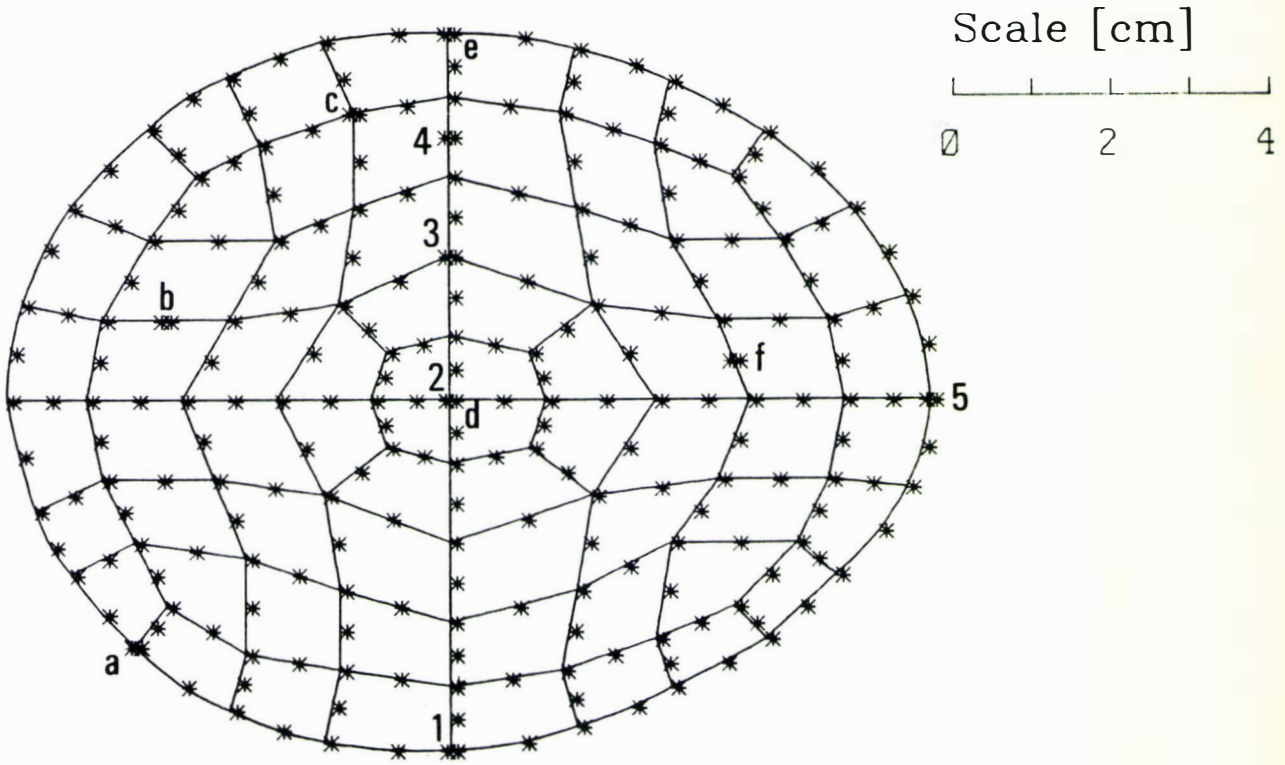
Fig. 5.20 Cross-section and Finite Element Method Grid For the
Two-Dimensional Irregular Shape Number Seven.
* - nodes, ** - nodes corrosponding to thermocouples
positions, _ - element boundaries.
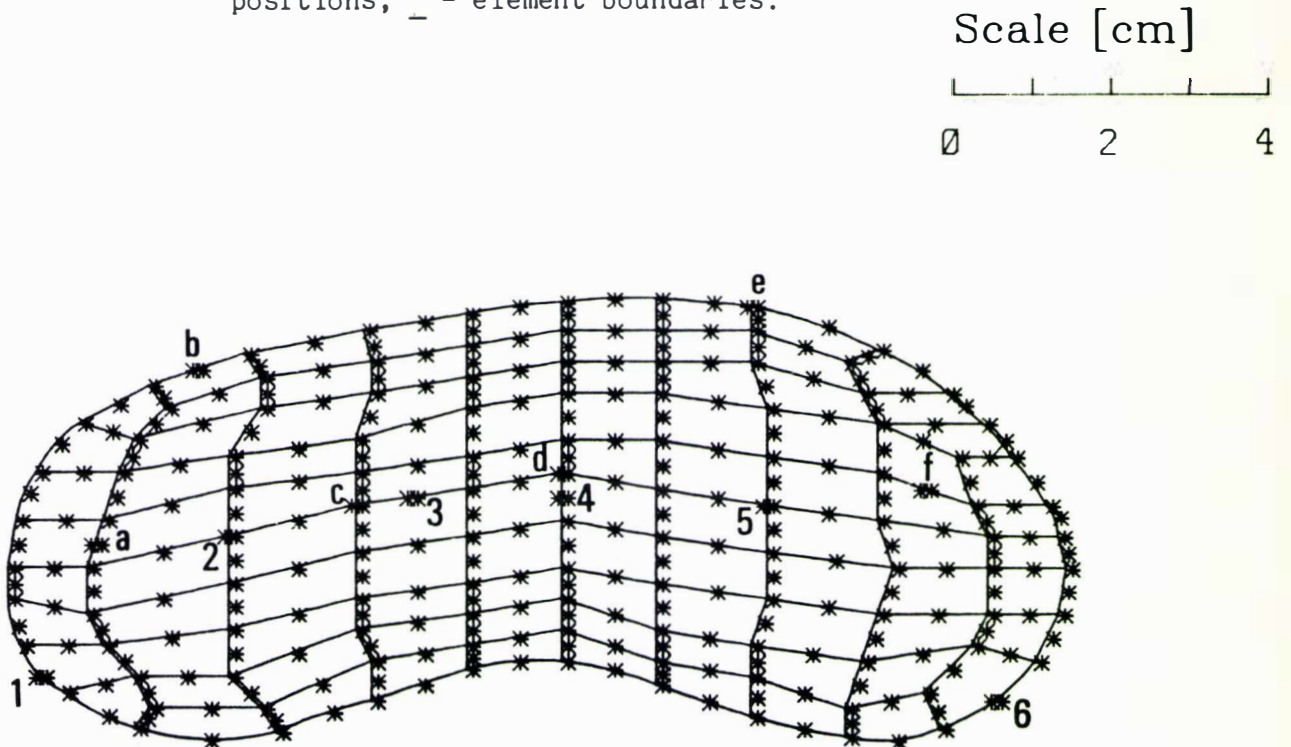
Fig. 5.21 Cross-section and Finite Element Method Grid For the
Two-Dimensional Irregular Shape Number Eight.
* - nodes, ** - nodes corrosponding to thermocouples
positions, _ - element boundaries.
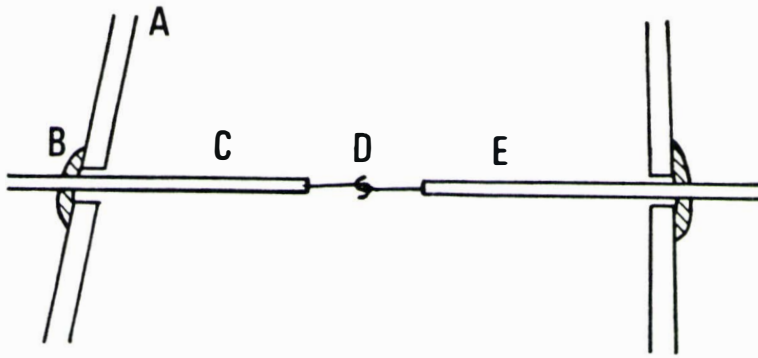
Fig. 5.22 Schematic Diagram Showing the Method of Thermocouple
          Insertion and Positioning Within the Multi-Dimensional
          Irregular Shapes. Not to scale.
          A - object wall, B - epoxy resin, C - insulated constantan
          lead, D - thermocouple junction, E - insulated copper lead.
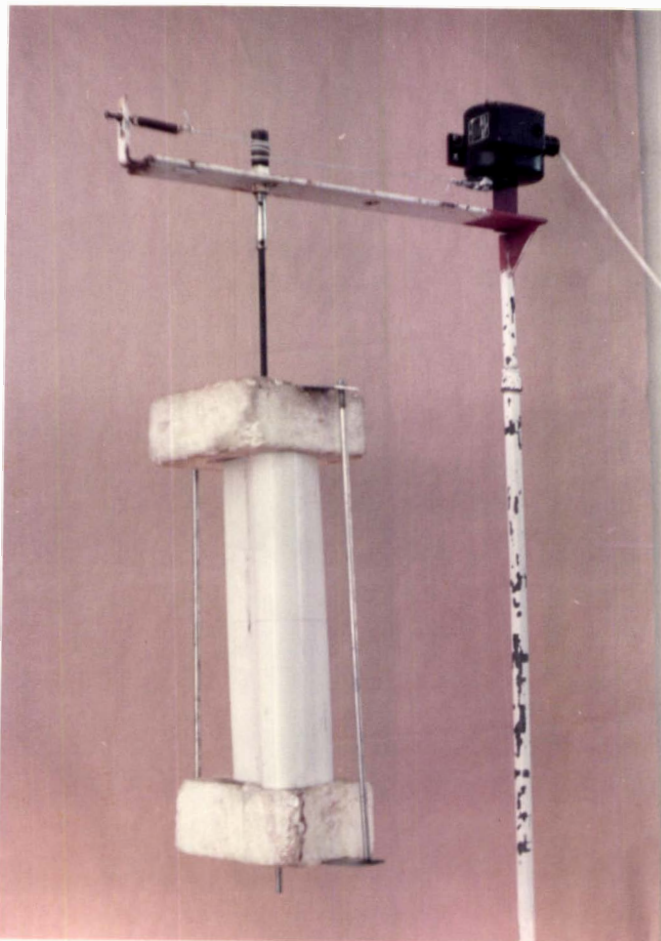
Fig. 5.23 The Sample Oscillator and Two-Dimensional Irregular Shape
          Freezing and Thawing Equipment Used in the Liquid Immersion
          Tank.

The liquid immersion tank was used. Because both freezing and thawing
experiments were carried out, the tank contained 29% calcium chloride
brine. Accurate temperature control across the temperature range -40°C
to 50°C was achieved. The test samples were oscillated to minimise
local variations of the surface heat transfer coefficient.

5.8.2 Dimensional Measurement and Control

The rigid nature of the PVC pipes meant that no variation in shape or
size was measured during experiments.   If any density change of the
Tylose or minced lean beef occurred during phase change, it resulted in
lengthwise change in volume which was absorbed by compression of the
polystyrene end caps.

There was some variation in the cross-sectional shape of each object
along its length. Cross-sectional profiles from each end of the object
were drawn and averaged to estimate the final shape and size for each
object (Fig. 5.15 to 5.21) as accurately as possible. Variations from
the mean shape were less than ±1.0mm in dimensions and less than 1.0%
in perimeter and cross-sectional area.

The characteristic thickness for the irregular shapes is defined as
either the minimum thickness measured through the thermodynamic centre
or double the minimum distance from the thermodynamic centre to the
surface. For all the shapes it was found that only one thermodynamic
centre existed, because the surface conditions were uniform and the
geometries used were relatively uniform in shape.   The characteristic
thicknesses determined from each definition were equal. The position
of the thermodynamic centre was found by analysis using the finite
element method (Sec. 4.2) for typical phase change conditions.

5.8.3 Measurement and Control of Surface Heat Transfer Coefficients

For the irregular shapes studied there were no satisfactory methods to
estimate the surface heat transfer coefficient directly   from
experiments for each shape. The two-dimensional irregular shapes were
remoulded from PVC cylinders for which surface heat transfer

coefficients can be determined (Sec. 5.5.3). As long as the liquid film heat transfer conditions are equivalent at all parts of the surface and the PVC wall thickness is constant over the whole surface, then the surface heat transfer coefficient would be expected to be approximately the same as that for the equivalent PVC cylinder. Use of the liquid immersion system plus oscillation of the test samples ensured that the liquid film heat transfer coefficient was constant to all surfaces of all the objects. The PVC wall thickness was the same for the remoulded shapes as for the original cylinders and did not vary significantly at different positions on the surface of the irregular shapes. Small random variations in wall thickness did occur due to changes in the degree of curvature of the PVC and heat shrinkage. The inside perimeters of the irregular shapes were measured to be within 1% of the original cylinder wall perimeter for the 0.15 m cylinders and within 2% for the 0.1 m cylinders, for all the irregular shapes. Therefore variation in the PVC wall thickness due to stretching during the moulding process had negligible effect on heat transfer.

Separate heating and cooling experiments with an unmoulded PVC cylinder were used to estimate h for the other (irregular) shapes in a similar manner to that used in infinite cylinder thawing experiments (Sec. 5.5.3). The curved surfaces of both the irregular shapes and the cylinder gave the same problems with voids and imperfect thermal contact at the surface, experienced for infinite cylinder and sphere thawing. It was assumed that the effect of these factors were the same for the irregular shapes as for the cylinder shapes so that the estimated surface heat transfer coefficients were still representative. Because Tylose packing conditions and the occurrance and distribution of the surface voids were similar in both cases, there is no reason to expect this assumption to be invalid.

To alter the surface heat transfer coefficient two layers of sheet rubber were glued onto the surface of all the irregularly shaped objects derived from the 0.1 m PVC pipes. The change in exposed surface area as more packaging material is added is slightly different for a cylinder and an irregular shape, so very small differences in h values are possible, but these were within the tolerance of the measurement system. The effect of the rubber and the above problems

with imperfect contact are discussed fully in Sec. 5.5.3.

The heat penetration method, based on cylinder centre temperature profiles, showed no statistically significant differences between replicates within the 26 runs used to estimate the three different values of h (for the 0.15 m PVC cylinder, the 0.1 m PVC cylinder and the 0.1 m PVC cylinder plus two layers of rubber) at the 95% level of confidence. The uncertainty in the mean values had 95% confidence bounds of ±12.7%, ±7.1% and ±2.8% for the above three values respectively. The values of h were different from those for the 0.1 m and 0.15 m PVC cylinders used in thawing (Sec. 5.5) because pipes of different thicknesses were used.

The surface heat transfer coefficient for the minced lean beef experiments was assumed to be the same as that determined for the Tylose experiments with the same shape. As discussed in Sec. 4.8.3 for rectangular bricks, this potentially leads to increased experimental uncertainty for the minced lean beef experiments because this assumption about h may not be valid.

5.8.4   Analysis of Heat Transfer in Two-Dimensional Irregular Shapes

Experiments for irregular shapes are subject to the same error to those for regular shapes. Voids in the Tylose and inhomogeneity caused by thermocouple wires had similar effects to those found in the infinite cylinder experiments, and were similarly insignificant.

Error in thermocouple placement was not a major source of uncertainty due to the way the leads were positioned and held in place. Dismantling of the objects showed that the thermocouple junctions remained within a 2 mm radius of the recorded position over a number of runs. However, the method used to insert the thermocouples did lead to errors due to heat conduction along the wires as they were not introduced along isothermal paths. Typically, four thermocouples were used to measure internal temperatures for each object. Only one of these was located in close proximity to the thermodynamic centre. Conduction along each thermocouple would be less than the 0.8% of the total heat flow calculated for the centre thermocouple in the smallest

sphere used for thawing (Sec. 5.6.4). The volume and surface area for
these two-dimensional irregular shapes were larger that those for the
smallest sphere.   Though up to four thermocouple wires conducted heat
towards the centre, because all but one of these were positioned well
away from the thermodynamic centre and the object volume and surface
areas were large, the effect of heat conduction along the thermocouple
wires was considered insignificant. Only 0.02% to 0.03% of the surface
area within the central 100 mm length of the pipes was affected by the
introduction of the thermocouple wire throught the walls.   This is
insignificantly small.

Heat transfer along the length of the irregularly shaped objects will
be of the same order of magnitude as that for the equivalent
cylindrical shapes due to the insulating caps, the high ratio of length
to thickness used and the central position used for temperature
measurement.   In Sec. 5.5.4 this was shown to be insignificant.

The problem with imperfect contact of the Tylose with the PVC wall,
noted for infinite cylinder experiments, occurred.   For infinite
cylinders it was analysed in the same manner by using centre
temperature profiles only to determine an average h for each object.
The effect of surface inhomogeneity, due to the imperfect contact, may
have been larger for irregular shapes if the presence of voids was not
evenly distributed over the surface. There was no evidence of this so
the approach used for infinite cylinders when considering accuracy of
surface temperature profiles was adopted.

For irregular shapes the position of the thermodynamic centre is not
known, and in fact it may move during any freezing or thawing run
(Fleming 1970). For this reason, the position of one thermocouple was
located as close as possible to the predicted thermodynamic centre of
the objects, as determined by a finite element analysis (Sec. 4.2) for
typical experimental conditions.   This may not be the   exact
thermodynamic centre so when the temperature profiles were analysed,
the breakpoint analysis discussed in Sec. 5.4.4 was used to increase
the precision of the experimentally determined thawing time where
necessary. This analysis is as applicable to irregular shapes as it is
to regular shapes.   When considering locations of other thermocouples

it was not important where they were positioned as long as the position was accurately known. A range of alternative positions were used to provide a number of typical temperature profiles from throughout each object.

For the two-dimensional irregular shape experiments an identical procedure to that used for thawing of regular infinite cylinders was adopted. Although the uncertainty in measured surface heat transfer coefficients was lower than for the infinite cylinder thawing experiments, the inability to control h to the same value for all the shapes introduced extra uncertainty. There is also an additional error in measuring and controlling the geometry so the overall experimental error was estimated to be of slightly greater magnitude than that for infinite cylinder thawing.

5.9   HEAT TRANSFER IN THREE-DIMENSIONAL IRREGULAR SHAPES

5.9.1   The Equipment

Only three different three-dimensional objects were investigated due to limitations in time and resources. Each was relatively uniform in shape, though irregular compared with slabs, infinite cylinders, spheres, infinite rods or rectangular bricks.

The first shape was the frustum of a square pyramid shown in Figs. 5.24 and 5.28. It was constructed from polypropylene plastic sheet in exactly the same manner as that used for rectangular brick shapes (Sec. 5.7.1). The other two irregular three-dimensional shapes were an ovoid (egg) shape and an fish shape smoothed to obtain a completely convex surface. To provide information about surface heat transfer conditions, two similarly sized regular spheres were used. Casts of each shape were made. For the egg shape, a two-dimensional cross-sectional profile was drawn and a block of wood turned in a lathe to this shape. The full wooden egg was set in plaster of paris so that two identical halves could be moulded. The plaster provided a flat surface to form a flange so the two halves could be joined together. An albacore tuna was frozen and then cut in half lengthwise down the backbone. A negative plaster of paris cast was then made of one half.

From this positive fish shaped casts were reconstructed. The spherical plaster of paris cast was made in the hollow metal hemispheres used to make the 0.128 m diameter sphere for thawing of regular shapes. The metal sphere was not suitable for moulding directly.

The casts were used to vacuum heat mould two halves for each object from CAB ethyl acetate plastic sheet. The fish, egg and two sphere moulds constructed were all of comparable size and curvature so that the vacuum moulding of the plastic gave similar thicknesses of plastic over each of the moulds. The casts had no concave sections so that bridging of the plastic between ridges on the cast was not a problem and the plastic mould closely resembled and fitted the original cast.

Each plastic half mould was filled with Tylose. Thermocouples were introduced to various pre-determined points in a similar manner to that used for two-dimensional irregular shapes. Holes were drilled in the plastic for the individual copper or constantan wire leads. The wires were joined and tensioned in the appropriate place in the shapes and the holes sealed by epoxy resin. Six thermocouples; two on the surface and four located internally, were used for each shape, except for the two spheres which each had three surface thermocouples and one at the geometric centre. One thermocouple was always placed as close as possible to the thermodynamic centre estimated by finite element analysis. The filled halves of the plastic objects were joined together and the plastic flanges held together with a solvent glue and screws. In this way the objects were totally sealed against liquid ingress.

The three shapes are shown in Fig. 5.25 to 5.28. All the shapes had a bolt attached through the flange to allow connection to the sample oscillator. The liquid immersion tank was used.

5.9.2 Dimensional Control and Measurement

The measurements of the moulded plastic objects were taken directly from the wood or plaster casts. The wooden egg closely followed the mathematical relationship for an ovoid because it was turned to fit a specific profile. Similarly, the moulds for the spheres and the

frustum of the square pyramid were uniform or flat sided and could be accurately measured. The fish shape was naturally derived and irregular in all respects except for a lengthwise plane of symmetry between the two halves. To accurately model it, the plaster cast was cut and the cross-sections at thirteen evenly distributed points along the length of the object mapped. The shape of the fish surface was then interpolated between these cross-sections. It was found that each of the cross-sections was closly approximated if a further vertical axis of symmetry was assumed. Hence only one quarter of the fish was modelled. Using these methods and because the plastic mould closely resembled the original casts the error in determining the surface shape and critical dimensions was considered to be ±2 mm at any point for both the fish and the egg, ±1.0 mm for the spheres and ±0.5 mm for the pyramid.

The characteristic thickness was determined from the grids shown in Fig. 5.24 to 5.27 once the thermodynamic centre was pinpointed by finite element analysis for typical phase change conditions. The measurements taken off the casts were confirmed by some measurements on the actual test objects. There was no observable difference in size or shape as the objects changed from the frozen to the unfrozen states.

5.9.3   Control and Measurement of Surface Heat Transfer Coefficient

The polypropylene pyramid was identical in all respects to the polypropylene rectangular brick shapes constructed previously for water immersion thawing (Sec. 5.7) and for brine immersion freezing (Cleland 1977), except for the irregularities in shape. The surface heat transfer coefficient had been found to be equal in both the rectangular brick freezing experiments using brine (Cleland 1977) and the thawing experiments using water. The same h value was assumed to hold for the polypropylene pyramid and no further experiments relating to it were undertaken. The error in the value of h for the polypropylene pyramid should be of the same order as that for thawing of the polypropylene rectangular bricks (1.5%). The sample was oscillated in a similar manner to that used for rectangular bricks.

For the plastic mould shapes, h cannot be measured directly without substantial difficulty. Hence the analagous regular spherical shapes constructed from the same plastic material, and the methods of Sec. 5.6.3, were used to measure h. Twelve separate heating and cooling runs without phase change, both above and below the phase change temperature range, for the two sphere shapes were undertaken. None of the differences between runs, between values for the two spheres or the correlation of h with temperature were statistically significant at the 95% confidence level. The error in the average value determined by the variablilty of replicates was ±21%. It was assumed that the h value determined in this way accurately represented h for the egg and fish shapes as wall thicknesses were essentially the same for all test objects, and the degrees of curvature were approximately equivalent. Some plastic thickness variation was noted, even between the two spheres moulded from identical casts, due to factors that were not controllable. During moulding the plastic tended to spread out thinly over some regions and accumulate at other parts. The effect was relatively randomly distributed except near the flanges for each half where the plastic was always thicker. Hence, there was in practice some violation of the assumption that external heat transfer was uniform on all surfaces of the test objects. No practical way to avoid this problem was found, so it was decided to carry out the experiments with the moulds as they were, and accept the consequential loss of accuracy in calculations for which a constant h value was assumed.

5.9.4 Analysis of Heat Transfer for Three-Dimensional Irregular Shapes

Sources of error for the three-dimensional irregular shapes were similar to those for other shapes. Problems with voids, inhomogeneity due to thermocouple wires, heat conduction along thermocouple wires and errors in placement of thermocouples were similar to those for two-dimensional irregular shapes and were consequently considered negligible. Because a thermocouple could not necessarily be located exactly at the thermodynamic centre (but usually close by), the breakpoint analysis was used to accurately determine experimental freezing and thawing times.

The three-dimensional shapes meant that end heat transfer effects were not a problem. Only the pyramid shape was affected by the presence of a bolt inserted through the wall. As was the case for rectangular brick thawing, the presence of this bolt was found to be insignificant. Disruptions due to the modular nature of the plastic moulds affected heat transfer. The flange retained on each half of the plastic moulds allowed a strong join to be made and it also allowed the attachment to the sample oscillator without further disruption to the object surface. The flange for the plastic moulded shapes ran in a lengthwise circumference around each shape. It therefore affected part of the surface area but the regions on the surface closest to the thermodynamic centre were only slightly affected. The effect of the flange on the surface heat transfer was considered unavoidable. As has been indicated, a lower degree of accuracy in these experiments was accepted.

Imperfect contact was a similar problem for the plastic moulded shapes to that which occurred for infinite cylinders, spheres and the two-dimensionally irregular shapes. As before, it was considered that the effect was equally frequent for all shapes and randomly distributed over the surface so that the effect on surface or overall heat transfer was not significant and could be accurately accounted for by an average surface heat transfer coefficient. Finite element predictions for the plastic shapes (Sec. 8.4) tend to show that surface heat transfer conditions were not uniform and that alternative means to control and measure h would be needed if experiments with less uncertainty were considered essential. In spite of these problems, the shape of the temperature profile for a thermocouple situated near the thermodynamic centre (predicted by finite element analysis assuming uniform surface heat transfer conditions), suggested that the non-uniformities at the surface had not moved the thermodynamic centre much, and that thawing times could be determined from this thermocouple by the breakpoint analysis.

For three-dimensional irregular shapes the uncertainty associated with controlling the surface heat transfer conditions by use of the plastic moulding could not be assessed. However the error in measuring h was large and there are further significant errors in measuring and

modelling the shapes of each object accurately. Other sources of uncertainty are of the same order of magnitude to those in the other experiments. Consequently, the overall experimental error for the three-dimensionally irregular shapes moulded from plastic was larger than for other shapes. This must be considered when comparing freezing and thawing time prediction methods with the experimental data. The exception was the polypropylene pyramid shape for which the overall experimental error was of the same order of magnitude as occurred for the thawing of rectangular bricks as the experimental techniques used were almost identical.
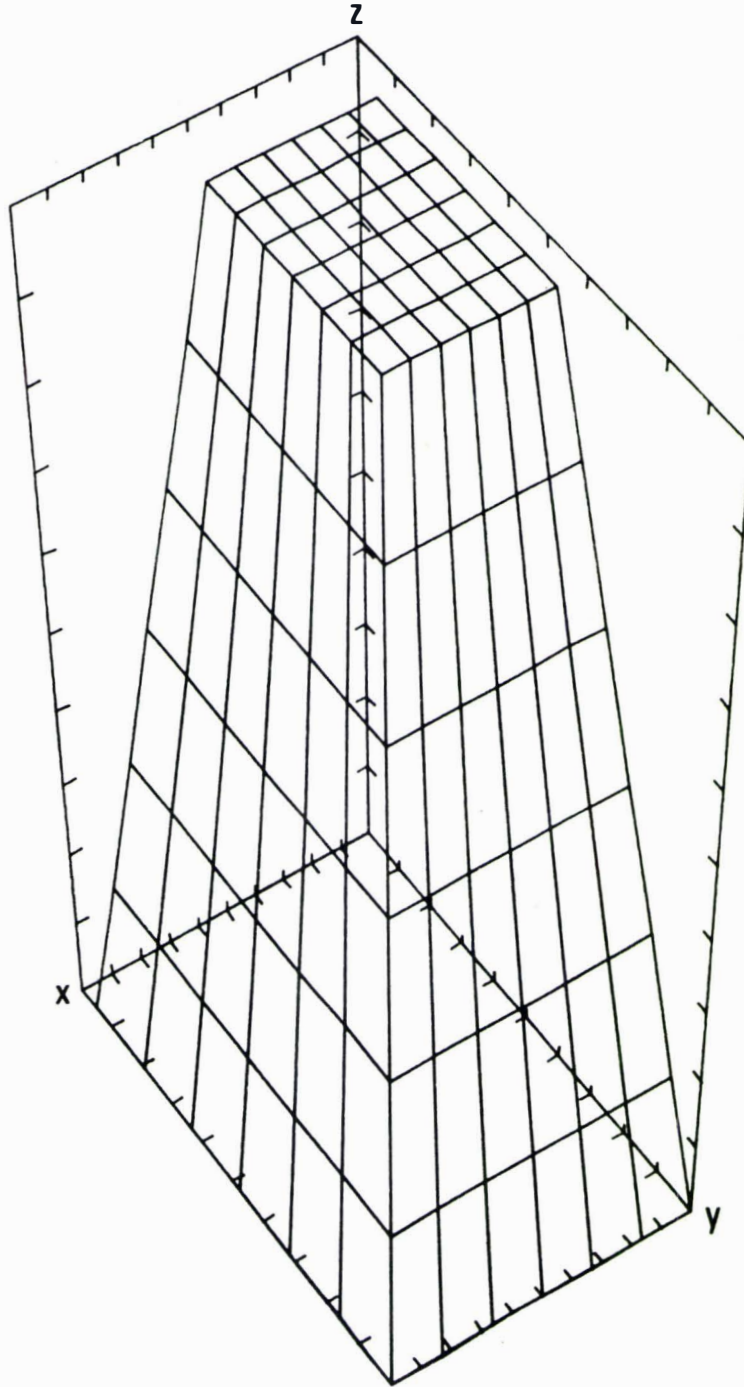
Fig. 5.24 The Pyramid Three-Dimensional Irregular Shape Finite Element
          Method Grid.
          Only a quadrant of the shape is modelled. The x,z and y,z
          faces are planes of symmetry. Only the boundary surface
          grids are shown. The x,y face is also a boundary surface.
          Scale - in the x direction 1 division = 0.005 m, in the y
          direction 1 division = 0.008 m and in the z direction 1
          division = 0.016 m.
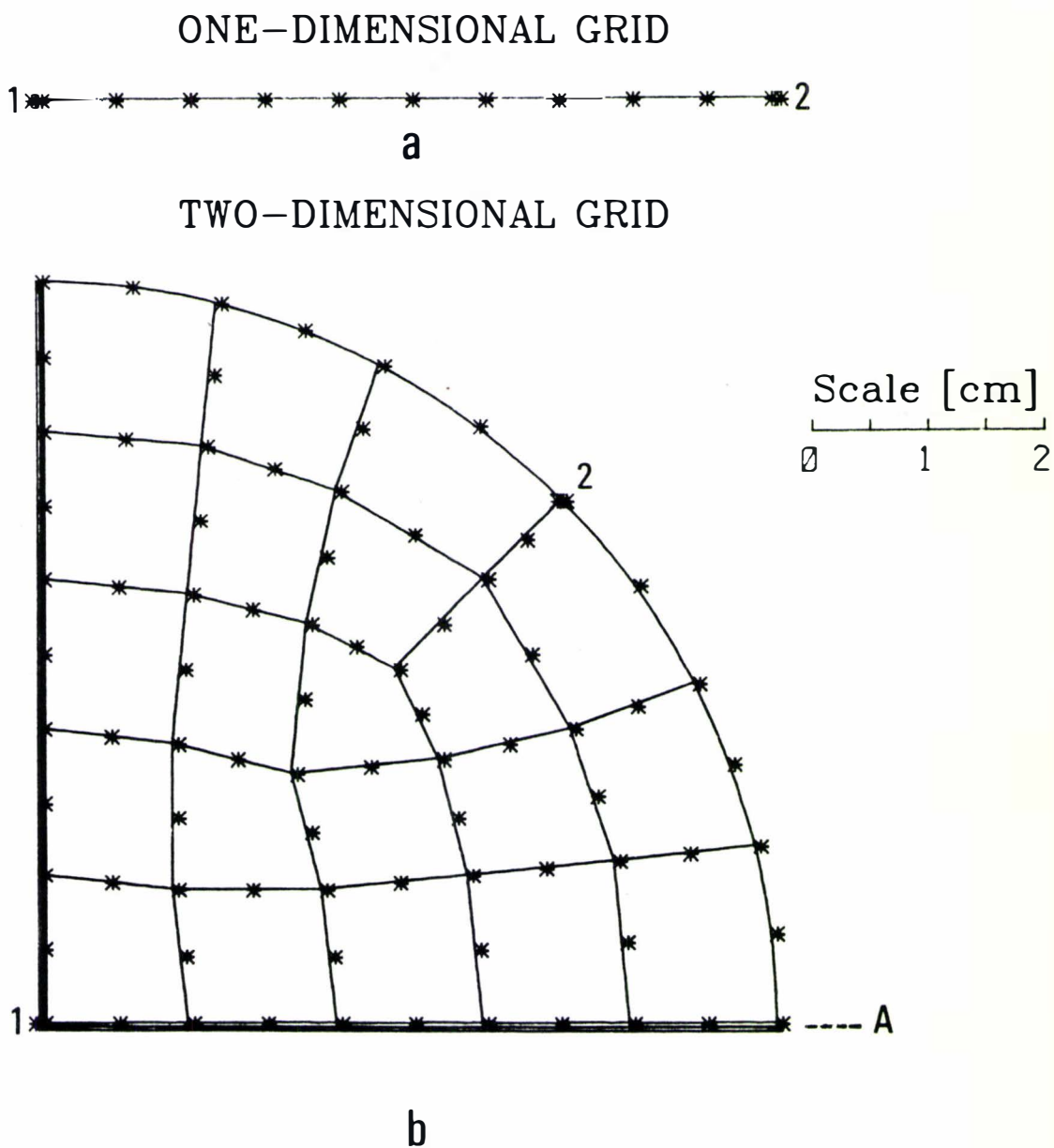
ONE–DIMENSIONAL GRID

a

TWO–DIMENSIONAL GRID

b

Fig. 5.25 The Sphere Three-Dimensional Irregular Shape Finite Element
Method Grids.

(a) and (b) the one- and two-dimensional grids

* - nodes, ** - nodes corrosponding to thermocouple

positions, _ - element boundaries, ≋ - planes of symmetry,

A - axis of rotational symmetry.

(c) the three-dimensional grid (p. 116).
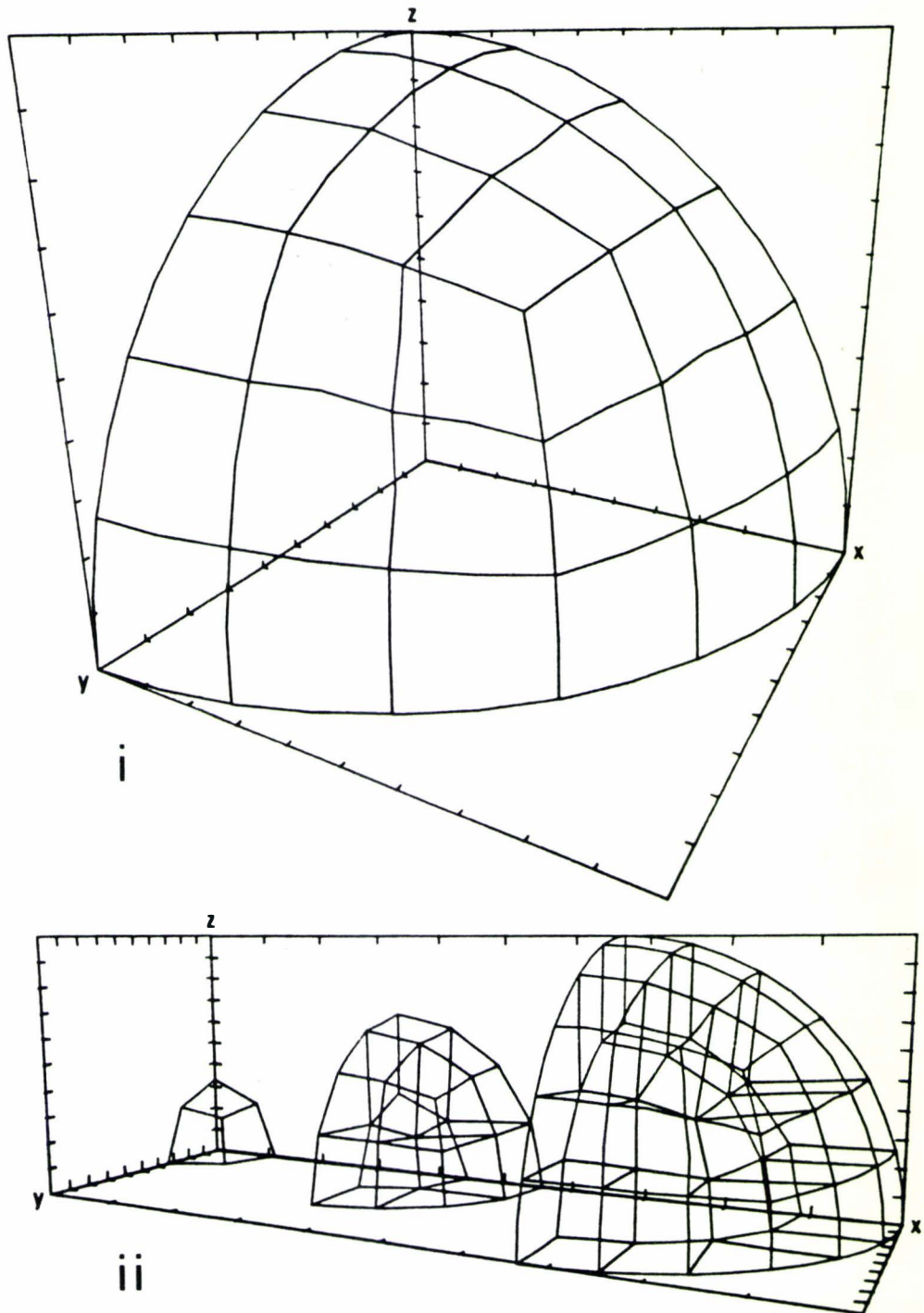
Fig. 5.25 The Sphere Three-dimensional Irregular Shape Finite Element
        Method Grids.
                (a) and (b) the one- and two-dimensional grids (p. 115)
                (c) the three-dimensional grid. Only an octant is modelled.
                The x,z and y,z faces are planes of symmetry. Scale for the
                three-dimensional grid is 1 division = 0.00635 m.
                (i) only the boundary surfaces are shown.
                (ii) an exploded view of the full sphere grid; each of the
                three shells of elements are shown.

TWO−DIMENSIONAL GRID
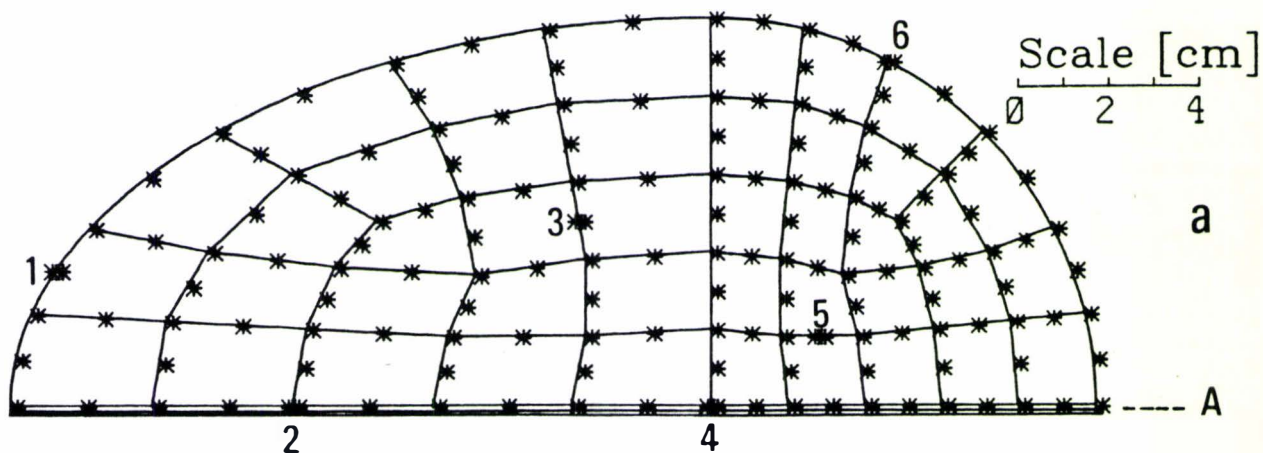
THREE−DIMENSIONAL GRID
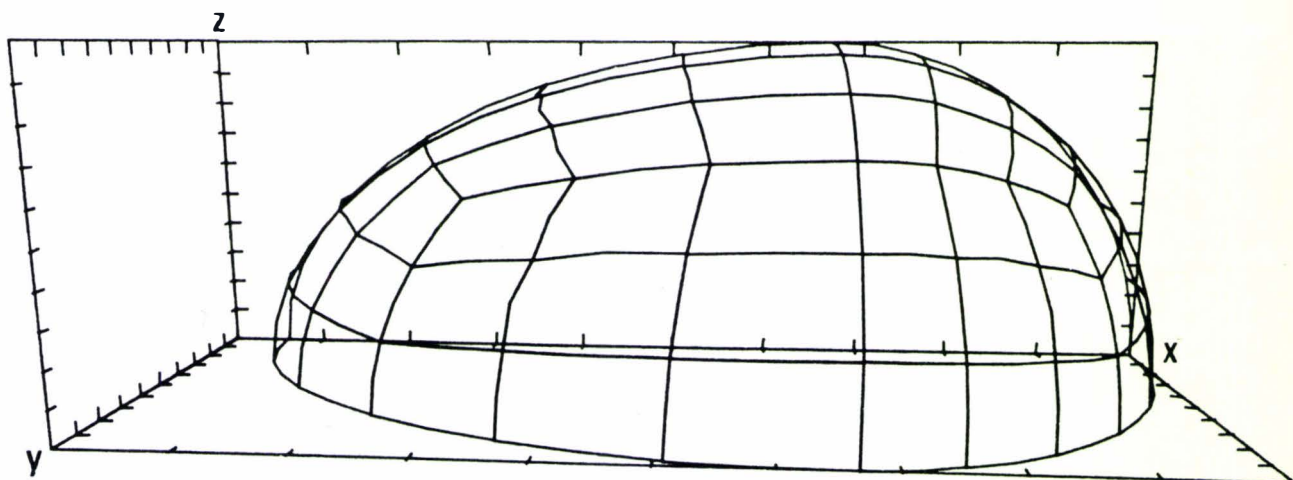
Fig. 5.26 The Egg Three-Dimensional Irregular Shape Finite Element
Method Grids.
  (a) the two-dimensional grid. * - nodes, ** - nodes
  corrosponding to thermocouple positions, _ - element
  boundaries, A - axis of rotational symmetry.
  (b) the three-dimensional grid. Only a quadrant is modelled.
  The x,y and x,z faces are planes of symmetry. Only the
  boundary surface grid is shown. The full grid is an
  elongated, double version of the sphere three-dimensional
  grid (Fig. 5.25c). Scales: in the x direction 1 division =
  0.0255 m, in the y and z directions 1 division = 0.0085 m.
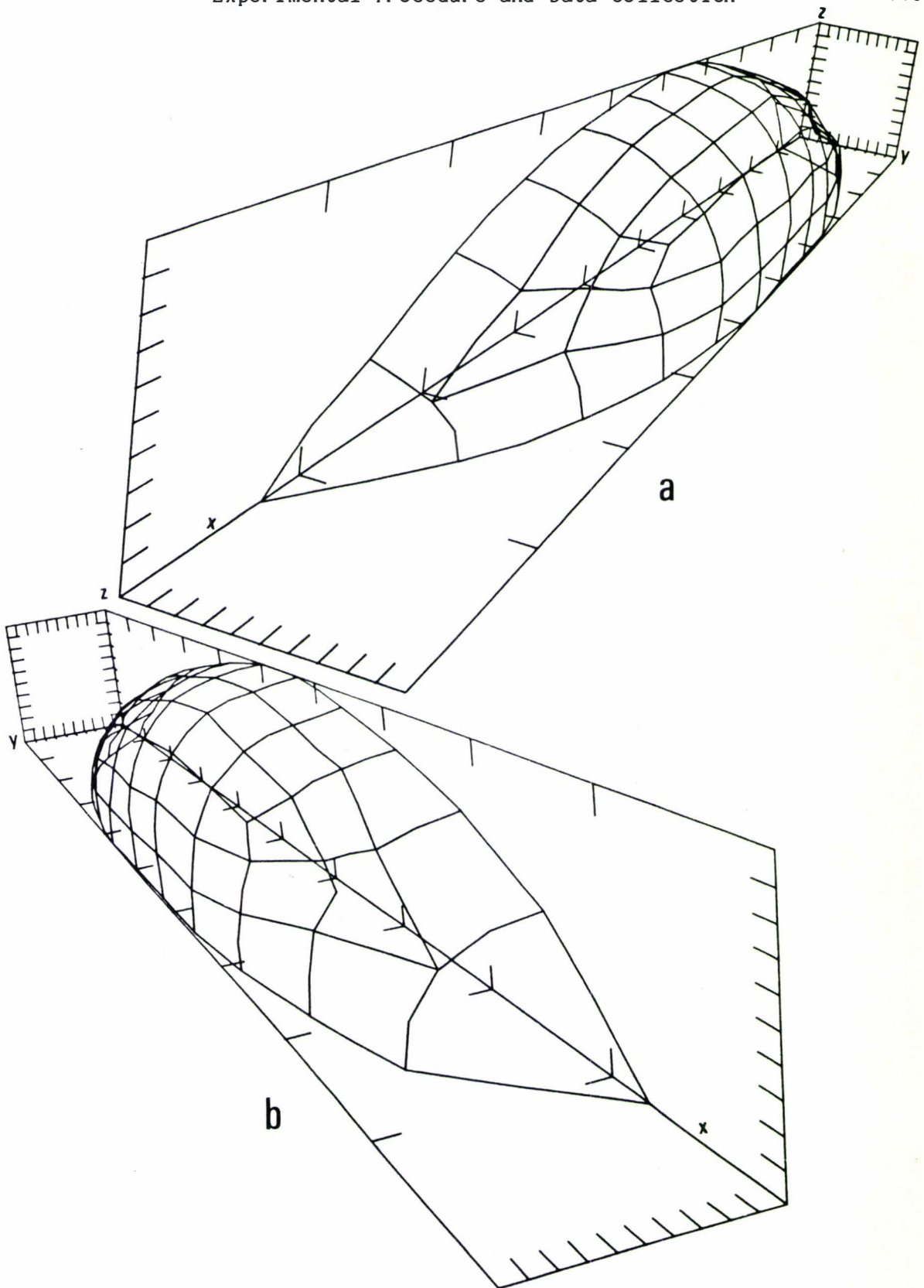
Fig. 5.27 The Fish Three-Dimensional Irregular Shape Finite Element
Method Grid. Only a quadrant is modelled. The x,y and x,z
faces are planes of symmetry. Only the boundary surface grid
is shown. The full grid is a distorted version of the egg
three-dimensional grid (Fig. 5.26b). Scales: in the x
direction 1 division = 0.060 m, in the y direction 1 division
= 0.007 m and in the z direction 1 division = 0.006 m.

(a) viewed from the tail, (b) viewed from the head.
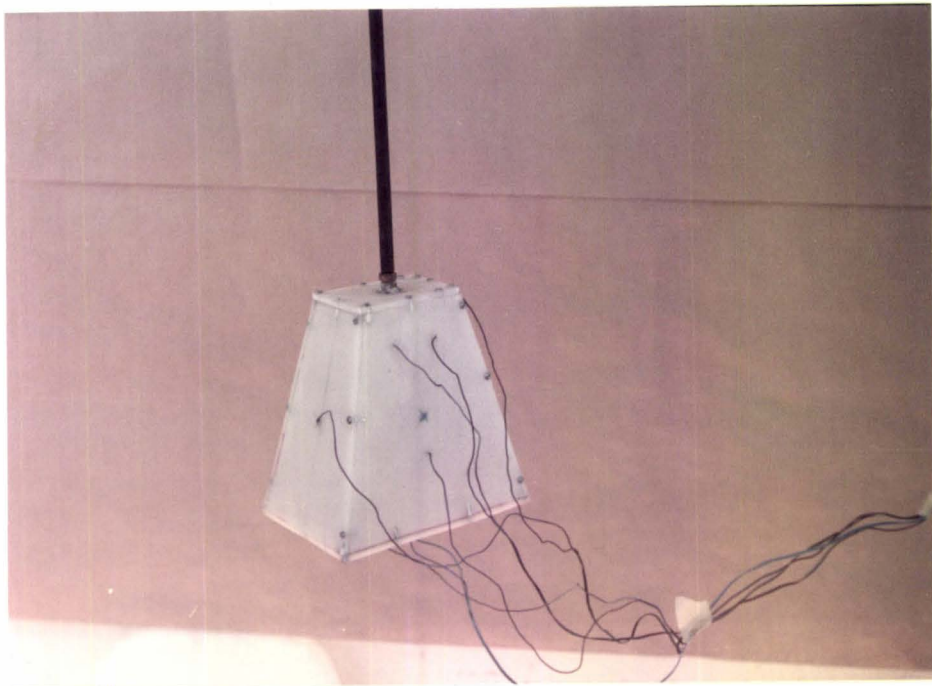
a
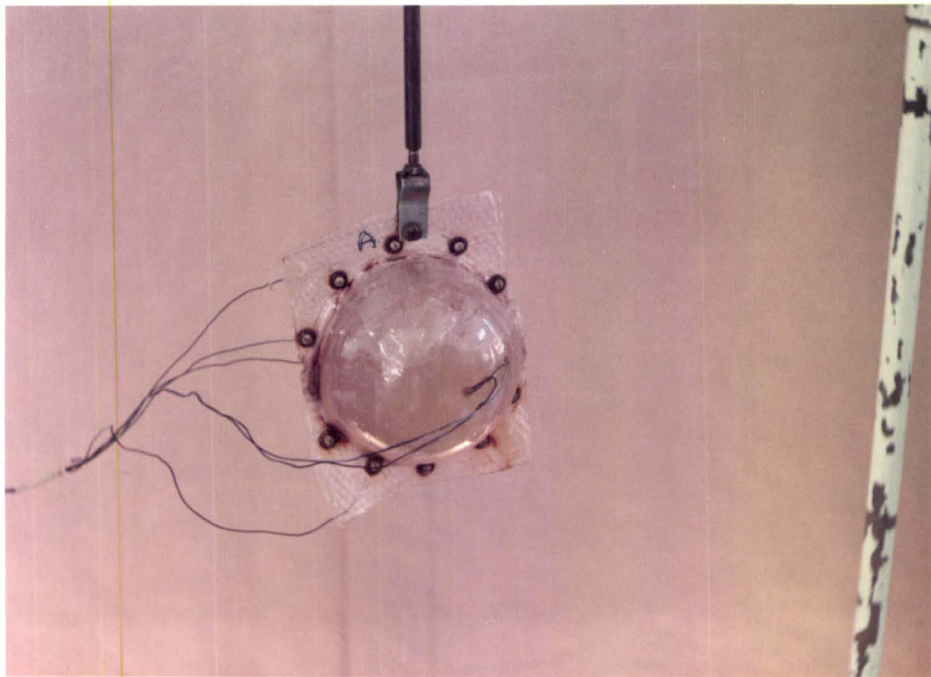
b

Fig. 5.28 The Sample Oscillator and Three-Dimensional Irregular Shapes
Used in the Liquid Immersion Tank.

(a) pyramid

(b) sphere

(c) egg (p. 120)

(d) fish (p. 120).
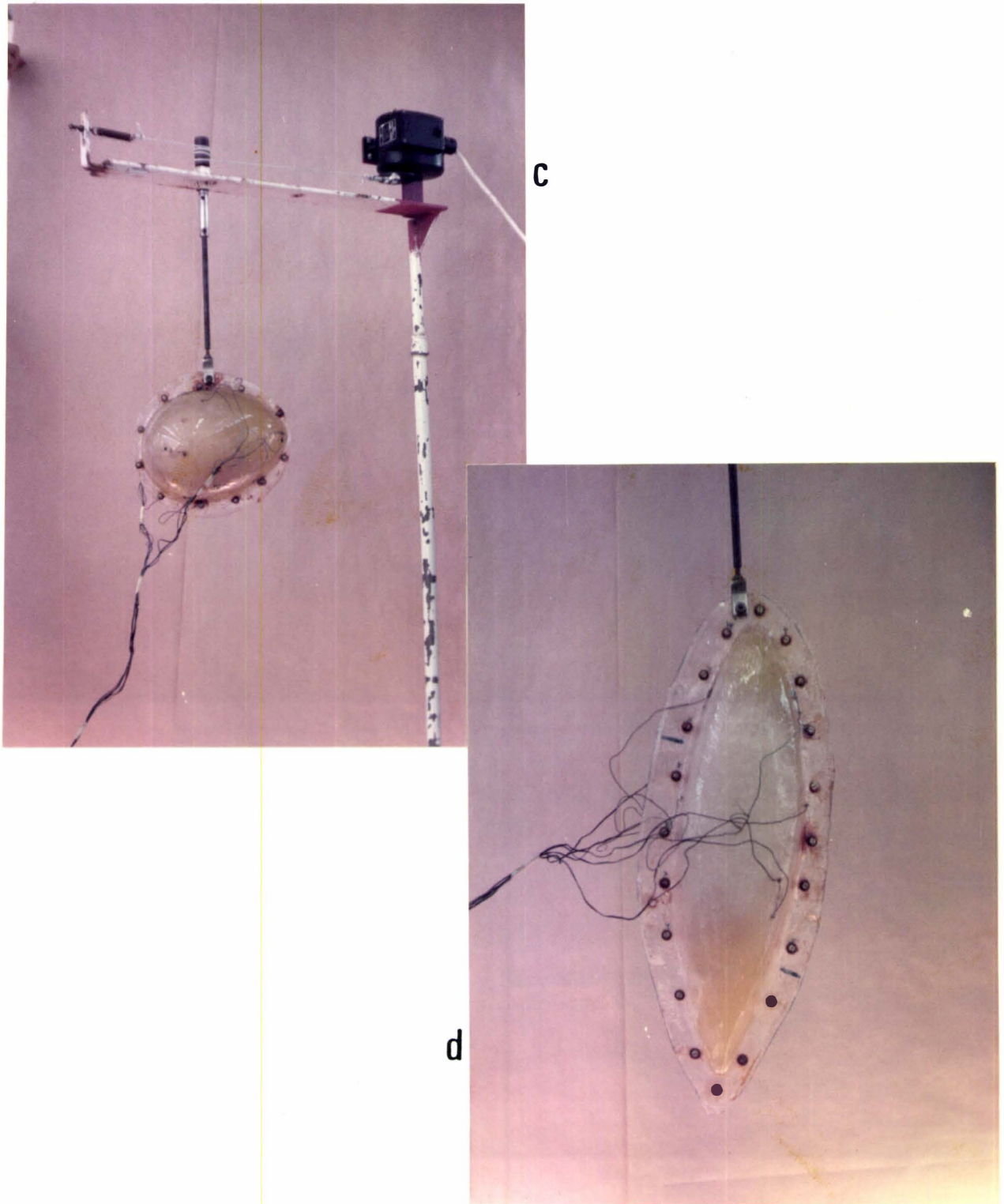
C

d

Fig. 5.28 The Sample Oscillator and Three-Dimensional Irregular Shapes
        Used in the Liquid Immersion Tank.
        (a) pyramid (p. 119)
        (b) sphere (p. 119)
        (c) egg
        (d) fish

6   EXPERIMENTAL DESIGN AND RESULTS

6.1   INTRODUCTION

To investigate the accuracy of methods for predicting freezing and thawing times for food, experiments must be conducted for a wide range of conditions covering those that occur in practical freezing and thawing situations.   In Chap. 3 five objectives for the present work were defined. The first two of these related to data collection so that prediction methods could be assessed:

(1) to collect thawing data for the basic slab, infinite cylinder, sphere and rectangular brick shapes

(2) to collect freezing and thawing data for other (irregular) shapes. It was decided to consider each shape separately and to limit the range of freezing and thawing conditions to situations described in Table 3.2. Essentially, this meant that the study was limited to homogeneous materials and constant conditions.   Even after these restrictions on the range of conditions are applied, seven important factors affecting freezing or thawing time can be identified (Table 3.3).

Pham (1983) used dimensional analysis to show that the six factors other than shape can be related by seven dimensionless groups to the freezing or thawing time. These are the Fourier number, the Biot number,   the Stefan number, the Plank number and three other dimensionless numbers.   The Fourier number:

$$\text{Fo} = \frac{k_s\,t}{C_s D^2} \text{ for freezing, } \text{Fo} = \frac{k_l\,t}{C_l D^2} \text{ for thawing} \tag{6.1}$$

takes account of the object size, the phase change time and the thermal properties of the material in the state it will be in after the phase change process has occurred. The Biot number:

$$\text{Bi} = \frac{hD}{k_s} \text{ for freezing, } \text{Bi} = \frac{hD}{k_l} \text{ for thawing} \tag{6.2}$$

is the ratio of internal to external resistances to heat transfer. The Stefan number:

$$\text{Ste} = \frac{C_s(T_{if}-T_a)}{\Delta H} \text{ for freezing, } \text{Ste} = \frac{C_l(T_a-T_{if})}{\Delta H} \text{ for thawing} \tag{6.3}$$

accounts for the ambient medium temperature and relates the heat
transfer after the phase change process to that due to latent heat
release or absorption itself. The Plank number (Cleland & Earle
1976b):

$$Pk = \frac{C_l(T_{in}-T_{if})}{\Delta H} \text{ for freezing, } Pk = \frac{C_s(T_{if}-T_{in})}{\Delta H} \text{ for thawing} \quad (6.4)$$

takes account of the initial superheating or subcooling and relates it
to the latent heat. Finally, three other numbers which take account of
the final temperature at the thermodynamic centre, T_{fin}, the initial
freezing temperature and other thermal properties of the food are:

$$N_1 = \frac{C_s(T_{if}-T_{fin})}{\Delta H} \text{ for freezing, } N_1 = \frac{C_l(T_{fin}-T_{if})}{\Delta H} \text{ for thawing} \quad (6.5)$$

$$N_2 = \frac{C_l}{C_s} \text{ and } N_3 = \frac{k_l}{k_s} \quad\quad\quad (6.6) \text{ and } (6.7)$$

In situations where it is assumed that all latent heat is released at a
unique phase change temperature the enthalpy change in the phase change
temperature region, ΔH, is defined as the latent heat of freezing or
thawing, whereas the enthalpy change between 0 °C and -10 °C is used in
all other cases. This definition ensures that ΔH includes the major
phase change effect yet is similarly defined and equally relevant for
both freezing and thawing analyses. For freezing, the very similar
definition of ΔH as the enthalpy change from T_{if} to -10 °C has been used
(Cleland 1977). This definition leads to ΔH values only 1.0% different
from ΔH from 0 °C to -10 °C and is therefore treated as being equivalent
in this study. This definition is also commensurate with an
alternative used by Hung & Thompson (1983) where ΔH was taken as the
enthalpy change from T_{in} to T_{fin}.

Both Hayakawa et al (1983a) and Succar & Hayakawa (1984) performed
numerically based screening experiments that showed that for slab and
infinite cylinder freezing over a range of typically encountered
conditions only five parameters, described in terms of Bi, Ste and Pk
above, had a statistically significant effect on the freezing time
(Fo). Neither the thermodynamic centre temperature nor the ratio of
the unfrozen to the frozen thermal properties (N_1, N_2, N_3) were
significant. Similar results would be expected for thawing. Cleland &
Earle (1984b) show that the effect on freezing time of different final
thermodynamic centre temperatures can be accurately related to the

Stefan number in a simple manner. For these reasons, and those outlined in Sec. 2.2.3 only freezing to a single final thermodynamic centre temperature of -10°C and thawing to 0°C were investigated experimentally.

Most foods, frozen or thawed inductrially are predominantly aqueous in composition and consequently the initial freezing temperature, T_{if}, and the ratios of the thermal properties, N_2 and N_3, differ only slightly for different foods (Table 6.1). For this reason only one typical phase change material (Tylose) was used and the changes in N_2 and N_3 were not considered of major practical importance. Some runs with a food material, minced lean beef, were performed to see if any noticeable effect due to N_2 or N_3 could be observed. A study encompassing a range of materials (Cleland & Earle 1984a) showed little deviation between predictions for the different food materials used, confirming this reasoning.

The full functional dependence of the phase change time to a given endpoint temperature, on the conditions considered in this work and the thermal properties is therefore given by:

$$Fo = f (Bi, Ste, Pk, geometry) \qquad\qquad (6.8)$$

The variables that were manipulated in order to investigate this relationship were the size, D, the surface heat transfer coefficient, h, the ambient medium temperature, T_a, the initial temperature, T_{in} and the object shape. To isolate the effect of geometry the other four variables were varied independently for a variety of different shapes. Table 6.1 shows typical values of these variables for common freezing and thawing processes. An experimental design was sought in which these variables were varied over as wide a range as possible within the the limitations of the experimental equipment.

Orthogonal experimental designs in terms of Bi, Ste and Pk were not feasible because of physical limitations in controlling the four variables, especially h and D, to pre-selected values. The object size and the surface heat transfer coefficients were, in most cases, determined more by considerations such as the availability of the appropriate types of container and their wall material, than by choice to give a specified Biot number. Variation in Bi was therefore

difficult to achieve and evenly spaced levels required for an orthogonal design were not practicable. Consequently it was decided to vary the Biot number as widely as possible by using different combinations of container size and wall materials. The addition of insulating rubber layers for some shapes gave some control and variability of h.

At each level of Biot number T_a and T_{in}, and hence Ste and Pk, were also varied to cover as wide a range and combinations of conditions as possible. The basis for the experimental design in these cases were either part or full factorial designs with two or three levels of T_a and T_{in}. It was decided not to attempt to control these two variables exactly to the pre-selected levels; provided a value close to the pre-selected level was obtained, it was considered satisfactory.

6.2   THAWING OF SLABS

For experiments using Tylose it was chosen to vary h and D to give seven approximately evenly spaced levels of Bi. At each of the extreme values, experiments at a central level of both T_a and T_{in} were performed. At each of the five intermediate Bi levels a factorial design with T_a and T_{in} each at two levels plus one centrepoint was conducted and some other runs at intermediate levels were made. Evenly spaced levels of 1/Ste, corrosponding to T_a values of about 5°C, 13°C and 45°C, and Pk with values of T_{in} of about -10°C, -20°C and -30°C were used, with h varying from 13.2 W m^{-2} °C^{-1} to 172.7 W m^{-2} °C^{-1} and D from 0.026 m to 0.105 m respectively. This design was considered to give a satisfactory data base for assessment of thawing time prediction methods.

The results of the full set of 35 slab thawing experiments including replicates to estimate the experimental error are shown in Table 6.2. Typical thawing temperature/time profiles are shown in Fig. 6.1. The replicates were performed as independently from each other as possible to give a true indication of variability due to experimental techniques. The only variable that could not be measured independently from the other slab experiments was the surface heat transfer coefficient. Any additional uncertainty introduced by errors in

measurement, and due to systematic error, could not be quantified from the spread of replicates.

Six thawing experiments were conducted with minced lean beef for a representative range of conditions to check that experiments with Tylose gave results consistent with those for real foodstuffs, and that N_2 and N_3 were not parameters significantly affecting prediction method accuracy. Results for the minced lean beef experiments are given in Table 6.8 and Fig. 6.17 is a typical temperature/time profile.

6.3   THAWING OF INFINITE CYLINDERS

For infinite cylinders the range of Biot numbers that could be considered was physically limited by the cylinder diameters and pipe wall materials and thicknesses used. By use of both metal and PVC walled cylinders and the addition of rubber insulation a range of h from 19.0 W m^{-2} ^{o}C^{-1} to 113.0 W m^{-2} ^{o}C^{-1} was obtained in the liquid immersion system.   In combination with different cylinder diameters this gave six approximate levels in Bi from 1.8 to 26.0. At each level a similar design to that used for slabs was set up to cover a wide range of ambient and initial temperature conditions.

The 34 experimental results for thawing infinite cylinders of Tylose are given in Tables 6.3, and a typical thawing curve is shown in Fig. 6.2.

6.4   THAWING OF SPHERES

Thirty-five thawing runs were conducted with Tylose spheres. A similar design to that used for infinite cylinder thawing was used. The metal walled spheres plus rubber coating gave surface heat transfer coefficients from 41.9 W m^{-2} ^{o}C^{-1} to 246.2 W m^{-2} ^{o}C^{-1}. For the three sphere diameters used there were six levels of the Biot number in the range 5.9 to 57.0.

Figure 6.3 gives a typical thawing temperature/time profile while the full set of results are given in Table 6.4.

6.5   THAWING OF RECTANGULAR BRICKS

The thawing time of a rectangular brick shaped object depends on its
geometry as well as the three parameters Bi, Ste and Pk. The shape of
a rectangular brick is defined by the ratio of each of the two longer
side lengths to the shortest (β_1 and β_2). The shortest side length is
equal to the characteristic dimension (D) so the two shape factors, β_1
and β_2, can be introduced. The experiments were designed to cover all
the five factors (Bi, Ste, Pk, β_1 and β_2) as widely as was practicable.

For each of twelve differently shaped and sized boxes a 2^2 factorial
design in Ste and Pk plus a centrepoint (corresponding to values of T_a
of 5 °C, 13 °C and 45 °C, and T_{in} of -10 °C, -20 °C and -30 °C) was
performed. The five runs for each brick were divided between two
levels of the Biot number (arising from the boxes both with and without
rubber sheets glued to the surface). The geometric factors, β_1 and β_2,
were varied from 1 to 4, this range covering practical applications.

The results for the 68 thawing experiments conducted are shown in Table
6.5. A typical thawing curve is shown in Fig. 6.4. Four thawing runs
were made with two different rectangular brick shapes using minced lean
beef.   These results is given in Table 6.8 and a typical
temperature/time profiles is shown in Fig. 6.18.

6.6   TWO-DIMENSIONAL IRREGULAR SHAPES

Eight different two-dimensional objects   were   used;   four   were
constructed by distortion of a 0.1 m diameter PVC pipe, and four from a
0.15 m diameter PVC pipe. Six of the objects were irregular in shape,
while two were cylindrical (one for each pipe size). Figs. 5.15 to
5.21 show the cross-sectional geometries for these objects. For each
shape at least four freezing and four thawing runs were conducted.

For freezing three levels of the Stefan number (corresponding to values
of T_a of about -20 °C, -28 °C and -35 °C) and four levels of the Plank
number (corresponding to T_{in} values of about 4 °C, 10 °C, 20 °C and 30 °C)
were used. A complete factorial design was not possible.   The
combinations of Ste and Pk used for individual experiments were chosen

so that the Ste and Pk levels were not statistically correlated over the full data set. For thawing a similar design to that used for the regular shapes was applied for T_a and T_{in}. The three values of h for each combination of pipe wall thickness and rubber led to eleven different levels of Biot number.

A total of 83 experiments were performed with Tylose. The results are given in Table 6.6 and Figs. 6.5 to 6.12 shown typical temperature/time profiles at different positions within each shape. As well, eight runs were conducted with minced lean beef for two of the irregular shaped objects. Table 6.8 gives the results of these experiments. Fig. 6.19 shows typical temeperature/time profiles for the minced lean beef runs.

6.7   THREE-DIMENSIONAL IRREGULAR SHAPES

Eighteen experiments were conducted with the three three-dimensional irregular Tylose objects chosen for study. The shapes are shown in Figs. 5.25 to 5.27. An additional six runs were performed using two spheres. The experimental design used was similar to that used for two-dimensional irregular shapes. Each shape was both frozen and thawed over a range of ambient and initial temperatures. The Biot number was completely pre-set for each shape by the material and size of construction for each object. Table 6.7 gives the full set of results. Figs. 6.13 to 6.16 show typical temperature/time profiles.

Table 6.1 <u>Typical Conditions in Food Freezing and Thawing Processes</u>

		Freezing	Thawing
D	(m)	0.001 to 0.5	0.001 to 0.5
h	$(W\ m^{-2}\ ^\circ C^{-1})$	7 to 600	2 to 10 000
Bi		0.05 to 60	0.01 to 1000
T_a	($^\circ$C)	-15 to -40	5 to 50
Ste		0.12 to 0.35	0.07 to 0.9
T_{in}	($^\circ$C)	0 to 40	-10 to -35
Pk		0 to 0.6	0.06 to 0.3
T_{fin}	($^\circ$C)	-10 to -30	0 to 10
N_1		0.05 to 0.25	0.01 to 0.1
N_2		1.7 to 2.0	1.7 to 2.0
N_3		0.27 to 0.35	0.27 to 0.35

Table 6.2 <u>Experimental Data For Thawing of Slabs of Tylose</u>

Run Number	D_x (m)	h (W m^{-2} °C^{-1})	T_a (°C)	T_{in} (°C)	t_{exp} (hrs)
T1	0.0260	13.2	12.8	-20.9	4.69
T2	0.0260	24.5	5.2	-29.4	5.63*
T3	0.0525	13.2	5.2	-11.4	19.32
T4	0.0260	24.5	45.9	-8.3	0.90
T5	0.0525	13.2	46.1	-28.6	3.89
T6	0.0525	13.2	12.8	-20.5	10.33
T7	0.0260	50.4	4.6	-26.3	3.49
T8	0.0525	24.5	5.2	-10.7	13.20
T9	0.1000	13.2	45.9	-8.3	7.82*
T10	0.1020	13.2	43.0	-13.7	8.83
T11	0.0770	18.2	46.2	-26.8	5.11
T12	0.0525	29.5	12.8	-20.9	6.26*
T13	0.0770	37.3	5.2	-30.2	18.49
T14	0.0525	50.4	5.1	-25.0	9.41
T15	0.0260	78.1	5.2	-12.3	2.51*
T16	0.1000	24.5	12.8	-9.4	16.92
T17	0.0525	50.4	46.0	-10.6	1.64
T18	0.0770	37.3	46.1	-24.7	3.72
T19	0.1000	24.5	45.8	-32.5	6.75
T20	0.0260	78.1	12.4	-27.7	1.42
T21	0.0525	50.4	13.4	-20.2	4.68
T22	0.0525	50.4	13.4	-24.1	4.65
T23	0.0525	50.4	13.4	-23.6	4.60
T24	0.0525	50.4	13.4	-23.6	4.50
T25	0.0525	78.1	5.2	-28.9	7.58*
T26	0.1050	37.3	5.2	-10.4	29.33
T27	0.0770	50.4	45.7	-13.5	2.99
T28	0.0280	172.7	43.0	-31.0	0.43
T29	0.0525	78.1	13.3	-22.5	3.91*
T30	0.1050	78.1	5.2	-28.8	23.62
T31	0.0770	78.1	5.0	-14.2	14.39
T32	0.0770	78.1	45.7	-9.4	2.61
T33	0.1000	78.1	46.2	-28.2	4.59
T34	0.0770	78.1	12.9	-21.0	7.25
T35	0.1050	172.7	13.4	-23.8	10.61

* indicates a run in which edge heat transfer was calculated to be greater than 1.0%.

Table 6.3 Experimental Data For Thawing of Infinite Cylinders of Tylose

Run Number	D_r (m)	h (W m^{-2} °C^{-1})	T_a (°C)	T_{in} (°C)	t_{exp} (hrs)
C1	0.158	23.5	43.3	-14.0	7.34
C2	0.158	23.5	21.1	-20.6	12.43
C3	0.158	23.5	5.1	-28.4	34.41
C4	0.156	90.7	43.2	-11.9	5.31
C5	0.156	90.7	13.0	-13.6	12.30
C6	0.156	90.7	5.1	-27.9	23.74
C7	0.156	43.5	40.3	-21.2	6.09
C8	0.156	43.5	11.9	-27.4	15.40
C9	0.156	43.5	8.2	-26.9	19.21
C10	0.156	43.5	5.3	-14.9	25.70
C11	0.106	113.0	43.3	-10.7	2.47
C12	0.106	113.0	8.5	-20.2	7.94
C13	0.106	113.0	5.1	-28.8	11.36
C14	0.103	37.4	43.3	-30.5	3.26
C15	0.103	37.4	13.0	-14.5	7.25
C16	0.103	37.4	5.3	-10.6	13.89
C17	0.103	25.1	40.3	-10.6	3.79
C18	0.103	25.1	18.7	-14.1	6.63
C19	0.103	25.1	13.2	-14.4	8.84
C20	0.103	25.1	5.3	-31.2	16.73
C21	0.103	19.5	43.9	-26.9	4.33
C22	0.103	19.5	18.3	-14.9	7.54
C23	0.103	19.5	5.8	-13.1	18.20
C24	0.051	46.5	44.0	-10.6	0.87
C25	0.051	46.5	8.5	-11.9	2.93
C26	0.051	46.5	5.1	-10.0	4.22
C27	0.051	27.9	40.3	-11.8	1.30
C28	0.051	27.9	18.9	-26.5	2.49
C29	0.051	27.9	13.2	-18.5	3.00
C30	0.051	27.9	5.3	-28.0	5.96
C31	0.051	19.0	43.9	-28.1	1.64
C32	0.051	19.0	14.6	-18.2	3.76
C33	0.051	19.0	9.6	-28.2	5.03
C34	0.051	19.0	5.8	-12.1	7.15

Table 6.4 Experimental Data For Thawing of Spheres of Tylose

Run Number	D_r (m)	h $(W\ m^{-2}\ ^{\circ}C^{-1})$	T_a ($^{\circ}C$)	T_{in} ($^{\circ}C$)	t_{exp} (hrs)
S1	0.128	246.2	43.3	-9.7	2.26
S2	0.128	246.2	21.1	-25.3	3.92
S3	0.128	246.2	13.0	-19.7	5.42
S4	0.128	74.8	44.0	-15.1	2.66
S5	0.128	74.8	18.3	-18.8	4.78
S6	0.128	74.8	11.9	-23.1	6.39
S7	0.128	74.8	5.3	-26.5	11.33
S8	0.128	51.6	43.3	-27.9	2.76
S9	0.128	51.6	22.0	-18.8	4.31
S10	0.128	51.6	14.5	-20.3	5.81
S11	0.128	51.6	5.1	-15.5	12.26
S12	0.128	41.9	43.6	-20.3	3.13
S13	0.128	41.9	12.0	-33.0	7.63
S14	0.128	41.9	5.5	-17.1	12.82
S15	0.112	76.0	43.9	-14.5	1.89
S16	0.112	76.0	8.0	-13.9	5.96
S17	0.112	76.0	5.3	-28.0	7.87
S18	0.112	59.4	43.6	-27.1	2.02
S19	0.112	59.4	14.5	-16.6	4.05
S20	0.112	59.4	5.0	-18.2	9.02
S21	0.112	45.7	43.6	-30.2	2.43
S22	0.112	45.7	8.9	-32.9	7.18
S23	0.112	45.7	5.5	-17.4	9.67
S24	0.056	137.2	18.3	-16.9	0.86
S25	0.056	137.2	11.9	-13.4	1.15
S26	0.056	137.2	5.3	-23.5	2.08
S27	0.056	87.0	43.6	-14.2	0.58
S28	0.056	87.0	22.2	-20.3	0.87
S29	0.056	87.0	14.5	-14.8	1.11
S30	0.056	87.0	7.0	-22.8	1.88
S31	0.056	87.0	5.0	-24.7	2.33
S32	0.056	57.5	43.6	-22.8	0.67
S33	0.056	57.5	22.3	-14.9	1.06
S34	0.056	57.5	12.1	-21.7	1.58
S35	0.056	57.5	5.5	-16.3	2.67

Table 6.5 <u>Experimental Data For Thawing of Rectangular Bricks of Tylose</u>

Run Number	D_x (m)	D_y (m)	D_z (m)	h (W m^{-2} $^{\circ}$C^{-1})	T_a ($^{\circ}$C)	T_{in} ($^{\circ}$C)	t_{exp} (hrs)
B1	0.075	0.075	0.075	41.0	43.2	-28.5	1.67
B2	0.075	0.075	0.075	41.0	5.2	-11.9	6.86
B3	0.075	0.075	0.075	23.7	39.1	-10.5	2.05
B4	0.075	0.075	0.075	23.7	21.5	-25.3	3.22
B5	0.075	0.075	0.075	23.7	15.1	-23.7	4.07
B6	0.075	0.075	0.075	23.7	5.8	-29.9	8.07
B7	0.104	0.125	0.152	41.0	45.0	-12.0	3.50
B8	0.104	0.125	0.152	41.0	13.8	-23.3	8.35
B9	0.104	0.125	0.152	41.0	5.2	-26.5	15.98
B10	0.104	0.125	0.152	23.7	39.1	-30.8	4.92
B11	0.104	0.125	0.152	23.7	5.7	-12.4	17.65
B12	0.052	0.078	0.202	41.0	13.8	-22.5	3.45
B13	0.052	0.078	0.202	41.0	5.3	-26.4	6.88
B14	0.052	0.078	0.202	41.0	5.2	-12.4	6.84
B15	0.052	0.078	0.202	23.7	39.1	-11.6	2.05
B16	0.052	0.078	0.202	23.7	21.5	-32.0	3.42
B17	0.081	0.151	0.151	41.0	46.1	-31.0	3.16
B18	0.081	0.151	0.151	41.0	13.8	-21.8	7.09
B19	0.081	0.151	0.151	41.0	5.2	-29.4	13.49
B20	0.081	0.151	0.151	23.7	39.1	-10.7	4.10
B21	0.081	0.151	0.151	23.7	5.7	-12.9	15.81
B22	0.054	0.127	0.201	41.0	45.6	-12.1	1.84
B23	0.054	0.127	0.201	41.0	5.2	-28.3	8.59
B24	0.054	0.127	0.201	23.7	21.6	-18.7	4.45
B25	0.054	0.127	0.201	23.7	15.1	-17.7	5.72
B26	0.054	0.127	0.201	23.7	5.7	-10.5	10.66
B27	0.060	0.201	0.201	41.0	5.3	-32.0	11.92
B28	0.060	0.201	0.201	41.0	5.2	-31.0	11.50
B29	0.060	0.201	0.201	23.7	43.3	-11.9	3.13
B30	0.060	0.201	0.201	23.7	21.5	-16.9	5.46
B31	0.060	0.201	0.201	23.7	13.9	-17.2	7.44
B32	0.060	0.201	0.201	23.7	5.7	-11.8	13.82
B33	0.109	0.156	0.207	281.0	42.9	-30.0	3.60
B34	0.109	0.156	0.207	281.0	24.5	-11.8	5.29
B35	0.109	0.156	0.207	79.1	13.2	-23.8	9.63
B36	0.109	0.156	0.207	79.1	10.0	-27.9	11.80
B37	0.109	0.156	0.207	79.1	5.4	-12.1	17.00
B38	0.158	0.159	0.164	281.0	42.9	-12.0	4.53
B39	0.158	0.159	0.164	281.0	12.8	-27.9	10.54
B40	0.158	0.159	0.164	281.0	5.6	-31.4	19.05
B41	0.158	0.159	0.164	79.1	41.3	-30.0	5.75
B42	0.158	0.159	0.164	79.1	10.0	-21.7	14.70
B43	0.158	0.159	0.164	79.1	5.4	-11.6	20.86

Table 6.5 continued...   133

Run Number	D_x (m)	D_y (m)	D_z (m)	h (W m^{-2} °C^{-1})	T_a (°C)	T_{in} (°C)	t_{exp} (hrs)
B44	0.081	0.093	0.196	281.0	42.9	-9.5	1.65
B45	0.081	0.093	0.196	281.0	20.4	-12.0	2.89
B46	0.081	0.093	0.196	281.0	9.3	-11.0	5.52
B47	0.081	0.093	0.196	281.0	5.6	-10.6	7.40
B48	0.081	0.093	0.196	79.1	41.3	-29.2	2.35
B49	0.081	0.093	0.196	79.1	13.2	-12.1	5.07
B50	0.081	0.093	0.196	79.1	5.4	-29.2	9.25
B51	0.082	0.154	0.233	281.0	42.9	-29.5	2.49
B52	0.082	0.154	0.233	281.0	12.8	-13.0	5.97
B53	0.082	0.154	0.233	281.0	5.6	-8.5	10.39
B54	0.082	0.154	0.233	281.0	5.1	-10.9	11.39
B55	0.082	0.154	0.233	79.1	41.3	-11.4	3.05
B56	0.082	0.154	0.233	79.1	20.7	-22.8	5.18
B57	0.082	0.154	0.233	79.1	5.4	-19.7	12.79
B58	0.079	0.079	0.156	281.0	43.3	-29.0	1.55
B59	0.079	0.079	0.156	281.0	9.3	-10.0	4.39
B60	0.079	0.079	0.156	281.0	5.6	-22.0	6.02
B61	0.079	0.079	0.156	79.1	20.7	-11.0	2.97
B62	0.079	0.079	0.156	79.1	13.2	-21.5	4.29
B63	0.079	0.079	0.156	79.1	5.4	-28.9	7.92
B64	0.086	0.303	0.306	281.0	14.6	-22.7	6.44
B65	0.086	0.303	0.306	281.0	5.6	-11.5	11.93
B66	0.086	0.303	0.306	79.1	41.3	-10.3	3.45
B67	0.086	0.303	0.306	79.1	13.2	-23.5	8.43
B68	0.086	0.303	0.306	79.1	5.4	-27.4	15.99

Table 6.6 Experimental Data For Freezing and Thawing of Two-Dimensional Irregular Shapes of Tylose

Run Number	Shape Code	D (m)	h (W m^{-2} °C^{-1})	T_a (°C)	T_{in} (°C)	t_{exp} (hrs)
I1	1	0.1525	28.0	21.1	-15.2	9.95
I2	1	0.1525	28.0	20.8	-16.6	10.60
I3	1	0.1525	28.0	13.7	-13.7	13.79
I4	1	0.1525	28.0	13.6	-17.2	16.12
I5	1	0.1525	28.0	5.6	-16.1	26.23
I6	1	0.1525	28.0	-19.7	18.1	9.83
I7	1	0.1525	28.0	-23.6	2.8	6.77
I8	1	0.1525	28.0	-25.0	33.6	7.88
I9	1	0.1525	28.0	-27.0	19.4	7.34
I10	1	0.1525	28.0	-30.6	2.7	5.82
I11	1	0.1525	28.0	-33.9	19.4	5.45
I12	1	0.1525	28.0	-38.5	23.9	5.18
I13	2	0.1115	28.0	40.6	-12.1	5.40
I14	2	0.1115	28.0	20.3	-31.3	9.98
I15	2	0.1115	28.0	13.7	-21.9	13.28
I16	2	0.1115	28.0	13.6	-17.2	13.11
I17	2	0.1115	28.0	5.6	-31.7	24.98
I18	2	0.1115	28.0	-19.7	31.8	9.53
I19	2	0.1115	28.0	-23.7	4.3	6.31
I20	2	0.1115	28.0	-25.1	34.9	7.30
I21	2	0.1115	28.0	-26.9	20.0	6.70
I22	2	0.1115	28.0	-38.6	1.8	3.96
I23	3	0.1370	28.0	20.3	-11.2	10.17
I24	3	0.1370	28.0	13.7	-19.9	14.47
I25	3	0.1370	28.0	8.4	-19.4	18.69
I26	3	0.1370	28.0	5.6	-18.4	27.32
I27	3	0.1370	28.0	-19.8	19.5	9.31
I28	3	0.1370	28.0	-26.9	20.1	7.13
I29	3	0.1370	28.0	-30.5	32.8	6.90
I30	3	0.1370	28.0	-38.5	13.4	4.63
I31	4	0.0990	28.0	20.1	-21.5	8.98
I32	4	0.0990	28.0	13.7	-32.5	12.28
I33	4	0.0990	28.0	8.4	-13.2	16.86
I34	4	0.0990	28.0	5.6	-9.5	21.19
I35	4	0.0990	28.0	-19.8	18.1	7.82
I36	4	0.0990	28.0	-27.1	19.9	6.17
I37	4	0.0990	28.0	-38.6	19.1	4.04

Table 6.6 continued...   135

Run Number	Shape Code	D (m)	h (W m^{-2} °C^{-1})	T_a (°C)	T_{in} (°C)	t_{exp} (hrs)
I38	5	0.1050	34.2	21.1	-15.7	5.13
I39	5	0.1050	34.2	13.6	-12.7	7.19
I40	5	0.1050	34.2	8.5	-12.6	9.35
I41	5	0.1050	34.2	5.6	-32.5	15.17
I42	5	0.1050	34.2	-19.8	3.3	4.51
I43	5	0.1050	34.2	-27.2	19.3	3.78
I44	5	0.1050	34.2	-30.6	3.1	3.01
I45	5	0.1050	34.2	-39.0	32.4	2.71
I46	5	0.1050	20.3	5.3	-28.1	18.83
I47	5	0.1050	20.3	-22.2	14.9	6.27
I48	5	0.1050	20.3	-34.1	19.7	4.12
I49	6	0.0850	34.2	40.4	-29.8	3.19
I50	6	0.0850	34.2	20.2	-20.1	5.23
I51	6	0.0850	34.2	13.7	-20.9	7.14
I52	6	0.0850	34.2	5.5	-9.7	13.08
I53	6	0.0850	34.2	-19.6	31.4	5.01
I54	6	0.0850	34.2	-26.9	20.0	3.55
I55	6	0.0850	34.2	-30.6	22.0	3.21
I56	6	0.0850	34.2	-39.1	2.3	2.05
I57	7	0.0910	34.2	20.2	-31.6	5.24
I58	7	0.0910	34.2	13.7	-21.4	7.32
I59	7	0.0910	34.2	8.4	-29.4	9.06
I60	7	0.0910	34.2	5.6	-28.4	13.60
I61	7	0.0910	34.2	-19.8	2.6	4.30
I62	7	0.0910	34.2	-26.9	20.6	3.82
I63	7	0.0910	34.2	-30.1	12.8	3.17
I64	7	0.0910	34.2	-38.8	28.4	2.58
I65	7	0.0910	20.3	32.5	-28.7	4.55
I66	7	0.0910	20.3	8.1	-26.6	12.18
I67	7	0.0910	20.3	5.3	-11.6	16.81
I68	7	0.0910	20.3	-21.3	19.9	6.56
I69	7	0.0910	20.3	-29.9	3.3	3.77
I70	7	0.0910	20.3	-34.1	20.4	3.87
I71	8	0.0475	34.2	40.6	-11.9	1.76
I72	8	0.0475	34.2	20.6	-11.4	3.01
I73	8	0.0475	34.2	13.7	-20.2	4.43
I74	8	0.0475	34.2	5.6	-15.1	7.99
I75	8	0.0475	34.2	-19.7	14.4	3.40
I76	8	0.0475	34.2	-27.1	19.4	2.65
I77	8	0.0475	34.2	-38.7	18.3	1.70
I78	8	0.0475	20.3	15.6	-12.1	4.70
I79	8	0.0475	20.3	8.1	-11.2	7.69
I80	8	0.0475	20.3	5.3	-27.6	11.77
I81	8	0.0475	20.3	-22.1	2.9	3.87
I82	8	0.0475	20.3	-29.6	33.7	3.48
I83	8	0.0475	20.3	-34.1	34.5	3.11

Table 6.7 Experimental Data For Freezing and Thawing of
         Three-Dimensional Irregular Shapes of Tylose

Run Number	Shape	D (m)	h (W m^{-2} °C^{-1})	T_a (°C)	T_{in} (°C)	t_{exp} (hrs)
TI1	Pyramid	0.0825	41.0	21.0	-13.5	4.52
TI2	Pyramid	0.0825	41.0	9.8	-15.6	7.65
TI3	Pyramid	0.0825	41.0	5.6	-28.2	12.28
TI4	Pyramid	0.0825	41.0	-25.6	35.8	3.62
TI5	Pyramid	0.0825	41.0	-29.2	5.1	2.70
TI6	Pyramid	0.0825	41.0	-38.0	19.8	2.48
TI7	Sphere	0.1270	51.4	12.8	-11.9	5.94
TI8	Sphere	0.1270	51.4	5.6	-20.9	11.14
TI9	Sphere	0.1270	51.4	-21.1	20.5	3.03
TI10	Sphere	0.1270	51.4	-22.5	36.7	3.55
TI11	Sphere	0.1270	51.4	-37.9	4.0	1.83
TI12	Sphere	0.1270	51.4	-38.1	30.7	1.99
TI13	Egg	0.1700	51.4	30.1	-14.9	5.62
TI14	Egg	0.1700	51.4	12.8	-28.6	11.46
TI15	Egg	0.1700	51.4	5.7	-12.0	21.22
TI16	Egg	0.1700	51.4	-22.6	20.6	5.76
TI17	Egg	0.1700	51.4	-29.1	34.9	4.55
TI18	Egg	0.1700	51.4	-38.6	19.6	4.11
TI19	Fish	0.1200	51.4	14.7	-13.0	8.29
TI20	Fish	0.1200	51.4	10.8	-13.7	10.48
TI21	Fish	0.1200	51.4	5.6	-28.4	18.76
TI22	Fish	0.1200	51.4	-21.9	5.9	4.13
TI23	Fish	0.1200	51.4	-29.1	34.4	3.65
TI24	Fish	0.1200	51.4	-38.5	16.3	2.81

Table 6.8 Experimental Data For Freezing and Thawing of Slabs and Multi-Dimensional Shapes of Minced Lean Beef

Run Number	Shape[1] & Code	D_x (m)	D_y (m)	D_z (m)	h (W m^{-2} °C^{-1})	T_a (°C)	T_{in} (°C)	t_{exp} (hrs)
M1	Slab	0.024			13.2	5.8	-19.1	8.58
M2	Slab	0.024			50.4	26.9	-15.6	0.84
M3	Slab	0.047			18.2	8.0	-27.1	12.07
M4	Slab	0.047			78.1	15.8	-24.4	2.85
M5	Slab	0.075			24.5	43.2	-29.0	5.21
M6	Slab	0.075			172.7	9.3	-16.9	8.94
M7	Brick	0.152	0.153	0.154	41.0	27.0	-28.4	7.22
M8	Brick	0.152	0.153	0.154	41.0	8.4	-15.0	18.01
M9	Brick	0.076	0.077	0.300	41.0	13.0	-22.3	5.23
M10	Brick	0.076	0.077	0.300	41.0	5.8	-23.9	9.32
M11	2DI 3	0.1370			28.0	21.0	-27.1	10.07
M12	2DI 3	0.1370			28.0	8.1	-13.2	19.50
M13	2DI 3	0.1370			28.0	-29.1	18.8	6.27
M14	2DI 3	0.1370			28.0	-30.2	24.5	6.33
M15	2DI 8	0.0475			20.3	13.9	-11.6	5.05
M16	2DI 8	0.0475			20.3	6.5	-16.3	8.75
M17	2DI 8	0.0475			20.3	-23.3	3.1	3.43
M18	2DI 8	0.0475			20.3	-37.8	32.2	2.59

[1] 2DI = two-dimensional irregular, code numbers from Table 6.6.
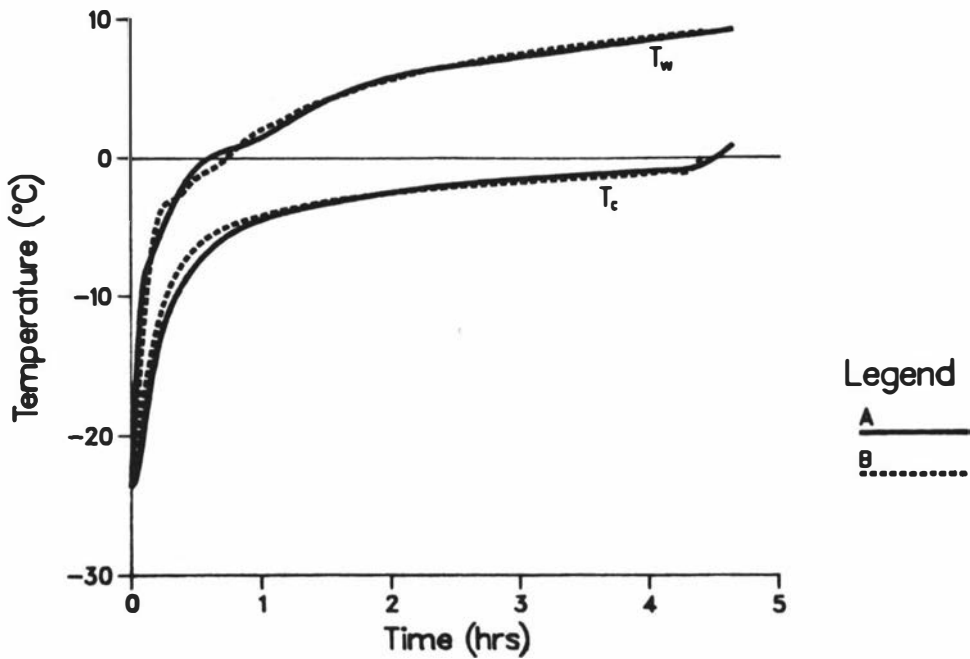
Fig. 6.1 A Typical Temperature/Time Profile For Thawing of Slabs of
Tylose.   Run T24, D_x = 0.0525 m, h = 50.4 W m^{-2} $^{\circ}$C^{-1},
T_a = 13.4°C, T_{in} = -23.6°C.   A - experimentally measured
temperatures, B - temperatures predicted by the full finite
element method formulation.   Results for all the numerical
methods are all virtually identical.
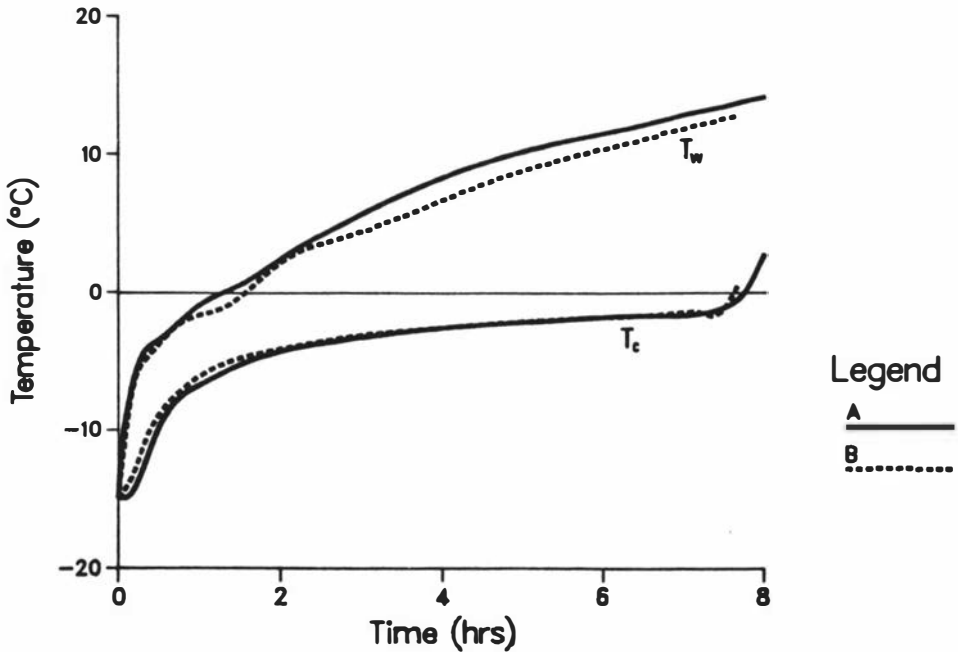
Fig. 6.2 A Typical Temperature/Time Profile For Thawing of Infinite
Cylinders of Tylose.
Run C22, D_r = 0.103 m, h = 19.5 W m^{-2} $^{\circ}$C^{-1}, T_a = -8.2°C,
T_{in} = -14.9°C.   A - experimentally measured temperatures,
B - temperatures predicted by the finite difference method.
Results for the finite difference method and both finite
element method formulations are all virtually identical.
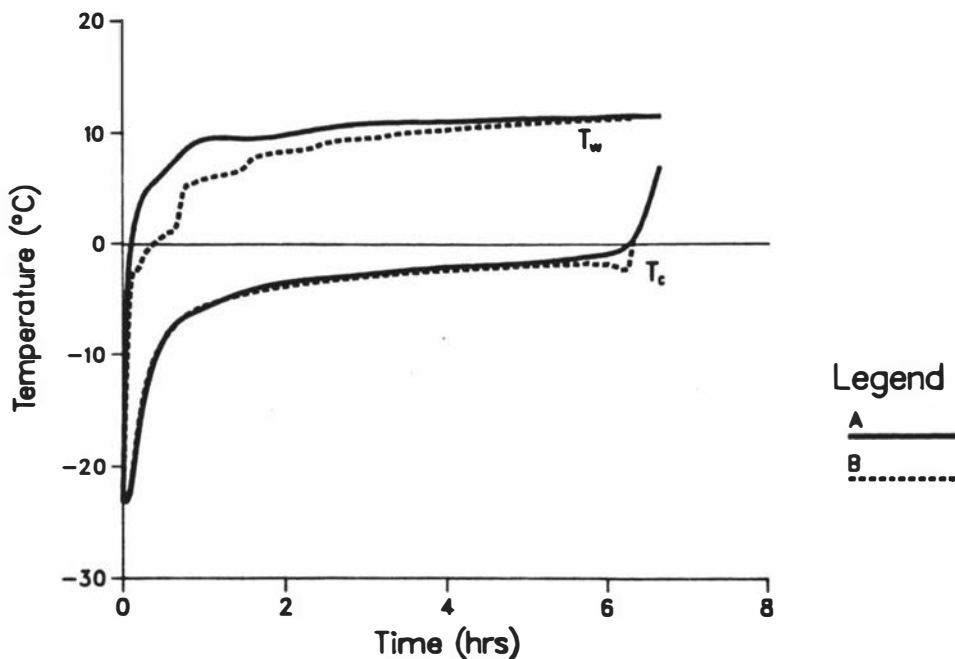
Fig. 6.3 A Typical Temperature/Time Profile For Thawing of Spheres of
Tylose.   Run S6, D_r = 0.128 m, h = 74.8 W m^{-2} °C^{-1},
T_a = 11.9°C, T_{in} = -23.1°C.   A - experimentally measured
temperatures, B - temperatures predicted by the simplified
finite element method.   Results for all the numerical methods
are virtually identical.
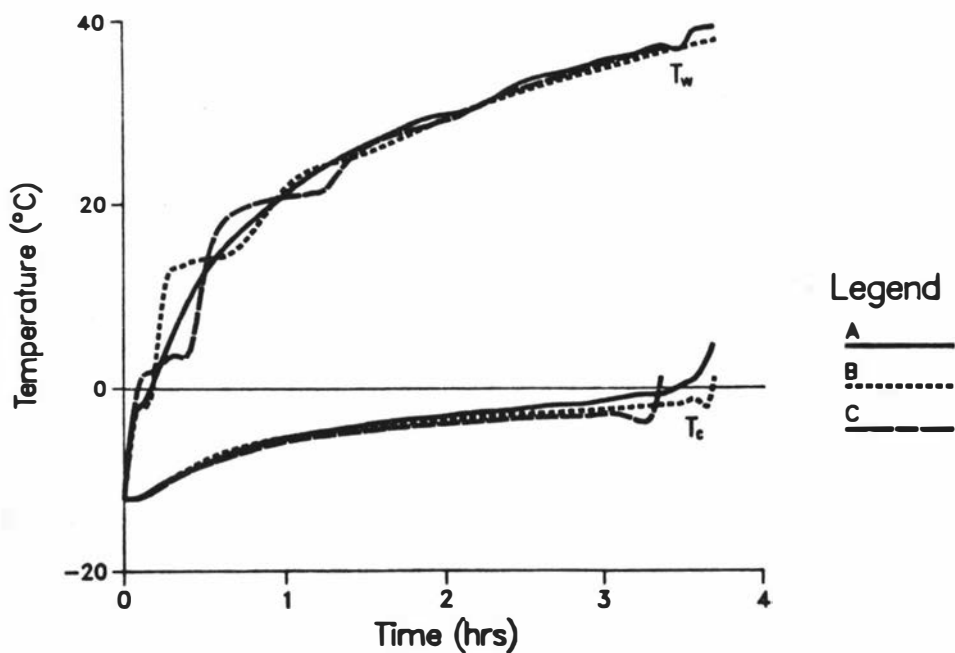
Fig. 6.4 A Typical Temperature/Time Profile For Thawing of Rectangular
Bricks of Tylose.   Run B7, D_x = 0.104 m, D_y = 0.125 m, D_z =
0.152 m, h = 50.4 W m^{-2} °C^{-1}, T_a = 45.0°C, T_{in} = -12.0°C.
A - experimentally measured temperatures, B - temperatures
predicted by the finite difference method, C - temperatures
predicted by the simplified finite element method, T_w =
temperature at the surface of the centre of the x,z face.
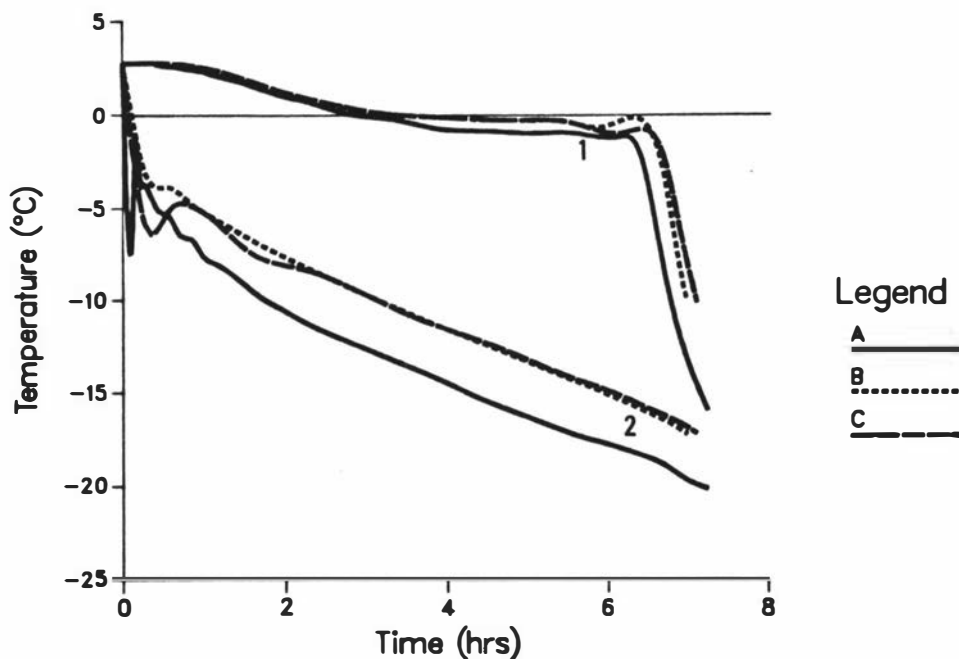
Fig. 6.5 A Typical Temperature/Time Profile For Freezing or Thawing of
the Tylose Two-Dimensional Irregular Shape Number One.
Run I7, h = 28.0 W m^{-2} $^{\circ}$C^{-1}, T_a = -23.6 $^{\circ}$C, T_{in} = 2.8 $^{\circ}$C.
A - experimentally measured temperatures, B - temperatures
predicted by the full finite element method, C - temperatures
predicted by the simplified finite element method. Calculated
using the two-dimensional grid in Fig. 5.15.
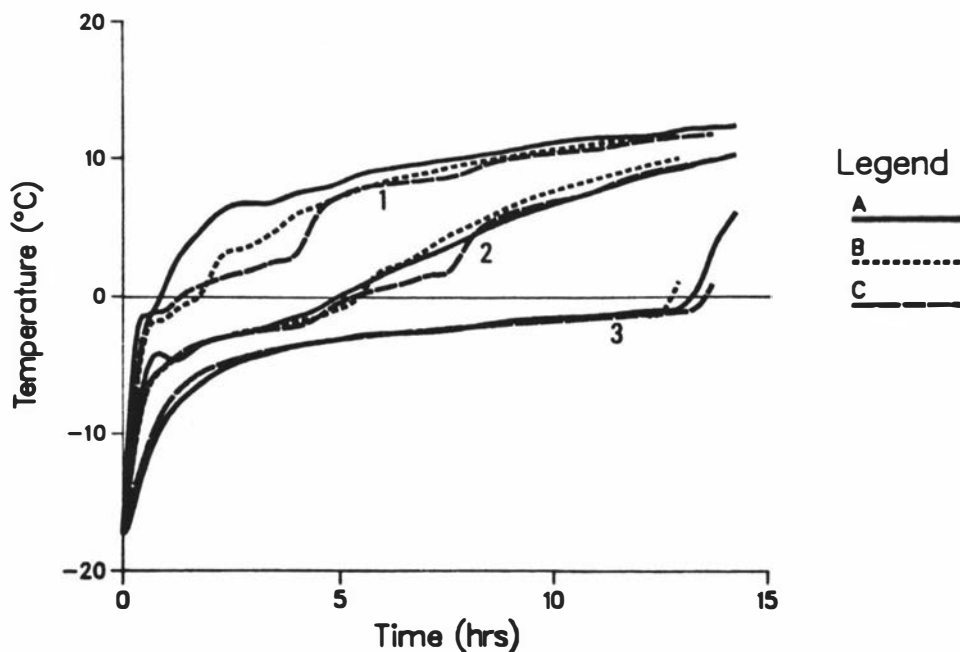
Fig. 6.6 A Typical Temperature/Time Profile For Freezing or Thawing of
the Tylose Two-Dimensional Irregular Shape Number Two.
Run I16, h = 28.0 W m^{-2} $^{\circ}$C^{-1}, T_a = 13.6 $^{\circ}$C, T_{in} = -17.2 $^{\circ}$C.
A - experimentally measured temperatures, B - temperatures
predicted by the full finite element method, C - temperatures
predicted by the simplified finite element method. Calculated
using the two-dimensional grid in Fig. 5.16.
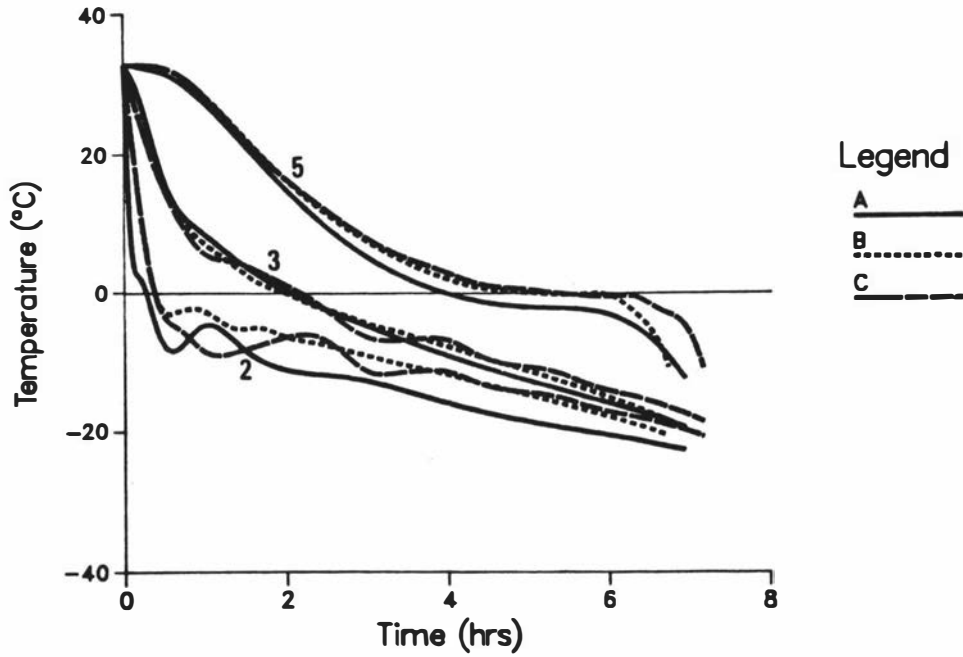
Fig. 6.7 A Typical Temperature/Time Profile For Freezing or Thawing of
the Tylose Two-Dimensional Irregular Shape Number Three.
Run I29, h = 28.0 W m^{-2} $^{\circ}$C^{-1}, T_a = -30.5°C, T_{in} = 32.8°C.
A - experimentally measured temperatures, B - temperatures
predicted by the full finite element method, C - temperatures
predicted by the simplified finite element method. Calculated
using the two-dimensional grid in Fig. 5.17.
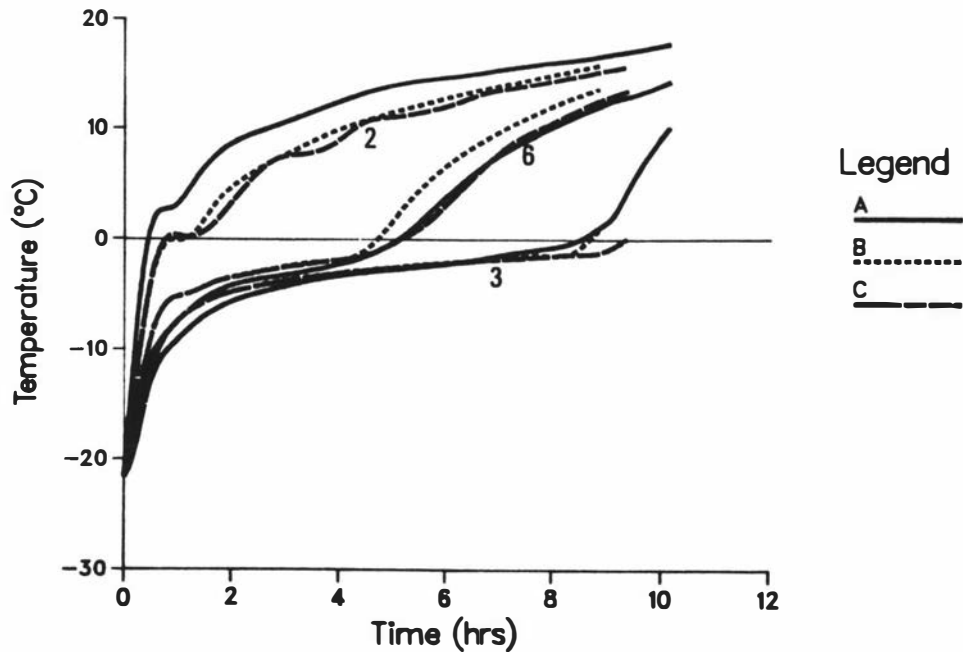
Fig. 6.8 A Typical Temperature/Time Profile For Freezing or Thawing of
the Tylose Two-Dimensional Irregular Shape Number Four.
Run I31, h = 28.0 W m^{-2} $^{\circ}$C^{-1}, T_a = 20.1°C, T_{in} = -21.5°C.
A - experimentally measured temperatures, B - temperatures
predicted by the full finite element method, C - temperatures
predicted by the simplified finite element method. Calculated
using the two-dimensional grid in Fig. 5.18.
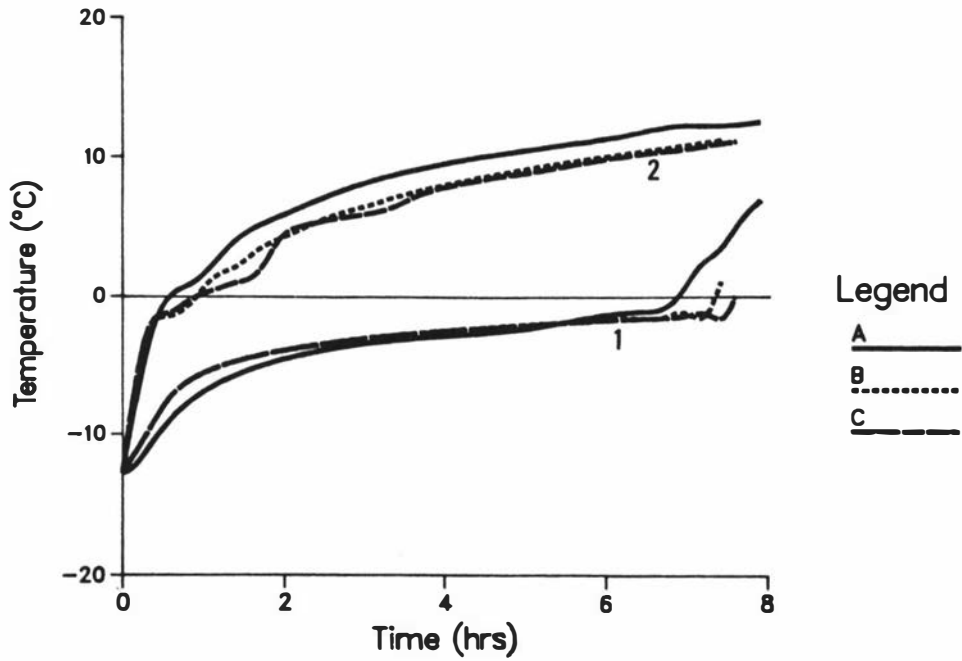
Fig. 6.9 A Typical Temperature/Time Profile For Freezing or Thawing of
the Tylose Two-Dimensional Irregular Shape Number Five.
Run I39, h = 34.2 W m^{-2} °C^{-1}, T_a = 13.6 °C, T_{in} = -12.7 °C.
A - experimentally measured temperatures, B - temperatures
predicted by the full finite element method, C - temperatures
predicted by the simplified finite element method. Calculated
using the two-dimensional grid in Fig. 5.15.
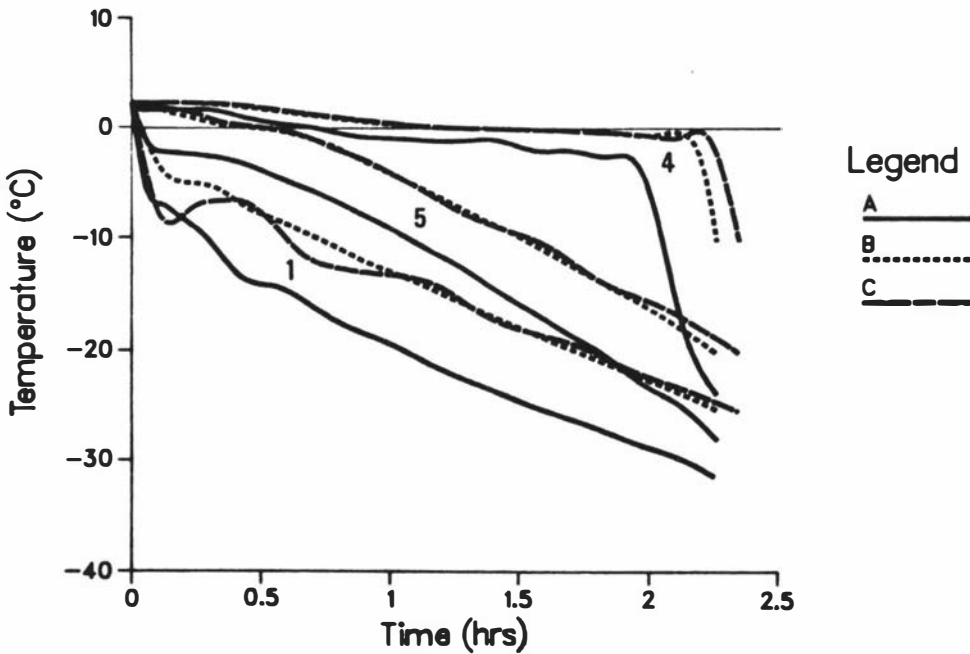
Fig. 6.10 A Typical Temperature/Time Profile For Freezing or Thawing of
the Tylose Two-Dimensional Irregular Shape Number Six.
Run I56, h = 34.2 W m^{-2} °C^{-1}, T_a = -39.1 °C, T_{in} = 2.3 °C.
A - experimentally measured temperatures, B - temperatures
predicted by the full finite element method, C - temperatures
predicted by the simplified finite element method.
Calculated using the two-dimensional grid in Fig. 5.19.
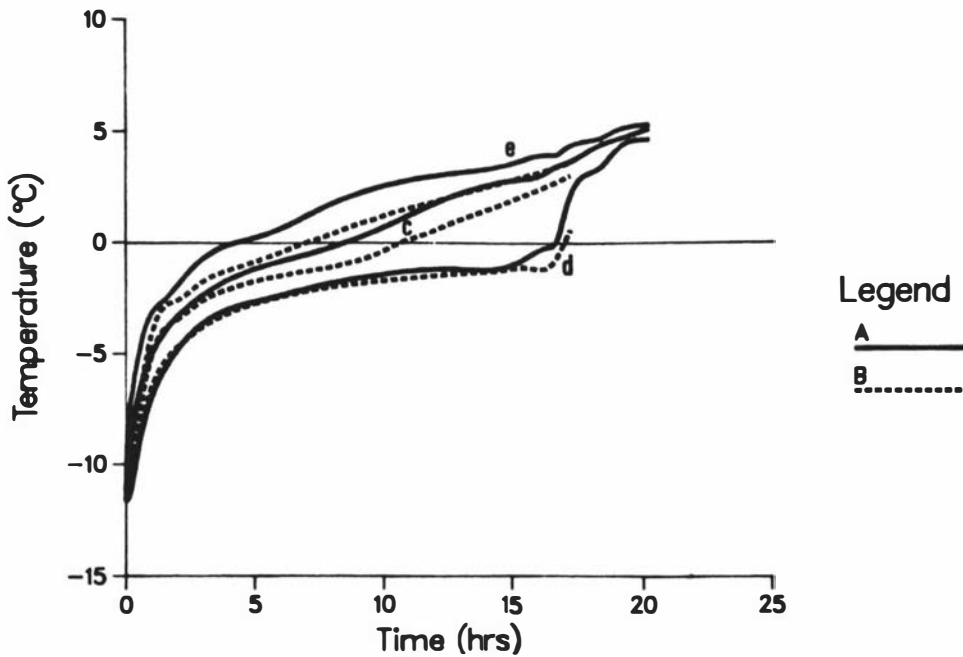
Fig. 6.11 A Typical Temperature/Time Profile For Freezing or Thawing of
the Tylose Two-Dimensional Irregular Shape Number Seven.
Run I29, h = 20.3 W m^{-2} °C^{-1}, T_a = 5.3 °C, T_{in} = -11.6 °C.
A - experimentally measured temperatures, B - temperatures
predicted by the full finite element method.   Calculated
using the two-dimensional grid in Fig. 5.20.
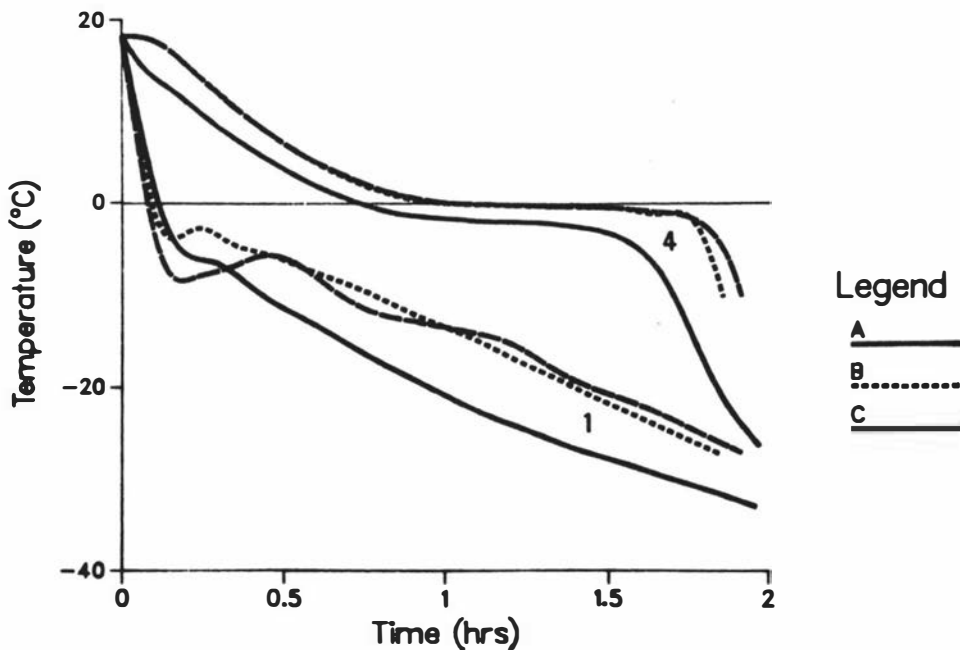
Fig. 6.12 A Typical Temperature/Time Profile For Freezing or Thawing of
the Tylose Two-Dimensional Irregular Shape Number Eight.
Run I77, h = 34.2 W m^{-2} °C^{-1}, T_a = -38.7 °C, T_{in} = 18.3 °C.
A - experimentally measured temperatures, B - temperatures
predicted by the full finite element method, C - temperatures
predicted by the simplified finite element method.
Calculated using the two-dimensional grid in Fig. 5.21.
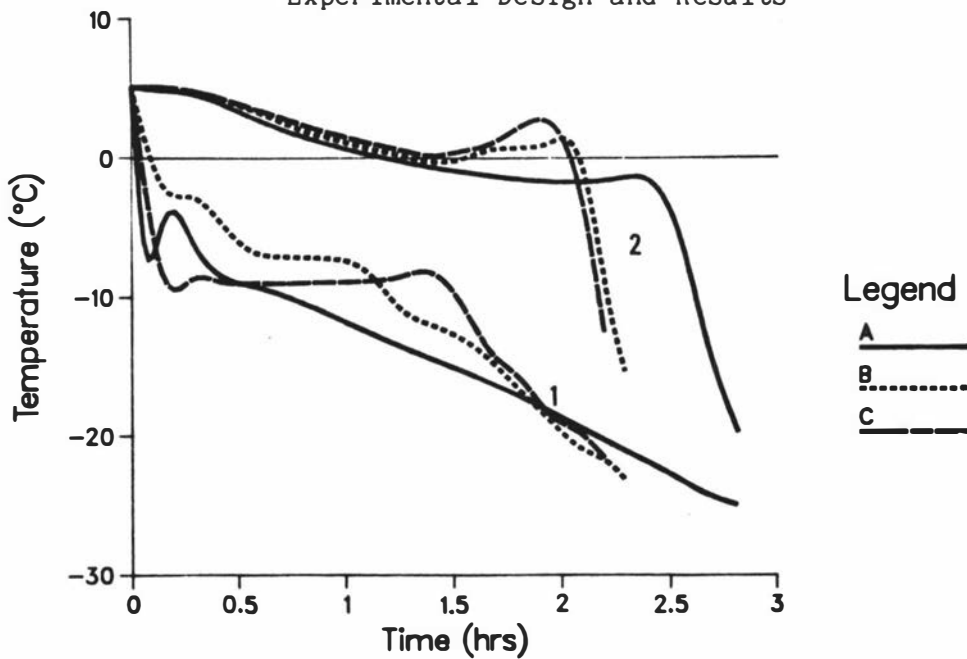
Fig. 6.13 A Typical Temperature/Time Profile For Freezing or Thawing of
the Tylose Three-Dimensional Irregular Pyramid Shape.
Run TI5, h = 41.0 W m^{-2} °C^{-1}, T_a = -29.2°C, T_{in} = 5.1°C.
A - experimentally measured temperatures, B - temperatures
predicted by the full finite element method, C - temperatures
predicted by the simplified finite element method.
Calculated using the three-dimensional grid in Fig. 5.24.
1 - at the centre of the x,y face (base) of the pyramid,
2 - 0.0765 m (mid-height) above position 1 (Fig. 5.24).
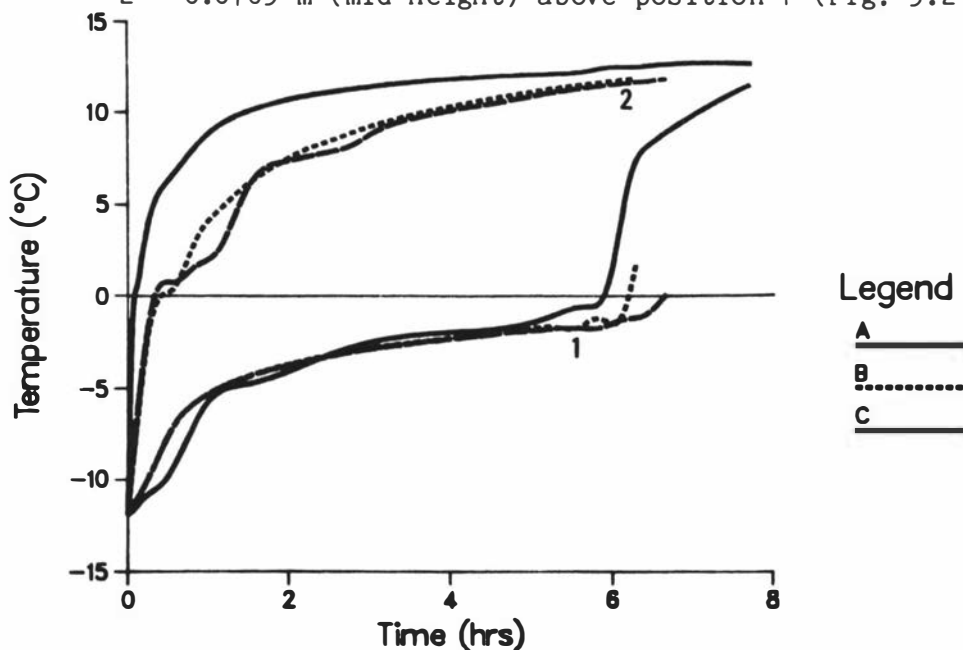
Fig. 6.14 A Typical Temperature/Time Profile For Freezing or Thawing of
the Tylose Three-Dimensional Irregular Sphere Shape.
Run TI5, h = 51.4 W m^{-2} °C^{-1}, T_a = 12.8°C, T_{in} = -11.9°C.
A - experimentally measured temperatures, B - temperatures
predicted by the full finite element method, C - temperatures
predicted by the simplified finite element method.
Calculated using the two-dimensional grid in Fig. 5.25b.
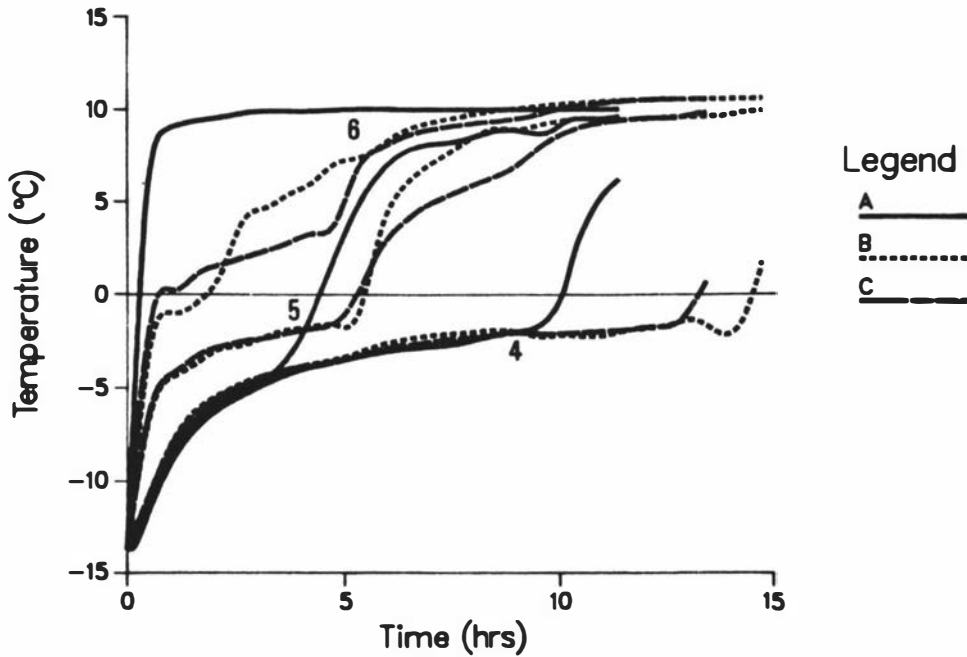
Fig. 6.15 A Typical Temperature/Time Profile For Freezing or Thawing of
the Tylose Three-Dimensional Irregular Fish Shape.
Run TI20, h = 51.4 W m^{-2} °C^{-1}, T$_a$ = 10.8°C, T$_{in}$ = -13.7°C.
A - experimentally measured temperatures, B - temperatures
predicted by the full finite element method, C - temperatures
predicted by the simplified finite element method.
Calculated using the three-dimensional grid in Fig. 5.27.
4 - 0.213 m along the x axis from the tip of the head shown
in Fig. 5.27b, 5 - 0.085 m along the x axis from the tip of
the head shown in Fig. 5.27b, 6 - 0.021 m along the x axis
from the tip of the head shown in Fig. 5.27b and on the fish
surface 0.021 m in the y direction from the x axis.
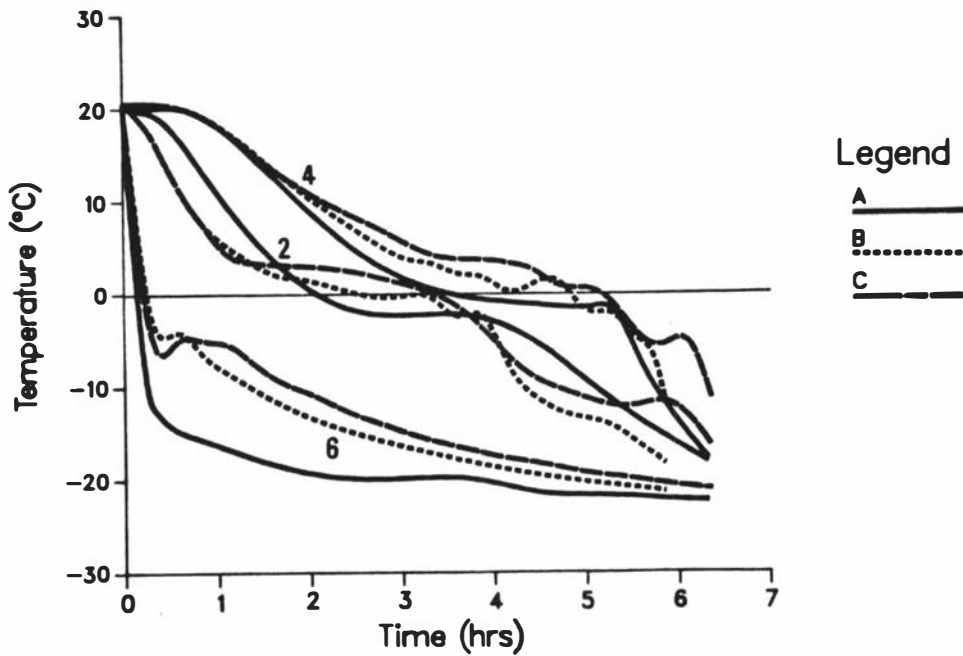
Fig. 6.16 A Typical Temperature/Time Profile For Freezing or Thawing of
the Tylose Three-Dimensional Irregular Egg Shape.
Run TI 16, h = 51.4 W m^{-2} °C^{-1}, T$_a$ = -22.6 °C, T$_{in}$ = 20.6 °C.
A - experimentally measured temperatures, B - temperatures
predicted by the full finite element method, C - temperatures
predicted by the simplified finite element method.
Calculated using the three-dimensional grid in Fig. 5.26b.
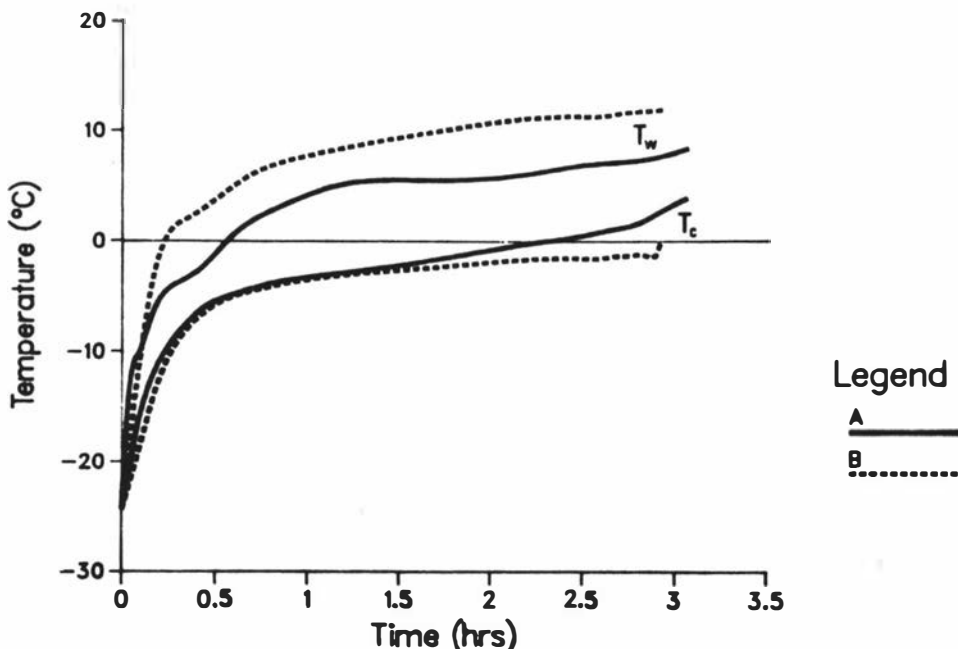
Fig. 6.17 A Typical Temperature/Time Profile For Thawing of Slabs of
Minced Lean Beef.
Run M4, D$_x$ = 0.047 m, h = 78.1 W m^{-2} °C^{-1}, T$_a$ = 15.8 °C,
T$_{in}$ = -24.2 °C. A - experimentally measured temperatures,
B - temperatures predicted by the finite difference method.
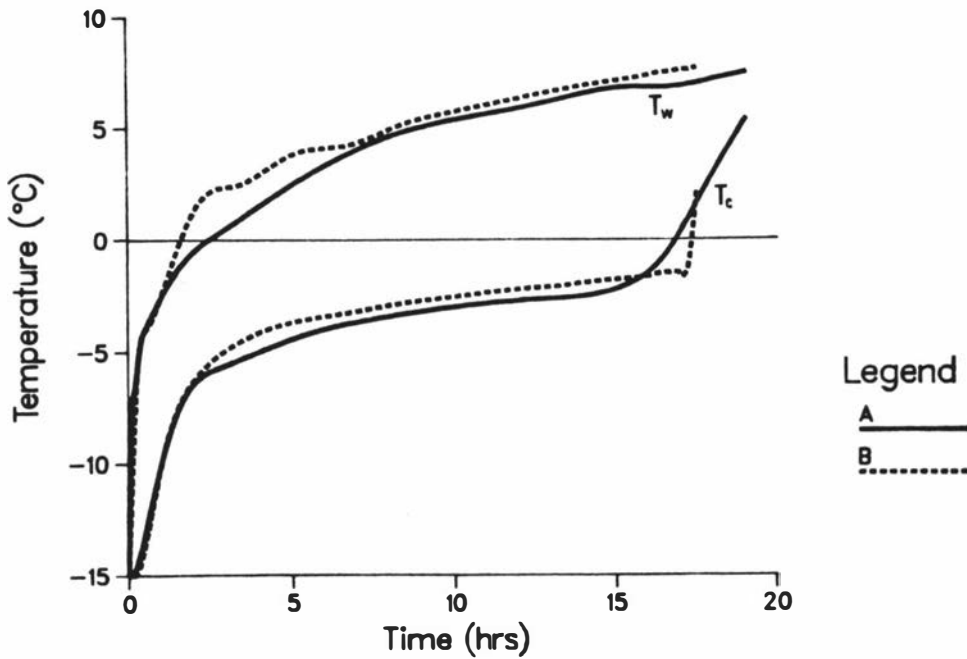
Fig. 6.18 A Typical Temperature/Time Profile For Thawing of Rectangular
Bricks of Minced Lean Beef.
Run M8, D_x = 0.152 m, D_y = 0.153 m, D_z = 0.154 m,
h = 41.0 W m^{-2} °C^{-1}, T_a = 8.4°C, T_{in} = -15.0°C.
A - experimentally measured temperatures, B - temperatures
predicted by the finite difference method.
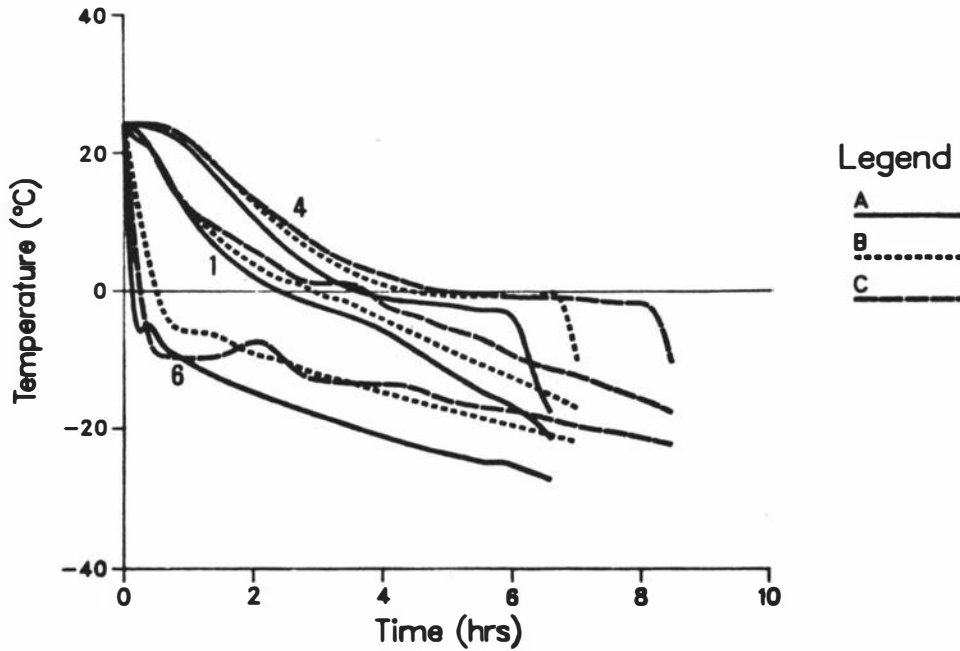
Fig. 6.19 A Typical Temperature/Time Profile For Freezing or Thawing of
a Minced Lean Beef Two-Dimensional Irregular Shape.
Run M14, two-dimensional irregular Shape No. 3,
h = 28.0 W m^{-2} °C^{-1}, T_a = -30.2°C, T_{in} = 24.5°C.
A - experimentally measured temperatures, B - temperatures
predicted by the full finite element method, C - temperatures
predicted by the simplified finite element method.
Calculated using the two-dimensional grid in Fig. 5.17.

7   PREDICTION OF THAWING TIMES FOR SLABS, INFINITE CYLINDERS AND SPHERES

In Chap. 3 prediction methods were classified into those requiring only hand calculation (Group I) and those requiring computer calculation (Group II).   The   third   objective for the present work set in Chap. 3 was to assess the   accuracy   of   Group   I   and   Group   II   methods   for prediction of   thawing   times   for   regular   shapes.   Chapter 7 reports results for Group I and Group II methods   applied   to   slabs,   infinite cylinders and   spheres.   Chapter   8   reports   the   results of Group II methods applied to rectangular   bricks   as   well   as   multi-dimensional irregular   shapes,   whilst   Chap. 9   considers   Group   I   methods   for multi-dimensional regular shapes.

7.1   VERIFICATION OF A UNIFIED APPROACH FOR SIMPLE SHAPES

Plank (1913) derived an equation for the time to freeze or thaw   slabs, infinite cylinders   and spheres.   This equation suggests that the ratio of times   for   phase   change   for   the   three   shapes   under   identical conditions and   with   the   same characteristic dimension is 6:3:2.   The ratio arises from consideration of the relationship between volume   and surface area   for   each   shape.   However the equation requires that the following conditions are met:
(a) that phase change occurs at a unique phase change temperature
(b) that thermal properties are constant and
(c) that sensible heat effects are negligible compared with the   latent heat.

In freezing or thawing of biological materials not all these conditions are met so the 6:3:2 ratio is not necessarily correct.   However   taking the ratio   as   constant   allows   a   single phase change time prediction method for one of the basic shapes   to   be   equally   applicable   to   the other two, which is a desirable feature of any prediction method.

Data are available for freezing of foods where latent heat is   released over   a   range   of   temperatures,   thermal   properties   change   with temperature and sensible heat effects both above and below the freezing temperature range are   significant   (Cleland   &   Earle   1977a,   1979a).

Within the tolerance of the data, previous studies (Cleland & Earle 1982b, Pham 1984a) suggested that there was no evidence that the ratio was not constant at 6:3:2. The predictions for all the shapes showed no trends with changes in shape or freezing conditions (Pham 1984c).

The hypothesis that the ratio of $t_{slab}:t_{cyl}:t_{sph}$ is constant at 6:3:2 for both freezing and thawing of foods and that it is independent of environmental conditions was tested more rigorously by use of numerical methods. The Tylose freezing data (Cleland & Earle 1976b, 1977a, 1979a, 1979b) and the Tylose thawing data (Chap. 6) for the slab, infinite cylinder and sphere shapes were predicted using the three numerical methods discussed in Chap. 4 - the finite difference method and the two finite element method formulations. For each experimental run nine predictions were made - one for each combination of the three numerical methods and the three geometry descriptions. Each prediction was modified by the appropriate ratio and the percentage difference from the experimental time calculated. For example, an infinite cylinder experimental run was predicted by results from slab, infinite cylinder and sphere versions of the three numerical methods multiplied by 0.5, 1.0 and 1.5 respectively. The percentage differences were calculated from:

$$\text{percentage difference} = \frac{\text{predicted time} - \text{experimental time}}{\text{experimental time}} \cdot \frac{100}{1} \quad (7.1)$$

The results for both the freezing and thawing data are summarised in Table 7.1. The finite difference method and the two finite element method formulations gave almost identical results so only the finite difference results are presented. The ratios of numerically predicted times: t_{slab}/t_{sph}, t_{slab}/t_{cyl} and t_{cyl}/t_{sph} were also examined for each set of experimental runs. The mean values and 95% confidence intervals were 3.02 ±0.20, 2.01 ±0.07 and 1.50 ±0.05 respectively for freezing and 3.00 ±0.37, 2.00 ±0.15 and 1.50 ±0.07 respectively for thawing.

The mean prediction accuracy was not significantly affected by the choice of geometry description used in the numerical calculations. Hence, on average, the ratio of 6:3:2 holds for both freezing and thawing.

Variations of the 6:3:2 ratio for individual experimental runs arose from two factors - both the overall change in enthalpy from the initial temperature to a specified final thermodynamic centre temperature and the mean "effective" thermal conductivity differ with shape. These are directly consequential on the different distribution of volume with respect to displacement from the geometric centre in the three shapes, which in turn affects the shape of the temperature/displacement profile. These factors mean that the $t_{slab}:t_{cyl}:t_{sph}$ ratio is dependent on Bi, Ste and Pk.

For freezing the dependence of the ratio on Ste and Pk is weak. For the ranges over which Bi, Ste and Pk vary in typical freezing operations (Table 6.1), there is no need to take account of these trends. The ratio can be considered constant at 6:3:2 without introducing any significant additional uncertainty into the predictions.

For thawing the effect of Pk is insignificant because values of Pk typically encountered are small (Table 6.1). Also thermal conductivity is high and temperature driving forces are large when the sensible heat represented by Pk is transferred so this heat transfer is easily achieved. Conversely, the sensible heat represented by Ste is transferred more slowly as temperature differences and the thermal conductivities are both lower at this stage in the thawing process. Typically in thawing Ste varies over a wide range so the Ste effect is larger. The Bi effect results from changes in the thermal conductivity with temperature and variation of the surface temperature and temperature/displacement profile at the end of the phase change process as Bi changes.

Although discernible in the numerical results, the Bi, Ste and Pk effects were sufficiently small compared with the experimental uncertainty in the data set (Tables 6.2, 6.3 and 6.4) that they could be ignored in the present work. By use of the 6:3:2 ratio all the slab, infinite cylinder and sphere data could be grouped together for analysis by a unified approach. If more accurate thawing data were available, parameters relating Bi, Ste and Pk to shape may be needed to give accurate predictions for all three shapes.

7.2   PREDICTION BY NUMERICAL METHODS

A wide range of numerical solutions to thawing problems were discussed in Chaps. 2 and 4. The three time level Lees' finite difference scheme and finite element method that accounted for thermal properties continuously variable with temperature, were shown to be the best numerical methods for prediction of phase change in foods.

Using the thermal data given in Table 5.1 the predictions by the finite difference method and the two finite element formulations are compared with the experimental slab, infinite cylinder and sphere thawing times in Table 7.3. Typical predicted temperature profiles are shown in Fig. 6.1 to 6.3. In all cases an evenly spaced 11 node grid (with 10 two node linear elements for the finite element methods) was used. Numerical approximation error could be reduced by using a more refined grid (and/or higher order elements for the finite element method). Testing of different grid sizes was carried out for some runs but as significantly different predictions did not result, the 11 node grid was considered satisfactory.

The 95% confidence limits of the percentage differences (Eq. (7.1)) between the calculated thawing times and the experimental results for all three shapes are -9.3% to 6.7% for the finite difference method, -9.6% to 7.9% for the full finite element formulation (Eqs. (4.2) to (4.5)) and -9.5% to 9.3% for the simplified finite element formulation (Eqs. (4.5) to (4.8)). These uncertainty limits include contributions from three sources - experimental error, thermal data error and errors in the application of the numerical methods.

Applying the criteria of Cleland & Earle (1984a) to comparisons of the numerical predictions with the experimental results showed no trends in the data that might suggest major systematic experimental or thermal data errors. The experimental error bounds could not be determined accurately but were estimated to be between ±5% and ±10% (Chap. 5, Table 12.2) for the slab, infinite cylinder and sphere thawing experiments. This is of the same order of magnitude as the total limits for the numerical predictions, suggesting that only minimal uncertainty has arisen in the application of the numerical methods.

This was expected because relatively fine space and time grids could be used (Chap. 4).

Some slab runs had a contribution from edge heat transfer that was estimated to exceed 1% (Sec. 5.4.4, App. B). The predicted thawing times calculated by the three numerical methods for these runs when compared with the experimental data agreed to within 1.3% ±8.4%, 0.2% ±8.8% and 0.2% ±8.8% respectively. If edge heat transfer was significant compared with sources of random error then the means of these percentage differences should be noticably offset from the mean of all the other percentage differences. It was concluded that the extra experimental uncertainty in these runs had not significantly increased the overall uncertainty.

Numerical methods, if formulated and implemented correctly, are the closest to exact prediction methods. Therefore as there is no significant and identifiable systematic trend or correlation in the experimental data the error bounds of the numerical predictions are the best estimate of the overall random experimental error (due to uncertainty in control and measurement of experimental conditions). Predictions better than those achieved by the numerical methods cannot be expected if the same experimental and thermal data are used unless a more exact or sophisticated form of the numerical methods is used (Heldman 1983, Cleland & Earle 1984a). Comparing the numerical predictions for each shape individually (Table 7.3) gives estimates of the experimental error for the experiments with each shape. The average 95% confidence bounds of the observed differences for the three numerical methods are on average ±7.1%, ±5.0% and ±11.3% for slabs, infinite cylinders and spheres respectively. As expected the uncertainty for slabs and infinite cylinders is lower than for spheres as better control and measurements of the experimental conditions, especially dimensions and surface heat transfer coefficients, were possible (Chap. 5). The above uncertainty bounds are consistent with experimental variability measured by summing that measured in replicate experiments, and systematic error from other sources not evident from the replicates (for example, measurement of h).

The mean prediction error arising from calculations by the simplified

finite element method formulation was higher than for the other two methods. This is due to the relatively crude way in which variations in the thermal properties are incorporated into this method. For this method increasing the number of nodes and elements did have some benefits and reduced the difference in prediction compared with the other methods. It is debatable whether the savings in computation costs justifies this loss in accuracy as the decrease in computer memory size requirements and increase in speed achieved by using the simple formulation for one-dimensional work is small.

Centre temperature profiles were accurately predicted by all the numerical methods though, for the reason outlined above, the simplified finite element formulations performed least well in this respect. Differences between predicted and experimental temperatures were more likely to have arisen from uncertainty in thermocouple placement rather than numerical method error. In Chap. 5 it was shown that thermocouple placement was a major problem. It did not affect thawing time prediction (because the breakpoint analysis was used), but did give significantly different experimental temperature profiles from those expected at the centre.

All three numerical methods tended to predict surface temperatures consistently lower than those measured experimentally for the infinite cylinder and sphere experiments. This was due to the problems with thermal contact, air voids and thermocouple placement at the surface for these shapes. As discussed in Secs. 5.5 and 5.6 the methods used to estimate the average surface heat transfer coefficient only used the centre temperature and not the surface temperature data. The experimentally determined surface temperature was taken from the thermocouple that exhibited the most rapid change in temperature. This thermocouple was not necessarily representative of the true average surface temperature. Numerical predictions made with the average surface heat transfer coefficient therefore underestimated the rate of change of the experimental values. For the slab shape the surface temperature predictions were consistently more accurate as problems with voids were avoided.

For the finite element methods some unexpected deviations of the

temperature profiles were observed when elements were near the latent heat temperature range. This occurred because of the way the finite element methods incorporated the thermal properties and was an effect of the integral nature of the finite element method, especially when thermal property change with temperature are rapid (Cleland et al 1984).

7.3   PREDICTION BY SIMPLE FORMULAE

7.3.1   Existing Prediction Formulae

In Chap. 2 a large number of simple formulae for calculation of freezing and thawing times in slabs, infinite cylinders and/or spheres were discussed. Many of these formulae were not expected to be accurate in the situations considered in this work. Solutions that only take account of the first kind of boundary condition are not suitable for general use as they give poor predictions except where the surface heat transfer coefficient is extremely high. These types of methods were therefore not considered any further. Similarly solutions for the second kind of boundary condition were considered impractical.

Thawing times for the slab, infinite cylinder and sphere experimental data were calculated using the methods that considered the third kind of boundary condition and that seemed most likely to lead to reasonable prediction accuracy. The percentage differences between the calculated results and the experimental thawing times were found (Eq. (7.1)). A summary of these values is given in Table 7.2.

Most of the methods tested assume that all the latent heat is absorbed at a unique thawing temperature and that the frozen and unfrozen phase have constant thermal properties (thermal conductivity and specific heat capacity). For these methods the thermal conductivity of the completely unfrozen material was used, and the latent heat component was obtained by subtracting the sensible heat component from the total enthalpy change between 0 °C and -10 °C. Except where a "mean" thawing temperature was defined, the unique thawing temperature was taken as the initial freezing temperature because this is well defined for most foods and the rate of change of the ice fraction with temperature is at

a maximium at this temperature. The choices of properties made fit the
concept of the analytical methods, are not ambiguous, and also use the
best known thermal data for most foods. The thermal property values
used are given in Table 5.2.

Some methods based on modifications to existing analytical formulae
define the thermal properties differently, generally to more closely
approximate the true thermal properties during the phase   change
process. Commonly, the enthalpy change is defined to include sensible
heat effects, and average thermal conductivities and mean phase change
temperatures are used.   In each such case the guidelines for thermal
property determination suggested by the proposer of the prediction
method were followed as closely as possible.

Some empirical formulae developed specifically for freezing   time
prediction were also tested.   If it was possible the analogous
empirical formula was developed for thawing.   Generally the methods
that could be adapted were those with a more complete theoretical
basis. Other formulae were situation or product specific and could not
be made applicable.

Prediction methods that did not predict the experimental thawing data
well were limited in one or more of the following ways.
(1) Methods developed for semi-infinite slabs cannot be applied to
    finite shapes if sensible heat effects prior to phase change are
    significant. This is because heat transfer is calculated to occur
    from a greater volume in the semi-infinite slab than is actually
    present in the finite geometry (Geuze et al 1972, Cleland 1977).
(2) Methods assuming a unique thawing temperature (taken as equal to
    the initial freezing temperature) lead to overprediction of thawing
    time because much of the latent heat (as well as subcooling
    sensible heat) is absorbed over a range of temperatures lower than
    T_{if}. Therefore the actual temperature driving force for heat
    transfer is greater than that used in calculations.
(3) Methods that used the unfrozen phase thermal conductivity during
    the phase change process tended to overpredict the thawing times.
    The true mean thermal conductivity during the thawing process is
    greater than or equal to the unfrozen value so more heat transfer

occurs in practice than calculated using the fully unfrozen value.

(4) Thawing time prediction methods ignoring sensible heat added to the thawed region tend to underpredict.

(5) Methods ignoring the sensible heat added to the frozen region underpredict. The extent of the underprediction from this cause is less than that from (4).

Numerical methods that solve the governing partial differential equation for heat transfer and take account of temperature dependent thermal properties correctly model the thawing process physically and therefore give predictions that are not affected by the above factors. Comparison with the results for the numerical methods helps to identify how well a prediction method performs in trying to give a physically correct description of these factors and how they affect thawing time. It is convenient to use the correlation coefficient (r) comparing percentage differences in the manner of Cleland & Earle (1984a).

The methods and results in Table 7.2 were divided into nine groups. The Group A methods are affected by the first of the above limitations and are not accurate. Other methods that solve for the semi-infinite slab do not account for initial subcooling and consequently predict differently to Group A methods.

Plank's (1913) equation (Group B) was limited by the latter four factors. The compensatory nature of (2) and (3) against (4) and (5) means that the mean prediction error was +6.0%. However, the spread of the predictions was large (±43% at the 95% level of confidence) and the correlation with the finite difference method results was low. This indicates that the compensation was not consistent between runs with different conditions, rendering the equation unreliable. In freezing, Plank's equation consistently underpredicted by 20% to 40% because the equivalent problems to factors (2) to (5) all lead to underprediction for that process.

The analytical methods due to Rutov (1936), Goodman (1958), Shih & Chou (1971), Shih & Tsay (1971), Huang & Shih (1975a, 1975b), Kern (1977), Glasser & Kern (1978), Yan & Huang (1979), Clyne & Garcia (1980), Cho & Sunderland (1981), Soliman (1981) and Hill & Kucera (1983), and the

empirical methods of Baxter (1962), Tao (1967, 1968) and Goodling & Khader (1974), form Group C. They are all limited in similar ways to Plank's equation except that they take account of the sensible heat in the unfrozen phase. All methods within this group gave similar prediction accuracy. The results for Goodman (1958) shown in Table 7.2 are typical of the whole group. The mean difference was higher than that for Plank's equation and the spread is reduced because factor (4) was taken into account. The predictions are still poor because of the other limitations.

Group D are the modified analytical methods (semi-analytical) that are based on multiplicative factors to account for sensible heat effects (factors (4) and (5)). They all tend to substantially overpredict thawing times, and predictions tend to have a large spread.

Group E methods use either a mean phase change temperature (Mott 1964, Fleming 1967), an average thermal conductivity (Mellor & Seppings 1976) or both (Modified Plank) to take account of factors (2) and (3). Such methods still do not take account of all the limitations in a physically realistic manner so the spread of predictions was still large.

The Group F methods break the phase change process into three stages and attempt to approximate the heat transfer in each stage. They perform better than Group D because they model the true physical conditions more realistically. To remain simple these methods use some averaging techniques. They tend to overpredict the thawing times usually because they do not take account of factors (2) and (3) properly.

The empirical formulae developed for freezing (Group G) all tend to overpredict thawing times as the empirical correction factors are not appropriate for thawing. The method of Succar & Hayakawa (1984) was not tested as it is possibly unnecessarily complex and yet was not expected to be more accurate, than the other methods in this group.

The two empirical methods (Group H) specifically developed for thawing time prediction gave the best prediction accuracy. Creed & James

(1981) gave an empirical formula for thawing of slabs of boneless beef based on both numerical predictions and experimental thawing data. It gave prediction with 95% confidence bounds of -17.7% to 18.1%. The method is product specific because it does not take account of different thermal properties (k_l, k_s, C_l, C_s, ΔH, T_{if}). Also the predicted thawing time is only valid for T_{in}=-30°C. Tylose has thermal properties similar to those of beef and thawing time is only weakly dependent on changes in initial temperature. Therefore the predictions have a mean difference of zero but a significantly greater variability than would occur if these factors were taken into account.

Calvelo (1981) presents an empirical formula based on Plank's equation derived by regression analysis of numerical predictions for thawing of beef slabs. Though k_l and C_l are incorporated in the equation, the other properties (ΔH, T_{if}, k_s, C_s) do not need to be specified and the method is therefore product specific. As Tylose and beef have similar thermal properties this method gave accurate predictions with error bounds of -11.8% to 11.8% at the 95% level of confidence. The correlation of the percentage differences with the finite difference predictions was high, suggesting that all major sources of thawing time variation are accounted for by this formula. The residual prediction uncertainty, apart from that due to experimental error, was small in magnitude and was not significantly correlated to any other individual factor.

Within Group I, only the method due to Golovkin et al (1974) gave reasonable prediction accuracy. As the predictions were no better than those for some other simpler methods, and because the published derivation is unclear, the method was not considered further.

7.3.2 Improved Prediction Methods

Of the existing methods tested, only three (Creed & James 1981, Calvelo 1981 and Pham 1984a) gave predictions of reasonable accuracy and reliability (mean percentage difference close to zero and a low standard deviation of the percentage differences). Further, they took account of most of the sources of variation in thawing times and were consequently highly correlated with results from numerical methods.

The best methods were those due to Calvelo (1981) and Creed & James (1981) but both have the disadvantage that they do not take account of different thermal properties for different foodstuffs. Creed & James' method was also independent of initial temperature. Pham's (1984a) method has the advantage of having a predominately analytical basis. It has a low standard deviation due to the three stage approach considering all sources of thawing time variation but the mean percentage difference was offset from zero.

Because all the existing methods have weaknesses it seemed worthwhile to seek a new prediction method. Empirically modified forms of Plank's equation similar to those found to be useful for freezing (Cleland & Earle 1982b, Hung & Thompson 1983) were investigated because of their simplicity and success for freezing time prediction. Also prediction formulae similar to those of Calvelo (1981) and Pham (1984a, 1984c) were investigated to see if they could be improved and made applicable to a wider range of situations. The Creed & James' approach may have yielded an accurate product-specific formula but was not considered as suitable for development of a general formula compared with the other methods.

The following four prediction formulae were found to be superior to others tried. Their predictions are summarised in Table 7.3.

(a) Use of the basic form of Calvelo's (1981) solution but representing it in terms of Fo, Bi, Ste and Pk so that all the thermal properties are included. Analysis of the experimental data by multiple non-linear regression gave the following prediction equation:

$$Fo \frac{AD}{2V} = 1.4291 \left[\frac{0.5}{Bi\ Ste} + \frac{0.125}{Ste} \right]^{1.0248} Ste^{0.2712}\ Pk^{0.0610} \qquad (7.2)$$

(b) Use of weighted multiple linear regression to find modified formulae for the shape factors in Plank's equation in a similar manner to that used by Cleland & Earle (1976b, 1977a, 1979a, 1979b, 1982b). The best formula developed was:

$$Fo \frac{AD}{2V} = \frac{P}{Bi\ Ste} + \frac{R}{Ste} \qquad (7.3)$$

where P   = 0.5 (0.7754 + 2.2828 Ste Pk)

R   = 0.125 (0.4271 + 2.1220 Ste - 1.4847 Ste^2)

Other terms were statistically significant in this model but did not lead to worthwhile reduction of the standard deviation of the percentage differences between experimental and predicted thawing times. These terms may have been fitting a systematic component of the experimental error.

(c) A three stage approach similar to Pham (1984a, 1984c). The best prediction formula of this type was:

$$t \frac{AD}{2V} = \sum_{1}^{3} \frac{\Delta H_i \, D}{\Delta T_i 2h} \left[1 + \frac{hD}{4k_i} \right] \tag{7.4}$$

where $\Delta H_1 = C_s (T_{ifave} - T_{in})$

$\Delta T_1 = T_a - (T_{in} + T_{ifave})/2$

$k_1 = k_s$

$\Delta H_2 = L$

$\Delta T_2 = T_a - T_{ifave}$

$k_2 = 0.25 \, k_s + 0.75 \, k_1 = 0.83$ for Tylose $\quad$ $(W \, m^{-1} \, {}^{\circ}C^{-1})$

$\Delta H_3 = C_1 (T_{ave} - T_{ifave})$

$\Delta T_3 = T_a - (T_{ave} + T_{ifave})/2$

$k_3 = k_1$

T_{ave} = average final temperature $\quad$ $(^{\circ}C)$

$\quad = T_{fin} - (T_{fin} - T_a)/(2 + 4k_1/h/D)$

$T_{ifave} = T_{if} - 1.5 = -2.1$ for Tylose $\quad$ $(^{\circ}C)$

Prediction accuracy was sensitive to the values of the mean freezing temperature, the average thermal conductivity in the phase change period and the average final temperature. To retain the analytical basis the values of the mean thawing temperature and the average final temperature were calculated by the methods suggested by Pham (1984a). For accurate predictions it was necessary to empirically fit the value for the mean thermal conductivity in the phase change period (k_2). The weighted value for k_2 of 0.83 $W \, m^{-1} \, {}^{\circ}C^{-1}$ for the phase change period, although physically reasonable, has no basis apart from convenience. Equation (7.4) is closely related to the methods of Pham (1984a, 1984c), which are both of similar prediction accuracy for freezing. Equation (7.4) was considered to be the empirical thawing equivalent of the Pham (1984c) freezing approach, rather than the equivalent of the Pham (1984a) method as the latter has more substantial analytical basis.

(d) Direct fitting of a correction to Plank's equation gave:

$$Fo \frac{AD}{2V} - \left[\frac{0.5}{Bi\ Ste} + \frac{0.125}{Ste}\right] \frac{\Delta H^*}{\Delta H} \left[0.8941 - \frac{0.0244}{Ste} + 0.6192 \frac{Pk}{Bi}\right] \quad (7.5)$$

where ΔH^* = enthalpy change from $-10\,°C$ to T_{ave} $(J\ m^{-3})$

Equation (7.5) is similar in form to the freezing time prediction method proposed by Pham (1983). The Pham prediction formula has not been published in the literature. It is:

$$Fo \frac{AD}{2V} = \left[\frac{0.5}{Bi\ Ste} + \frac{0.125}{Ste}\right] \left[1 + 0.04\ \sqrt{(Bi\ Ste)} + 1.27\ \sqrt{(Pk\ Ste)}\right] \quad (7.6)$$

All four possibilities gave accurate predictions and the predictions take account of all major sources of variation in thawing time as indicated by the high correlation with the finite difference method. All the methods are simple and have some physical basis though their derivations were not analytical.

Further refinement of these methods may be possible. It is unlikely that significant increase in prediction accuracy could be achieved without introducing further terms (that could be fitting systematic experimental error), or empirically fitting the equations separately for each of the three shapes. For all four formulae above, the spread of predictions for each of the three shapes was slightly higher than for the numerical methods. This is because the unified approach using the 6:3:2 ratio is not completely accurate. If data for each shape are analysed separately, three slightly different forms of Eqs. (7.2) to (7.5), specific for each shape, can be derived. The percentage differences for these shape specific formulae have similar standard deviations to the numerical methods for each shape.

The possibility must still exist that a different approach to any of those investigated could conceivably lead to a more accurate formula, but this is not considered likely.

Because Eqs. (7.2) to (7.5) were derived for Tylose thawing data only, they are restricted in pratice to those foods with thermal properties similar to those of Tylose. This includes a wide range of medium to high moisture foods and is not unduly limiting. Other ranges of applicability are:

$$0.6\quad < Bi\ < 57.3$$

$$0.085 < Ste < 0.768$$
$$0.065 < Pk < 0.272$$

7.3.3 Comparison With Freezing Time Prediction Formulae

Methods similar in principle to Eqs. (7.3) to (7.5) have been
successfully used for freezing time prediction (Cleland & Earle 1982b,
Pham 1983 (Eq. (7.6)), Pham 1984c). The main advantages of these types
of method are their simplicity, accuracy and minimal requirement for
thermal property data.

Zaritzky et al (1982) used an approach for freezing similar to
Eq. (7.2), basing it on numerically predicted data. The method
predicted the data of Cleland(1977) poorly so multiple non-linear
regression was used to derive a more accurate formula of this type for
freezing:

$$Fo\,\frac{AD}{2V} = 1.3179 \left[\frac{0.5}{Bi\ Ste} + \frac{0.125}{Ste}\right]^{0.9576} Ste^{0.0550}\ 10^{0.0017Bi+0.1727Pk} \qquad (7.7)$$

Equation (7.7) has a mean prediction error of 0.1% ±7.3% at the 95%
confidence level and a correlation coefficient of 0.61 compared with
the finite difference method predictions errors, when tested against
the freezing data of Cleland & Earle (1977a, 1979a, 1979b). This
compares favourably with the prediction accuracy of the other proven
freezing time prediction formulae (Cleland & Earle 1982b, Pham 1983,
1984a, 1984c).

Cleland & Earle (1984a, 1984b) and Pham (1983, 1984a, 1984c) showed
that their methods were superior to other recent freezing time
prediction methods due to Mascheroni & Calvelo (1982), de Michelis &
Calvelo (1983) and Hung & Thompson (1983) for a large composite
freezing data set. Consequently, the number of accurate simple
freezing time prediction methods for further study was reduced to four.
These were that of Cleland & Earle (1982b, 1984a), that of Pham (1983)
(Eq. (7.6)), that of Pham (1984c) and Eq. (7.7). The method of Pham
(1984a) was not considered further as it performs no better than the
Pham (1984c) method. Similarly Eqs. (7.2) to (7.5), which are the
thawing equivalent of the these four freezing methods, were the only
simple thawing time prediction methods considered further.

7.4 SUMMARY

Within the accuracy of the present freezing and thawing data, it was valid to take the ratio of phase change times for slabs, infinite cylinders and spheres to be constant at 6:3:2 justifying a unified approach for freezing and thawing time prediction for these shapes.

The three numerical methods (the finite difference method and two finite element method formulations) that accounted for thermal properties continuously variable with temperature, accurately predicted thawing times for the three basic shapes. The numerical methods predicted temperature profiles during thawing as accurately as could be expected taking into account the imprecision of some of the measured data.

No previously published simple prediction formula was both sufficiently accurate and suitably expressed for it to be adopted as a general thawing time prediction method. Four improved formulae (Eqs. (7.2) to (7.5)), that gave comparable results with the numerical methods were developed. Each of these formulae represents a different conceptual approach in modifying the well-known Plank's equation in ways that had been previously successful for freezing time prediction.

For both freezing and thawing, all the approaches yielded formulae that are of similar accuracy and simplicity. All are limited more by the accuracy of the data from which they were derived rather than the inherent inaccuracy of the approach used. Within the limits of the testing against experimental data, all of these approaches are of comparable usefulness. It is unlikely that significantly better methods can be developed that retain the advantage of simplicity.

None of the four approaches can be recommended as being significantly more accurate than the others for the three basic shapes. If a method can be easily made compatible with techniques to account for more complex geometry then this would be a useful feature. Therefore, the choice between the four approaches for thawing time prediction is best delayed until a fuller consideration of a range of geometric shapes is made.

Table 7.1 Summary of Percentage Differences Between Experimental
          Freezing and Thawing Times For Simple Tylose Shapes and
          Freezing and Thawing Times Calculated By Slab, Infinite
          Cylinder and Sphere Versions of the Finite Difference Method

Data[1] Type	FDM[2] Version	Corr[3] FDM	Mean (%)	Std Dev[4] (%)	Min[4] (%)	Max[4] (%)
S	S	1.00	0.8	6.1	-14.6	9.3
	C	0.98	-0.3	5.6	-14.1	7.4
Freezing[5]	SP	0.92	-0.8	5.2	-13.5	6.4
C	S	0.97	-3.1	6.1	-15.9	5.6
	C	1.00	-3.6	4.7	-14.1	3.0
Freezing[5]	SP	0.93	-3.4	4.3	-13.3	1.8
SP	S	0.71	-2.6	5.4	-13.2	6.1
	C	0.92	-2.8	4.0	-11.8	2.6
Freezing[5]	SP	1.00	-2.2	3.5	-10.3	4.1
S,C,SP	S	0.93	-1.3	6.1	-15.9	9.3
	C	0.97	-2.0	5.1	-14.1	7.4
Freezing[5]	SP	0.93	-2.0	4.6	-13.5	6.5
	Unmod.	1.00	-1.4	5.4	-14.6	9.3
S	S	1.00	-0.8	3.5	-6.3	6.8
	C	0.79	0.4	6.0	-8.5	13.0
Thawing[6]	SP	0.69	1.3	7.9	-9.7	17.7
C	S	0.45	-2.4	4.1	-9.6	4.8
	C	1.00	-2.2	2.4	-6.8	3.6
Thawing[6]	SP	0.71	-2.4	3.6	-8.3	6.1
SP	S	0.64	0.4	8.1	-13.7	13.7
	C	0.92	-0.2	5.9	-9.0	10.4
Thawing[6]	SP	1.00	-0.9	5.5	-9.5	9.1
S,C,SP	S	0.68	-0.9	5.7	-13.7	13.7
	C	0.86	-0.6	5.1	-9.0	13.0
Thawing[6]	SP	0.78	-0.6	6.1	-9.7	17.7
	Unmod.	1.00	-1.3	4.0	-9.5	9.1

[1] S = slab (43 freezing and 35 thawing runs), C = infinite cylinder (30 freezing and 34 thawing runs), SP = sphere (30 freezing and 35 thawing runs).

[2] Version of the finite difference method.

[3] Correlation coefficient (r) compared with the percentage differences for the unmodified version of the finite difference method.

[4] Std Dev = standard deviation, Min = minimum, Max = maximum.

[5] Data from Cleland & Earle (1977a, 1979a, 1979b).

[6] Data from Tables 6.2, 6.3 and 6.4.

Table 7.2 Summary of Percentage Differences Between Experimental
          Thawing Times For Tylose Slabs, Infinite Cylinders and
          Spheres and Thawing Times Calculated By Simple Prediction
          Formulae

Data from Tables 6.2, 6.3 and 6.4.

Total of 104 runs - 35 for slabs, 34 for infinite cylinders
and 35 for spheres.

Group	Method & Reference	Mean (%)	Std Dev[1] (%)	Min[1] (%)	Max[1] (%)	Corr[2] FDM
A	Neumann (1912) in Carslaw & Jaeger (1959), p.282	69.6	110.5	-68.8	411.7	-0.13
	Charm & Slavin (1962)	173.0	142.6	16.5	536.6	-0.08
	Hrycak (1963,1967)	168.9	147.0	6.9	343.0	-0.09
B	Plank (1913)	6.0	21.4	-28.0	50.5	0.08
C	Goodman (1958)	13.3	17.6	-15.3	53.7	0.14
D	Nagaoka et al (1955)	79.1	15.2	45.4	122.6	0.33
	Levy (1958), Eddie & Pearson (1958)	95.3	21.7	56.2	160.1	0.18
	Earle & Freeman (1966)	52.0	30.6	3.0	115.2	0.08
	Walker (1970)	38.2	17.9	7.9	86.3	0.15
	Vanichseni (1972) Vanichseni et al (1972)	33.7	18.8	-2.8	78.1	0.14
	Frazerhurst (1972)	69.7	59.8	-10.3	304.7	-0.16
	Slatter & Jones (1974)	29.6	17.0	0.3	74.0	0.14
E	Mott (1964)	12.3	15.7	-18.2	49.7	0.14
	Fleming (1967)	13.4	17.7	-16.7	48.7	0.15
	Mellor & Seppings (1976)	-4.0	14.4	-36.4	30.7	0.28
	Modified Plank	-19.9	13.3	-53.1	9.3	0.22
F	Cowell (1967)	34.5	19.9	3.4	85.5	0.09
	Lotz (1974)	13.8	21.3	-22.0	59.3	0.09
	Mascheroni & Calvelo (1982) de Michelis & Calvelo (1983)	15.5	16.8	-16.6	54.1	0.16
	Pham (1984a)	14.7	7.2	0.6	35.0	0.54
	Pham (1984c)	18.3	48.8	-51.4	136.5	0.00

Table 7.2 continued...   166

Group	Method & Reference	Mean (%)	Std Dev[1] (%)	Min[1] (%)	Max[1] (%)	Corr[2] FDM
	Cleland & Earle (1982b)	66.4	17.7	29.6	112.4	0.16
G	Zaritzky et al (1982)	40.1	77.9	-64.2	208.0	-0.11
	Hung & Thompson (1983)	92.2	26.6	14.7	134.2	0.23
	Pham (1983)	53.6	18.4	21.9	100.7	0.14
H	Calvelo (1981)	0.0	6.0	-12.1	17.1	0.66
	Creed & James (1981)	0.2	9.1	-20.0	21.9	0.52
	Khatchaturov (1958)	12.0	27.4	-45.7	86.6	-0.02
	Golovkin et al (1974)	7.8	10.5	-13.6	35.2	0.34
I	Schwartzberg (1977)	-86.1	4.6	-94.3	-71.8	-0.07
	Churchill & Gupta (1977)	-49.5	12.2	-73.5	-25.4	0.16
	Levy (1984)	-35.8	9.3	-64.8	-17.7	0.30
	Sastry (1984)	-57.4	10.7	-71.8	-33.0	0.31

[1] Std Dev = standard deviation, Min = minimum, Max = maximum.

[2] Correlation coefficient (r) compared with the percentage differences for the finite difference method.

Table 7.3 Summary of Percentage Differences Between Experimental
Thawing Times For Tylose Slabs, Infinite Cylinders and
Spheres and Thawing Times Calculated By the Best Present
Methods

Method[1]	Data[2]	Mean (%)	Std Dev[3] (%)	Min[3] (%)	Max[3] (%)	Corr[4] FDM
FDM	S,C,SP	-1.3	4.0	-9.5	9.1	1.00
	S	-0.8	3.5	-6.3	6.8	1.00
	C	-2.2	2.4	-6.8	3.6	1.00
	SP	-0.9	5.5	-9.5	9.1	1.00
FEM$_f$	S,C,SP	-0.9	4.4	-9.2	11.4	0.94
	S	-2.0	3.6	-7.0	6.5	0.99
Eqs. (4.2)-(4.5)	C	-1.7	2.5	-6.0	4.6	0.97
	SP	1.2	5.8	-9.2	11.4	0.99
FEM$_s$	S,C,SP	-0.1	4.8	-7.6	13.1	0.88
	S	-2.2	3.6	-7.6	6.5	0.98
Eqs. (4.5)-(4.8)	C	-1.0	2.6	-5.2	5.4	0.96
	SP	2.9	5.9	-7.2	13.1	0.98
Eq. (7.2)	S,C,SP	0.1	5.7	-10.2	15.2	0.72
	S	0.4	6.0	-7.2	15.2	0.71
	C	-1.6	3.2	-7.7	5.2	0.66
	SP	1.5	6.9	-10.2	14.6	0.76
Eq. (7.3)	S,C,SP	-0.2	4.9	-9.2	12.0	0.80
	S	-0.2	4.5	-7.0	10.2	0.72
	C	-1.8	3.3	-9.2	5.9	0.61
	SP	1.3	6.0	-9.0	12.0	0.89
Eq. (7.4)	S,C,SP	0.0	5.4	-12.6	14.3	0.80
	S	1.7	6.0	-7.0	14.3	0.77
	C	-1.1	3.1	-7.1	4.4	0.64
	SP	-0.5	6.2	-12.6	10.7	0.90
Eq. (7.5)	S,C,SP	0.3	5.6	-10.2	10.3	0.76
	S	0.1	5.2	-8.8	11.1	0.72
	C	-1.3	3.9	-8.8	5.9	0.69
	SP	2.1	6.9	-10.2	14.8	0.79

[1] FDM = finite difference method, FEM$_f$ = full finite element method
formulation, FEM$_s$ = simplified finite element method formulation.

[2] S = slab (35 runs), C = infinite cylinder (34 runs), SP = sphere (35
runs), data from Tables 6.2, 6.3, and 6.4.

[3] Std Dev = standard deviation, Min = minimum, Max = maximum.

[4] Correlation coefficient (r) compared with the percentage differences
for the finite difference method.

8 PREDICTION OF FREEZING AND THAWING TIMES FOR MULT-DIMENSIONAL SHAPES BY NUMERICAL METHODS

The fourth research objective set in Chap. 3 was to assess the accuracy of Group II (numerical) methods for prediction of freezing and thawing times of irregular shapes. Chapter 8 deals with part of the third objective (assessment of the accuracy of prediction methods for regular shapes) and the fourth objective. Results are reported for numerical methods applied to both regular and irregular multi-dimensional shapes.

8.1 INTRODUCTION

The development of numerical methods that solve the governing partial differential equation for heat conduction with temperature dependent thermal properties for objects of any two or three-dimensional geometry was discussed in Chap. 4. The finite difference method is limited by practical considerations to regular shaped objects (infinite rods, finite cylinders and rectangular bricks), whereas the finite element method can take account of the more complex, irregular, multi-dimensional geometries as well as the regular shapes. Thermal property data used in all the numerical calculations are listed in Table 5.1.

8.2 PREDICTIONS FOR REGULAR SHAPES

The only experimental thawing data collected for multi-dimensional regular shapes were those for Tylose rectangular bricks (Table 6.5). The full finite element method formulation (Eqs. (4.2) to (4.5)) was not used as computation costs were too high but the simpler finite element method formulation (Eqs. (4.5) to (4.8)) and the finite difference method were applied. Table 8.1 summarises the calculation results.

Because of symmetry only an octant of each rectangular brick was considered. Within this octant a 9x9x9 node grid was used in finite difference method calculations. The finite element method calculations used a 7x7x7 node grid with 216 evenly sized, 8 node, linear,

isoparametric, brick shaped elements. A finer grid was not practicable
due to computation cost and computer memory size limitations.

Table 8.1 shows that the simplified finite element method formulation
had slightly greater off-set of the mean prediction error than the
predictions for the finite difference method. As was the case for the
simple slab, infinite cylinder and sphere shapes this difference was
thought to be due to the relatively crude way in which variations in
the thermal properties are incorporated into the simplified finite
element method. The three-dimensional geometry and the coarse nodal
grid used, accentuated this problem so the difference between the
finite difference method and the simplified finite element method is
greater than for slabs, infinite cylinders and spheres (Table 7.3).

Results for the full finite element method formulation would be
expected to be close to the finite difference method results (Cleland
et al 1984). For thirteen representative rectangular brick freezing
runs the full finite element method results were calculated as well as
the results for the other two numerical methods. The mean prediction
errors for these runs were -5.7% for the finite difference method,
-8.2% for the simplified finite element method and -6.3% for the full
finite element method respectively. The correlation coefficients for
the finite element method percentage differences with the finite
difference percentage differences for these thirteen runs were 0.96 and
0.99 for the simplified and full formulations respectively. Hence, if
the full finite element method had been used for the full set of data,
the results would have closely matched the finite difference method
results.

Predicted temperature profiles agreed closely with experimentally
measured profiles as illustrated in Fig. 6.4. A large part of the
difference between the predicted and measured temperatures was probably
due to uncertainty in thermocouple placement which was discussed in
Sec. 5.7.4. Both the finite difference method and the simplified
finite element method formulation predicted surface temperatures that
oscillated about the experimental values immediately after the phase
change temperature region. This was due to the discrete nature of the
numerical methods and for the simple finite element method formulation

was magnified by the coarse element grid used for predictions.

The differences between predicted and measured thawing times were not statistically correlated with any independent variable in the experiments and displayed comparable accuracy with numerical predictions for freezing of Tylose rectangular bricks (Cleland & Earle 1979b, Cleland et al 1984). Further the 95% confidence bounds for the numerical methods are similar in magnitude to the estimated experimental uncertainty (Sec. 5.7.4, Table 12.2). This suggests that for the finite difference method and the full finite element method formulation, most of the difference between the predictions and experimental values was due to experimental uncertainty and not errors in the implementation of the numerical methods themselves. That is, the time steps and the space grid used yielded results negligibly different from those that would have been obtained if finer grids had been used. The only significant inaccuracy arising from the numerical methods themselves was that introduced by the crude thermal property estimation in the simpler finite element method formulation; this indicates that care should be exercised in using it for rectangular brick shapes.

8.3   PREDICTIONS FOR TWO-DIMENSIONAL IRREGULAR SHAPES

The experimental freezing and thawing times for the two-dimensional irregular Tylose shapes are given in Table 6.6. Predictions were carried out by both finite element method formulations using the grids shown in Figs. 5.15 to 5.21. The grids were prepared from 8 node, quadratic, isoparametric, rectangular elements. These elements allowed curved boundaries to be approximated by quadratic functions. The grids prepared ensured that at least five elements (11 nodes) existed between the thermodynamic centre and the outside surface of each object, in all directions.

The results summarised in Table 8.1 show that both the finite element formulations gave accurate predictions of both freezing and thawing times (within tolerances allowed for experimental error), for all the shapes tested. The 95% confidence bounds for the percentage differences of the full finite element formulation of -9.7% to 10.3%

are of similar magnitude to the estimated experimental error
(Sec. 5.8.4) indicating that most of the difference was explainable by
the experimental uncertainty. Again, the full finite element method
formulation used sufficiently small space and time intervals that
numerical approximation errors were negligible, but the simple finite
element method formulation did introduce significant inaccuracy by
crude thermal property estimation.

Predicted temperature profiles (Figs. 6.5 to 6.12) generally compared
well with those measured experimentally. Differences between predicted
and measured temperatures may have arisen due to uncertainty in
thermocouple placement for all the thermocouples. Also the possibility
of air voids, poor contact and therefore variations in the local
surface heat transfer coefficient meant that measured temperatures at
points on or near the surface had significant uncertainties associated
with them. The surface temperatures predicted by the simplified finite
element method formulation oscillated significantly compared with the
predictions for the full finite element method formulation. Again this
difference was attributed to the crude thermal property estimation in
the simple formulation and the relatively small number of quadratic
elements used in the grids for the predictions.

8.4   PREDICTIONS FOR THREE-DIMENSIONAL IRREGULAR SHAPES

Table 8.2 summarises the percentage differences between experimental
freezing and thawing times and the predictions by the two finite
element method formulations for the three-dimensional irregular shapes.

The grid used for the first shape (the frustum of a square pyramid) is
shown in Fig. 5.24. Because of the straight sides it is basically the
same 7x7x7 node grid used for the rectangular brick predictions, but
was distorted to the pyramid dimensions. Because of the
three-dimensional irregularity a full quadrant of the shape was
modelled. Consequently the grid was rather coarse with only three
linear elements between surface and centre along the height of the
pyramid. The experimental procedure for the pyramid was identical in
all respects to that used for the rectangular brick shape so it was
considered that the experimental conditions were controlled and

measured to the same level of precision as in the rectangular brick experiments, and that the same surface heat transfer coefficient applied.

The predictions have similar spread to those for the rectangular brick freezing and thawing but the mean was offset by about 10%. The low standard deviation of the prediction errors suggests that the problem is systematic, and not random. Two possible reasons are: (a) the coarse grid leading to significant prediction inaccuracy and (b) the assumption that h was the same for the pyramid and rectangular brick shapes may not hold.

The amount of offset was greater for the freezing runs where Bi was low suggesting that the second reason was an important contributor according to the criteria of Cleland & Earle (1984a).

In the numerical calculations, freezing and thawing were considered complete when the slowest cooling or heating node reached the desired final temperature. If the true thermodynamic centre of the object does not coincide with a node, at this time, then the object is not completely frozen or thawed. Under-prediction of the time for the complete process will result from this effect. The effect is smallest for fine finite element grids, but for coarse grids the extra time could be substantial. Further, linear elements magnify the problem because they use linear approximation functions between nodes. The true temperature profile and any local maximum or minimum values of the temperature within each element cannot be modelled. Quadratic and higher order elements allow more accurate approximations to the temperature profile to be made and therefore give more accurate predictions.

Finite element method calculations for the pyramid shape were affected in the manner just described, as a coarse grid of linear elements was used. Also the position of the thermodynamic centre could not be accurately determined prior to grid preparation so the true thermodynamic centre was not necessarily close to a node. Therefore the observed under-prediction of freezing and thawing times was not unexpected. Predicted temperature profiles were adequate considering

these problems with the coarse grid and the experimental uncertainty in thermocouple positioning (Fig. 6.13).

The other three shapes used were a sphere, an egg and a fish shape. The sphere runs were used to provide information about the surface heat transfer coefficient for the other two three-dimensional shapes moulded in plastic. The sphere is a regular shape and can be modelled by a one- or two-dimensional grid rather than three-dimensionally if the axisymmetrical formulation of the finite element method is used. However modelling the sphere with a three-dimensional grid allowed some measure of the accuracy of the modelling of curved surfaces by the finite element method to be made. The three different grids shown in Fig. 5.25 were used: (a) an 11 node, 10 linear element, one-dimensional grid; (b) a two-dimensional grid modelling a quadrant of the cross-section (a circle) with 21, eight node, quadratic, isoparametric, elements and (c) a 208 node, 27 element, three-dimensional grid modelling an octant of the sphere. Due to the limitations in computation power available and the high data preparation time, the three-dimensional grid was coarse with only three 20 node, quadratic, isoparametric elements between the surface and the centre. These were arranged in three expanding shells so that the elements were all approximately the same size and none were too highly distorted from the basic regular rectangular brick shape.

The results generated for the sphere shape using both the finer one- and two-dimensional grids with the full finite element formulation were very similar. The coarser three-dimensional grid results were significantly less accurate. This was attributed to the coarse grid rather than incorrect implementation of the three-dimensional part of the program (Sec. 4.2.3). The three quadratic elements between the centre and surface meant that the temperature profiles could be modelled only approximately. The position of the thermodynamic centre was known exactly for the sphere, and quadratic elements were used. Therefore the problem with the coarse grid was less acute than for the pyramid shape predictions and the amount of under-prediction for the coarser three-dimensional grid, compared with the finer one- and two-dimensional grids, was less than the under-prediction for the pyramid shape.

For the sphere shape the simplified finite element method formulation gave comparable results with the full formulation, but where the element size was larger in the two- and three-dimensional grids the results had a larger variation attributed to the less representative incorporation of thermal properties into the finite element scheme as well as the coarse grid. For both finite element methods the freezing and thawing time prediction accuracy as well as the prediction of temperature profiles was similar to that achieved for the full set of sphere thawing data analysed in Sec. 7.2. The experimental techniques were similar, except for use of the plastic moulding, so similar prediction accuracy was expected.

The egg shape has one axis of rotational symmetry so it could be modelled by either a two- or three-dimensional grid. Both the finite element method grids used are shown in Fig. 5.26. The two-dimensional grid is similar to that use for the sphere shape except that it was distorted to fit the elliptical shape and a half, rather than a quarter, of the cross-sectional profile was modelled. The three-dimensional grid used was also a distorted , double version of the sphere three-dimensional grid. The full quadrant needed was described by 54 twenty node, quadratic, isoparametric, rectangular elements. The fish shape though irregular in all three dimensions was closely approximated by a shape with two planes of symmetry so only a quadrant was modelled. The grid is shown in Fig. 5.27. It is the same basic three-dimensional grid used for the egg shape but the grid point coordinates, especially for the surface nodes were modified to fit the actual shape.

For the egg and fish shapes it was assumed that the surface heat tranfer coefficient was the same as that measured on the moulded plastic spheres (Sec. 5.9.3). The inaccuracy introduced by this assumption was not easily assessed. Variations in plastic thickness and the presence of air voids and poorer or better surface contact at the surface of these objects may have contributed to the uncertainties. This extra experimental uncertainty, plus the uncertainty due to difficulties in measuring and describing these shapes mathematically, as well as approximating the shape with a coarse finite element method grid, meant that poorer predictions were expected for the egg and fish

shapes than for the sphere and pyramid shapes.

For the egg shape the mean prediction error was close to zero so the assumption that the surface heat transfer coefficient was the same as it was for the sphere seemed reasonable. The higher standard deviation of the predictions for the egg shape compared with the pyramid and sphere shapes was mainly the result of the extra uncertainty in the experiments rather than uncertainty due to the implementation of the finite element method. If a finer grid had been used, the finite element method would have introduced no significant prediction inaccuracy.

Predicted temperature profiles for the egg shape (Fig. 6.16) were also quite accurate and reflected the accuracy of the freezing and thawing time predictions. Temperature profiles for some surface positions may have been affected by any localised variation in h. Predicted temperature profiles were affected by the coarse three-dimensional grids used, and therefore displayed some oscillatory behaviour. As expected, this was particularly obvious for the simple finite element method formulation predictions, for positions near the object surface and at temperatures close to the phase change temperature range (Cleland et al 1984, Sec. 4.2.1).

For the fish shape the predictions were consistently high by 20% to 40% but the standard deviation of prediction errors was comparable with that for the egg shape. The off-set mean was probably caused by systematic error in the surface heat transfer coefficient. The surface heat transfer coefficient may not have been the same as that for the sphere due to: (a) a thinner plastic thickness arising during moulding and/or (b) better thermal contact between the Tylose and the plastic mould for the fish shape than the sphere. As discussed in Sec. 5.9.4 these factors could not not be quantatively assessed as it was not possible to measure h directly for the fish shape. However, measurement of the plastic thickness showed variations of up to 15% of the average total thickness over the surface of the fish shape and differences of up to 10% in the thickness between the fish and sphere shapes. It was unknown whether these observed variations were sufficiently large to cause the differences between the predicted and

measured freezing and thawing times. Because the finite element method
displayed accurate predictions for other regular and irregular shapes
it was considered unlikely that these differences were the result of
deficiencies in the finite element method or program.

Predicted temperature profiles for the   fish   shapes   (Fig. 6.15)
reflected the accuracy of the predicted freezing and thawing times and
problems with the coarse element grid used. The finite element method
consistently under-predicted the changes in the temperature at all
positions in the fish shape.   Temperature profiles   for   surface
positions would have been affected by any localised variation in the
surface heat transfer coefficient as well as the possible systematic
error in the h value, but the predicted values showed trends consistent
with a systematic underprediction of h.

8.5 FINITE ELEMENT METHOD USER GUIDELINES

Some guidelines for application of the finite element method were
established   in Sec. 4.2.   In the light of the testing against
experimental data it is possible to refine these.   Adherence to the
guidelines will lead to predictions in which the error arising from the
numerical approximations is negligible compared with experimental and
data uncertainty. The guidelines are:
(a) to use at least 8 to 10 nodes and at least 5 elements between the
    thermodynamic centre and the surface,
(b) to use the full finite element formulation if computational
    limitations allow,
(c) to accurately predict the position of the thermodynamic centre
    prior to grid preparation so that a node can be positioned
    accurately near it, and
(d) to use sufficiently small time steps that the heat balance agrees
    to within 2% (Sec. 4.2.2).
In almost all situations, using more refined grids and smaller time
steps than those suggested here, will only give small increases in
accuracy and reliability of the predictions and will probably not
justify the increase in computational costs.

8.6 SUMMARY

The finite difference method used for regular two- and three-dimensional shapes predicted thawing times as accurately as it predicted freezing times. The method could be implemented with negligible inaccuracy arising from the numerical approximations used.

The spreads of the numerical method predictions were low for all data, but mean prediction errors for some three-dimensional irregular shapes were off-set from zero. This indicates that systematic data errors, probably in estimation of surface heat transfer coefficients, were important compared with random experimental uncertainty. Predicted temperature profiles confirmed these trends.

The implementations of the finite element method used for both regular and irregular multi-dimensional shapes do not lead to significant inaccuracy in predictions provided the guidelines in Sec. 8.6 are followed. Use of coarse grids and/or the simplified finite element method formulation did lead to significant inaccurracy in the predictions and therefore worsened overall agreement with experimental freezing and thawing data.

Practical contraints on computation power means that users of the finite element method will have to work close to the limits of grid and method refinement for which prediction method uncertainty is significant, so care must be exercised in using these methods.

Table 8.1 Summary of Percentage Differences Between Experimental
Freezing and Thawing Times For Tylose Multi-Dimensional
Shapes and Freezing and Thawing Times Calculated By Numerical
Methods

Shape	Type[1]	Reference	Method[2]	Mean (%)	Std Dev[3] (%)	Min[3] (%)	Max[3] (%)
Rectangular Brick	F	Cleland & Earle (1979b) (72 runs)	FDM	-4.4	6.6	-20.7	9.8
			FEM_s	-5.9	7.1	-24.1	9.8
	T	Table 6.5 (68 runs)	FDM	0.6	3.1	-6.0	7.9
			FEM_s	-6.3	3.4	-12.9	1.2
Two-Dimensional Irregular	F,T	Table 6.6 (83 runs)	FEM_f	0.3	5.1	-11.4	11.3
			FEM_s	4.2	6.1	-9.1	21.9
	F	Table 6.6 (42 runs)	FEM_f	-1.0	4.5	-11.4	7.6
			FEM_s	2.6	4.8	-9.1	12.0
	T	Table 6.6 (41 runs)	FEM_f	1.5	5.5	-7.1	11.3
			FEM_s	5.8	7.0	-6.7	21.9

[1] F = freezing, T = thawing.

[2] FDM = finite difference method, FEM_f = full finite element method
formulation (Eqs. (4.2) to (4.5)), FEM_s = simplified finite element
method formulation (Eqs. (4.5) to (4.8)).

[3] Std Dev = standard deviation, Min = minimum, Max = maximum.

Table 8.2 Summary of Percentage Differences Between Experimental
Freezing and Thawing Times For Tylose Three-Dimensional
Irregular Shapes and Freezing and Thawing Times Calculated By
the Finite Element Method

Shape	Grid[1]	Method[2]	Mean (%)	Std Dev[1] (%)	Min[1] (%)	Max[1] (%)
Pyramid		FEM_f	-10.3	6.7	-18.2	-2.0
	3D					
(6 runs)		FEM_s	-14.5	4.8	-20.2	-8.9
		FEM_f	-5.5	6.8	-12.1	5.3
	3D					
		FEM_s	-1.2	12.7	-16.1	13.9
Sphere		FEM_f	0.6	7.0	-8.7	13.9
	2D					
(6 runs)		FEM_s	7.7	8.3	-1.6	18.2
		FEM_f	0.4	6.7	-7.7	9.6
	1D					
		FEM_s	2.6	6.5	-4.9	11.6
		FEM_f	5.2	13.0	-12.9	25.1
	3D					
Egg		FEM_s	9.8	14.9	-9.4	28.8
(6 runs)		FEM_f	3.7	13.8	-16.1	24.7
	2D					
		FEM_s	16.4	18.7	-4.1	48.4
Fish		FEM_f	35.3	8.9	20.8	44.2
	3D					
(6 runs)		FEM_s	33.5	16.3	8.6	58.4

[1] 1D = one-dimensional, 2D = two-dimensional, 3D = three-dimensional.

[2] FEM_f = full finite element method formulation (Eqs. (4.2) to (4.5)),
FEM_s = simplified finite element method formulation (Eqs. (4.5) to
(4.8)).

[3] Std Dev = standard deviation, Min = minimum, Max = maximum.

9 PREDICTION OF FREEZING AND THAWING TIMES FOR MULTI-DIMENSIONAL REGULAR SHAPES BY SIMPLE METHODS

In Chapter 9 Group I (simple) methods for regular multi-dimensional shapes are considered. This completes the analysis required for the third research objective set in Chap. 3.

9.1 ANALYTICAL TREATMENT OF THE EFFECT OF GEOMETRY

For slabs, infinite cylinders and spheres the 6:3:2 ratio of freezing and thawing times, which arises from the value of 2V/AD, was successfully used to describe the effect of the geometry so that simple prediction methods could be made universal for all three basic shapes. Rutov (1936) and Mott (1964) proposed the use of the same 2V/AD ratio for all shapes. The prediction equation becomes:

$$t = \frac{2V}{AD}\, t_{slab} \tag{9.1}$$

where t   = freezing or thawing time for the multi-dimensional
              object of characteristic dimension D   (s)

   t_{slab} = freezing or thawing time for a slab of
              thickness D under equivalent conditions   (s)

   A   = surface area of the object (m^2)

   V   = volume of the object (m^3)

   D   = characteristic dimension of the object   (m)

          = length of shortest dimension for regular
            shaped objects.

For two- and three-dimensional regular shapes (infinite rods, finite cylinders and rectangular bricks) an alternative approach was used by Plank (1941) and Shamsundar (1982). They made the quasi-steady state assumption and assumed both a particular shape for the phase change front and that the surface was isothermal with respect to position. This led to geometric factors to modify the basic slab formulae that tend to 2V/AD as Bi→0 but included a small correction to the internal conduction term, in the resulting analytical formula, for other Bi values.

For all two- and three-dimensional shapes (apart from infinite cylinders and spheres) the surface is not isothermal with respect to position unless $Bi \to 0$ or $Bi \to \infty$. In addition the phase change front shape varies with time. Consequently the true geometric factors for multi-dimensional shapes are in reality highly dependent on the Biot number. As $Bi \to 0$ the ratio of $2V/AD$ holds for all shapes. For higher Bi values, some parts of the surface are more effective in transferring heat to or from the centre than others. Therefore none of the analytical developments based only on the area to volume ratio are successful for freezing (Cleland & Earle 1982b). The complexity of the heat transfer in multi-dimensional objects is such that an accurate geometric factor is unlikely to be derived analytically.

9.2 FEASIBLE GEOMETRIC FACTORS

Alternative geometric factors have been developed, partly by fitting to experimental data and partly by considering some known limiting cases.

Cleland & Earle (1982b) defined the equivalent heat transfer dimensionality, EHTD, as:

$$EHTD = \frac{t_{slab}}{t} \qquad (9.2)$$

The formula for rectangular brick shapes:

$$EHTD = 1 + \frac{2}{Bi+2}\left[\frac{2}{\beta_1(\beta_1+1)} + \frac{2}{\beta_2(\beta_2+1)}\right] + \frac{Bi}{Bi+2}\left[\frac{0.625}{\beta_1^3} + \frac{0.625}{\beta_2^3}\right] \qquad (9.3)$$

where β_1 = ratio of second longest to shortest side length

$\qquad\qquad$ = D_y/D_x

$\qquad \beta_2$ = ratio of longest to shortest side length

$\qquad\qquad$ = D_z/D_x

$\qquad D_x$ = shortest side length $\qquad\qquad\qquad\qquad$ (m)

$\qquad D_y$ = second longest side length $\qquad\qquad\quad$ (m)

$\qquad D_z$ = longest side length $\qquad\qquad\qquad\qquad$ (m)

was developed by fitting experimental data with Bi in the range 0.5 to 22.0. It does not conform to the limiting case that $EHTD=AD/2V$ as $Bi \to 0$ but does fit published experimental data for rectangular bricks undergoing freezing. It covers ranges of Bi, β_1 and β_2 typically encountered in practice. Used in conjunction with the freezing time prediction formula for slabs due to Cleland & Earle (1982b) it

predicted the experimental Tylose rectangular brick freezing data of Cleland & Earle (1979b) with percentage differences with a mean of -1.2% ±11.4% at the 95% level of confidence.

Pham (1984b) used the 2V/AD geometric factor but modified the internal conduction term in the simple prediction formula based on Plank's slab equation by a factor called the "mean conducting path length", MCP. MCP is based on the same principle as the corrections derived analytically by Plank (1941) and Shamsundar (1982) but because it was developed based on fit to experimental data it includes compensation for effects such as the non-isothermal surface, that Plank and Shamsundar ignored. For rectangular bricks the formula developed to calculate MCP was:

$$\frac{MCP}{D} = 1 + \left[\left(1.5\sqrt{\beta_1} - 1\right)^{-4} + \left[(\frac{1}{\beta_1} + \frac{1}{\beta_2})(1 + \frac{4}{Bi}) \right]^{-4} \right]^{-0.25} \qquad (9.4)$$

For finite cylinders, an equivalent rectangular brick shape was defined so that Eq. (9.4) could be used (Pham 1984c). Equation (9.4), combined with the slab prediction method of Pham (1984a), predicted the Tylose rectangular brick freezing data (Cleland & Earle 1979b) with 95% confidence bounds of -13.0% to 13.0% and a mean prediction error close to zero, which is similar to the results for EHTD (Pham 1984b).

MCP and EHTD are essentially equivalent geometric corrections to the basic slab prediction methods but are incorporated into the simple formulae in different manners. EHTD is a divisor and can be applied to any slab prediction method by rearrangement of Eq. (9.2) to give:

$$t = \frac{t_{slab}}{EHTD} \qquad (9.5)$$

MCP can be directly incorporated into simple prediction formulae where contributions due to external and internal resistance to heat transfer can be separated (such as Plank's equation), by the relationship:

$$t \propto \frac{V}{A} \left[\text{External Resistance} + \text{Internal Resistance} \frac{MCP}{D} \right] \qquad (9.6)$$
$$\phantom{t \propto \frac{V}{A} \left[\right.} \text{Term} \phantom{+ \text{Internal Resistance} \frac{MCP}{D}}$$

A more general form which allows it to be applied to any slab prediction method is:

$$t = t_{slab} \frac{2V}{AD} \left[1 + \frac{Bi}{4} \frac{MCP}{D} \right] / \left[1 + \frac{Bi}{4} \right] \qquad (9.7)$$

The values for the two variables can be related by the equations:

$$EHTD = \frac{AD}{2V} \left[1 + \frac{Bi}{4} \right] / \left[1 + \frac{Bi}{4} \frac{MCP}{D} \right] \tag{9.8}$$

and

$$\frac{MCP}{D} = \left[\frac{4}{Bi} + 1 \right] \frac{AD}{2V} \frac{1}{EHTD} - \frac{4}{Bi} \tag{9.9}$$

EHTD and MCP defined by Eqns. (9.3) and (9.4) are both accurate
geometric factors for the rectangular brick shape with the intermediate
β and Bi values that occur in the rectangular brick freezing data from
which they were developed. For other conditions they may not be
accurate.

One possible approach for the current work was to seek to extend the
MCP and EHTD definitions to a wider range of geometries and
environmental conditions to enhance their versatility. If this was
successful then there would be little benefit in seeking to develop
completely different geometric factors. Therefore the approach taken
was to investigate the MCP and EHTD concepts in detail, and then to
assess whether their lack of fit to data was sufficiently great to
justify considering other alternative geometric factors.

If both MCP and EHTD can be made accurate for a wide range of
conditions and geometries then the choice between the two concepts must
be made by considering other criteria such as:
(a) conceptual understanding and simplicity
(b) ease and accuracy of calculation for a wide range of object
    geometries.
Because the equations to calculate MCP and EHTD, such as Eqs. (9.3) and
(9.4) are partly empirically developed it is possible that the second
criterion allows a distinction to be made.

9.3 VERIFICATION OF THE EFFECT OF ENVIROMENTAL CONDITIONS
   ON GEOMETRIC FACTORS

As defined by Eqs. (9.5) and (9.7) EHTD and MCP are both related to the
ratio of t_{slab}/t. For infinite cylinders and spheres it was found
(Sec. 7.1) that the dependence of this ratio on Bi, Ste and Pk was
sufficiently weak for both freezing and thawing that the variation

could be ignored. For other multi-dimensional shapes the Bi effect
would be expected to be larger because the surface is not isothermal
with respect to position and the degree of approach to a constant
surface temperature is Biot number dependent. Where most of the
resistance is internal (Bi→∞), surface area not directly adjacent to
the thermodynamic centre will have little effect on the change in
temperature at the centre. Conversely if most of the resistance is
external (Bi→0), then all the surface area of the object is equally
effective and no further correction to 2V/AD is needed.

Freezing and thawing times were calculated for different Bi, Ste and Pk
values using the finite difference and finite element methods.
Calculations were made for a range of different infinite rod, finite
cylinder and rectangular brick shapes as well as for the equivalent
slab shape so that the dependence of t_{slab}/t on Bi, Ste and Pk could be
examined.

The finite difference method results for freezing and thawing of two
infinite rod shapes are shown in Table 9.1. These are typical for all
the shapes, for both freezing and thawing, and for both the numerical
methods used. For each of the shapes tested the effect of changes in
Ste and Pk, due to changes in T_a and T_{in}, were far less than the effect
of changes in Bi for the ranges of conditions typically encountered in
practice. The Biot number effect must be taken into account but the
Ste and Pk effects are small. The Ste and Pk effects were most
important for thawing, and for that process changed t_{slab}/t by less
than ±5% over the full range of Ste and Pk values typically encountered
in practice. The initial approach was to ignore the Pk and Ste
effects.

9.4   DEVELOPMENT OF IMPROVED GEOMETRIC FACTORS FOR MULTI-DIMENSIONAL
   REGULAR SHAPES

The analysis of the previous section confirmed that for regular
multi-dimensional shapes, accurate geometric factors can probably be
defined solely as functions of Bi and parameters that describe the
shape, without introducing significant error into the prediction
method:

Geometric Factor $= f \left(Bi, \beta_1, \beta_2 \right)$ (9.10)

The existing formulae for EHTD and MCP (Eqs. (9.3) and (9.4)) were curve-fitted to experimental data for freezing of rectangular brick shapes which were both limited in range of β_1, β_2 and Bi, and affected by experimental error. To develop an improved empirical geometric factor better data were considered necessary. An alternative data set that shows the geometry effect without masking by experimental uncertainty was developed by using numerical prediction methods for regular multi-dimensional shapes.

The numerical calculations were carried out over a wider range of conditions than the published experimental data. Freezing times were calculated for freezing of the infinite rod, finite cylinder and rectangular brick shapes using the finite difference method. Biot number was varied from 0.01 to 100.0, and β_1 and β_2 from 1.0 to 10.0. For the rectangular brick shape only the ten possible combinations derived from β_1 and β_2 values of 1.0, 1.582, 2.50 and 4.0 were investigated due to limitations in computation resources. The equivalent slab shape freezing times were also calculated using the finite difference method. Equations (9.2) and (9.9) were used to calculate EHTD and MCP. Using the same prediction method for both the multi-dimensional shapes and the equivalent slab gives a systematic error cancelling effect so that the results reflect almost entirely the variations in geometric factors. Calculations for some runs using the full finite element method formulation gave identical results to the finite difference method, so the full finite element method formulation was not used for the full set of data. As slight changes in the geometric factors can occur with environmental conditions, all calculations were made at intermediate Ste and Pk values to average these effects. A full set of data was not calculated for thawing as a trial of some representative calculations yielded very similar MCP and EHTD values to those calculated for freezing.

The numerically calculated results are are tabulated in App. C (Table C.1). Apart from some random error introduced by slight imprecision in the numerical calculations, especially at extremes of the range of Bi, the results showed a number of consistent patterns. Each shape was considered to have three dimensions, taken in order of size. The first

dimension was the characteristic dimension and had an effect equal to that of a slab for infinite rods, rectangular bricks and squat cylinders (finite cylinders with $D_r \geq D_y$), and an effect equal to that of an infinite cylinder for short cylinders (finite cylinders with $D_r \leq D_y$). The effect of each of the other dimensions on the ratio of t_{slab}/t for each shape could be separated. A number of trends were evident :

(a) the effect of the second dimension for infinite rods and rectangular bricks was equal

(b) the effect of the second and third dimensions for the squat cylinders (considering the thickness as the first dimension and the diameter as two equivalent dimensions) were both the same, and were equal to the effect of the second dimension in infinite rods and rectangular bricks

(c) the effect of the third dimension in short cylinders (considering the diameter as the first two dimensions and the height or length as the third) was the same as the effect of the third dimension in rectangular bricks, but was less than the effect of the second dimension in infinite rods and rectangular bricks.

The value of t_{slab}/t changed with Biot number. The value of Bi at which the change with respect to Bi was greatest depended on the ratio of dimensions :

(d) as β_1 or β_2 increased the change occurred at lower Bi values

(e) for high β_1 and β_2 values as Bi→∞, the values of MCP and EHTD both tended to slab limits (for infinite rods, rectangular bricks and squat cylinders) or infinite cylinder limits (for short cylinders)

(f) for low β_1 and β_2 values as Bi→∞, the values of MCP and EHTD both tend to some other limits which are fractions of the values as Bi→0.

(g) as Bi→0 the values of MCP and EHTD both depend only on 2V/AD.

Using non-linear regression of the numerical data set, a number of functions were developed to calculate EHTD and MCP for all the regular shapes. The simplest forms that gave reasonable prediction accuracy were:

$$EHTD = G1 + G2 \left[f_{12}(\beta_1) \frac{1}{\beta_1} + \left(1 - f_{12}(\beta_1)\right) \frac{0.73}{\beta_1^{2.50}} \right]$$
$$+ G3 \left[f_{12}(\beta_2) \frac{1}{\beta_2} + \left(1 - f_{12}(\beta_2)\right) \frac{0.50}{\beta_2^{3.69}} \right] \qquad (9.11)$$

and
$$\frac{MCP}{D} = 1 + (2 - G1) \, f_{14}\left(\, f_{13}(G2,\beta_1) \, \right) 0.63 \, Bi^{0.39} \left(1.34 \, \beta_1^{1.43} - 1\right)$$

$$+ G3 \, f_{14}\left(\, f_{13}(G3,\beta_2) \, \right) 0.63 \, Bi^{0.39} \left(1.51 \, \beta_2^{1.22} - 1\right)$$

$$+ \left[\, 1 - f_{14}\left(\, (f_{13}(G2,\beta_1) + f_{13}(G3,\beta_2))/(G2 \, G3 + 1) \, \right) \, \right] \cdot$$
$$\cdot \left[\frac{(G1 + G2/\beta_1 + G3/\beta_2)}{(G1 + G2 \, 0.73/\beta_1^{2.50} + G3 \, 0.50/\beta_2^{3.69})} - 1 \right] \qquad (9.12)$$

where $f_{12}(\beta) \quad = 2.32/\beta^{1.77}/\left(Bi^{1.34} + 2.32/\beta^{1.77}\right)$
$\quad\quad f_{13}(G,\beta) = G \, 2.00/\beta^{1.92}$
$\quad\quad f_{14}(X) \quad = X/\left(Bi^{1.34} + X\right)$

and the values of G1, G2 and G3 are given in Table 9.2.

The principles behind the methods to calculate EHTD and MCP were developed from the above observed trends in the t_{slab}/t data. For the MCP concept the AD/2V ratio was incorporated independently (Eq. (9.7)) whereas for the EHTD concept it was included in the geometric factor itself.

The geometric factor can be influenced by up to three dimensions for any shape. Firstly, the effect of the first (characteristic) dimension is added (G1 for EHTD and 1.0 for MCP). Where the characteristic dimension can be measured in more than one dimension, the effect of each of the additional dimensions is to increase the value of G1 by one. The data in Table 9.2 illustrate this idea. The effects of each of the other dimensions are then calculated and summed as needed.

As Bi→0 the effect depends on the AD/2V ratio only. For regular shapes AD/2V = G1+G2/β_1+G3/β_2 so for EHTD the additions are G2/β_1 and/or G3/β_2, while for MCP there is zero addition as the effect of AD/2V has already been included.

As Bi→∞ the effect of each dimension is less than that suggested by the AD/2V ratio so the effect of each dimension is a fraction of G2/β_1

and/or $G3/\beta_2$ for EHTD and is greater than zero for MCP. The fractional values, which are different for each dimension because the effect of the third dimension is less than the effect of the second dimension, are given by $0.73/\beta_1^{1.50}$ and $0.52/\beta_2^{2.69}$ respectively for EHTD.

For MCP the final term calculates the modification to MCP required to alter the effect of the AD/2V ratio. It is based on the fact that as $Bi \to 0$, $MCP \to EHTD(Bi \to 0)/EHTD(Bi \to \infty)$.

For the EHTD concept the expression is completed by a Biot number weighting function that calculates the relative contribution of the $Bi \to 0$ and the $Bi \to \infty$ terms in the effect of each dimension. The equation can be written in general terms as:

$$EHTD = X_1 \left(EHTD_{Bi \to 0} \right) + \left(1 - X_1 \right) \left(EHTD_{Bi \to \infty} \right) \qquad (9.13)$$

where X_1 = Biot number weighting function ($0 \le X_1 \le 1$). The Bi value at which the maximum rate of change, from one term to the other, occurs is dependent on the relative size of that dimension compared with the characteristic dimension.

For the MCP concept the transition is more difficult to calculate as MCP goes through a maximum value between the two Biot number extremes. Therefore the expression includes an extra Biot number correction as well as a Bi weighting function similar to that used for EHTD. Written in general terms:

$$MCP = X_2 MCP_{Bi \ne \infty} + \left(1 - X_2 \right) \left(EHTD_{Bi \to 0} / EHTD_{Bi \to \infty} \right) \qquad (9.14)$$

where X_2 = Biot number weighting function ($0 \le X_2 \le 1$) and $MCP_{Bi \ne \infty}$ is a function including a term that increases as Bi increases.

Table 9.3 shows the adequacy of the fit to the numerical t_{slab}/t data of (a) the old EHTD formula (Eq. (9.3)), (b) the new EHTD formula (Eq. (9.11)), (c) the old MCP formula (Eq. (9.4)) and (d) the new MCP formula (Eq. (9.12)). The new versions of EHTD and MCP are significant improvements over the older versions. This was expected because Eqs.(9.3) and (9.4) were both developed from data for the rectangular brick shape only and for a limited range of Bi, β_1 and β_2 values. The inaccuracy in the improved MCP and EHTD formulae (about ±3% at the 95% level of confidence) is likely to be insignificant compared with experimental uncertainties. Therefore the introduction of further new

terms into Eqs. (9.11) and/or (9.12) (or development of a new empirical formula), to relate EHTD and MCP more closely to β_1, β_2 and Bi would be difficult to justify. It must be remembered that the Ste and Pk effects (of up to ±5%) have been ignored.

Equations (9.11) and (9.12) were fitted for Bi in the range 0.01 to 100.0 and β from 1.0 to 10.0 for finite cylinders and infinite rods, and β_1 and β_2 from 1.0 to 4.0 for rectangular bricks. The range for the brick shape may appear more restrictive. However, the relationship of EHTD and MCP for rectangular bricks was found to be a summation of the infinite rod and the finite cylinder terms. Therefore the finite cylinder and infinite rod data provided information that allowed an accurate form of the relationship for the rectangular brick shape to be found that was applicable beyond the range of the data for the rectangular brick shape itself.

9.5 TESTING OF IMPROVED GEOMETRIC FACTORS AGAINST EXPERIMENTAL DATA FOR MULTI-DIMENSIONAL REGULAR SHAPES

By use of Eqs. (9.5) and (9.7), both EHTD and MCP can be applied to any slab prediction method. A number of accurate simple prediction formulae for both freezing and thawing are available or were developed in Chap. 7. All of these methods are of similar prediction accuracy and calculate process times highly correlated with numerical method predictions. Rather than test the geometric factors with each slab prediction method individually, it was decided to initially use only one slab prediction method. The finite difference method was chosen as it best allows the geometry effect to be studied on its own.

The previous, and the improved versions of the expressions to calculate MCP and EHTD were tested against the Tylose rectangular brick freezing and thawing data (Cleland & Earle 1979b and Table 6.5). A summary of the predictions is given in Table 9.4.

For Tylose rectangular brick freezing the mean prediction error was off-set from zero for both the geometric factors. The full finite difference method results also displayed an off-set mean prediction error of the same magnitude. Cleland et al (1982) showed that this was

probably due to non-equilibrium freezing rate effects not taken into account in calculations by the finite difference method. Using the finite difference method as the slab prediction method would therefore be expected to lead to a similar off-set of the mean.

For freezing, the standard deviation of predictions was low, and the correlation coefficient (compared with the full finite difference method results) was high for both geometric factors. This verifies the assumption that the Ste and Pk effects on t_{slab}/t and hence EHTD and MCP were sufficiently small to be ignored, and also provides confirmation that for freezing the lack of fit of Eqs. (9.11) and (9.12) has not decreased the overall agreement with experimental data.

For Tylose rectangular brick thawing, the mean prediction errors for Eqs. (9.11) and (9.12) were not significantly different from zero. However, the standard deviation of the prediction error was higher than that for the full finite difference method predictions and the correlation coefficient compared with the full finite difference method results was low, for both the geometric factors. This suggests that the inaccuracy arising from the improved EHTD and MCP formulae is sufficiently large to be distinguished from the experimental uncertainty. Two reasons exist. Firstly the rectangular brick thawing experiments had less experimental uncertainty than the rectangular brick freezing data so the lack of fit is more discernible for thawing but not for freezing. Secondly, it was shown in Sec. 9.3 that the effect of Ste and Pk on t_{slab}/t was as much as ±5% during thawing. These effects were ignored by Eqs. (9.11) and (9.12), so correlation of prediction errors with Ste or Pk would indicate whether this was a contributing factor. The correlation coefficients with Ste and Pk were -0.73 and 0.06 respectively, indicating that neglect of the effect of Ste was significant.

Although better predictions for thawing could be achieved by adding terms involving Ste, especially, into Eqs. (9.11) and (9.12) this step was not taken as the improvement would only be evident with very accurate experimental data. In commercial practice, food engineers making thawing time predictions cannot determine data to represent the conditions as accurately as is possible in a research laboratory, so

the extra terms would not be helpful to them.

An interesting facet of Table 9.4 is that overall the old MCP and EHTD formulae perform as well as the new ones. This might suggest that the introduction of the new formulae was not worthwhile. However, it must be noted that the experimental data set does not cover as wide a range of conditions or geometries as the numerical data set of Table 9.3. The old EHTD and MCP formulae are inaccurate in parts of the wider range of conditions and shapes covered by Table 9.3 so their use for some β and Bi combinations, or shapes other than rectangular bricks, could lead to substantial prediction errors.   Therefore their replacement by Eqs. (9.11) and (9.12) is justified because of the reduced prediction inaccuracy risks, despite some additional complexity.

9.6   TESTING OF IMPROVED GEOMETRIC FACTORS IN COMBINATION WITH SIMPLE PREDICTION FORMULAE

The predictions of the improved geometric factors in combination with the simple freezing and thawing time prediction methods of Sec. 7.3 are summarised in Table 9.5.

For freezing they all perform similarly - those appearing to be better due to lower standard deviations also have lower correlation coefficients with the full finite difference method predictions.   The means are not off-set from zero like the finite difference mean, but the standard deviations are of similar size to the finite difference method standard deviation. The off-set mean for the finite difference method predictions arises from the rate effects discussed by Cleland et al (1982). The closeness of the standard deviation for the finite difference method and those for the simple methods indicates that for freezing time prediction any of the eight combinations in Table 9.5 can be used without introducing significant prediction method uncertainty.

The situation for thawing time predictions was similar.   All eight method combinations are comparable, but the neglect of Ste and Pk effects on EHTD and MCP has both lowered the correlation coefficient with the finite difference method predictions, and led to the standard

deviation being slightly higher than for the finite difference method.

Because Eq. (9.11) and (9.12) were developed from numerical data they are applicable over a wide range of conditions. For all the regular shapes considered the limits are:

$$0.0 < Bi < 100$$
$$1.0 < \beta_1 < 10$$
$$1.0 < \beta_2 < 10$$

The formulae may be applicable outside these ranges but at the expense of reduced accuracy. However, virtually all practical food freezing and thawing situations are covered.

9.7   SUMMARY

The effect of geometry on freezing and thawing times, even for regular multi-dimensional shapes, is sufficiently complex that no accurate geometric factor has been derived analytically.

There are two useful concepts to account for geometry - EHTD and MCP. Formulae to calculate both geometric factors for freezing of rectangular brick shapes under a limited range of conditions had been previously developed by empirically fitting rectangular brick freezing experimental data.

By fitting an alternative data set calculated by numerical methods, improved formulae for MCP and EHTD were developed. These are accurate for both freezing and thawing of an extended range of regular multi-dimensional shapes, and for a wider range of conditions than the original formulae.

Used in combination with accurate slab freezing and thawing time prediction methods, both of the improved geometric factors gave good fit to experimental data for freezing and thawing of rectangular bricks. Neither of the geometric factors introduced significant prediction uncertainty.

For prediction of freezing and thawing of regular shaped multi-dimensional objects there were no grounds to recommend either of

the two geometric concepts ahead of the other (similarly, none of the slab prediction approaches stood out as being significantly more accurate or simple to use).

Table 9.1 The Effect of Bi, Ste and Pk on the Ratio of Freezing and Thawing Times For Infinite Rods To the Times For the Equivalent Slab

β_1	Bi	T_a	T_{in}	t_{slab}/t	Effect of
1.0	0.1	−40.0	20.0	1.99	
1.0	0.1	−30.0	20.0	1.99	Ste
1.0	0.1	−20.0	20.0	2.00	
1.0	1.0	−40.0	5.0	1.85	
1.0	1.0	−30.0	20.0	1.91	Ste and Pk
1.0	1.0	−20.0	35.0	1.96	
1.0	1.0	5.0	−10.0	1.93	
1.0	1.0	20.0	−20.0	1.84	Thawing
1.0	1.0	35.0	−30.0	1.80	
1.0	10.0	−30.0	5.0	1.69	
1.0	10.0	−30.0	20.0	1.72	Pk
1.0	10.0	−30.0	35.0	1.75	
2.0	0.1	−40.0	20.0	1.47	
2.0	0.1	−30.0	20.0	1.48	Ste
2.0	0.1	−20.0	20.0	1.48	
2.0	1.0	−40.0	5.0	1.26	
2.0	1.0	−30.0	20.0	1.31	Ste and Pk
2.0	1.0	−20.0	35.0	1.35	
2.0	1.0	5.0	−10.0	1.35	
2.0	1.0	20.0	−20.0	1.26	Thawing
2.0	1.0	35.0	−30.0	1.23	
2.0	10.0	−30.0	5.0	1.10	
2.0	10.0	−30.0	20.0	1.11	Pk
2.0	10.0	−30.0	35.0	1.12	

Table 9.2 Constants For Prediction Of EHTD and MCP

Shape	G1	G2	G3
Slabs	1	0	0
Infinite Cylinders	2	0	0
Spheres	3	0	0
Finite Cylinders $D_r \geq D_y$	1	2	0
Finite Cylinders $D_r \leq D_y$	2	0	1
Infinite Rods	1	1	0
Two-Dimensional Irregular Shapes	1	1	0
Rectangular Bricks	1	1	1
Three-Dimensional Irregular Shapes	1	1	1

Table 9.3 Summary of Percentage Differences Between Numerically Calculated Freezing Times For Finite Cylinders, Infinite Rods and Rectangular Bricks and Freezing Times Calculated By Simple Prediction Formulae[1]

Shape	Geometric Factor	Equation	Mean (%)	Std Dev[2] (%)	Min[2] (%)	Max[2] (%)
All Data (270 runs)	EHTD	(9.3)	3.8	7.2	-7.0	24.8
	EHTD	(9.11)	-0.5	1.6	-7.0	5.2
	MCP	(9.4)	-2.4	9.2	-31.5	25.0
	MCP	(9.12)	-0.3	1.7	-7.0	4.1
Finite Cylinders $D_r \leq D_y$ (63 runs)	EHTD	(9.3)	0.1	3.9	-6.6	7.8
	EHTD	(9.11)	-0.4	0.8	-2.5	1.2
	MCP	(9.4)	-11.3	10.5	-31.5	0.3
	MCP	(9.12)	0.5	1.3	-2.2	4.1
Finite Cylinders $D_r \geq D_y$ (54 runs)	EHTD	(9.3)	6.4	9.0	-5.9	24.8
	EHTD	(9.11)	-0.5	2.3	-7.0	5.0
	MCP	(9.4)	-4.2	6.3	-25.7	0.3
	MCP	(9.12)	-0.7	2.1	-7.0	3.5
Infinite Rods (63 runs)	EHTD	(9.3)	3.6	4.7	-2.9	13.8
	EHTD	(9.11)	-0.6	1.2	-3.7	2.4
	MCP	(9.4)	4.2	7.1	-1.2	25.0
	MCP	(9.12)	-0.5	1.3	-4.2	2.1
Rectangular Bricks (90 runs)	EHTD	(9.3)	4.9	8.2	-7.0	24.4
	EHTD	(9.11)	-0.5	1.7	-4.4	5.3
	MCP	(9.4)	0.3	4.7	-7.6	12.5
	MCP	(9.12)	-0.7	1.7	-6.0	3.1

[1] Using the finite difference method as the slab prediction method.

[2] Std Dev = standard deviation, Min = minimum, Max = maximum.

Table 9.4 Summary of Percentage Differences Between Experimental
Freezing and Thawing Times For Tylose Rectangular Bricks and
Freezing and Thawing Times Calculated Using Simple Geometric
Factors[1]

Data	Geometric Factor	Equation	Mean (%)	Std Dev[2] (%)	Min[2] (%)	Max[2] (%)	Corr[3] FDM
	FDM[4]		-4.4	6.6	-20.7	9.8	1.00
Freezing	FEM$_s$[4]		-5.9	7.1	-24.1	9.8	0.97
(Cleland & Earle 1979b)	EHTD	(9.3)	-5.7	7.3	-23.0	9.8	0.90
	EHTD	(9.11)	-3.8	6.6	-21.3	9.2	0.86
(72 runs)	MCP	(9.4)	-6.0	5.5	-16.8	7.3	0.67
	MCP	(9.12)	-4.9	7.1	-22.7	10.9	0.89
	FDM[4]		0.6	3.1	-6.0	7.9	1.00
	FEM$_s$[4]		-6.3	3.4	-12.9	1.2	0.66
Thawing	EHTD	(9.3)	-3.5	5.4	-15.0	6.4	0.06
(Table 6.6)	EHTD	(9.11)	-2.2	5.3	-12.9	10.9	0.06
(68 runs)	MCP	(9.4)	-0.6	5.8	-12.6	13.7	-0.03
	MCP	(9.12)	-3.4	5.2	-13.0	7.1	0.11

[1] Using the finite difference method as the slab prediction method.

[2] Std Dev = standard deviation, Min = minimum, Max = maximum.

[3] Correlation coefficient (r) compared with the percentage differences
for the full finite difference method.

[4] FDM = full finite difference method, FEM$_s$ = simplified finite element
method.

Table 9.5 Summary of Percentage Differences Between Experimental
Freezing and Thawing Times For Tylose Rectangular Bricks and
Freezing and Thawing Times Calculated By Simple Prediction
Formulae

Data	Slab Prediction Method	Geometric[1] Factor	Mean (%)	Std Dev[2] (%)	Min[2] (%)	Max[2] (%)	Corr[3] FDM
Freezing (Cleland & Earle 1979b) (72 runs)	FDM[4]		-4.4	6.6	-20.7	9.8	1.00
	Eq. (7.7)	EHTD	-0.1	4.9	-8.9	9.7	0.57
		MCP	-1.3	5.2	-11.0	8.0	0.66
	Cleland & Earle 1982b	EHTD	0.8	5.3	-9.0	15.5	0.49
		MCP	-0.4	5.5	-10.5	12.7	0.59
	Pham 1984c	EHTD	-0.8	6.3	-16.4	11.2	0.91
		MCP	-1.9	6.8	-17.9	13.4	0.94
	Pham 1983 (Eq. (7.6))	EHTD	-2.1	6.0	-15.9	11.2	0.87
		MCP	-3.3	6.5	-17.4	10.8	0.89
Thawing (Table 6.5) (68 runs)	FDM[4]		0.6	3.1	-6.0	7.9	1.00
	Eq. (7.2)	EHTD	-1.6	4.3	-9.1	11.5	0.28
		MCP	-2.8	4.2	-9.8	7.7	0.36
	Eq. (7.3)	EHTD	-2.3	5.3	-12.9	10.6	0.36
		MCP	-3.5	5.1	-13.4	6.6	0.42
	Eq. (7.4)	EHTD	-2.6	6.0	-15.6	11.9	0.35
		MCP	-3.9	5.5	-16.1	7.8	0.43
	Eq. (7.5)	EHTD	-1.1	4.3	-11.5	7.9	0.35
		MCP	-2.4	4.4	-11.5	6.3	0.40

[1] EHTD from Eq. (9.11), MCP from Eq. (9.12).

[2] Std Dev = standard deviation, Min = minimum, Max = maximum.

[3] Correlation coefficient (r) compared with the percentage differences
for the full finite difference method.

[4] full finite difference method.

10   PREDICTION OF FREEZING AND THAWING TIMES FOR MULTI-DIMENSIONAL
IRREGULAR SHAPES BY SIMPLE METHODS

The previous three chapters have covered the third and fourth research
objectives set in Chap. 3 - assessment both of the accuracy of Group I
(simple) and Group II (numerical) prediction methods for regular shapes
and of Group II methods for irregular shapes. Chapter 10 is concerned
with the fifth objective - investigation of the possibility of
developing a Group I method to predict freezing and thawing times for
irregular shapes.

10.1   INTRODUCTION

No simple methods suggested for calculation of geometric factors from
first principles for freezing and thawing of irregular shaped objects
have proved accurate. Rutov (1936) and Mott (1964) used the AD/2V
ratio as a shape factor but it is known that this is not accurate when
$Bi \neq 0$. Smith et al (1967), Smith et al (1968), Clary et al (1968),
Smith & Nelson (1969) and Clary et al (1971) defined a geometry index
(the forerunner to EHTD), for the case of heat conduction without
change of phase and $Bi \rightarrow \infty$.   For irregular geometries they calculated
their geometry index from an ellipsoidal model shape that has equal
orthogonal cross-sectional areas and the same characteristic thickness
as those of the anomalous shape that it replaces.   The orthogonal
cross-sections taken were generally the small and largest that pass
through the thermodynamic centre and lie in the same plane as the
characteristic dimension. It was unknown how this method would perform
for phase change and when $Bi \neq \infty$.

For regular multi-dimensional shapes use of the concepts of EHTD and
MCP led to accurate methods to take account of geometry in freezing and
thawing time predictions. EHTD and MCP are calculated as functions of
the Biot number and the two other geometry parameters (β_1 and β_2) that
describe the regular geometries. It was considered sensible to try to
extend the methods to calculate EHTD and MCP to irregular geometries.
It was decided to ignore any variation of these geometric factors with
Ste and Pk as this variation would probably be small compared with the

Bi and shape effects (Sec. 9.3).

10.2   GEOMETRY PARAMETERS

Using Eqs. (9.2) and (9.9) the values of EHTD and MCP can be defined from individual experiments for a particular shape (Cleland & Earle 1982b). However these determinations are both geometry and condition specific and do not necessarily allow accurate and simple calculations for other conditions or geometries. A major problem with developing methods to determine EHTD and MCP from first principles is that apart from D, A and V, there are few other easily measured parameters that can be used to characterise all irregular shapes.

Even the characteristic (first) dimension, D, is not always straightforward to estimate. For an irregular shape D is defined either as (a) the smallest thickness measured by a line that passes through the thermodynamic centre, or (b) twice the shortest distance from the thermodynamic centre to the objects surface. The position of the thermodynamic centre is not always obvious from examination of the object and may move during the phase change process (Fleming 1970). For most common shapes where surface boundary conditions are not position variable (such as those considered in this work), the two definitions of D are virtually equivalent.

Possibly useful measures of the effect of the second and third dimensions are:
(a) The ratio between the maximum distance from the thermodynamic centre to the surface and D/2.
(b) The ratio of the major axis length to the minor axis length for an elliptical model cross-sections equal in area to the orthogonal cross-sections of the anomalous shape (Smith et al 1967).
(c) The ratio of the volume of the object compared with the volume for a infinite cylinder (two-dimensional shapes) or sphere (three-dimensional shapes) of the same surface area.
These three parameters are highly correlated with each other as they all measure in some way, the distortion of the shape from a infinite cylinder or sphere. Each has some different properties so all three were investigated to see if they could individually, or in combination,

provide simple methods to calculate geomeric factors for irregular shapes.

A fourth but, very different, way to describe an objects shape is to define a regular shape that freezes or thaws in the same time as the object under the same environmental conditions. For example, Pham (1984c) defined an equivalent rectangular brick shape for finite cylinders, but this led to uncertainty in the shape factor and consequently underprediction of freezing and thawing times, especially at high Bi values (Table 9.3). This was because the size of the equivalent brick (brick with the same freezing or thawing time) changes with Biot number. Although this approach has proved successful for some specifically studied irregular shapes by approximation to slabs, infinite cylinders or spheres and defining equivalent diameters (Sec. 2.5, Table A.8), it is unlikely to lead to a method that can be applied systematically to a wide range of shapes with accuracy. It was decided not to consider it further unless all of the other approaches proved unsuitable.

10.3 DEVELOPMENT OF GEOMETRIC FACTORS FOR MULTI-DIMENSIONAL IRREGULAR SHAPES

Both EHTD and MCP are defined for any shape as Bi→0 by the AD/2V ratio. Therefore the requirement is to develop a method to calculate the change in these factors with Biot number, in as simple and as accurate a manner as possible. The calculation method should only use easily measured or estimated geometry parameters such as those discussed in Sec. 10.2.

There are few experimental data for freezing and thawing of irregular shaped objects available in the literature, for which the geometry and conditions are sufficiently accurately described, measured and controlled to allow their use in the present study. For this reason, the method of analysis applied was the same as that used for regular shapes (Sec. 9.4). Initially only the ratios of numerically calculated freezing and thawing times for the actual shape, and for the reference slab were used in the development of the geometric factors. Only the variations due to geometry and the effect of Bi were apparent in these

data as mid-range Ste and Pk values were used. The choice of approach
was especially important for the three-dimensional irregular shapes
where there was the possibility of systematic sources of experimental
error in the experimental data (Secs. 5.9.3, 5.9.4 and 8.4).

Even though an infinite number of shapes are possible, due to
limitations in grid preparation time and computation resources,
numerical data were only calculated for the eight two-dimensional
objects and the four three-dimensional objects used in experiments
(Figs. 5.15 to 5.21 and 5.24 to 5.27). Also computer process time
limitations meant that computations were not possible for the full
range of Bi values; only the important case where Bi→∞ was calculated.
The data are given in Table C.2. To supplement the data base, the
numerical data for the regular shapes were also used (Table C.1). Any
method to calculate the geometric factor for irregular shapes should
also be applicable to regular shapes. However, lower accuracy compared
with the methods specific for regular shapes, described in Chap. 9,
would be expected because for the method to be universal, less detailed
information about the geometry can be incorporated. The regular shape
data both increased the range of geometry types and added information
about how the geometric factors behave at intermediate Bi values.   The
composite data set was still limited in scope.

By curve fitting of the numerical data the following expressions were
found to be of reasonable accuracy, but as simple as possible:

$$\text{EHTD} = G1 + G2 \left[\frac{L_1 D}{2A_1} - 1 \right] \left(f_{15}(\nabla_1) + (1 - f_{15}(\nabla_1))/\nabla_1^{1.47} \right)$$

$$+ G3 \left[\frac{L_2 D}{2A_2} - 1 \right] \left(f_{15}(\nabla_2) + (1 - f_{15}(\nabla_2))/\nabla_2^{2.75} \right) \quad (10.1)$$

and

$$\frac{\text{MCP}}{D} = 1 + (2-G1) f_{17}\left(f_{16}(G2,\nabla_1) \right) 0.65 \, Bi^{0.39} \left(\nabla_1^{1.39} - 1 \right)$$

$$+ G3 \, f_{17}\left(f_{16}(G3,\nabla_2) \right) 0.65 \, Bi^{0.39} \left(\nabla_2^{1.26} - 1 \right)$$

$$+ \left[\frac{AD}{2V} / \left(G1 + G2 \left[\frac{L_1 D}{2A_1} - 1 \right] / \nabla_1^{1.47} + G3 \left[\frac{L_2 D}{2A_2} - 1 \right] / \nabla_2^{2.75} \right) - 1 \right] \cdot$$

$$\cdot \left[1 - f_{17}\left((f_{16}(G2,\nabla_1) + f_{16}(G3,\nabla_2))/(G2 \, G3 + 1) \right) \right] \quad (10.2)$$

where $f_{15}(\nabla) = 3.56/\nabla^{1.77} / \left(Bi^{1.34} + 3.56/\nabla^{1.77} \right)$

$f_{16}(G,\nabla) = G \, 3.08/\nabla^{1.90}$

$f_{17}(X) = X / (Bi^{1.35} + X)$

L_1, L_2 = perimeter length of the first and second
orthogonal cross-sections   (m)

A_1, A_2 = area of the first and second orthogonal
cross-sections (m^2)

∇ = ratio of major axis length to minor axis length for
an ellipse modelling an orthogonal cross-section

$\nabla_1 = 4A_1 / \pi D^2$

$\nabla_2 = 4A_2 / \pi D^2$

and the values of G1, G2 and G3 are given in Table 9.2. Table 10.1 gives the geometry parameters used in Eqs. (10.1) and (10.2) for the shapes used in this study (Tables 6.6 and 6.7).

These equations use the second of the shape parameters discussed in Sec. 10.2 yet are still definite extensions of the methods developed in Sec. 9.4 for regular shapes. The techniques are similar to that of Smith et al (1967) in that the orthogonal cross-sections that pass through the thermodynamic centre are used and the contributions to the geometric factor calculated from each cross-section are summed (this is also the case in Eqs. (9.11) and (9.12)). Due to the lack of data, accurate fitting of all the coefficients was not possible so many of the coefficients have been defined by analogy to the methods developed for the regular shape geometric factors (for example, $3.08/\nabla^{1.77}$ approximates $2.32/\beta^{1.77}$ and $Bi^{1.34}$ is retained to give the Biot number weighting functions in the equation for EHTD). Equations (10.1) and (10.2) are very similar to Eqs. (9.11) and (9.12) because ∇ is a parameter that is closely related to β for regular shapes. However, this means that for shapes increasingly distorted from regular shapes the accuracy may be reduced. All of the irregular shapes used in the analysis were either relatively oval with no sharp contour changes or were rectangular with square corners or edges; so this was not a problem with this data set.

Table 10.2 shows the fit of Eqs. (10.1) and (10.2) to the numerical data for regular shapes. Overall the agreement is good and is only slightly inferior to that displayed by the specialised methods (Table 9.3).

10.4   TESTING OF GEOMETRIC FACTORS AGAINST EXPERIMENTAL DATA FOR MULTI-DIMENSIONAL SHAPES

Equations (10.1) and (10.2) can be used in conjunction with any of the slab prediction method that had previously been used with Eqs. (9.5) and (9.7), to predict freezing and thawing times for objects of any shape. Table 10.3 summarises the predictions against the experimental data of Cleland & Earle (1979b) and Tables 6.5, 6.6 and 6.7 for rectangular bricks, two-dimensional irregular shapes and three-dimensional irregular shapes.

10.4.1   Rectangular Brick Freezing and Thawing

The predictions were almost identical to those displayed for Eq. (9.11) and (9.12) in Tables 9.4 and 9.5.   This confirms that for regular shapes, the general calculation methods for EHTD and MCP (Eqs. (10.1) and (10.2)) are equivalent to the specialised methods (Eqs. (9.11) and (9.12)), and do not add significant uncertainty to freezing or thawing time predictions.

10.4.2   Freezing and Thawing of Two-Dimensional Irregular Shapes

For the two-dimensional irregular shape data the mean prediction errors using Eq. (10.1) and (10.2) to describe geometry were slightly off-set from zero for both the geometric factors, and for both freezing and thawing. The standard deviation was low and the correlation coefficient (compared with the full finite element method results) was high. The magnitude of the 95% confidence bounds for the prediction errors was similar to the estimated experimental error bounds for this data (Sec. 5.8.4, Table 12.2). Hence for the two-dimensional irregular shapes used (all of which had curved, oval surfaces) the lack of fit of the geometric factors calculated by Eqs. (10.1) and (10.2) does not significantly worsen the overall agreement with experimental data although there is a slight shift of the mean.

10.4.3 Freezing and Thawing of Three-Dimensional Irregular Shapes

In general the accuracy of predictions for the three-dimensional irregular shapes was poorer than for the other shapes. This was expected due to a higher experimental uncertainty for these shapes (Sec. 5.9.4). The standard deviation of the predictions were similar to those for the full finite element method results and the correlation coefficient of the percentage differences were high.

However, the mean prediction errors displayed different trends to those for the full finite element results (Table 8.2). For the pyramid shape the mean prediction error was closer to zero compared with the under-prediction shown by the full finite element method results. As discussed in Sec. 8.4 the off-set for the numerical results was partly caused by use of a coarse spatial grid for the calculations. The simple slab prediction methods and Eqs. (10.1) and (10.2) were not affected by this problem so, as expected, for an accurate slab prediction method the mean prediction error was not significantly different from zero.

The same explanation applies for the sphere shape results. The predictions for the full finite element method using a three-dimensional grid were off-set from zero, but both the predictions for the finite element method using a finer one-dimensional grid and those for the simple prediction methods were not.

For the egg and fish shapes different trends were observed. The mean prediction error was higher for the simple prediction methods than the numerical methods for the egg shape, but lower for the fish shape. It was difficult to assess whether the differences in the mean prediction errors were apparent due to systematic error in the geometric factors for these shapes, because the numerical calculations were influenced by factors such as the coarse spatial grid (Sec. 8.4), or because the predictions were affected by systematic error in the value of the surface heat transfer coefficient used in calculations (Sec. 8.4). All three reasons probably contributed in both cases.

Because the predictions for the two-dimensional irregular shapes were based on data for shapes with both rectangular and oval cross-sections and were quite precise, it was considered that the effect of the second dimension was accurately modelled by Eqs. (10.1) and (10.2) for both ovoid and rectangular shapes. Therefore any uncertainty due to the geometric factors for the egg and fish shapes was thought to be in the modelling of the effect of the third dimension. This is not surprising as there were very few data available to analysis the effect of the third dimension in three-dimensional irregular shapes. The main reason for this was the large computation costs involved in numerical calculation for three-dimensionally irregular shapes. A typical calculation using the full finite element method for the fish shape took 150 000 sec. process time on a Prime 750 computer. This meant that the analysis was forced to rely heavily on the rectangular brick and finite cylinder shape data. These regular shapes have rectangular cross-sections in the third dimension, not oval as found in the egg and fish shapes. Consequently the coefficients in Eqs. (10.1) and (10.2) fitted data for shapes with rectangular cross-sections in the third dimension and do not seem to be as accurate for shapes with other geometries. To develop more accurate methods to calculate the geometric factors, EHTD and MCP, more data are required. If more three-dimensional irregular shape data were available, including data for shapes with oval cross-sections in the third dimension, it was felt that the principles of the methods to calculate EHTD and MCP (Sec. 9.4) would not need to be changed; only the values of the coefficients in Eq. (10.1) and (10.2) (and possibly the geometry parameter used), would alter to fit the data.

Overall, the off-set of the mean for the predictions using Eq. (10.1) and (10.2) was not considered large in relation to the inaccuracy of the experimental data and the lack of suitable data to develop and test the geometric factor expressions for three-dimensional irregular shapes.

10.4.4   Comparison of Slab Prediction Methods

All of the five slab prediction methods (the finite difference method plus the four simple formulae approaches), used in conjunction with the expressions for EHTD and MCP gave adequate prediction accuracy. As discussed for rectangular brick freezing (Sec. 8.2), use of numerical slab methods lead to under-prediction compared with the other simple slab prediction methods (Chap. 7). Otherwise the mean prediction error was almost identical for all the slab prediction methods. The five slab prediction methods also gave very similar standard deviations of prediction errors and correlation coefficients with numerical method predictions.

10.4.5   Analysis of Geometric Factors

The accuracy of the predictions obtained using the simple geometric factors, EHTD and MCP, was sufficiently good for most of the shapes tested that no further geometry parameters or geometric factor concepts were investigated.

The expressions for EHTD and MCP gave almost identical freezing and thawing time predictions for all shapes and could not be differentiated by the accuracy criterion alone. The expression for EHTD was slightly less complex in its final form than the expression for MCP. Because of the peak in MCP values at intermediate Biot numbers it was more difficult to find and curve-fit a suitable expression for MCP than it was for EHTD.

It was difficult to assess the ranges of applicability of Eqs. (10.1) and (10.2) because of the large variety of geometries that are common in practice. Their accuracy has been proven for two-dimensional shapes with both oval and rectangular cross-sections so it seems reasonable to suggest that the equations should apply equally well to most two-dimensional objects. For three-dimensional shapes Eqs. (10.1) and (10.2) have only been proven accurate for objects with rectangular cross-sections in the third dimension. Therefore the limits of their application should be to objects with this type of geometry. The formulae can be used for other shapes, but at the expense of reduced

accuracy. The accuracy of Eqs. (10.1) and (10.2) for both two- and three-dimensional objects with extreme distortion of geometry would be expected to be lower. More refinement of the expressions for ETHD and MCP can be justified, especially to make them applicable to a wider range of three-dimensional geometries.

The way in which the equations for EHTD and MCP take account of the effect of Bi was thought to be universally correct so the limits of applicability with regard to this parameter are the same as for Eqs. (9.11) and (9.12) for regular shapes:

$$0.0 < Bi < 100.$$

10.5 SUMMARY

The principles underlying the methods to calculate geometric factors using the EHTD and MCP concepts were satisfactorily extended to irregular geometries. In a similar manner to that used for regular shapes in Chap. 9 and by Smith et al (1967) for irregular shapes, the effect of each dimension was calculated separately by considering each of the orthogonal cross-sections that pass through the thermodynamic centre. The parameter $\nabla = 4A/\pi D^2$ for these cross-sections was similar to the parameter β used for regular shapes and allowed expressions to calculate the two geometric factors to be developed along similar lines to those used for regular shapes.

Used in conjunction with accurate slab freezing and thawing time prediction methods the expressions developed for EHTD and MCP both gave predictions of similar accuracy to those achieved by numerical methods for rectangular bricks and two-dimensional irregular shapes.   The geometric factors did not add significant uncertainty to the predictions for these shapes.

For the three-dimensional irregular shapes the accuracy of the geometric factors was lower than for the two-dimensional irregular shapes. This was attributed to less accurate modelling of the effect of the third dimension rather than error in modelling of the effect of the second dimension or because the principles of the calculation method were inappropriate as the predictions for the two-dimensional

shapes were accurate.

The methods developed are accurate for most two-dimensional objects but are restricted to three-dimensional objects with rectangular cross-sections in the third dimension. For these shapes the methods do not add significantly to the prediction uncertainty. For other shapes lower accuracy was apparent.

The present analysis was limited by the small data set, and by difficulties in obtaining accurate experimental measurements especially for three-dimensional irregular shapes. More data would enable more accurate and universally applicable expressions to calculate EHTD and MCP to be developed. Substantial computing costs would have to be borne in order to do this work.

Table 10.1 <u>Parameters For Calculation of the Effect of Geometry For</u>
           <u>Irregular Shapes</u>

Shape[1] & Code	D (m)	$V^{[2]}$ (m^3)	$A^{[2]}$ (m^2)	A_1 (m^2)	L_1 (m)	∇_1	A_2 (m^2)	L_2 (m)	∇_2
2DI 1	0.1525	0.0183	0.479	0.0183	0.479	1.00			
2DI 2	0.1115	0.0164	0.475	0.0164	0.475	1.68			
2DI 3	0.1370	0.0177	0.475	0.0177	0.475	1.20			
2DI 4	0.0990	0.0152	0.478	0.0152	0.478	1.97			
2DI 5	0.1050	0.00866	0.330	0.00866	0.330	1.00			
2DI 6	0.0850	0.00796	0.323	0.00796	0.323	1.40			
2DI 7	0.0910	0.00811	0.324	0.00811	0.324	1.25			
2DI 8	0.0475	0.00586	0.325	0.00586	0.325	3.30			
Pyramid	0.0825	0.00136	0.0780	0.0103	0.416	1.93	0.0115	0.460	2.15
Sphere	0.1270	0.00107	0.0507	0.0127	0.399	1.00	0.0127	0.399	1.00
Egg	0.1700	0.00363	0.1175	0.0227	0.534	1.00	0.0320	0.652	1.41
Fish	0.1200	0.00437	0.1625	0.0143	0.424	1.26	0.0488	1.076	4.31

[1] 2DI = two-dimensional irregular shape, code number from Table 6.6.

[2] For the 2DI shapes these values are for a 1.0 m long object.

Table 10.2 <u>Summary of Percentage Differences Between Numerically</u>
<u>Calculated Freezing Times For Finite Cylinders, Infinite</u>
<u>Rods and Rectangular Bricks and Freezing Times Calculated By</u>
<u>Simple Prediction Formulae</u>[1]

Shape	Geometric Factor	Equation	Mean (%)	Std Dev[2] (%)	Min[2] (%)	Max[2] (%)
All Data (270 runs)	EHTD	(9.11)	-0.5	1.6	-7.0	5.2
	EHTD	(10.1)	-0.3	1.7	-6.8	5.7
	MCP	(9.12)	-0.3	1.7	-7.0	4.1
	MCP	(10.2)	-0.3	1.7	-6.9	4.2
Finite Cylinders $D_r \leq D_y$ (63 runs)	EHTD	(9.11)	-0.4	0.8	-2.5	1.2
	EHTD	(10.1)	-0.4	0.8	-2.8	1.2
	MCP	(9.12)	0.5	1.3	-2.2	4.1
	MCP	(10.2)	0.2	1.5	-4.1	4.2
Finite Cylinders $D_r \geq D_y$ (54 runs)	EHTD	(9.11)	-0.5	2.3	-7.0	5.0
	EHTD	(10.1)	-0.3	2.5	-6.8	5.7
	MCP	(9.12)	-0.7	2.1	-7.0	3.5
	MCP	(10.2)	-0.5	2.2	-6.9	4.0
Infinite Rods (63 runs)	EHTD	(9.11)	-0.6	1.2	-3.7	2.4
	EHTD	(10.1)	-0.3	1.3	-3.7	2.6
	MCP	(9.12)	-0.5	1.3	-4.2	2.1
	MCP	(10.2)	-0.3	1.3	-4.2	1.9
Rectangular Bricks (90 runs)	EHTD	(9.11)	-0.5	1.7	-4.4	5.3
	EHTD	(10.1)	-0.2	1.7	-4.3	5.6
	MCP	(9.12)	-0.7	1.7	-6.0	3.1
	MCP	(10.2)	-0.6	1.7	-6.1	3.9

[1] Using the finite difference method as the slab prediction method.

[2] Std Dev = standard deviation, Min = minimum, Max = maximum.

Table 10.3 Summary of Percentage Differences Between Experimental
Freezing and Thawing Times For Tylose Multi-Dimensional
Shapes and Freezing and Thawing Times Calculated By Simple
Prediction Formulae

Data	Slab Prediction Method	Geometric[1] Factor	Mean (%)	Std Dev[2] (%)	Min[2] (%)	Max[2] (%)	Corr[3] FDM
	FDM[4]		-4.4	6.6	-20.7	9.8	1.00
	FDM	EHTD	-3.4	6.7	-21.1	9.6	0.86
		MCP	-4.9	7.2	-22.8	11.3	0.89
Rectangular Brick	Eq. (7.7)	EHTD	0.3	5.1	-8.5	10.1	0.56
		MCP	-1.3	5.4	-11.1	8.3	0.65
Freezing	Cleland & Earle 1982b	EHTD	1.2	5.5	-8.7	15.9	0.48
(Cleland & Earle 1979b)		MCP	-0.4	5.7	-10.6	13.1	0.58
(72 runs)	Pham 1984c	EHTD	-0.4	6.4	-16.2	11.7	0.91
		MCP	-2.0	6.9	-18.0	13.9	0.93
	Pham 1983 (Eq. (7.6))	EHTD	-1.8	6.1	-15.7	11.4	0.86
		MCP	-3.3	6.6	-17.5	11.3	0.89
	FDM[4]		0.6	3.1	-6.0	7.9	1.00
	FDM	EHTD	-1.6	5.4	-12.3	11.2	0.06
		MCP	-3.2	5.3	-12.8	6.8	0.10
Rectangular Brick	Eq. (7.2)	EHTD	-1.0	4.3	-8.8	11.8	0.29
		MCP	-2.6	4.2	-9.8	7.4	0.34
Thawing	Eq. (7.3)	EHTD	-1.7	5.3	-12.7	10.8	0.36
(Table 6.5)		MCP	-2.2	5.1	-13.3	7.0	0.41
(68 runs)	Eq. (7.4)	EHTD	-2.1	5.9	-15.4	12.1	0.36
		MCP	-3.7	5.3	-16.0	7.4	0.43
	Eq. (7.5)	EHTD	-0.6	4.4	-11.1	8.2	0.35
		MCP	-2.2	4.6	-11.7	7.4	0.38

Table 10.3 continued...   212

Data	Slab Prediction Method	Geometric[1] Factor	Mean (%)	Std Dev[2] (%)	Min[2] (%)	Max[2] (%)	Corr[3] FDM
	FEM[4]		-1.0	4.5	-11.4	7.6	1.00
	FDM	EHTD	2.5	4.6	-8.3	11.4	0.85
		MCP	2.8	4.6	-8.3	11.8	0.84
Two-Dimensional Irregular	Eq. (7.7)	EHTD	3.9	5.1	-9.6	13.5	0.72
		MCP	4.1	5.1	-8.9	14.0	0.72
Freezing	Cleland & Earle 1982b	EHTD	4.5	5.6	-9.6	16.8	0.83
(Table 6.6)		MCP	4.7	5.6	-8.9	16.8	0.83
(42 runs)	Pham 1984c	EHTD	5.5	4.1	-5.0	14.1	0.86
		MCP	5.8	4.1	-4.2	14.4	0.86
	Pham 1983 (Eq. (7.6))	EHTD	3.5	5.0	-7.3	12.9	0.84
		MCP	3.8	5.0	-6.6	13.3	0.84
	FEM[4]		1.5	5.5	-7.1	11.3	1.00
	FDM	EHTD	5.1	5.2	-6.7	19.0	0.79
		MCP	5.0	5.3	-6.7	19.2	0.80
Two-Dimensional Irregular	Eq. (7.2)	EHTD	5.2	5.2	-6.7	19.2	0.85
		MCP	5.2	5.3	-6.7	19.3	0.86
Thawing	Eq. (7.3)	EHTD	5.6	5.4	-7.4	16.5	0.82
(Table 6.6)		MCP	5.6	5.5	-7.4	16.7	0.83
(41 runs)	Eq. (7.4)	EHTD	6.4	5.6	-7.8	18.9	0.82
		MCP	6.3	5.7	-7.8	19.1	0.83
	Eq. (7.5)	EHTD	6.0	5.6	-5.1	20.2	0.86
		MCP	5.9	5.7	-5.1	20.3	0.87
	FEM[4]		-10.3	6.7	-18.2	-2.0	1.00
	FDM	EHTD	0.8	10.2	-12.8	13.2	0.89
		MCP	-3.9	9.7	-16.8	7.9	0.89
	Eq. (7.7) or Eq. (7.2)	EHTD	2.5	8.0	-9.0	12.0	0.91
Pyramid		MCP	-2.3	7.6	-13.2	6.8	0.91
(Table 6.7)	Cleland & Earle 1982b or Eq. (7.3)	EHTD	2.8	7.4	-6.5	11.1	0.95
(6 runs)		MCP	-2.0	7.0	-10.8	5.9	0.95
	Pham 1984c or Eq. (7.4)	EHTD	2.3	8.1	-8.3	13.2	0.93
		MCP	-2.5	7.6	-12.5	7.8	0.93
	Pham 1983 (Eq. (7.6)) or Eq. (7.5)	EHTD	2.6	9.3	-7.0	15.9	0.95
		MCP	-2.2	8.8	-11.3	10.5	0.95

Table 10.3 continued... 213

Data	Slab Prediction Method	Geometric[1] Factor	Mean (%)	Std Dev[2] (%)	Min[2] (%)	Max[2] (%)	Corr[3] FDM
	FEM[4] (3-Dal Grid)		-5.5	6.8	-12.1	15.3	1.00
	FEM[4] (1-Dal Grid)		0.4	6.7	-7.7	9.6	0.91
	FDM	EHTD	2.3	8.8	-13.1	13.6	0.72
		MCP	2.1	8.8	-13.3	13.4	0.71
	Eq. (7.7) or Eq. (7.2)	EHTD	5.0	5.2	-1.6	13.7	0.92
Sphere		MCP	4.8	5.2	-1.8	13.5	0.92
(Table 6.7)	Cleland & Earle 1982b or Eq. (7.3)	EHTD	6.9	7.6	-1.2	16.5	0.94
(6 runs)		MCP	6.7	7.5	-1.4	16.2	0.94
	Pham 1984c or Eq. (7.4)	EHTD	2.1	7.3	-6.9	14.5	0.94
		MCP	2.0	7.3	-7.1	14.2	0.94
	Pham 1983 (Eq. (7.6)) or Eq. (7.5)	EHTD	3.6	7.4	-6.5	11.3	0.77
		MCP	3.5	7.4	-6.7	11.1	0.77
	FEM[4]		5.2	13.0	-12.9	25.1	1.00
	FDM	EHTD	14.4	14.3	-11.5	28.8	0.89
		MCP	13.3	14.4	-12.8	27.9	0.89
	Eq. (7.7) or Eq. (7.2)	EHTD	17.2	12.7	-4.1	31.6	0.96
Egg		MCP	16.0	12.8	-5.4	30.6	0.96
(Table 6.7)	Cleland & Earle 1982b or Eq. (7.3)	EHTD	20.5	13.5	3.0	39.8	0.97
(6 runs)		MCP	19.3	13.5	1.6	38.8	0.97
	Pham 1984c or Eq. (7.4)	EHTD	13.7	12.4	-6.9	30.2	0.98
		MCP	12.5	12.5	-8.2	29.3	0.98
	Pham 1983 (Eq. (7.6)) or Eq. (7.5)	EHTD	17.0	13.5	-4.1	34.6	0.95
		MCP	15.8	13.6	-5.4	33.7	0.94

Table 10.3 continued...   214

Data	Slab Prediction Method	Geometric[1] Factor	Mean (%)	Std Dev[2] (%)	Min[2] (%)	Max[2] (%)	Corr[3] FDM
	FEM[4]		35.3	8.9	20.8	44.2	1.00
	FDM	EHTD	15.3	7.3	6.2	24.6	0.88
		MCP	12.3	7.0	2.5	20.4	0.89
	Eq. (7.7) or Eq. (7.2)	EHTD	17.9	7.1	7.7	28.5	0.72
Fish		MCP	14.8	6.3	5.9	24.1	0.79
(Table 6.7)	Cleland & Earle 1982b or Eq. (7.3)	EHTD	19.1	10.3	2.9	34.8	0.67
(6 runs)		MCP	16.0	9.3	1.1	30.2	0.73
	Pham 1984c or Eq. (7.4)	EHTD	15.3	8.1	2.2	25.1	0.74
		MCP	12.3	7.3	0.5	20.8	0.80
	Pham 1983 (Eq. (7.6)) or Eq. (7.5)	EHTD	18.1	7.4	4.8	25.3	0.96
		MCP	15.0	7.0	3.0	21.0	0.99

[1] EHTD from Eq. (10.1), MCP from Eq. (10.2).

[2] Std Dev = standard deviation, Min = minimum, Max = maximum.

[3] Correlation coefficient (r) compared with the percentage differences for either the full finite difference method or the full finite element method.

[4] Full finite difference method or full finite element method.

11   TESTING OF PREDICTION METHODS FOR OTHER
MATERIALS AND DATA SETS

11.1   INTRODUCTION

In Sec. 6.1 it was decided to exclude variation of N_2 (the ratio of the unfrozen to the frozen volumetric specific heat capacity), and N_3 (the ratio of the unfrozen to the frozen thermal conductivity), in the main thawing experimental design as the effect of these factors was expected to be small. However some testing was required to ensure that this was the case. Also to complete the testing of freezing and thawing time prediction methods, all available accurate experimental data - for as many geometries, conditions and phase change materials as possible - should be used.

In the literature no experimental thawing data for foods were found for which the conditions and geometries were sufficiently accurately measured, described and controlled for them to be used to test prediction methods. However, in the present study fourteen thawing experiments were conducted with minced lean beef (Table 6.8).

For freezing a comprehensive set of data for a range of regular geometries, food materials and final thermodynamic centre temperatures exists (Cleland & Earle 1984a, Pham 1984c). The only additional data collected were four freezing runs using two-dimensional irregular shapes of minced lean beef. The composite freezing and thawing data set is described in Table 11.1.

11.2   NUMERICAL PREDICTION METHODS

It was expected that the finite difference and finite element numerical methods would introduce negligible prediction inaccuracy when applied to foods if the space and time step intervals used were sufficiently small. However, an increase in thermal property data uncertainty relative to Tylose data would be expected (Sec. 5.2). Also the nature of food materials means that experimental error is likely to exceed that for experiments using Tylose, which is a homogenous gel

(Sec. 5.7.3)

The numerical methods to predict freezing and thawing times had previously been compared with most of the composite data set for freezing (Cleland & Earle 1984a) and for thawing of Tylose (Sec. 7.2 and Chap. 8). Numerical method predictions were made for the remaining thawing data for minced lean beef and the more recently published freezing data, (marked in Table 11.1), to complete the comparison. The finite difference method was used for regular shapes and the finite element method for irregular shapes. The thermal property data used were those given by Cleland & Earle (1984a). For Tylose and minced lean beef these are consistent with, although slightly different to, the data in Table 5.1. The predictions are summarised in Table 11.2 (for thawing of minced lean beef) and Table 11.4 (for freezing of multi-dimensional shapes).

Offset of the mean percentage difference between predicted and experimental times from zero was significant for the two-dimensional irregular shapes, for finite cylinder experiments carried out by de Michelis & Calvelo (1983), and for all the data collected by Hayakawa et al (1983a) and Succar & Hawakawa (1984). Consistent offset can arise from systematic experimental error (particularly in estimates of the surface heat transfer coefficient) or from thermal property data used in calculations not truly representing the samples of the test materials used.

For the two-dimensional irregular shapes the former was considered most likely. Measured rates of temperature change with time were consistently under-predicted by the finite element method throughout both the freezing or thawing processes for both the shapes used (Fig. 6.19). Although thermocouple placement error may have contributed to occasional under-prediction, the under-prediction was too consistent for this factor alone to explain the observed temperature profiles. Hence the assumption made in Sec. 5.8.3 that both the contact resistance between the Tylose and the mould wall and the contact resistance between the minced lean beef and the mould wall were equal, may not be correct. The difference may have arisen because Tylose is a dry gel, whereas minced lean beef has a fibrous, moist

nature (Sec. 5.7.3).

The other data sets for which offsets from zero were significant were all taken from the literature. It was difficult to assess whether inappropriate thermal data, or experimental inaccuracy caused the problems in these data sets. In several cases surface heat transfer coefficients were not determined independently of the freezing experiments. It is very unlikely that problems in the finite difference or finite element method calculations were the cause as the programs were tested rigorously (Chap. 4) and it has been demonstrated in this study that they performed well for 90% of the whole data set.

The standard deviations of prediction errors were generally larger for food experiments than for Tylose experiments (for example - Tylose slab thawing, 3.5%; minced lean beef slab thawing, 5.9%). This reflects the difficulties discussed previously in experimenting with food materials (Sec. 5.2).

It should be noted that some individual sets of data are very small (less than six runs), so prediction error means and standard deviations calculated for these sets are less meaningful than those for large data sets. Similarly, when simple prediction methods are evaluated in Sec. 11.3, the correlation coefficients between these methods and the numerical method prediction results for such small data sets should be viewed in the same way.

11.3 SIMPLE PREDICTION METHODS

If the effects of N_2 and N_3 are unimportant, results calculated using previously-recommended simple prediction formulae (Sec. 7.3.3) would be expected to match results for the numerical methods (similar mean prediction error and high correlation coefficients), as well as being in general agreement with the experimental times. Very good agreement with all of the experiments would not be expected in the light of the poor numerical method predictions for some data.

Table 11.2 summarises the prediction accuracy for the four simple slab thawing time prediction formulae (Eqs. (7.2) to (7.5)) used in

conjunction with the two geometric factors (Eqs. (10.1) and (10.2)) for the minced lean beef data (Table 6.8). The thermal property data used are given in Table 5.2. As both the mean and standard deviations of the prediction errors are similar to those for the numerical methods it was concluded that any inaccuracy arising from neglect of N_2 and N_3 was sufficiently small to be ignored.

Cleland & Earle (1984a, 1984b) and Pham (1983, 1984c) used the data of Cleland & Earle (1977a, 1979a, 1979b), de Michelis & Calvelo (1983) and Hung & Thompson (1983) to test methods to predict freezing times. It was considered worthwhile to calculate results equivalent to Table 1 of Cleland & Earle (1984b) for Eq. (7.7), the one new freezing method under consideration here. The results are given in Table 11.3. For data to a final thermodynamic centre temperature other than -10 °C, the modification of Cleland & Earle (1984b) was used to correct the prediction of Eq. (7.7) which is based on a final thermodynamic centre temperature of -10 °C. The thermal property data given by Cleland & Earle (1984a) were used to be consistent with the previously published results.

Since the previous studies, some new slab data have been published by Succar & Hayakawa (1984). These are also included in Table 11.3. With the thermal property data used, neither these nine runs, nor results from the same laboratory for other shapes (Hawakawa et al 1983a) shown in Table 11.4 could be predicted accurately by any of the methods considered, including the finite difference method.

Comparison of Table 11.3 with Table 1 of Cleland & Earle (1984b) shows that Eq. (7.7) was equally good as the best previously proposed methods of Cleland & Earle (1984b), and Pham (1983, 1984a, 1984c) (Sec. 7.3.3). Neither ignoring the effects of N_2 and N_3 nor using the method of Cleland & Earle (1984b) to account for different final temperatures significantly affected the prediction accuracy.

The four simple slab freezing and thawing time prediction approaches discussed in this section and in Sec. 7.3, can all be extended to any other shape by either of the geometric factors EHTD or MCP. Both geometric factors have been tested for most of the Tylose

multi-dimensional shape freezing and thawing data (Chap. 10 and Table 11.2). In Table 11.4, the prediction results of these simple prediction methods are summarised for the remaining multi-dimensional shape data from the composite data set of Table 11.1. Because all four slab approaches are approximately equivalent, only one was used in this analysis. The method of Pham (1984c) was arbitrarily chosen. Again, the simple prediction method results closely follow the numerical method predictions and agree as well as could be expected with the experimental data. No significant difference in prediction accuracy between MCP and EHTD could be discerned.

11.4   SUMMARY

Numerical freezing and thawing time prediction methods were slightly less accurate for food materials than for Tylose due to larger thermal property data and experimental uncertainties.

Simple slab prediction methods and geometric factors developed to predict freezing and thawing times for Tylose have been shown to be equally applicable to food materials and for a wider range of conditions and shapes than previously considered.

The effects of N_2 and N_3 on freezing times were sufficiently small compared with experimental uncertainty, that no justification existed for inclusion of terms involving N_2 and N_3 in the simple empirical methods. Fewer test data exist for thawing, but there is no indication from these that N_2 and N_3 are any more significant for thawing than for freezing.

Table 11.1 <u>Composite Data Set For Testing of Freezing and Thawing Time</u>
           <u>Prediction Methods</u>

Type	Source	Material	Shape[1]	Final Centre Temperature (°C)	No. of Runs
Thawing	Table 6.2	Tylose	Slab	0.0	35
	Table 6.3	Tylose	Cylinder	0.0	34
	Table 6.4	Tylose	Sphere	0.0	35
	Table 6.5	Tylose	Brick	0.0	68
	Table 6.6	Tylose	2DI	0.0	41
	Table 6.7	Tylose	3DI	0.0	11
	Table 6.8	Lean Beef	Slab	0.0	6[*]
	Table 6.8	Lean Beef	Brick	0.0	4[*]
	Table 6.8	Lean Beef	2DI	0.0	4[*]
Freezing	Table 6.6	Tylose	2DI	-10.0	42
	Table 6.7	Tylose	3DI	-10.0	13
	Table 6.8	Lean Beef	2DI	-10.0	4[*]
Freezing		Tylose	Slab	-10.0	43
	Cleland & Earle 1977a	Lean Beef	Slab	-10.0	6
		Potato	Slab	-10.0	6
	Cleland & Earle 1979a	Tylose	Cylinder	-10.0	30
	Cleland & Earle 1979a	Tylose	Sphere	-10.0	30
	Cleland & Earle 1979b	Tylose	Brick	-10.0	72
Freezing	Hung & Thompson 1983	Tylose	Slab	-18.0	23
		Lean Beef	Slab	-18.0	9
		Potato	Slab	-18.0	9
		Ground Beef	Slab	-18.0	9
		Carp	Slab	-18.0	9

Table 11.1 continued...   221

Type	Source	Material	Shape[1]	Final Centre Temperature (°C)	No. of Runs
Freezing	de Michelis & Calvelo 1983	Lean Beef	Slab	-18.0	5
		Lean Beef	Finite Cyl.	-18.0	4
		Lean Beef	Inf. Rod	-18.0	3
		Lean Beef	Brick	-10.0	17
Freezing	Hayakawa et al 1983a	Lean Beef	Inf. Rod	-15.0	6*
		Tylose	Finite Cyl.	-15.0	6*
Freezing	Succar & Hayakawa 1984	Tylose	Slab	Various	9*
THAWING				Total	238
FREEZING				Total	355
FREEZING AND THAWING				TOTAL	593

[1] 2DI = two-dimensional irregular shapes, 3DI = three-dimensional irregular shapes.

* Data not previously used to test prediction methods.

Table 11.2 Summary of Percentage Differences Between Experimental Thawing Times and Predicted Thawing Times For Minced Lean Beef

Data	Slab Prediction Method	Geometric[1] Factor	Mean (%)	Std Dev[2] (%)	Min[2] (%)	Max[2] (%)	Corr[3] FDM
Slab (Table 6.8) (6 runs)	FDM[4]		-4.5	5.9	-11.9	2.5	1.00
	Eq. (7.2)		-7.2	8.5	-15.4	3.6	0.81
	Eq. (7.3)		-7.0	6.9	-16.0	1.1	0.91
	Eq. (7.3)		-6.4	7.9	-19.4	3.6	0.92
	Eq. (7.5)		-5.4	6.0	-10.6	2.5	0.96
Rectangular Brick (Table 6.8) (4 runs)	FDM[4]		4.8	7.0	-3.0	17.3	1.00
	Eq. (7.2)	EHTD	1.8	6.0	-3.5	10.1	1.00
		MCP	1.8	6.0	-4.1	9.4	0.99
	Eq. (7.3)	EHTD	1.7	8.5	-5.3	14.1	0.99
		MCP	1.7	8.3	-5.9	13.4	0.99
	Eq. (7.4)	EHTD	-0.6	5.5	-6.1	6.3	0.97
		MCP	-0.7	5.5	-7.5	5.6	0.93
	Eq. (7.5)	EHTD	2.5	4.6	-2.1	8.6	0.94
		MCP	2.4	4.3	-1.5	7.9	0.95
Two-Dimensional Irregular (Table 6.8) (4 runs)	FEM[4]		13.8	3.0	9.5	16.2	1.00
	Eq. (7.2)	EHTD	14.6	2.8	12.4	18.8	0.16
		MCP	14.8	2.8	12.5	18.9	0.16
	Eq. (7.3)	EHTD	15.7	3.7	11.6	19.9	0.55
		MCP	15.8	3.7	11.8	20.0	0.56
	Eq. (7.4)	EHTD	17.0	3.3	13.5	21.0	0.76
		MCP	17.2	3.3	13.6	21.2	0.76
	Eq. (7.5)	EHTD	16.9	1.4	15.4	18.5	0.81
		MCP	17.0	1.4	15.6	18.7	0.82

[1] EHTD calculated from Eq. (10.1), MCP calculated from Eq. (10.2).

[2] Std Dev = standard deviation, Min = minimum, Max = maximum.

[3] Correlation coefficient (r) compared with the percentage differences for either the full finite difference method or the full finite element method.

[4] Full finite difference method or full finite finite element method.

Table 11.3 <u>Summary of Percentage Differences Between Experimental</u>
<u>Freezing Times and Predicted Freezing Times Calculated By</u>
<u>Eq. (7.7)</u>

Source	Shape	Material	Geometric Factor[1]	No.	Mean (%)	Std Dev[2] (%)	Min[2] (%)	Max[2] (%)	Corr[3] FDM
Cleland & Earle 1977a	Slab	Tylose		43	0.8	2.8	-5.9	5.7	0.32
	Slab	Lean Beef		6	2.9	4.0	-1.8	9.4	0.64
	Slab	Potato		6	-0.5	2.2	-3.2	2.2	0.35
Cleland & Earle 1979a	Cylinder	Tylose		30	-1.4	4.0	-9.8	5.3	0.81
	Sphere	Tylose		30	0.5	4.0	-7.2	10.6	0.92
Cleland & Earle 1979b	Brick	Tylose	EHTD	72	0.3	5.1	-8.5	10.1	0.56
			MCP	72	-1.3	5.4	-11.1	8.3	0.65
Hung & Thompson 1983	Slab	Tylose		23	-3.9	8.0	-24.8	9.2	0.78
		Lean Beef		9	-4.8	9.0	-17.2	9.3	0.89
		Potato		9	-8.0	4.9	-16.5	0.0	0.20
		Ground Beef		9	2.8	15.8	-21.6	22.2	0.93
		Carp		9	-1.7	12.1	-22.2	16.7	0.89
de Michelis & Calvelo 1983	Slab	Lean Beef		5	4.4	4.6	-1.5	10.9	0.91
	Finite Cylinder Rod & Brick	Lean Beef	EHTD	24	8.7	11.5	-12.0	29.3	0.84
			MCP	24	7.4	10.8	-12.3	29.0	0.87
Succar & Hayakawa 1984	Slab	Tylose		9	31.5	8.3	23.0	43.1	1.00

[1] EHTD calculated from Eq. (10.1), MCP calculated from Eq. (10.2).

[2] Std Dev = standard deviation, Min = minimum, Max = maximum.

[3] Correlation coefficient (r) compared with the percentage differences for the finite difference method.

Table 11.4 <u>Summary of Percentage Differences Between Experimental</u>
<u>Freezing Times For Multi-Dimensional Shapes and Freezing</u>
<u>Times Calculated By Simple Prediction Methods[1]</u>

Source	Shape	Material	Geometric Factor[2]	Mean (%)	Std Dev[3] (%)	Min[3] (%)	Max[3] (%)	Corr[4] FDM
	Infinite Rod		FDM[5]	-2.7	3.9	-6.7	1.0	1.00
		Lean Beef	EHTD	-5.3	9.8	-16.6	0.5	0.91
	(3 runs)		MCP	-5.6	9.7	-16.8	0.2	0.91
de Michelis	Finite Cylinder		FDM[5]	13.6	9.3	6.1	25.6	1.00
& Calvelo		Lean Beef	EHTD	14.4	8.3	10.6	30.0	0.97
1983a	(4 runs)		MCP	18.2	8.9	10.1	29.7	1.00
	Rectangular Brick		FDM[5]	1.00	8.6	6.5	-4.2	17.7
		Lean Beef	EHTD	4.2	6.9	-12.6	13.6	0.84
	(17 runs)		MCP	2.8	6.0	-12.5	10.0	0.89
	Infinite Rod		FDM[5]	23.8	8.0	14.9	37.9	1.00
		Lean Beef	EHTD	28.8	8.2	19.5	43.0	1.00
Hayakawa	(6 runs)		MCP	28.4	8.3	18.9	42.7	1.00
et al 1983	Finite Cylinder		FDM[5]	66.9	19.9	45.2	91.5	1.00
		Tylose	EHTD	80.8	21.5	57.5	107.3	1.00
	(6 runs)		MCP	80.9	22.3	56.8	108.2	1.00
	2DI[6]		FEM[5]	10.8	2.2	8.2	13.5	1.00
Table 6.8		Lean Beef	EHTD	12.5	1.8	10.5	14.6	0.46
	(4 runs)		MCP	13.2	2.3	10.7	15.9	0.37

[1] Using Pham's (1984c) slab prediction method for freezing.

[2] EHTD calculated from Eq. (10.1), MCP calculated from Eq. (10.2).

[3] Std Dev = standard deviation, Min = minimum, Max = maximum.

[4] Correlation coefficient (r) compared with the percentage differences for either the full finite difference method or the full finite element method.

[5] Full finite difference method or full finite element method.

[6] 2DI = two-dimensional irregular shapes.

12 OVERALL EVALUATION OF FREEZING AND THAWING TIME PREDICTION METHODS

12.1 INTRODUCTION

In Chaps. 7, 8, 9, 10 and 11 a number of prediction methods were evaluated against a large composite data set of 593 freezing and thawing runs. Table 12.1 summarises the overall performance of the best numerical methods (the finite difference method for regular shapes and the finite element method for irregular shapes) and the four best simple slab freezing and thawing time prediction approaches (used in conjunction with both simple geometric factors). It was decided to exclude from Table 12.1 the data against which all the prediction methods performed badly. This decision was made so that these experimental runs did not unduly influence the comparison of prediction methods. Only 33 runs were excluded. These were the data of Hayakawa et al (1983a), Succar & Hayakawa (1984) plus the egg and fish three-dimensional irregular shapes (Table 6.8). Detailed comments on why poor predictions arose for these runs are given in Secs. 10.4 and 11.2.

It was also considered useful to compare prediction method performance to estimates of the random experimental uncertainty. In this study an estimate of the experimental uncertainty could only be derived for the experimental work of Cleland (1977) and the present work. Table 12.2 compares the estimated random experimental uncertainty with the 95% confidences bounds for the prediction errors of both the best numerical and simple prediction methods, for each shape tested.

Important sources of random experimental error were discussed in Sec. 5.1. In order to obtain a good estimate of the experimental error, expressed as a 95% confidence bound, the following calculation procedure was used:
(a) the spread of replicate slab experiments was assessed — this was used to estimate the uncertainty arising from control in all of the experiments,
(b) a component was added for the surface heat transfer coefficient.

The importance of error in h is a function of the Biot number. Plank's equation suggests a weighting of $4/(Bi+4)$ so this was used,

(c) further allowances were added for multi-dimensional irregular shapes where the experimental techniques and problems with measuring and controlling the geometries suggested greater uncertainty than that found for the slab experiments.

It was considered that all other sources of random experimental error were negligibly small. Thermal data uncertainties and systematic experimental error were not included in the estimates. The 95% confidence bounds based on fit to experimental data for the four best simple slab prediction approaches were averaged to give the data in Table 12.2 as all four approaches gave predictions with very similar offset and spread of prediction errors (Table 12.1).

12.2 NUMERICAL PREDICTION METHODS

Throughout the testing against experimental data (summarised in Tables 12.1 and 12.2) it has been shown that the finite difference and finite element numerical methods do not introduce significant prediction uncertainty provided that they are correctly formulated and implemented. The users of these methods need to meet the guidelines for space and time step intervals established in Sec. 8.5 for the finite element method.

The difference between the prediction error 95% confidence bounds for the numerical methods and the estimated random experimental uncertainty bounds in Table 12.2 give in most cases an indication of the thermal property uncertainty.

The off-set mean error for the rectangular brick freezing data and the larger numerical prediction error bounds for both the slab and rectangular brick freezing data are most probably the result of freezing rate effects that the numerical method calculations did not take into account (Cleland et al 1982). The larger spread of prediction errors and the off-set mean for the three-dimensional irregular numerical predictions have probably arisen as a result of being forced to use coarse spatial grids. They could also reflect substantial systematic experimental errors (particularly in measurement

of the surface heat transfer coefficient and in describing and measuring the object geometries).

12.3 SIMPLE PREDICTION METHODS

All four empirical approaches gave similar prediction accuracy for the composite data set for both freezing and thawing. The simple method predictions all generally matched the numerical method predictions, and the mean prediction errors were not significantly off-set from zero. For freezing the formulae for the two approaches of Calvelo (1981) and Cleland & Earle (1976b) (Eq. (7.7) and Cleland & Earle (1982b)), were not quite as highly correlated with the numerical method results as the other approaches; probably because these formulae were based on curve-fitting to a smaller data set than the other formulae.

In Table 12.1 it can be observed that the standard deviations for simple freezing time prediction methods were very similar to the numerical methods standard deviations, but a small difference occurred for thawing. Numerical methods were ±4.9%, but the best simple methods were about ±6.1%. This suggests that for thawing a small simple prediction method uncertainty does exist. It has almost certainly arisen from neglect of the effect of Ste in deriving empirical equations for EHTD and MCP (Sec. 9.5). The decrease in prediction method accuracy is small, and can only just be observed with a large, accurate experimental data set. Whilst new terms for the Ste effect could be included in MCP and EHTD for thawing this would destroy the unified approach to take account of geometry. Further, the practising food engineer would not obtain significantly better predictions because data uncertainties in industrial practice far exceed those in the research laboratory.

Table 12.2 shows that the confidence bounds for the simple methods are consistent with the numerical predictions and with the experimental error bounds. Hence, there is no evidence in this table that simple prediction method inaccuracy is significant compared to experimental or thermal property data error.

The accuracy of all four approaches was such that development of other empirical methods was not considered worthwhile. It is unlikely that significantly better prediction accuracy could be achieved unless better experimental data are collected. Marginal increases in accuracy could be achieved if further terms were added, but at the risk that a systematic component of the experimental error was being fitted.

Two ways of calculating each of the geometric factors, EHTD and MCP, were proposed - Eqs. (9.11) and (9.12) for EHTD and MCP respectively for regular shapes and Eqs. (10.1) and (10.2) respectively for irregular shapes. For regular shapes the latter equations to calculate EHTD and MCP (Eqs. (10.1) and (10.2)) gave almost equal values as Eqs. (9.11) and (9.12). Therefore only Eq. (10.1) (EHTD) and Eq. (10.2) (MCP) were compared directly.

The two geometric factors gave virtually identical overall prediction accuracy for the composite data set as well as almost identical individual predictions. The formula for EHTD (Eq. (10.1)) was less complex than the formula for MCP because the MCP function goes through a maximum value at intermediate Biot number values, which was difficult to curve-fit in a simple manner. It was found easier to fit the EHTD relationship first and use the inter-relationship between EHTD and MCP to derive the MCP equations.

There may be no need for other geometric concepts because both EHTD and MCP seem capable of giving sufficient accuracy for a wide range of shapes. The proposed calculation formulae are least accurate for calculating the effect of the third dimension in irregular shapes. This situation has arisen more from the sparsity of suitable data, than from inappropriate principles in the geometric factors themselves. Collection of the necessary data would be expensive, but no problems in modifying the EHTD and MCP equations are envisaged because all the present work has shown that the principles on which they are based are sound. Table 12.1 includes few data with irregular third dimensions so this one area of weakness is not apparent in it.

If the detailed comparisons in Chaps. 7 to 10 are examined it can be seen that each of the simple approaches has data sets on which it

performs relatively better, and data sets on which its performance is poor compared with the other three approaches. Table 12.1 shows that there is nothing systematic in these observations for the full data set so all four simple approaches and both geometric factors can be used with equal confidence. All eight individual freezing and eight thawing time prediction methods are therefore recommended as suitable for general use. Engineers may have preferences amongst them. Possible criteria are discussed in Sec. 12.4. Should very accurate predictions be required users may wish to make predictions by more than one method, and take an average. This procedure also helps guard against the possibility of calculation error as predictions disagreeing by more than a few percent have almost certainly arisen from user error.

The choice between the geometric factors is probably best made by individuals on the basis of ease of understanding of the concepts. Some may find EHTD easier to visualise and others MCP.

12.4   OTHER ATTRIBUTES OF SIMPLE PREDICTION METHODS

The desirable attributes of a freezing or thawing time prediction method other than accuracy are listed in Table 3.1. All four simple approaches investigated had some of these attributes. Each approach led to freezing and thawing time prediction formulae with similar forms so that a unified approach for freezing and thawing time prediction could be used.

In terms of simplicity, none of the approaches was significantly better. For all four approaches, most of the time required to obtain a prediction would be spent estimating representative environmental conditions and thermal property data, rather than in using the formulae themselves. Sample calculations for all of the approaches are given in App. E.

Comments can be made on some of the slab methods. The freezing formulae of Pham (1984c) uses a variable, the mean freezing temperature, that does not take physically realistic values in calculations. The approach of Pham (1983) for freezing assumes that the basic form of Plank's (1913) equation correctly models phase change

in foods without superheating or subcooling, which in reality it does not do (Sec. 2.3.2.3). Otherwise the four approaches led to formulae that are physically realistic. The method of Pham (1984c) for freezing builds on an earlier method Pham (1984a) which had a more complete physical and analytical basis. It proved impossible to extend the earlier method to thawing without incorporating empirical terms (Eq. (7.4) in Sec. 7.3.2). Therefore for the present analysis, Eq. (7.4) was regarded as the thawing equivalent of the approach of Pham (1984c) for freezing because both are empirical methods, and the approach of Pham (1984a) was not considered further.

12.5   COMPARISON OF NUMERICAL AND SIMPLE PREDICTION METHODS

Comparisons of the merits of numerical methods and simple formulae for freezing and thawing time predictions are made by Cleland (1977), Cleland & Earle (1977a, 1984a) and Heldman (1983). Briefly, numerical methods have the advantages of flexibility and reliability for a wide range of conditions, whereas simple methods are less complex, easier and less costly to use in calculations, have fewer thermal property data requirements but have a more restricted range of applicability.

Tables 12.1 and 12.2 show that the numerical and simple prediction methods gave comparable prediction accuracy. The simple method results deviated from the numerical results for only three sets of data, but these deviations can be explained. Firstly, the numerical results for slab and rectangular brick freezing were particularly affected by rate effects (Cleland et al 1982). Secondly, coarse spatial grids were used in the calculations for three-dimensional irregular shapes, and this introduced numerical method error. Thirdly, the lack of suitable data meant that the simple methods geometric factors were not as accurate for three-dimensional irregular shapes as they may have been with an extended data set.

12.6   NON-CONSTANT ENVIRONMENTAL CONDITIONS

In Chap. 3 it was decided that the entire field of freezing and thawing time prediction could not be covered comprehensively. The present study therefore considered only phase change with constant conditions

and concentrated particularly on the effect of shape. Future research
may address the accuracy of freezing and thawing time predictions under
time and/or position variable environmental conditions.

Until such research is carried out the most appropriate ways to handle
non-constant conditions with simple methods are those described by
Cleland (1977) in the case of non-uniform initial temperature, and
Loeffen et al (1981) and Cleland & Earle (1982c) in the case of time
variable h and T_a. The problem of a position variable surface heat
transfer coefficient introduces another level of complexity. Teider
(1963), de Michelis (1982) and Mascheroni et al (1982), describe ways
to handle only the simplest case of a slab with different h values on
each face.

Numerical methods, by comparison with simple formulae, are very
versatile and can take account of any of these time or position
variations directly, but at the expense of more complex computer
implementation and more expensive computations.

12.7 SUMMARY

The accuracy of the finite difference and finite element methods for
freezing and thawing time prediction were limited more by inaccuracy in
the thermal data and experimental uncertainty than uncertainty due to
the methods themselves provided that the guidelines to   ensure
sufficiently small spatial and time steps are obeyed.

All four simple empirical approaches in combination with both EHTD and
MCP are accurate freezing and thawing time predictors, performing very
similarly to the numerical methods. None of the methods had attributes
that particularly recommended it so all are advocated as suitable for
routine use.   The highest level of precision is probably obtainable by
averaging prediction from more than one of the methods.

Table 12.1 <u>Summary of the Percentage Differences Between Experimental</u>
<u>Freezing and Thawing Times From a Composite Data Set and</u>
<u>Freezing and Thawing Times Calculated By Numerical and</u>
<u>Simple Prediction Methods</u>

Geometric Factor	EHTD			MCP		
Slab Prediction Method	Mean (%)	Std Dev[1] (%)	Corr[2] FDM	Mean (%)	Std Dev[1] (%)	Corr[2] FDM
FREEZING (328 runs)						
Numerical[3]	-0.8	7.9	1.00			
Eq. (7.7)	1.0	7.3	0.70	0.5	7.3	0.73
Cleland & Earle 1982b	1.8	7.5	0.68	1.3	7.5	0.72
Pham 1984c	1.8	7.4	0.80	1.3	7.6	0.81
Pham 1983 (Eq. (7.6))	0.8	7.4	0.86	0.3	7.6	0.87
THAWING (232 runs)						
Numerical[3]	-0.1	4.9	1.00			
Eq. (7.2)	1.0	6.1	0.64	0.4	6.2	0.64
Eq. (7.3)	0.8	6.2	0.67	0.2	6.3	0.67
Eq. (7.4)	1.0	6.7	0.64	0.5	6.8	0.65
Eq. (7.5)	1.4	6.2	0.67	0.9	6.4	0.66

[1] Std Dev = standard deviation, Min = minimum, Max = maximum.

[2] Correlation coefficient (r) compared with the percentage differences
for either the full finite difference method or the full finite
element method.

[3] The full finite difference method for regular shapes and the full
finite element method for irregular shapes.

Table 12.2 Comparison of the Estimated Experimental Uncertainty Bounds and the Means and 95% Confidence Bounds For the Numerical[1] and Simple[2] Freezing and Thawing Time Prediction Methods

Data[3]	Type[4]	Estimated[5] Experimental Uncertainty (%)	Numerical Methods[1]		Simple Methods[2]	
			Mean (%)	CB[6] (%)	Mean (%)	CB[6] (%)
Slab	F	±4.2[7]	0.8	±12.2	1.9	±8.7
	T	±5.3	-0.8	±7.0	0.5	±10.9
Cylinder	F	±6.5[7]	-3.6	±9.5	-1.0	±8.4
	T	±6.1	-2.2	±4.7	-1.4	±6.8
Sphere	F	±7.0[7]	-2.2	±6.9	-0.3	±7.9
	T	±8.0	-0.9	±11.1	1.1	±13.0
Brick	F	±8.0[7]	-4.4	±13.1	-0.9	±12.0
	T	±5.4	0.6	±6.3	-1.9	±9.8
2DI	F,T	±8.9	0.3	±10.2	5.1	±10.5
3DI[8] Rect	F,T	±9.6	-10.3	±13.4	0.2	±15.9
Oval	F,T	±14.3	11.7	±40.2	12.3	±21.6

[1] The finite difference method for regular shapes and the full finite element method for irregular shapes.

[2] Average of the four best slab prediction methods, results were nearly identical using either EHTD or MCP as the geometric factor.

[3] Data from Cleland 1977 and Tables 6.2, 6.3, 6.4, 6.5, 6.6, and 6.7.

[4] F = freezing, T = thawing.

[5] Estimated experimental uncertainty 95% confidence bounds.

[6] CB = 95% confidence bounds of the predictions about the mean.

[7] Estimates given by Cleland (1977).

[8] 2DI = two-dimensional irregular shapes, 3DI = three-dimensional irregular shapes, Rect = rectangular cross-sections in third dimension, Oval = oval cross-sections in the third dimension.

13 CONCLUSIONS

The data measured in the present work represent a major addition to the sets of accurately measured and controlled experimental data for freezing and thawing of foods. The 297 experiments include 182 for thawing of regular shapes and 115 for both freezing and thawing of irregular shapes.

Of the numerical methods available those that take account of the continuously temperature-variable thermal properties model the true physical behaviour during freezing and thawing of foods most closely. Testing showed that these methods were accurate predictors of temperature/time profiles.

The finite difference method is restricted by practical considerations to use for regular shapes. Testing against experimental data indicated that provided sufficiently small space and time steps were used in a correctly formulated and implemented computer program, the prediction method uncertainty in predicting freezing and thawing times of regular shapes was insignificant.

The finite element method was formulated and implemented in a computer program that was able to solve heat conduction with phase change for multi-dimensional regular and irregular shapes. Computation costs were high. A simplified finite element method formulation was derived that considerably reduced costs but should be used cautiously because of the crude way in which thermal property variations are incorporated. Quantitative guidelines were developed for application of the two finite element method formulations to freezing and thawing problems where there are limits to computing resources. Comparison of predicted phase change times with experimental data for both regular and irregular shapes showed that adherence to these guidelines ensured that prediction method uncertainty was negligible.

No accurate simple method to predict thawing times that was not product specific was found in the literature. For thawing of slabs, infinite cylinders and spheres, four simple but generally applicable formulae were developed. They were all equally accurate with 95% confidence

bounds of -11.0% to +11.0% when compared with experimentally determined
thawing times.

The two existing concepts to take account of the effect of geometry on
freezing and thawing times, EHTD and MCP, were both increased in
accuracy and extended to cover a wider range of multi-dimensional
geometries.   Used in conjunction with accurate simple prediction
methods for slabs, they gave prediction accuracy similar to that of the
numerical methods.   For two-dimensional shapes the 95% confidence
bounds of the percentage differences for the prediction compared with
the experimentally measured freezing and thawing times were -5.0% to
+15.5%; for three-dimensional shapes with rectangular cross-sections
the bounds were -12.5% to +9.5%; but for three-dimensional shapes with
oval cross-sections the bounds were wider and off-set further from zero
at -4% to 37%.

Refinement of the methods to calculate EHTD and MCP so as to increase
the accuracy for some three-dimensional shapes was prevented by lack of
suitable data.   However the principles underlying the methods to
calculate EHTD and MCP are considered valid so further data would
enable the coefficients in the equations to be more accurately fitted
for a wider range of shapes.   Improvement of the empirical EHTD and MCP
expressions for the effect of the third dimension for irregular shapes
is an area in which future work might be most valuable.

When compared with the composite experimental freezing and thawing data
set for a range of materials, geometries and conditions, both the
numerical and simple prediction methods gave accurate predictions.
None of the four simple slab prediction method approaches has any
advantage that particularly recommended it so all are advocated as
suitable for routine use. Both EHTD and MCP gave virtually identical
predictions for multi-dimensional shapes. Users may wish to base the
choice of which to use on their conceptual understanding of the
principles involved.   In practice it would be expected that any of the
prediction methods advocated in this study would be limited more by the
accuracy of data to be used in the predictions, than by limitations in
the accuracy of the methods themselves.

NOMENCLATURE

a	constant for radial geometry	
A	surface or cross-sectional area	m^2
Bi	$= hD/k$, Biot number	
Bi	$= hD/k_s$, Biot number for freezing	
	$= hD/k_1$, Biot number for thawing	
c	specific heat capacity	$J\ kg^{-1}\ °C^{-1}$
C	volumetric specific heat capacity	$J\ m^{-3}\ °C^{-1}$
C	thermal capacitance matrix	
D	thickness, diameter or characteristic dimension	m
E	percentage error	%
EHTD	equivalent heat transfer dimensionality	
f	arbitrary function	
FDM	finite difference method	
FEM	finite element method	
F	thermal forcing vector	
Fo	$= kt/CD^2$, Fourier number	
Fo	$= k_s t/C_s D^2$, Fourier number for freezing	
	$= k_1 t/C_1 D^2$, Fourier number for thawing	
G	constants for calculation of EHTD and MCP	
h	surface heat transfer coefficient	$W\ m^{-2}\ °C^{-1}$
H	enthalpy	$J\ m^{-3}$
I	number of nodes in x direction	
J	number of nodes in y direction	
k	thermal conductivity	$W\ m^{-1}\ °C^{-1}$
K	thermal conductance matrix	
l	direction cosine to the outward normal	
L	latent heat capacity	$J\ m^{-3}$
L	edge or perimeter length	m
m	position in r direction	
M	number of nodes in r direction	
MCP	mean conducting path length	m
n	number of nodal points	
N	shape function	
N_1	$= C\ \lvert T_{if} - T_{fin} \rvert / \Delta H$	

N_1 $= C_s(T_{if}-T_{fin})/\Delta H$ for freezing

        $= C_l(T_{fin}-T_{if})/\Delta H$ for thawing

N_2 $= C_l/C_s$

N_3 $= k_l/k_s$

P   geometric factor in versions of Plank's equation

Pk $= C\ |T_{in}-T_{if}|/\Delta H$, Plank number

Pk $= C_l(T_{in}-T_{if})/\Delta H$, Plank number for freezing

        $= C_s(T_{if}-T_{in})/\Delta H$, Plank number for thawing

Q   internal heat generation $W\ m^{-3}$

r   distance in radial direction   m

R   half thickness or radius   m

R   geometric factor in versions of Plank's equation

S   surface area m^2

Ste $= C\ |T_{if}-T_a|/\Delta H$, Stefan number

Ste $= C_s(T_{if}-T_a)/\Delta H$, Stefan number for freezing

        $= C_l(T_a-T_{if})/\Delta H$, Stefan number for thawing

t   time   s or hrs

T   temperature   °C or K

T   vector of nodal temperatures   °C or K

V   volume m^3

W   factor for axisymmetric finite element integrations

x   distance in x direction   m

X   Biot number weighting function for EHTD and

        MCP calculations

X   constant in the FDM schemes

y   distance in y direction   m

Y   fractional unaccomplished temperature change

        $= (T_a-T)/(T_a-T_{in})$

Y   constant in the FDM schemes

z   distance in z direction   m

β ratio of side lengths for regular shapes

ΔH enthalpy change between 0 °C and -10 °C $J\ m^{-3}$

∇ ratio of major axis length to minor axis length

        for an ellipse

        $= 4A/\pi D^2$

σ Stefan-Boltzmann constant $W\ m^{-2}\ K^{-4}$

        $= 5.67 \times 10^{-8}$

ε surface radiation emissivity

ρ density $kg\ m^{-3}$

α thermal diffusivity $m^2\ s^{-1}$

ϕ heat flux $W\ m^{-2}$

Δ change in

$\sum$ summation of

Subscripts

a   ambient value

ac   ambient convective value

ar   ambient radiative value

ave   average value

c   centre value

con   value for convection

cyl   value for cylinder

e   element or surface value

exp   experimental value

f   for freezing

f   full method

fdm   value predicted by the finite difference method

fem   value predicted by the finite element method

femf   full finite element method formulation

fems   simplified finite element method formulation

fin   final value

i   denotes position of node in x direction

i   value for ith node

if   value at initial freezing point

in   initial value

j   denotes position of node in y direction

j   value for jth node

k   denotes position of node in z direction

l   unfrozen phase value

m   denotes position of node in r direction

r   value in the radial direction

rad   value for radiation

s   frozen phase value

s   simplified method

slab   value for slab

sph   value for sphere

t   for thawing

w   value at a wall or surface

x   value in the x axial direction

y   value in the y axial direction

z   value in the z axial direction

1,2,3 indicates relative time, state or case

Superscripts

i   indicates time level in numerical methods

+   at values just greater than

−   at values just less than

REFERENCES

Albasiny, E.L. (1956): The solution of non-linear heat conduction problems on the Pilot Ace. Proc. Inst. Electric Engng 103 Part B, Supplement 1: 158

Albasiny, E.L. (1960): On the numerical solution of a cylindrical heat conduction problem. Quart. J. Mech. Appl. Maths 13: 374

Albin, F.V., Srinivasa Murthy, S. & Krishna Murthy, M.V. (1976): Analytical estimation of the freezing characteristics of packages of food products. Bull. I.I.R. Annexe-1: 385

Albin, F.V., Srinivasa Murthy, S. & Frishna Murthy, M.V. (1979): Prediction of the freezing characteristics of spherical-shaped food products. Int. J. Refrig. 2: 129

Allada, S.R. & Quan, D. (1966): A stable explicit numerical solution of the heat conduction equation for multi-dimensional nonhomogeneous media. Chem. Engng Prog. Symp. Ser. 62(64): 151

Allen, D.N.de G. & Severn, R.T. (1962): The application of relaxation methods to the solution of non-elliptic partial differential equations. Quart. J. Mech. Appl. Maths 15: 53

Arce, J.A. & Sweat, V.E. (1980): Survey of published heat transfer coefficients encountered in food refrigeration processes. ASHRAE Trans 86(2): 235

Arce, J.A., Potluri, P.L., Schneider, K.C., Sweat, V.E. & Dutson, T.R. (1983): Modelling beef carcass cooling using finite element techniques. Trans ASAE 26: 950

Badari Narayana, K. & Krishna Murthy, M.V. (1975): Thermal properties of a model food gel. Ind. J. Technol. 13: 415

Baghe-Khandan, M.S., Okos, M.R. & Sweat, V.E. (1982): The thermal conductivity of beef as affected by temperature and composition. Trans ASAE 25: 1118

Bailey, C. & James, S.J. (1974): Air-, water- and vacuum-thawing of frozen pork legs and meat blocks. Meat Freezing - How and Why?, M.R.I. Symp. No. 3, p.42.1.

Bailey, C., James, S.J., Kitchell, A.G. & Hudson, W.R. (1974): Air-, water-, and vacuum-thawing of frozen pork legs. J. Sci. Food Agric. 25: 81

Bailey, C. (1976): Thawing methods for meat. Proc. 6th Eur. Symp. Food: Engng Food Quality, p.175.

Bakal, A. & Hayakawa, K. (1973): Heat transfer during freezing and thawing of food. Adv. Food Res. 20: 217

Baker, D.W. & Charm, S.E. (1969): Freezing rates of sea foods as influenced by heat transfer coefficients of liquid refrigerants. Freezing and Irradiation of Fish, p.94. Fishing News(Books) Ltd., London.

Bald, W.D. (1981): Numerical Stability of Finite Element Solution Applied to the Freezing of Biological Materials. Ouel Report, Dept. Engng Sci., University of Oxford.

Bankoff, S.G. (1964): Heat conduction or diffusion with change of phase. Adv. Chem. Engng 5: 75

Baxter, D.C. (1962): The fusion times of slabs and cylinders. J. Heat Transfer 84: 317

Beaubouef, R.T. & Chapman, A.J. (1967): Freezing of fluids in forced flow. Int. J. Heat Mass Transfer 10: 1581

Beck, J.V. (1969): Determination of optimum, transient experiments for thermal contact conductance. Int. J. Heat Mass Transfer 12: 621

Bell, G.E. (1978): A refinement of the heat balance integral method applied to a melting problem. Int. J. Heat Mass Transfer 21: 1357

Bell, G.E. (1979a): Solidification of a liquid about a cylindrical pipe. Int. J. Heat Mass Transfer 22: 1681

Bell, G.E. (1979b): The accurate solution of one-dimensional melting problems by the heat balance integral method. Numerical Methods in Thermal Problems, R.W. Lewis & K. Morgan, eds., p.196. Pineridge Press, Swansea.

Bell, G.E. (1982): On the performance of the enthalpy method. Int. J. Heat Mass Transfer 25: 587

Biot, M.A. (1957): New methods in heat flow analysis with application to flight structures. J. Aeronaut. Sci. 24(12): 857

Boles, M.A. & Ozisk, M.N. (1983): Exact solution for freezing in cylindrically symmetric porous moist media. J. Heat Transfer 105: 401

Boley, B.A. (1961): A method of heat conduction analysis of melting and solidification problems. J. Math. Phys. 40: 300

Boley, B.A. (1963): Upper and lower bounds for the solution of a melting problem. Quart. Appl. Maths 21(1): 1

Boley, B.A. (1968): A general solution for melting and solidifying slabs. Int. J. Engng Sci. 6: 89

Bonacina, C. & Comini, G. (1971): On a numerical method for the solution of the unsteady state heat conduction equation with temperature dependent parameters. Proc. 13th Int. Congr. Refrig. 2: 329

Bonacina, C. & Comini, G. (1972): Calculation of convective heat transfer coefficients from time-temperature curves. Bull. I.I.R. Annexe-1: 157

Bonacina, C. & Comini, G. (1973): On the solution of the non-linear heat conduction equations by numerical methods. Int. J. Heat Mass Transfer 16: 581

Bonacina, C., Comini, G., Fasano, A. & Primicerio, M. (1973): Numerical solution of phase change problems. Int. J. Heat Mass Transfer 16: 1825

Bonacina, C., Comini, G., Fasano, A. & Primicerio, M. (1974): On the estimation of thermophysical properties in non-linear heat conduction problems. Int. J. Heat Mass Transfer 17: 861

Bonacina, C. & Comini, G. (1976): The freezing point equation for food products. I.I.R. Conference Paper B1.74.

Bonnerot, R. & Jamet, P. (1974): A second order finite element method for the one-dimensional Stefan problem. Int. J. Num. Meth. Engng 8: 811

Brebbia, C.A. & Walker, S. (1980): Boundary Element Techniques in Engineering. Butterworths, London.

Brennan, J.G. (1969): Food Engineering Operations. McGraw Hill, New York.

Brian, P.L.T. (1961): A finite difference method of high order accuracy for the solution of three-dimensional heat conduction problems. AIChE J. 7: 367

Brisson-Lopes J.M. & Domingos, J.J.D. (1979): The numerical computation of freezing processes in bodies of arbitrary shape. Proc. 15th Int. Congr. Refrig. 2: 605

Bruch, J.C. & Zyroloski, G. (1974): Transient two-dimensional heat conduction problems solved by the finite element method. Int. J. Num. Meth. Engng}] 8: 481

Budhia, H. & Kreith, F. (1973): Heat transfer with melting or freezing in a wedge. Int. J. Heat Mass Transfer 16: 195

Calvelo, A. (1981): Recent studies on meat freezing. Developments in Meat Science - 2, R. Lawrie, ed., p.125. Applied Science Publishers Ltd., England.

Carslaw, H.S. & Jaeger, J.C. (1959): Conduction of Heat in Solids (2nd ed.). Claredon Press, Oxford.

Chan, A.M.C., Smereka, P. & Shoukri, M. (1983): An approximate analytical solution to the freezing problem subject to convective cooling and with arbitrary initial liquid temperatures. Int. J. Heat Mass Transfer 26: 1712

Chang, H.D. & Tao, L.C. (1981): Correlations of enthalpies of food systems. J. Food Sci. 46: 1493

Charm, S.E. & Slavin, J.W. (1962) A method for calculating freezing times of a rectangular package of food. Bull. I.I.R. Annexe-1: 567

Charm, S.E. (1963): A method for experimentally evaluating heat transfer coefficients in freezers and thermal conductivity of frozen foods. Food Technol. 17(10): 93

Charm, S.E. (1971): Fundamentals of Food Engineering (2nd ed.). Avi, Westport.

Charm, S.E., Brand, D.H. & Baker, D.W. (1972): A simple method for estimating freezing and thawing times of cylinders and slabs. ASHRAE J. 14(11): 39

Chattopadhay, P., Raychaudhuri, B.C. & Bose, A.N. (1975): Prediction of temperature of iced fish. J. Food Sci. 40: 1080

Chavarria, V.M. & Heldman, D.R. (1984): Measurement of convective heat transfer coefficients during food freezing processes. J. Food Sci. 49: 810

Cho, S.H. & Sunderland, J.E. (1969): Heat conduction problems with melting or freezing. J. Heat Transfer 91: 421

Cho, S.H. & Sunderland, J.E. (1970): Phase change of spherical bodies. Int. J. Heat Mass Transfer 13: 1231

Cho, S.H. & Sunderland, J.E. (1974): Phase change problems with temperature dependent thermal conductivity. J. Heat Transfer 96: 214

Cho, S.H. & Sunderland, J.E. (1981): Approximate temperature distribution for phase change of a semi-infinite body. J. Heat Transfer 103: 401

Chuang, Y.K. & Szekely, J. (1971): On the use of Green's functions for solving melting or solidification problems. Int. J. Heat Mass Transfer 14: 1285

Chuang, Y.K. & Szekely, J. (1972): The use of Green's functions for solving melting or solidification problems in the cylinderical co-ordinate system. Int. J. Heat Mass Transfer 15: 1171

Chung, B.T.F. & Yeh, L.T. (1975): Solidification and melting of materials subject to convection and radiation. J. Spacecraft 12(6): 329

Chung, B.T.F. & Yeh, L.T. (1976): Freezing and melting of materials with variable thermal properties and arbitrary heat fluxes. AIAA J. 14(3): 388

Chung, B.T.F., Chang, T.Y., Hsiao, J.S. & Chang, C.I. (1983): Heat transfer with ablation in a half space subjected to time-variant heat fluxes. J. Heat Transfer 105: 200

Chung, K.S. (1981): The fourth-dimension concept in the finite element analysis of transient heat transfer problems. Int. J. Num. Meth. Engng 17: 315

Churchill, S.W. & Evans, L.B. (1971): Coefficients for calculation of freezing in a semi-infinite region. J. Heat Transfer 93: 234

Churchill, S.W. & Gupta, J.P (1977): Approximations for conduction with freezing or melting. Int. J. Heat Mass Transfer 20: 1251

Cichy, A., Lasocki, S. & Marcak, H. (1981): Efficient numerical technique for determining two-dimensional temperature distribution for n-arbitrarily located heat receivers with phase change. Int. J. Heat Mass Transfer 24: 1573

Clary, B.L., Nelson, G.L. & Smith, R.E. (1968): Heat transfer from hams during freezing by low temperature air. Trans ASAE 11: 496

Clary, B.L., Nelson, G.L. & Smith, R.E. (1971): Application of the geometry analysis technique in determining the heat transfer rates from biological materials. Trans ASAE 14: 586

Cleland, A.C. & Earle, R.L. (1976a): A new method for prediction of surface heat transfer coefficients in freezing. Bull. I.I.R. Annexe-1: 361

Cleland, A.C. & Earle, R.L. (1976b): A comparison of freezing calculations including modification to take into account initial superheat. Bull. I.I.R. Annexe-1: 369

Cleland, A.C. (1977) Heat Transfer During Freezing of Foods and Prediction of Freezing Times. Ph.D. thesis, Massey University, New Zealand.

Cleland, A.C. & Earle, R.L. (1977a): A comparison of analytical and numerical methods for predicting the freezing times of foods. J. Food Sci. 42: 1390

Cleland, A.C. & Earle, R.L. (1977b): The third kind of boundary condition in numerical freezing calculations. Int. J. Heat Mass Transfer 20: 1029

Cleland, A.C. & Earle, R.L. (1979a): A comparison of methods for predicting the freezing times of cylindrical and spherical foodstuffs. J. Food Sci. 44: 958

Cleland, A.C. & Earle, R.L. (1979b): Prediction of freezing times for foods in rectangular packages. J. Food Sci. 44: 964

Cleland, A.C. (1979) Prediction of freezing times of foods. A summary of available methods. Proc. Biotech. Conf. on Engng in Biotech., p.161. Massey University, New Zealand.

Cleland, A.C. & Earle, R.L. (1982a): A simplified method for prediction of heating and cooling rates in solids of various shapes. Int. J. Refrig. 5: 98

Cleland, A.C. & Earle, R.L. (1982b): Freezing time prediction for foods - a simplified procedure. Int. J. Refrig. 5: 134

Cleland, A.C. & Earle, R.L. (1982c): Freezing of irregular shapes under time variable conditions. Bull. I.I.R. Annexe-1: 447

Cleland, A.C., Earle, R.L. & Cleland, D.J. (1982): The effect of freezing rate on the accuracy of numerical freezing calculations. Int. J. Refrig. 5: 294

Cleland, A.C. & Earle, R.L. (1984a): Assessment of freezing time prediction methods. J. Food Sci. 49: 1034

Cleland, A.C. & Earle, R.L. (1984b): Freezing time prediction for different final product temperatures. J. Food Sci. 49: 1230

Cleland, D.J., Cleland, A.C., Earle, R.L. & Byrne, S.J. (1984): Prediction of rates of freezing, thawing and cooling in solids of arbitrary shape using the finite element method. Int. J. Refrig. 7: 6

Clyne, T.W. & Garcia, A. (1980): Assessment of a new model for heat flow during uni-directional solidification of metals. Int. J. Heat Mass Transfer 23: 773

Cochran, D.L. (1955): An investigation of rate of solidification. Refrig. Engng 63(8): 49

Comini, G. (1972): Design of transient experiments for measurement of convective heat transfer coefficients. Bull. I.I.R. Annexe-1: 169

Comini, G. & Bonacina, C. (1974): Application of computer codes to phase-change problems in food engineering. Bull. I.I.R. Annexe-3: 15

Comini, G., Bonacina, C. & Barina, S. (1974a): Thermal properties of foodstuffs. Bull. I.I.R. Annexe-3: 163

Comini, G., Del Guidice, S., Lewis, R.W. & Zienkiewicz, O.C. (1974b): Finite element solution of non-linear heat conduction problems with special reference to phase change. Int. J. Numerical Methods Engng 8: 613

Comini, G. & Del Guidice S. (1976): Thermal aspects of cryosurgery. J. Heat Transfer 98: 543

Comini, G. & Lewis, R.W. (1976): A numerical solution of two-dimensional problems involving heat and mass transfer. Int. J. Heat Mass Transfer 19: 1387

Comini, G., Del Guidice, S., Strada, M. & Rebellato, L. (1978): The finite element method in refrigeration engineering. Int. J. Refrig. 1: 113

Cordell, J.M. & Webb, D.C. (1972): The freezing of ice cream. Proc. Int. Symp. Heat Mass Transfer Problems Food Engng 2: D3.1

Cowan, W.B. (1958): Freezing methods and trends in Canada. Bull. I.I.R. Annexe-1: 65

Cowell, N.D. (1967): The calculation of food freezing times. Proc. 12th Int. Congr. Refrig. 2: 667

Cowell, N.D. (1974): The meaning of the term "freezing time". Meat Freezing - How and Why?, M.R.I. Symp. No. 3, p.14.1.

Cowell, N.D. & Namor, M.S.S. (1974): Heat transfer coefficients in plate freezers - effect of packaging materials. Bull. I.I.R. Annexe-3: 45

Crank, J. & Nicholson, P. (1947): A practical method for numerical integration of solutions of partial differential equations of heat conduction type. Proc. Cam. Phil. Soc. 43: 50

Crank, J. & Gupta, R.S. (1975): Isotherm migration method in two dimensions. (Int. J. Heat Mass Transfer 18: 1101

Crank, J. (1981): How to deal with moving boundaries in thermal problems. Numerical Methods in Heat Transfer, R.W. Lewis, K. Morgan & O.C. Zienkiewicz, eds., p.177. John Wiley & Sons Ltd., London.

Creed, P.G., Bailey, C., James, S.J. & Harding, C.D. (1979): Air thawing of lamb carcasses. J. Food Technol. 14: 181

Creed, P.G. & James, S.J. (1981): Predicting thawing time of frozen boneless beef blocks. Int. J. Refrig. 4: 355

Cullwick, T.D.C. & Earle, R.L. (1971): Prediction of freezing times of meat in plate freezers. Proc. 13th Int. Congr. Refrig. 2: 397

Danckwerts, P.V. (1950): Unsteady-state diffusion or heat conduction with a moving boundary. Trans Faraday Soc. 46: 701

de Michelis, A. & Calvelo, A. (1982): Mathematical models for non-symmetric freezing of beef. J. Food Sci. 47: 1211

de Michelis, A. & Calvelo, A. (1983): Freezing time prediction for brick and cylindrical shaped foods. J. Food Sci. 48: 909

Dickerson, R.W. (1977): Relationships between water content, enthalpy, specfic heat and thermal diffusivity of foods. ASHRAE Trans 38(1): 525

Donea, J. (1974): On the accuracy of finite element solutions to the transient heat conduction equation. Int. J. Num. Meth. Engng 8: 103

Dorney, D.C. & Glew, G. (1977): Rapid thawing of pre-cooked frozen foods in catering. J. Food Technol. 12: 523

Douglas, J. (1955): On the numerical integration of $d^2u/dx^2 + d^2u/dy^2 = du/dt$ by implicit methods. J. SIAM 3(1): 42

Douglas, J. & Gallie, T.M. (1955): On the numerical integration of a parabolic differential equation subject to a moving boundary condition. Duke Math. J. 22: 557

Douglas, J. & Rachford, H.H. (1956): On the numerical solution of heat conduction problems in two and three space variables. Trans Am. Maths Soc. 82: 421

Duda, J.L. & Vrentas, J.S. (1969): Perturbation solutions of diffusion controlled moving boundary problems. Chem. Engng Sci. 24: 461

Duda, J.L., Malone, M.F. & Notter, R.H. (1975): Analysis of two-dimensional diffusion-controlled moving boundary problems. Int. J. Heat Mass Transfer 18: 901

Durbin, J.R., MacDonald, B.R. & Loeffen, M.P.F. (1979): Short Investigation of Air Thawing of Lamb and Mutton Carcasses. MIRINZ Report No. RM100, Hamilton, New Zealand.

Dusinberre, G.M. (1945): Numerical method for transient heat flow. Trans A.S.M.E. 67: 703

Dusinberre, G.M. (1949): Numerical Analysis of Heat Flow, p.114. McGraw-Hill, New York.

Earle, R.L. & Earl, W.B. (1966): Freezing rate studies in blocks of meat of simple shape. Proc. 3rd Int. Heat Transfer Congr. 4: 152

Earle, R.L. & Freeman, N.W. (1966): Continuous tunnel freezing of boneless meat in cartons. Bull. I.I.R. Annexe-1: 663

Earle, R.L. & Fleming, A.K. (1967): Cooling and freezing of lamb and mutton carcasses - 1. Cooling and freezing rates in legs. Food Technol. 21(1): 79

Earle, R.L. (1971): Simple probe to determine cooling rates in air. Proc. 13th Int. Congr. Refrig. 2: 373

Earle, R.L. & Cleland, A.C. (1979): Prediction of surface heat transfer coefficients in industrial situations. Proc. Biotech. Conf. on Engng in Biotech., p.201. Massey University, New Zealand.

Eddie, G.G. & Pearson, S.F. (1958): The freezing time of fish in air-blast freezers. J. Refrig. 1: 75

Ede, A.J. (1949): The calculation of the rate of freezing and thawing of foodstuffs. Mod. Refrig. 52: 52

Ehrlich, L.W. (1958): A numerical method of solving a heat problem with a moving boundary. Assoc. Comp. Mach. J. 5: 161

El-Genk, M.S. & Cronenberg, A.W. (1979): Some improvements to the solution of Stefan-like problems. Int. J. Heat Mass Transfer 22: 167

Emery, A.F. & Carson, W.W. (1971): An evaluation of the use of the finite element method in the computation of temperature. J. Heat Transfer 93: 136

Evans, G.W., Isaacson, E., MacDonald, J.K.C. (1950): Stefan-like problems. Quart. Appl. Maths 8(1): 312

Everington, D.W. (1971): Thawing of frozen foodstuffs. Chem. Ind. 35: 973

Everington, D.W. & Cooper, A. (1972a): Vacuum heat thawing of frozen foodstuffs. Food Trade Rev. 42: 7

Everington, D.W. & Cooper, A. (1972b): Vacuum heat thawing of frozen foodstuffs. Bull. I.I.R. Annexe-2: 327

Eyres, N.R., Hartree, D.R., Ingham, J., Jackson, R., Sarjant, R.J. & Wagstaff, J.B. (1946): The calculation of variable heat flow in solids. Trans Roy. Soc. Lond. A240: 1

Fairweather, G. & Mitchell, A.R. (1965): A new alternating direction method for parabolic equations in three space variables. J. SIAM 13(4): 957

Fleming, A.K. (1967): Immersion Freezing of Small Meat-Products. Proc. 12th Int. Congr. Refrig. 2: 684

Fleming A.K. (1970): Physical aspects of meat cooling. Bull. I.I.R. Annexe-1: 151

Fleming, A.K. (1971a): The numerical calculation of freezing processes. Proc. 13th Int. Congr. Refrig. 2: 303

Fleming, A.K. (1971b): Applications of a computer programme to freezing processes. Proc. 13th Int. Congr. Refrig. 2: 403

Fleming, A.K. (1971c): The numerical calculation of freezing processes. Technical Licentiate Degree thesis, The Technical University of Norway, Trondheim, Norway.

Forgac, J.M., Schur, T.P. & Angus, J.C. (1979): Solidification of a sphere: the effects of thermal contraction and density change upon freezing. J. Appl. Mech. 46: 83

Fox, L. (1975): What are the best numerical methods? Moving Boundary Problems in Heat Flow and Diffusion, J.R. Ockenden & W.R. Hodgkins, eds., p.210. Claredon Press, Oxford.

Frazerhurst, L.F., Haughey, D.P. & Wyborn, L.G. (1972): Prototype development of an immersion freezer for fancy meats in monopropIyene glycol. MIRINZ Report No. 259, Hamilton, New Zealand.

Frivik, P.E., Thorbergsen, E., Del Guidice, S. & Comini, G. (1977): Thermal design of pavement structures in seasonal frost areas. J. Heat Transfer 99: 533

Frivik, P.E. & Thorbergson, E. (1981): Thermal design of artificial soil freezing systems. Engng Geology 18: 189

Frivik, P.E. & Comini, G. (1982): Seepage and heat flow in soil freezing. J. Heat Transfer 104: 323

Gau, C. & Viskanta, R. (1984): Melting and solidification of a metal system in a rectangular cavity. Int. J. Heat Mass Transfer 27: 113

Geuze, C.A., Betten, A. & Touber, S. (1972): Non-steady heat transfer in a freezing model substance. Bull. I.I.R. Annexe-1: 211

Glasser, D. & Kern, J. (1978): Bounds and approximate solutions to linear problems with non-linear boundary conditions: solidification of a slab. AIChE J. 24: 161

Golovkin, N.A., Geinz, R.G., Maslova, G.V. & Nozdrunkova, I.R. (1974): Studies of meat sub-freezing processes and it's application for cold storage of animal products. Proc. 13th Int. Congr. Refrig. 3: 221

Goodling, J.S. & Khader, M.S. (1974): Inward solidification with radiation-convection boundary condition. J. Heat Transfer 96: 114

Goodling, J.S. & Khader, M.S. (1975): Results of the numerical solution of outward solidification with flux boundary conditions. J. Heat Transfer 97: 307

Goodman, T.R. (1958): The heat balance integral and its application to problems involving a change of phase. Trans A.S.M.E. 80: 335

Goodman, T.R. & Shea, J.J. (1960): The melting of finite slabs. J. Appl. Mech. 27: 16

Goodman, T.R. (1961): The heat balance integral - further considerations and refinements. J. Heat Transfer 83: 83

Goodman, T.R. (1964): Application of integral methods to transient non-linear heat transfer. Adv. Heat Transfer 1: 51

Goodrich, L.E. (1978): Efficient numerical technique for one-dimensional thermal problems with phase change. Int. J. Heat Mass Transfer 21: 615

Gorenflo, D. & Mertz, K. (1975): Experimental investigation into the freezing of packets of Tylose in domestic freezers. L.W.T. Report 8(4): 185

Gupta, R.S. & Kumar, D. (1980): A modified variable time step method for the one-dimensional Stefan problem. Comp. Meth. Appl. Mech. Engng 23: 101

Gupta, R.S. & Kumar, D. (1981): Variable time step methods for one-dimensional Stefan problems with mixed boundary conditions. Int. J. Heat Mass Transfer 24: 251

Gupta, R.S. & Kumar, D. (1984): An efficient approach to isotherm migration in two dimensions. Int. J. Heat Mass Transfer 27: 1939

Hahne, E. & Grigull, U. (1975): Shape factor and shape resistance for steady multi-dimensional heat conduction. Int. J. Heat Mass Transfer 18: 751

Haji-Sheikh, A. & Sparrow, E.M. (1967): The solution of heat conduction problems by probability methods. J. Heat Transfer 89: 121

Hale, N.W. & Viskanta, R. (1980): Solid-liquid phase change heat transfer and interface motion in materials cooled or heated from above or below. Int. J. Heat Mass Transfer 23: 283

Hamill, T.D. & Bankoff, S.G. (1963): Maximum and minimum bounds on freezing-melting rates with time-dependent boundary conditions. AIChE J. 9: 741

Hamill, T.D. & Bankoff, S.G. (1964): Similarity solutions of the plane melting problem with temperature-dependent thermal properties. Ind. Engng Chem. Fund. 3(2): 177

Hashemi, H.T. & Sliepcevich, C.M. (1967a): A numerical method for solving two-dimensional problems of heat conduction with change of phase. Chem. Engng Prog. Symp. Ser. 63(79): 34

Hashemi, H.T. & Sliepcevich, C.M. (1967b): A diffusion-analogue method for solving problems of heat conduction with change of phase. Chem. Engng Prog. Symp. Ser. 63(79): 42

Hayakawa, K. & Bakal, A. (1973): Formula for predicting transient temperatures in food during freezing or thawing. Chem. Engng Prog. Symp. Ser. 69(132): 14

Hayakawa, K. (1977): Estimation of heat transfer during freezing or defrosting of food. Bull. I.I.R. Annexe-1: 293

Hayakawa, K., Nonino, C. & Succar,J. (1983a): Two-dimensional heat conduction in food undergoing freezing: predicting freezing times of rectangular or finitely cylindrical food. J. Food Sci. 48: 1841

Hayakawa, K., Nonino, C., Comini, G. & Del Giudice, S. (1983b): Two-dimensional heat conduction in food undergoing freezing: development of computerised model. J. Food Sci. 48: 1849

Hayashi, Y., Katoh, S. & Hattori, M. (1979): Heat conduction in freezing of cellular material involving aqueous solution. Proc. 15th Int. Congr. Refrig. 2: 617

Hayashi, Y. & Komori, T. (1979): Investigation of salt solutions in cells. J. Heat Transfer 101: 459

Heiss, R. (1958): The course of temperature in meat cubes during freezing and thawing. Bull. I.I.R. Annexe-1: 429

Heitz, W.L. & Westwater, J.W. (1970): Extension of the numerical method for melting and freezing problems. Int. J. Heat Mass Transfer 13: 1371

Heldman, D.R. (1974a): Computer simulation of food freezing processes. Proc. 4th Int. Congr. Food Sci. Technol. 4: 397

Heldman, D.R. (1974b): Predicting the relationship between unfrozen water fraction and temperature during food freezing using freezing point depression. Trans ASAE 17: 63

Heldman, D.R. & Gorby, G.P. (1974): Computer simulation of ice-cream freezing. Bull. I.I.R. Annexe-3: 29

Heldman, D.R. & Gorby, G.P. (1975): Prediction of thermal conductivity in frozen foods. Trans ASAE 18: 740

Heldman, D.R. (1981): Food properties in freezing processes. Symp. Physical Properties of Food, Food Engineering Division, Inst. Food Technologists.

Heldman, D.R. (1982): Food properties during freezing. Food Technol. 36(2): 92

Heldman, D.R. (1983): Factors influencing food freezing rates. Food Technol. 37(4): 103

Hewitt, M.R., Nicholson, F.J., Hill, G.P. & Smith, G.L. (1974): Freezing times for blocks of fish in vertical plate freezers - effect of contact area and bulk density. Bull. I.I.R. Annexe-3: 39

Heurtault, S., Badii, J.M., Rouanet, A. & Arnaud, G. (1982): Solidification of superheated liquid spheres with temperature dependent properties. Int. J. Heat Mass Transfer 25: 1671

Hill, J.M. & Kucera, A. (1983): Freezing a saturated liquid inside a sphere. Int. J. Heat Mass Transfer 26: 1631

Hills, A.W.D. & Moore, M.R. (1967): Use of integral-profile methods to treat heat transfer during solidification. Heat and Mass Transfer in Process Metallurgy, p.141. Institute Min. Met., London.

Hills, A.W.D. (1969): A generalised integral-profile method for the analysis of unidirectional flow during solidification. Trans Met. Soc. A.I.M.E. 245: 1471

Hills, A.W.D. & Moore, M.R. (1969): The solidification of pure metals under uni-directional heat flow conditions. I - Solidification with zero super-heat. Trans Met. Soc. A.I.M.E. 245: 1481

Hirai, E. & Komori, T. (1971): A proposal to solve Neumann's problem approximately, taking account of bulk dilatation by phase change - a semi-infinite solid. J. Chem. Engng Jap. 4(1): 96

Horvay, G. (1960): Freezing of a growing liquid column. J. Heat Transfer 82: 37

Hrycak, P. (1963): Problem of solidification with Newton's cooling at the surface. AIChE J. 9: 585

Hrycak, P. (1967): Heat conduction with solification in a stratified medium. AIChE J. 13: 160

Hsieh, R.C., Lerew, L.E. & Heldman, D.R. (1977): Prediction of freezing time for food as influenced by product properties. J. Food Process Engng 1: 183

Hsu, C.F., Sparrow, E.M. & Patankar, S.V. (1981): Numerical solution of moving boundary problems by boundary immobilisation and a control-volume-based finite difference scheme. Int. J. Heat Mass Transfer 24: 1335

Hsu, T.R. & Pizey, G. (1981): On the prediction of fusion rate of ice by finite element analysis. J. Heat Transfer 103: 727

Huang, C-L & Shih, Y-P (1975a): Perturbation solutions of planar diffusion-controlled moving boundary problems. Int. J. Heat Mass Transfer 18: 689

Huang, C-L & Shih, Y-P (1975b): Perturbation solution for planar solidification of a saturated liquid with convection at the wall. Int. J. Heat Mass Transfer 18: 1481

Hung, Y.C. & Thompson, D.R. (1983): Freezing time prediction for slab shape foodstuffs by an improved analytical method. J. Food Sci. 48: 555

Ichikawa, Y. & Kikuchi, N. (1979): A one-phase multi-dimensional Stefan problem by the method of variational inequalities. Int. J. Num. Meth. Engng 14: 1197

International Institute of Refrigeration (1972): Recommendations for the Processing and Handling of Frozen Foods (2nd ed.). Paris.

Imber, M. & Huang, P.N.S. (1973): Phase change in a semi-infinite solid with temperature dependent thermal properties. Int. J. Heat Mass Transfer 16: 1951

Jackson, F. (1964): The solution of problems involving the melting and freezing of a finite slab by a method due to Portnov. Proc. Edinburgh Maths Soc. 14: 109

James, S.J., Bailey, C. & Ono, S. (1976): Determination of freezing and thawing times in the centre of blocks of meat by measurement of surface temperature. (J. Food Technol. 11: 505

James, S.J., Creed, P.G. & Roberts, T.A. (1977)): Air thawing of beef quarters. J. Sci. Food Agric. 28: 1109

James, S.J., Creed, P.G. & Bailey, C. (1979): The determination of freezing time of boxed meat blocks. Proc. Inst. Refrig.(G.B.), p.74.

James, S.J. & Bailey, C. (1980): Air- and vacuum-thawing of unwrapped boneless meat blocks. Proc. Inst. Refrig.(G.B.), p.44.

James, S.J. & Creed, P.G. (1980): Predicting thawing times of frozen beef fore and hind-quarters. Int. J. Refrig. 3: 237

Jayaram, B. & Streider, W. (1983): An analysis of substrate heat losses in Stefan's problem with a constant heat flux. Int. J. Heat Mass Transfer 26: 786

Jiji, L.M., Rathjen, K.A. & Drzewiecki, T. (1970): Two-dimensional solidification in a corner. Int. J. Heat Mass Transfer 13: 215

Jiji, L.M. & Weinbaum, S. (1978): Perturbation solutions for melting or freezing in annular regions initially not at the fusion temperature. Int. J. Heat Mass Transfer 21: 581

Joshi, C. & Tao, L.C. (1974): A numerical method for simulating the axisymmetrical freezing of food systems. J. Food Sci. 39: 623

Kassai, D. (1969): A modern thawing technology for frozen carcasses. Bull. I.I.R. Annexe-6: 263

Keller, G.J. & Ballard, J.H. (1956): Predicting temperature changes in frozen liquids. Ind. Engng Chem. 48(2): 188

Kern, J. (1977): A simple and apparently safe solution to the generalised Stefan problem. Int. J. Heat Mass Transfer 20: 467

Khatchaturov, A.B. (1958): Thermal processes during air blast freezing of fish. Bull. I.I.R. Annexe-2: 365

Kikuchi, N. & Ichikawa, Y. (1979): Numerical methods for a two-phase Stefan problem by variational inequalities. Int. J. Num. Meth. Engng 14: 1221

Kinder, E. & Lamb, J. (1974): The prediction of freezing times of foodstuffs. Meat Freezing - How and Why?, M.R.I. Symp. No. 3, p.17.1.

Komori, T. & Hirai, E. (1970): An application of Stefan's problem to the freezing of a cylindrical foodstuff. J. Chem. Engng Jap. 3(1): 39

Komori, T. & Hirai, E. (1972): Solutions of heat conduction problem with change of phase - a slab. J. Chem. Engng Jap. 5(3): 242

Kopelman, I.J., Borrero, C. & Pflug, I.J. (1970): Evaluation of surface film heat transfer coefficients using transient methods. Proc. 12th Int. Congr. Refrig. 2: 291

Koskelainen, L. (1979): CONFID - a general finite difference program for heat conduction problems. Numerical Methods in Thermal Problems, R.W. Lewis & K. Morgan, eds., p.31. Pineridge Press, Swansea.

Kouwenhoven, H.L.J. (1972): The evaluation of heat removal during freezing of poultry in air blast freezers. Bull. I.I.R. Annexe-2: 195

Kreith, F. & Romie, F.E. (1955): A study of the thermal diffusion equation with boundary conditions corresponding to solidification or melting of materials initially at the fusion temperature. Proc. Phys. Soc. Lond. B68: 277

Kroeger, P.G. & Ostrach, S. (1974): The solution of a two-dimensional freezing problem including convection effects in the liquid region. Int. J. Heat Mass Transfer 17: 1191

Lamb, J. (1976): Influence of water on thermal properties of foods. Chem. Ind. 40: 1046

Landau, H.G. (1950): Heat conduction in a melting solid. Quart. Appl. Maths 8(1): 81

Langford, D. (1966): The freezing of spheres. Int. J. Heat Mass Transfer 9: 827

Langford, D. (1973): The heat balance integral method. Int. J. Heat Mass Transfer 16: 2424

Lappadula, C. & Mueller, W.K. (1966): Heat conduction with solidification and a convection boundary condition at the freezing front. Int. J. Heat Mass Transfer 9: 702

Larkin, J.L., Heldman, D.R. & Steffe, J.F. (1984): An analysis of factors influencing precision of thermal property values during freezing. Int. J. Refrig. 7: 86

Lazaridus, A. (1970): A numerical solution of the multidimensional solidification (or melting) problem. Int. J. Heat Mass Transfer 13: 1459

Lederman, J.M. & Boley, B.A. (1970): Axisymmetric melting or solidification of circular cylinders. Int. J. Heat Mass Transfer 13: 413

Lees, M. (1966): A linear three level difference scheme for quasi-linear parabolic equations. Maths Comput. 20: 516

Lemmon, E.C. (1979): Phase change techniques of finite element conduction codes. Numerical Methods in Thermal Problems, R.W. Lewis & K. Morgan, eds., p.149. Pineridge Press, Swansea.

Lentz, C.P. (1961): Thermal conductivity of meats, fats, gelatin gels and ice. Food Technol. 15(5): 243

Lentz, C.P. & Van Den Berg, L. (1977): Thermal conductivity data for foods: their significance and use. ASHRAE Trans 83(1): 533

Levy, F.L. (1958): Calculating the freezing time of fish in air-blast freezers. J. Refrig. 1: 55

Levy, F.L. (1979): Enthalpy and specific heat capacity of meat and fish in the freezing range. J. Food Technol. 14: 549

Levy, F.L. (1981): A modified Maxwell-Eucken equation for calculating the thermal conductivity of two-component solutions or mixtures. Int. J. Refrig. 4: 223

Levy, F.L. (1982a): Calculating the thermal conductivity of meat and fish in the freezing range. Int. J. Refrig. 5: 149

Levy, F.L. (1982b): A simplified method for calculating the thermal conductivity of meat and fish in the freezing range. Zeitschr f Lebensmitteltechnologie 33: 455

Levy, F.L. (1982c): Enthalpy and specific heat capacity of meat and fish in the freezing range and their presentation in diagrams. Zeitschr f Lebensmitteltechnologie 33: 509

Levy, F.L. (1983a): The coefficient of thermal diffusion of meat and fish in the freezing range. Zeitschr f Lebensmitteltechnologie 34: 16

Levy, F.L. (1983b): Calculating the chilling and freezing time of meat. Zeitschr f Lebensmitteltechnologie 34: 294

Levy, F.L. (1983c): Calculating the thawing time of meat. Zeitschr f Lebensmitteltechnologie 34: 691

Levy, F.L. (1984): A guide towards programming chilling and freezing operations of meat. Zeitschr f Lebensmitteltechnologie 35* 614

Lewis, R.W. & Bass, B.R. (1976): The determination of stresses and temperatures in cooling bodies by finite elements. J. Heat Transfer 98: 478

Libby, P.A. & Chen, S. (1968): The growth of a deposited layer on a cold surface. Int. J. Heat Mass Transfer 8: 395

Liebmann, G. (1956): Solution of transient heat transfer problems by the resistance network analogue method. Trans A.S.M.E. 78: 1267

Lim, C.P. (1975): The Effects of Temperature on Reinforced Concrete Beam Column Junctions. M.E. thesis, University of Canterbury, New Zealand.

Linge, D.V. (1973): Zum Problem der Instationaren Warmeleitung in Gefrierbereich von Lebensmitteln. D.Ing. thesis, University of Karlsruhe, German Federal Republic

Lock, G.H.S., Gunderson, J.R., Quan, D. & Donnelly, J.K. (1969): A study of one-dimensional ice formation with particular reference to periodic growth and decay. Int. J. Heat Mass Transfer 12: 1343

Lockwood, F.C. (1966): Simple numerical procedure for the digital computer solution of non-linear transient heat conduction with change of phase. J. Mech. Engng Sci. 8(3): 259

Loeffan, M.P.F., Earle, R.L. & Cleland, A.C. (1981): Two simple methods for predicting food freezing time with time variable boundary conditions. J. Food Sci. 46: 1032

London, A.L. & Seban, R.A. (1943): Rates of ice formation. Trans A.S.M.E. 65: 771

Longwell, P.A. (1958): A graphical method for solution of freezing problems. AIChE J. 4: 53

Lorentzen, G. & Rosvik, S. (1959): Investigation of Heat Transfer and Weight Loss During Freezing of Meat. Norges Tekniske, Hogskole, Institutt for Kjoleteknikk, Trondhiem.

Lotkin, M. (1960): Calculation of heat flow in melting solids. Quart. Appl. Maths 18(1): 79

Lotz, H. (1974): Heat transfer and freezing capacity of foodstuffs in household freezers. Bull. I.I.R. Annexe-3: 61

Lunardini, V.J. (1981): Phase change around a circular pipe. J. Heat Transfer 103: 598

Lynch, D.R. & O'Neill, K. (1981): Continuously deforming finite elements for the solution of parabolic problems with and without phase change. Int. J. Num. Meth. Engng 17: 81

Mascheroni, R.H., Ottino, J. & Calvelo, A. (1977): A model for the thermal conductivity of frozen meat. Meat Sci. 1: 235

Mascheroni, R.H. & Calvelo, A. (1980): Relationship between heat transfer parameters and the characteristic damage variables for the freezing of beef. Meat Sci. 4: 267

Mascheroni, R.H. & Calvelo, A. (1982): A simplified model for freezing time calculations in foods. J. Food Sci. 47: 1201

Mascheroni, R.H., De Michelis, A. & Calvelo, A. (1982): A simplified mathematical model for freezing time calculations in plate freezers. Bull. I.I.R. Annexe-1: 431

McAdams, W.H. (1954): Heat Transmission (3rd ed.). McGraw Hill, Tokyo.

McKee, S. & Mitchell, A.R. (1971): Alternating direction methods for parabolic equations in three space dimensions with mixed derivatives. Comp. J. 14(3): 295

Meffert, H.F.Th. (1984): Cost 90: results on an international project on thermal properties. Int. J. Refrig. 7: 21

Mellor, J.D. & Seppings, A.H. (1976): Thermophysical data for designing a refrigerated food chain. Bull. I.I.R. Annexe-1: 349

Mellor, J.D. (1976): Thermophysical properties of foodstuffs. 1. Introductory Review. Bull. I.I.R. 56(3): 551

Mellor, J.D. (1978): Thermophysical properties of foodstuffs. 2. Theoretical Aspects. Bull. I.I.R. 58(3): 569

Mellor, J.D. (1979): Thermophysical properties of foodstuffs. 3. Measurements. Bull. I.I.R. 59(3): 551

Mellor, J.D. (1980): Thermophysical properties of foodstuffs. 4. General Bibliography. Bull. I.I.R. 60(3): 493

Merritt, J.H. & Banks, A. (1964): Thawing of frozen cod in air and in water. Bull. I.I.R. Annexe-1: 65

Mikhailov, M.D. (1976): Exact solution for freezing of humid porous half space. Int. J. Heat Mass Transfer 19: 651

Miki, H., Kikukawa, H. & Nishomoto, J. (1978): Fundamental studies on the thawing of frozen fish - 3.Numerical analysis for the thawing process. Mem. Fac. Fisheries Kagoshima Univ. 27(1): 107

Miki, H., Kikukawa, H. & Nishomoto, J. (1982): Numerical calcultions of three-dimensional heat conduction on the freezing process of a marine foodstuff. Bull. Jap. Soc. Sci. Fisheries 48(6): 775

Moleeratanond, W., Ashby, B.H., Kramer, A. & Bailey, W.A. (1982): Criteria for energy efficient packaging and freezing of boxed beef. Trans ASAE 25: 502

Moore, F.E. & Bayazitoglu, Y. (1982): Melting within a spherical enclosure. J. Heat Transfer 104: 19

Moran, T. (1930): The frozen state in mammalian muscle. Proc. Royal Soc. Lond. B106: 182

Morgan, K., Lewis, R.W. & Zienkiewicz, O.C. (1978): An improved algorithm for heat conduction problems with phase change. Int. J. Num. Meth. Engng 12: 1191

Morley, M.J. (1966): Thermal conductivities of muscles, fats and bones. J. Food Technol. 1: 303

Morley, M.J. (1972): Thermal Properties of Meat: Tabulated Data. Special Report No. 1. Agricultural Research Council, M.R.I., Langford, Bristol.

Morrison, M.E. (1970): Numerical evaluation of temperature profiles and interface position in filaments undergoing solidification. AIChE J. 6: 57

Mott, L.F. (1964): The prediction of product freezing time. Aust. Refrig.Air Cond. Heat 18(12): 16

Muehlbauer, J.C. & Sunderland, J.E. (1965): Heat conduction with freezing or melting. Appl. Mech. Rev. 18: 951 or 16

Muehlbauer, J.C., Hatcher, J.D., Lyons, D.W. & Sunderland, J.E. (1973): Transient heat transfer analysis of alloy solidification. J. Heat Transfer 95: 324

Murray, W.D. & Landis, F. (1959): Numerical and machine solutions of transient heat conduction problems involving melting or freezing. J. Heat Transfer 81: 106

Myers, G.E. (1978): The critical time step for finite element solutions to two-dimensional heat conduction transients. J. Heat Transfer 100: 120

Nagaoka, J., Takaji, S. & Hohani, S. (1955): Experiments on the freezing of fish in an air blast freezer. Proc. 9th Int. Congr. Refrig. 4: 105

Newman, A.B. (1936): Heating and cooling rectangular and cylindrical solids. Ind. Engng Chem. 28(5): 545

O'Brien, G.G., Hyman, M.A. & Kaplan, S. (1951): A study on the numerical solution of partial differential equations. J. Maths Phys. 29: 223

O'Callaghan, M.J., Cravalho, E.G. & Huggins, C.E. (1980): Instability of the planar freeze front during solidification of an aqueous binary solution. J. Heat Transfer 102: 673

Ockendon, J.R. & Hodgkins, W.R., eds. (1975): Moving Boundary Problems in Heat Flow and Diffusion. Clarendon Press, Oxford.

Okada, M. (1984): Analysis of heat transfer during melting from a vertical wall. Int. J. Heat Mass Transfer 27: 2057

Ozisik, M.N. (1978): A note on the general formulation of phase change problems as heat conduction problems with a moving heat source. J. Heat Transfer 100: 370

Ozisik, M.N. & Uzzell, J.C. (1979): Exact solution for freezing in cylindrical symmetry with extended freezing temperature range. J. Heat Transfer 101: 331

Padmanabhan, T.V. & Subba Raji, K. (1975): Numerical solution for heat conduction problem with freezing. Ind. J. Technol. 13: 477

Patel, P.D. & Boley, B.A. (1969): Solidification problems with space and time varying thermal properties and imperfect mould contact. Int. J. Engng Sci. 7: 1041

Peaceman, D.W. & Rachford, H.H. (1955): The numerical solution of parabolic and elliptic differential equations. J. SIAM 3(1): 28

Pedroso, R.I. & Domoto, G.A. (1973a): Perturbation solution for spherical solidification of saturated liquids. J. Heat Transfer 95: 42

Pedroso, R.I. & Domoto, G.A. (1973b): Technical note on planar solidification with fixed wall temperature and variable thermal properties. J. Heat Transfer 95: 553

Pedroso, R.I. & Domoto, G.A. (1973c): Inward spherical solidification by the method of strained co-ordinates. Int. J. Heat Mass Transfer 16: 1037

Pedroso, R.I. & Domoto, G.A. (1973d): Exact solution by perturbation method for planar solidification of a saturated liquid with convection at the wall. Int. J. Heat Mass Transfer 16: 1816

Pekeris, C.L. & Slichter, L.B. (1939): Problem of ice formation. J. Appl. Phys. 10: 135

Pham, Q.T. (1983): Personal communication.

Pham, Q.T. (1984a): An extension to Plank's equation for predicting freezing times of foodstuffs of simple shape. Int. J. Refrig. (in press).

Pham, Q.T. (1984b): An analytical method for predicting freezing times of rectangular blocks of foodstuffs. Int. J. Refrig. (in press).

Pham, Q.T. (1984c): A simplified equation for predicting freezing time. Submitted to J. Food Sci.

Plank, R. (1913): Die gefrierdauer von eisblocken. Zeitschrift fur die gesamte Kalte-Industrie 20(6): 109

Plank, R. (1941) Bietrage zur berechnung und bewertung der gefriergesch windigkeit von lebensmitteln. Beiheft zur Zeitschrift fur die gesamte Kalte-Industrie Reihe 3 Heft 10: 1

Polley, S.L. (1980): A compilation of thermal properties of foods. Food Technol. 34(11): 76

Poots, G. (1962a): An approximate treatment of a heat conduction problem involving a two-dimensional solidification front. Int. J. Heat Mass Transfer 5: 339

Poots, G. (1962b): On application of integral methods to the solution of problems involving solidification of liquids initially at the fusion temperature. Int. J. Heat Mass Transfer 5: 525

Price, P.H. & Slack, M.R. (1954): The effect of latent heat on numerical solutions of the heat flow equation. Brit. J. Appl. Phys. 5: 285

Purwadaria, H.K. (1980): A Numerical Prediction Model for Food Freezing Using the Finite Element Method. Ph.D. thesis, Michigan State University.

Purwadaria, H.K. & Heldman, D.R. (1983): A finite element model for prediction of freezing rates in food products with anomalous shapes. Trans ASAE 25: 827

Ramakrishna, R.G. & Sastri, V.M.K. (1984): Efficient numerical method for two-dimensional phase change problems. Int. J. Heat Mass Transfer 27: 2077

Ramaswamy, H.S. & Tung, M.A. (1981): Thermophysical properties of apples in relation to freezing. J. Food Sci. 46: 724

Rathjen, K.A. & Jiji, L.M. (1971): Heat conduction with melting or freezing in a corner. J. Heat Transfer 93: 101

Raymond, J.F. & Rubinsky, B. (1983): A numerical study of the thawing process of a frozen coal particle. J. Heat Transfer 105: 197

Rebellato, L., Del Guidice, S. & Comini, G. (1978): Finite element analysis of freezing processes in foodstuffs. J. Food Sci. 43: 237

Riedel, L. (1957): Kalorimetrische untersuchungen uber das gefrieren von fleish. Kaltetechnik 9(2): 38

Riedel, L. (1960): Eine prufsubstanz fur gefrierversuche. Kaltetechnik 12: 222

Riedel, L. (1961): On the problem of bound water in meat. Kaltetechnik 13: 122

Riley, D.S., Smith, F.T. & Poots, G. (1974): The inward solidification of spheres and circular cylinders. Int. J. Heat Mass Transfer 17: 1507

Riley, D.S. & Duck, P.W. (1977a): Application of the heat balance integral method to freezing of a cuboid. Int. J. Heat Mass Transfer 20: 294

Riley, D.S. & Duck, P.W. (1977b): An extension of existing solidification results obtained from the heat balance integral method. Int. J. Heat Mass Transfer 20: 297

Rolfe, E.J. (1968): The chilling and freezing of foodstuffs. Biochemical and Biological Engineering Science (Vol. 2), N. Blakebrough, ed., p.137. Academic Press, London.

Rolphe, W.D. & Bathe, K-J. (1982): An efficient algorithm for analysis of non-linear heat transfer with phase change. Int. J. Num. Meth. Engng 18: 119

Roshan, H.Md., Ramachandran, E.G., Seshadri, M.R. & Ramachandran, A. (1974): Analytical solution to the heat transfer in mould walls during solidification of metals. A.F.S. Cast Metals Res. J. 10: 39

Rubinsky, B. & Cravahlo, E.G. (1981): An finite element method for the solution of one-dimensional phase change problems. Int. J. Heat Mass Transfer 24: 1987

Rutov, D.G. (1936): Thermal processes involved in the freezing of perishable foodstuffs. Proc. 7th Int. Congr. Refrig. 1: 211

Saitoh, T. (1978): Numerical method for multi-dimensional freezing problems in arbitrary domains. J. Heat Transfer 100: 294

Sastry, S.K. (1984): Freezing time prediction: an enthalpy-based approach. J. Food Sci. 49: 1121

Savino, J.M. & Siegel, R. (1969): An analytical solution for solidification of a moving warm liquid onto an iosthermal cold wall. Int. J. Heat Mass Transfer 12: 803

Scott, K.R. (1975): Hot water thawing of deboned mullet blocks. Can. Inst. Food Sci. Technol. J. 9(3): 160

Schwartzberg, H.G. (1976): Effective heat capacities for the freezing and thawing of food. J. Food Sci. 41: 152

Schwartzberg, H.G. (1977): Effective heat capacities for the freezing and thawing of foods. Bull. I.I.R. Annexe-1: 303

Schwartzberg, H.G., Rosenau, J.R. & Haight, J.R. (1977): The prediction of freezing and thawing temperature verses time behaviour through the use of effective heat capacity equations. Bull. I.I.R. Annexe-1: 311

Seeniraj, R.V. & Bose, T.K. (1982): One-dimensional phase change problems with radiation-convection. J. Heat Transfer 104: 811

Segerlind, L.J. (1976): Applied Finite Element Analysis. John Wiley & Sons, New York.

Seider, W.D. & Churchill, S.W. (1965): The effect of insulation on freezing front motion. Chem. Engng Prog. Symp. Ser. 61(59): 179

Selim, M.S. & Seagrave, R.C. (1973a): Solution of moving boundary transport problems in finite media by integral transforms. I. Problems with a plane moving boundary. Ind. Engng Chem. Fund. 12(1): 1

Selim, M.S. & Seagrave, R.C. (1973b): Solution of moving boundary transport problems in finite media by integral transforms. II. Problems with a cylindrical or spherical moving boundary. Ind. Engng Chem. Fund. 12(1): 9

Shamsundar, N. & Sparrow, E.M. (1975): Analysis of multidimensional phase change via the enthalpy model. J. Heat Transfer 97: 333

Shamsundar, N. & Sparrow, E.M. (1976): Effect of density change on multidimensional conduction phase change. J. Heat Transfer 98: 550

Shamsundar, N. & Srinivasan, R. (1979): A new similarity method for analysis of multi-dimensional solidification. J. Heat Transfer 101: 585

Shamsundar, N. (1981): Similarity rule for solidification heat transfer with change in volume. J. Heat Transfer 103: 173

Shamsundar, N. (1982): Approximate calculation of multi-dimensional solidification by using conduction shape factors. J. Heat Transfer 104: 8

Shih, Y-P & Tsay, S-Y (1971): Analytical solution for freezing a saturated inside or outside cylinders. Chem. Engng Sci. 26: 809

Shih, Y-P & Chou, T-C (1971): Analytical solution for freezing a saturated liquid inside or outside spheres. Chem. Engng Sci. 26: 1787

Siegel, R. & Savino, J.M. (1966): An analysis of the transient solidification of a flowing warm liquid on a convectively cooled wall. Proc. 3rd Int. Heat Transfer Conf. 4: 141

Slatter, M.A. & Jones, M.C. (1972): Development of an accurate method of predicting freezing rates in watery solids. Proc. Int. Symp. Heat Mass Transfer Problems Food Engng 2: D2-2

Slavin, J.W. (1964): Freezing seafood - now and in the future. ASHRAE J. 6(5): 43

Smith, R.E., Nelson, G.L. & Henrickson, R.L. (1967): Analyses on transient heat transfer from anomalous shapes. Trans ASAE 10: 236

Smith, R.E., Nelson, G.L. & Henrichson, R.L. (1968): Applications of geometry analysis of anomalous shapes to problems in transient heat transfer. Trans ASAE 11: 296

Smith, R.E. & Nelson, G.L. (1969): Transient heat transfer in solids: theory verses experimental. Trans ASAE 12: 833

Sokulski, M.B. (1972a): Sharp freezer room calculations. Bull. Int. Inst. Refrig. Annexe-2: 343

Sokulski, M.B. (1972b): A graphical method of temperature determination in freezing and defrosting processes. Bull. Int. Inst. Refrig. Annexe-2: 355

Soliman, M.A. (1981): An approximate analytical solution for the one-dimensional planar freezing of a supersaturated liquid. Chem. Engng J. 21: 65

Sparrow, E.M., Lee, L. & Shamsundar, N. (1976): Convective instability in a melt layer heated from below. J. Heat Transfer 98: 88

Steinhagen, H.P. & Myers, G.E. (1983): Numerical solution to axisymmetric thawing of frozen logs. J. Heat Transfer 105: 195

Stephan, K. (1969): Influence of heat transfer on melting and solidification in forced flow. Int. J. Heat Mass Transfer 12: 199

Succar, J. & Hayakawa, K. (1984): Parametric analysis for predicting freezing time of infinitely slab-shaped food. J. Food Sci. 49: 468

Sunderland, J.E. & Grosh, R.J. (1961): Transient temperature in a melting solid. J. Heat Transfer 83: 409

Talmon, Y. & Davis, H.T. (1981): Analysis of propagation of freezing and thawing fronts. J. Food Sci. 46: 1478

Talmon, Y., Davis, H.T. & Scriven, L.E. (1981): Progressive freezing of composites analysed by isotherm migration methods. AIChE J. 27: 928

Talmon, Y., Davis, H.T. & Scriven, L.E. (1983): Moving boundary problems in simple shapes solved by isotherm migration. AIChE J. 29: 795

Tanaka, K. & Nishimoto, J. (1959): Determination of time required for freezing of skip-jack. J. Tokyo Univ. Fisheries 45(2): 205

Tanaka, K. & Nishimoto, J. (1960): Determination of the time required for freezing of whalemeat. J. Tokyo Univ. Fisheries 47(1): 81

Tanaka, K. & Nishimoto, J. (1964): Determination of the time required for contact freezing of whalemeat. J. Tokyo Univ. Fisheries 50(2): 49

Tao, L.C. (1967): Generalised numerical solutions of freezing a saturated liquid in cylinders and spheres. AIChE J. 13: 165

Tao, L.C. (1968): Generalised solution for freezing a saturated liquid in a convex container. AIChE J. 14: 720

Tao, L.C. (1975): Effect of linear approximation of enthalpy-temperature curve in simulating heat transfer during freezing. J. Food Sci. 40: 1099

Tarnawski, W. (1976): Mathematical model for frozen consumption foods. Int. J. Heat Mass Transfer 19: 15

Tchigeov, G.B. (1958): Criterional generalisation of experimental data on the freezing of foods. Bull. I.I.R. Annexe-2: 423

Teider, V.A. (1963): Determination of freezing time with different conditions of heat exchange at the body surface. Proc. Refrig. Sci. Technol. 2: 953

Teller, A.S. & Churchill, S.W. (1965): Freezing outside a sphere. Chem. Engng Prog. Symp. Ser. 61(59): 185

Theofanous, T.G. & Lim, H.C. (1971): An approxiamte analytical solution for non-planar moving boundary problems. Chem. Engng Sci. 26: 1297

Tien, R.H. & Geiger, G.E. (1967): A heat transfer analysis of the solidification of a binary eutectic system. J. Heat Transfer 89: 230

Tien, R.H. & Geiger, G.E. (1968): The unidimensional solidification of a binary eutectic system with time dependent surface temperature. J. Heat Transfer 90: 27

Tien, R.H. & Koump, V. (1968): Unidimensional solidification of a slab - variable surface temperature. Trans Met. Soc. A.I.M.E. 242: 283

Tien, R.H. (1980): A heat transfer analysis for solidification of rounds. J. Heat Transfer 102: 378

Turner, M.J., Clough, R.W., Martin, H.C. & Topp, L.J. (1956): Stiffness and deflection analysis of complex structures. J. Aeronaut. Sci. 23(9): 805

Vanichseni, S. (1971): Thawing of Frozen Lamb Shoulders. MIRINZ Report No. 233, Hamilton, New Zealand.

Vanichseni, S., Haughey, D.P. & Nottingham, P.M. (1972): Water and air-thawing of frozen lamb shoulders. J. Food Technol. 7: 259

Voller, V. & Cross, M. (1981a): Accurate solutions of moving boundary problems using the enthalpy method. Int. J. Heat Mass Transfer 24: 545

Voller, V. & Cross, M. (1981b): Estimating the solidification/melting times of cylindrically symmetric regions. Int. J. Heat Mass Transfer 24: 1457

Voller, V. & Cross, M. (1983): An explicit method to track a moving phase change front. Int. J. Heat Mass Transfer 26: 147

Walker, R.B. (1970): Heat Transfer in Frozen Food. M. Phil. thesis, University of Leeds. Cited by Dorney & Glew (1977).

Weinbaum, S. & Jiji, L.M. (1977): Singular perturbation theory for melting or freezing in finite domains not at the fusion temperature. J. Appl. Mech. 44: 25

Wellford, L.C. & Ayer, R.M. (1977): A finite element free boundary formulation for the problem of multiphase heat conduction. Int. J. Num. Meth. Engng 11: 933

Westphal, K.O. (1967): Series solution of a freezing problem with the fixed surface radiating into a medium of arbitrary varying temperature. Int. J. Heat mass Transfer 10: 195

Wilson, D.G., Solomon, A.D. & Boggs, P.T., eds. (1978): Moving Boundary Problems. Academic Press, London.

Wood, W.L. & Lewis, R.W. (1975): A comparison of time marching schemes for the transient heat conduction equation. Int. J. Num. Meth. Engng 9: 679

Woodams, E.E. & Nowrey, J.E. (1968): Literature values of thermal conductivities of food. Food Technol. 22(4): 494

Woolrich, W.R. (1966): Specific and latents heat of food in the freezing range. ASHRAE J. 8(3): 43

Wrobel, L.C. & Brebbia, C.A. (1979): The boundary element method for steady state and transient heat conduction. Numerical Methods in Thermal Problems, R.W. Lewis & K. Morgan, eds., p.59. Pineridge Press, Swansea.

Wrobel, L.C. & Brebbia, C.A. (1981): A formulation of the boundary element method for axisymmetric transient heat conduction. Int. J. Heat Mass Transfer 24: 843

Yalmanchilli, R.V.S. & Chu, S.C. (1973): Stability and oscillation characteristics of finite element, finite difference and weighted residual methods for transient two-dimensional heat conduction in solids. J. Heat Transfer 95: 235

Yan, M.M. & Huang, P.N.S. (1979): Perturbation solutions to phase change problems subject to convection and radiation. J. Heat Transfer 101: 96

Yeh, L.T. & Chung, B.T.F. (1979): A variational analysis of freezing or melting in a finite medium subject to radiation and convection. J. Heat Transfer 101: 593

Yuen, W.W. (1980): Application of the heat balance integral to melting problems with initial sub-cooling. Int. J. Heat Mass Transfer 23: 1157

Yuen, W.W. & Kleinman, A.M. (1980): A application of variable time step finite difference methods for the one-dimensional melting problem including the effect of subcooling. AIChE J. 26: 828

Zaritzky, N.E., Anon, M.C. & Calvelo, A. (1982): Rate of freezing effect on the colour of frozen beef liver. Meat Sci. 7: 299

Zienkiewicz, O.C. & Parekh, C.J. (1970): Transient field problems: two-dimensional and three-dimensional analysis by isoparametric elements. Int. J. Num. Meth. Engng 2: 61

Zienkiewicz, O.C. (1971): Finite Elements in Engineering Science (2nd ed.). McGraw Hill, New York.

Zienkiewicz, O.C., Parekh, C.J. & Wills, A.J. (1973): The application of finite elements to heat conduction involving latent heat. Rock Mechanics 5: 65

APPENDIX A

SUMMARY OF PUBLISHED SOLUTIONS
TO PHASE CHANGE PROBLEMS

A.1 ABBREVIATIONS USED IN TABLES A.1 TO A.8

[1] Geometric shapes: SS = semi-infinite slab, S = slab, C = infinite cylinder, SP = sphere, 1D = one-dimensional, 2D = two-dimensional, 3D = three-dimensional.

[2] BC = boundary conditions: 1 = first kind, 2 = second kind, 3 = third kind, 4 = fourth kind, R = radiation.

[3] T_{in} = initial condition. = means intial temperature is equal to the phase change temperature and ≠ means initial temperature is not equal to the phase change temperature.

[4] Num Eval = numerical evaluation required for solution. Y = yes, N = no, P = probably.

[5] HBI = heat balance integral method, VT = variational technique, PER = perturbation method, QSS = using the quasi-steady state assumption, EM = embedding technique, AI = analytical iteration method, IT = integral transformation, MHS = solved as heat conduction with a moving heat source, APT = assumes interface position proportional to the square root of time, LRT = latent heat released or absorbed over a range of temperatures, DHG = discontinuous heat generation.

[6] Form Soln = form that the solutions takes, CH = chart, G = graph, N = nomogram, RE = regression based best fit equation.

[7] Type: F = freezing, T = thawing.

[8] Comments include product type and ambient media, EXP = based on experimental data, FDM = based on finite difference method results.

[9] Basic Shape = reference regular geometric shape that the actual irregular shape is related to by the equalivalent diameter. See note[1].

A.2 ANALYTICAL SOLUTIONS TO PHASE CHANGE USING THE ASSUMPTION OF A UNIQUE PHASE CHANGE TEMPERATURE

Table A.1 Exact Analytical Solutions Assuming a Unique Phase Change Temperature

Reference	Shape[1]	BC[2]	T_{in}[3]	Num[4] Eval	Method and Comments[5]
Stefan in Carslaw & Jaeger 1959, p.282	SS	1	=	N	
Neumann in Carslaw & Jaeger 1959, p.282	SS	1	≠	N	Churchill & Evans 1971 tabulate functions.
Danckwerts 1950	SS	1	≠	N	Density of phases different.
Evans et al 1950	SS	2	=	P	Series solution.
Landau 1950	SS	2	=	N	Ablation, transformation to immobilise boundary.

Table A.2 <u>Approximate Analytical Solutions For Slabs Assuming a Unique</u>
<u>Phase Change Temperature</u>

Reference	Shape[1]	BC[2]	T_{in}[3]	Num[4] Eval	Method and Comments[5]
Heat Balance Integral and Variational Technique					
Goodman 1958	SS	1,2,3	=	N	HBI, ablation, QSS.
Goodman & Shea 1960	S	2	≠	P	HBI, series expansion.
Goodman 1961	SS	1,2	=	N	HBI, different temperature profiles.
Poots 1962b	S	1	=	P	HBI, series solution.
Hrycak 1963	SS	3	≠	N	HBI, QSS, phase front α penetration distance.
Goodman 1964	SS	1,2	=	N	HBI
Libby & Chen 1965	SS	1	=	Y	HBI
Lappadula & Mueller 1966	SS	1	=	N	VT
Siegel & Savino 1966	SS	3	≠	Y	HBI, AI
Hrycak 1967	SS	3	≠	N	See Hrycak 1963, stratified media.
Hills & Moore 1967	SS	3	=	Y	HBI
Cho & Sunderland 1969	SS,S	1	≠	N	HBI, APT
Hills 1969	SS	1,2	=	Y	HBI
Hills & Moore 1969	SS	3	=	Y	HBI
Imber & Huang 1973	SS	1	=	Y	HBI, C & k temperature dependent.
Chung & Yeh 1975	S	3,R	≈	Y	HBI, VT
Albin et al 1976	S	4	≠	Y	HBI, six stages.
Chung & Yeh 1976	SS	2	=	Y	HBI, C & k temperature dependent.
Bell 1978	SS	1	=	Y	HBI, subdivides region.
Bell 1979b	S	1	≠	Y	HBI, subdivides region.
El-Genk & Cronenberg 1979	SS	1	=	N	HBI
Yeh & Chung 1979	S	3,R	≠	Y	VT

Reference	Shape[1]	BC[2]	T_{in}[3]	Num[4] Eval	Method and Comments[5]
Hale & Viskanta 1980	SS	1	=	Y	HBI
O'Callaghan et al 1980	S	2	≠	Y	HBI
Yuen 1980	SS	1,2,3	≠	Y	HBI
Chung et al 1983	SS	2	≠	Y	HBI, two stage ablation.
Jayaram & Streider 1983	SS	2	=	Y	HBI, series solution.
Gau & Viskanta 1984	S	1	=	Y	HBI

Perturbation and Series Solutions

Reference	Shape	BC	T_{in}	Num Eval	Method and Comments
Jackson 1964	S	2	≠	P	Series solution.
Westphal 1967	SS	3	≠	P	Series solution.
Duda & Vrentas 1969	S	1	≠	N	PER
Lock et al 1969	SS	4	≠	N	PER
Pedroso & Domoto 1973b	SS	1	=	Y	PER, C & k temperature dependent.
Pedroso & Domoto 1973d	SS	3	=	Y	PER
Huang & Shih 1975a	SS	1,3	=	N	PER
Huang & Shih 1975b	SS	3	=	N	PER
Weinbaum & Jiji 1977	S	1	≠	N	PER
Yan & Huang 1979	S	3,R	=	P	PER
Soliman 1981	SS	3	=	P	PER

Solutions Using Other Approaches

Reference	Shape	BC	T_{in}	Num Eval	Method and Comments
Plank 1913	S	3	=	N	QSS
Rutov 1936	S	3	=	N	Modified Plank 1913 for sensible heat removal.
London & Seban 1943	S	3	=	N	See Plank 1913.
Cochran 1955	S	1	=	N	QSS, lumped capacity method.
Kreith & Romie 1955	S	3	=	N	See Plank 1913.
Chan et al 1983	SS	3	≠	P	QSS, temperature profile approximated by isothermal boundary.

Reference	Shape[1]	BC[2]	T_{in}[3]	Num[4] Eval	Method and Comments[5]
Boley 1961	SS,S	3	≠	P	EM, ablation, series solution.
Boley 1963	S	2	≠	P	EM, ablation, short times.
Boley 1968	S	1,2,3	=	P	EM, ablation, short times.
Patel & Boley 1969	SS	4	=	Y	EM, short times.
Hamill & Bankoff 1964	SS	1	≠	N	AI
Beaubouef & Chapman 1967	SS	1	=	N	AI
Savino & Siegel 1969	SS	1	=	N	AI
Hamill & Bankoff 1963	SS	1,2	=	N	IT, solution bounded.
Selim & Seagrave 1973a	S	1,2,3	=	Y	IT
Kern 1977	SS	3	=	N	IT, considers effect of QSS.
Glasser & Kern 1978	SS	3	=	N	See Kern 1977, solution bounded.
Chuang & Szekely 1971	SS	3	≠	Y	MHS, ablation, Green's functions.
Hirai & Komori 1971	SS	3	≠	P	APT
Komori & Hirai 1972	S	3	≠	P	APT
Cho & Sunderland 1974	SS	1	≠	Y	APT, k temperature dependent, density of phases different.
Mikhailov 1976	SS	1	≠	N	APT, moisture migration.
Hayashi & Komori 1979	SS	1	≠	N	APT
Clyne & Garcia 1980	SS	3	=	N	APT, virtual adjunct method.
Cho & Sunderland 1981	SS	3	=	N	APT, temperature profile same as for no phase change.

Table A.3 Approximate Analytical Solutions For Radial Geometry Assuming
         a Unique Phase Change Temperature

Reference	Shape[1]	BC[2]	T_{in}[3]	Num[4] Eval	Method and Comments[5]
Poots 1962b	C,SP	1	=	P	HBI, series solution.
Langford 1966	SP	2	=	N	HBI, known interface velocity at zero time.
Albin et al 1979	SP	4	≠	Y	HBI, six stages.
Bell 1979a	C	1	=	Y	HBI, subdivides region.
Bell 1979b	C	1	≠	Y	HBI, subdivides region.
Tien 1980	C	3	=	Y	HBI
Lunardini 1981	C	1	≠	Y	HBI
Pekeris & Slichter 1939	C	1	=	N	Series solution.
Pedroso & Domoto 1973a	SP	1	=	N	PER
Pedroso & Domoto 1973c	SP	1	=	N	PER
Riley et al 1974	C,SP	1	=	N	PER
Jiji & Weinbaum 1978	C	1	≠	N	PER
Seeniraj & Bose 1982	C,SP	3,R	=	Y	PER
Hill & Kucera 1983	SP	3	=	N	Series solution.
Plank 1913	C,SP	3	=	N	QSS
London & Seban 1943	C,SP	3	=	N	See Plank 1913.
Lederman & Boley 1970	C	2	≠	Y	EM, ablation.
Shih & Tsay 1971	C	3	=	N	AI
Shih & Chou 1971	SP	3	=	N	AI
Theofanous & Lim 1971	SP	1	=	N	AI
Selim & Seagrave 1973b	C,SP	1	=	Y	IT
Chuang & Szekely 1972	C	3	≠	Y	MHS, ablation, Green's functions.
Cho & Sunderland 1970	SP	1	=	N	APT
Komori & Hirai 1970	C	3	=	P	APT
Boles & Ozisik 1983	C	2	≠	N	APT

Table A.4 <u>Approximate Analytical Solutions For Multi-Dimensional Shapes</u>
<u>Assuming a Unique Phase Change Temperature</u>

Reference	Shape[1]	BC[2]	T_{in}[3]	Num[4] Eval	Method and Comments[5]
Poots 1962a	2D	1	=	Y	HBI, series solution.
Riley & Duck 1977a	3D	1	=	Y	HBI, cuboid.
Riley & Duck 1977b	2,3D	1	=	Y	HBI, rectangular prisms, ellipses, ellipsoids.
Plank 1941	2,3D	3	=	N	QSS, isothermal surface, surface & interface parallel, rod & brick.
Tanaka & Nishimoto 1959	3D	3	=	N	See Plank 1941, conical & square pyramid shapes.
Tanaka & Nishimoto 1960	3D	3	=	N	See Plank 1941, bricks & finite cylinders.
Tanaka & Nishimoto 1964	3D	3	=	N	See Plank 1941, trapezoids.
Shamsundar 1982	2,3D	3	=	N	See Plank 1941, but surface & interface not parallel, uses shape factors of Hahne & Grigull 1975.
Jiji et al 1970	2D	1	≠	Y	MHS, Green's functions, corner.
Rathjen & Jiji 1971	2D	1	≠	Y	MHS, Green's functions, corner.
Budhia & Kreith 1973	2D	1	=	Y	MHS, Green's functions, wedge.

Table A.5 Empirical Solutions Assuming A Unique Phase Change
          Temperature

Reference	Shape[1]	BC[2]	T_{in}[3]	Num[4] Eval	Method[6],[7] and Comments[8]
Charm & Slavin 1962	SS	3	≠	N	Adds fictitious thickness to modify method of Neumann 1912.
Baxter 1962	S,C	3	=	N	RE, F, FDM
Tao 1967	C,SP	3	=	N	CH, F, FDM
Tao 1968	S,C,SP	3	=	N	RE, F, FDM
Everington & Cooper 1972a	S	1	≠	N	G, T, correction to Neumann 1912.
Goodling & Khader 1974	S,C,SP	3,R	=	N	CH, F, FDM
Churchill & Gupta 1977	1,2,3D	1,2,3	≠	P	Derive an "effective" C value that is used to modify solutions for heat conduction without phase change.
Albin et al 1979	SP	4	≠	N	RE, F, based on analytical results.
Shamsundar & Srinivasan 1979	1,2,3D	1,2,3	≠	Y	QSS, isothermal surface assumed, similarity rule so less numerical results are required.
Shamsundar 1981	1,2,3D	1,2,3	≠	Y	See Shamsundar & Srinivasan 1979, density of phases different.
Voller & Cross 1981b	C	1	≠	N	RE, F, FDM

A.3 SOLUTIONS FOR PHASE CHANGE OVER A RANGE OF TEMPERATURES

Table A.6 Approximate Analytical Solutions For Alloy Solidification

Reference	Shape[1]	BC[2]	T_{in}[3]	Num[4] Eval	Method and Comments[5]
Tien & Geiger 1967	SS	1	=	N	HBI, LRT, DHG
Tien & Geiger 1968	SS	4	=	Y	HBI, LRT, DHG
Tien & Koump 1968	S	4	=	Y	HBI, LRT, DHG
Cho & Sunderland 1969	SS,S	1	≠	N	HBI, APT, LRT, DHG
Geuze et al 1972	SS,S	1	=	Y	HBI, LRT
Hayakawa & Bakal 1973	S	3	≠	P	HBI, six stages, LRT
Muelbauer et al 1973	S	3	≠	P	HBI, six stages, LRT
Hayashi et al 1979	SS	1	≠	N	APT, five stages, LRT, DHG
Ozisik & Uzzell 1979	C	2	≠	N	Solid fraction depends on temperature or distance, DHG

Table A.7 <u>Empirical Solutions For Phase Change Over a Range of</u>
          <u>Temperatures</u>

Reference	Form[6] Soln	Type[7]	Comments[8]
Cowan 1958	CH	F	EXP, poultry immersed in brine or glycol.
Lorentzen & Rosvik 1959	CH	F	EXP, beef carcasses in air.
Merritt & Banks 1964	G	T	EXP, fish in water & air.
Slavin 1964	N	F	Fish in air, based on the method of Nagaoka et al 1955.
Earle & Fleming 1967	CH	F	EXP, lamb & mutton in air.
Fleming 1967	CH	F	EXP, lamb brains & kidneys in brine & air.
Kassai 1969	G	T	EXP, beef & pork legs in air.
Everington 1971	G	T	EXP, beef blocks in vacuum steam.
Everington & Cooper 1972b	G	T	EXP, food in vacuum steam.
Frazerhurst et al 1972	CH	F	EXP, fancy meats immersed in glycol.
Bailey & James 1974	CH	T	EXP, FDM, pork legs & meat blocks in air, water & vacuum steam.
Bailey et al 1974	G	T	EXP, FDM, pork legs in air, water & vacuum steam.
Hewitt et al 1974	RE	F	EXP, fish in plate freezer.
Scott 1975	G,RE	T	EXP, fish in water.
Cleland & Earle 1976b	RE	F	EXP, food slabs.
Cleland 1977	RE	F	EXP, food slabs, cylinders, spheres and bricks.
Cleland & Earle 1977a	RE	F	EXP, food slabs.
James et al 1977	CH	T	EXP, FDM, beef quarters in air.
Cleland & Earle 1979a	RE	F	EXP, food cylinders and spheres.
Cleland & Earle 1979b	RE	F	EXP, food bricks.
Creed et al 1979	CH,RE	T	EXP, lamb carcasses in air.
Durbin et al 1979	G	T	EXP, lamb & mutton carcasses in air.
James et al 1979	CH	F	EXP, FDM, boxed meat blocks in air.

Reference	Form[6] Soln	Type[7]	Comments[8]
James & Bailey 1980	G	T	EXP, FDM, beef blocks in air & vacuum steam.
James & Creed 1980	CH	T	EXP, FDM, beef fore & hind quarters air, water & vacuum steam.
Calvelo 1981	RE	T	FDM, meat slabs.
Creed & James 1981	CH,RE	T	EXP, FDM, beef blocks in air, water vacuum steam.
Loeffan et al 1981	RE	F	Differential form of Cleland & Earle 1979b for time variable conditions.
Cleland & Earle 1982b	RE	F	EXP, food slabs, cylinders, spheres and bricks.
Cleland & Earle 1982c	RE	F	Differential form of Cleland & Earle 1982b for time variable conditions.
Moleeratanond et al 1982	N,RE	F	EXP, boxed beef blocks in air.
Zaritzky et al 1982	RE	F	FDM, beef liver slabs.
Hayakawa et al 1983a	RE	F	Predicted by finite element methods for food in finite cylinders & rods.
Hung & Thompson 1983	RE	F	EXP, food slabs.
Pham 1983	RE	F	EXP, food slabs, cylinders & spheres.
Succar & Hayakawa 1984	RE	F	FDM, food slabs.
Pham 1984c	RE	F	EXP, food slabs, cylinders, spheres and bricks

Table A.8 <u>Solutions Using Equivalent Diameters to Account For Irregular</u>
          <u>Shape</u>

Reference	Basic[9] Shape	Type[7]	Comments[8]
Nagaoka et al 1955	C	F	Fish, elliptic shape.
Eddie & Pearson 1958	Brick	F	Fish.
Levy 1958	C	F	Fish.
Earle & Fleming 1967	C	F	Lamb & mutton carcasses.
Tao 1968	C,SP	F	Food, relate to nearest basic shape.
Fleming 1970	C	F	Lamb carcass.
Kouwenhoven 1972	SP	T	Poultry.
Vanichseni et al 1972	Brick	T	Lamb shoulders.
Bailey & James 1974	SP	T	Pork legs.
Bailey et al 1974	SP	T	Pork legs & meat blocks.
James et al 1977	C,SP	T	Beef hind- & fore-quarters.

APPENDIX B

ESTIMATION OF EDGE HEAT TRANSFER IN
SLAB THAWING EXPERIMENTS

In slab thawing experiments a number of measures were taken to minimise all heat transfer other than that which is one-dimensional between the slab faces. Each slab was surrounded by at least 0.09 m of polystyrenne foam board insulation on the other two sides. The Tylose slab itself was at least 2.1 times greater in width than it was thick.

Even with these measures some unwanted edge heat transfer is inevitable, especially where the temperature driving forces are small, the slab is thick, the surface heat transfer coefficient is low and the thawing process is therefore long. The insulation was largely effective in preventing heat transfer from the room conditions to the slab. However, heat transfer also occurred from the plates directly to the insulation and thence to the side faces of the slabs. This effect was thought to have significant effect on thawing times of the slabs so an investigation was made to predict this effect.

This effect could not be studied experimentally so simulation by the finite element method was used. The finite element method can deal with heat transfer in both the Tylose and in the insulation. Calculations were made with the grids shown in Fig. B.1. The two cases were (a) the ideal slab situation with only one-dimensional heat transfer (perfect insulation) and (b) where heat transfer through the insulating material was possible. The difference between the predicted thawing times was considered to be due to the unwanted edge heat transfer.

In the simulation the most pessimistic view that the contact resistance between the thawing plate and the polystyrene foam insulation surface was the same as that between the plate and the Tylose surface was taken. In the actual situation it should be greater because of the porous nature of the polystyrene and because the Tylose thickness was slightly larger than the surrounding insulation. Most of the contact

pressure was therefore between the Tylose and the plate. The extent to which the actual contact resistance from the plate to the insulation was greater than that from the plate to the Tylose could not be measured or estimated, but gives a further safety factor when interpreting the results of this investigation.

The conditions investigated were those used in the slab thawing runs (Sec. 6.2). For the runs most affected by edge effects the conditions used and the calculated thawing times, both assuming perfect insulation and with the possibility of heat transfer through the insulation, are given in Table B.1. The results show the six cases where the difference in thawing time was greater than 1.0%. The effect of the edge heat transfer quickly reduced for higher ambient thawing temperatures, higher surface heat transfer coefficients and smaller slab thicknesses. Consequently, for the other slab thawing experiments the simulated thawing times were less than 1.0% different. These results confirm that although the edge heat transfer was not negligible in all cases, for most of the slab thawing experiments it was small enough to be tolerated. Particular care must be taken in interpreting results for Runs T3, T16 and T3.

Table B.1 Results of the Finite Element Method Simulation of Edge Heat
          Transfer During Thawing of Slabs

Run	D (m)	h (W m^{-2} °C^{-1})	T_a (°C)	T_{in} (°C)	t_{exp} (hrs)	t_1^* (hrs)	t_2^* (hrs)	E^1 (%)
T26	0.1050	37.3	5.2	-24.7	29.33	29.43	28.09	4.6
T3	0.0525	13.2	5.2	-11.4	19.32	20.85	20.23	3.0
T16	0.1000	24.5	12.8	-9.4	16.92	16.37	15.91	2.8
T10	0.1020	13.2	43.0	-13.7	8.83	9.29	9.10	2.0
T30	0.1050	78.1	5.2	-28.8	23.62	23.51	23.07	1.9
T13	0.0770	37.3	5.2	-30.2	18.49	18.12	17.87	1.4

* t_1 = thawing time calculated from the finite element method using the
grid given in Fig. B.1a, t_2 = thawing time calculated from the finite
element method using the grid given in Fig. B.1b.

[1] E = percentage difference between the thawing times predicted by
finite element analysis with perfect insulation (t_1) and that with
imperfect insulation (t_2) at the slab edges.
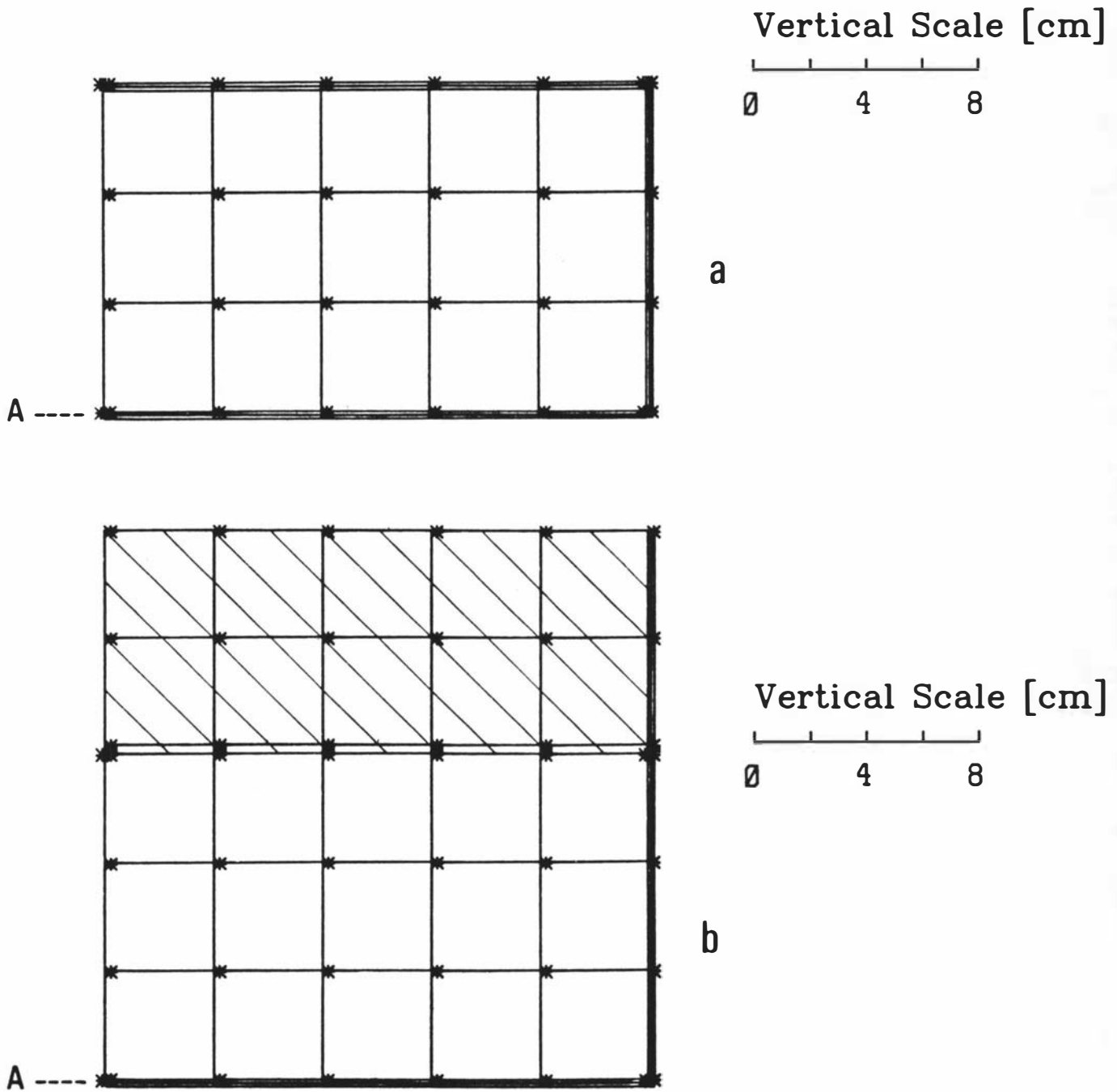
Fig. B.1 The Finite Element Method Grids Used To Investigate the Effect of Edge Heat Transfer During Thawing of Slabs of Tylose. * - nodes, ** - nodes where temperature recorded, _ - element boundaries, ≡ - planes of symmetry, A - axis of symmetry. Shaded regions show elements representing polystyrene, $k = 0.03$ W m^{-2} ^{o}C^{-1}, $C = 3.388$ MJ m^{-3} ^{o}C^{-1}. Horizontal axis scale is variable depending on the slab thickness modelled. (a) a perfectly insulated slab (b) an actual slab.

APPENDIX C

GEOMETRIC FACTOR DATA FOR MULTI-DIMENSIONAL SHAPES

Table C.1 Results of Finite Difference Method Calculations To Determine Geometric Factors For Multi-Dimensional Regular Shapes

Using Tylose thermal property data (Table 5.1), D = 0.0165 m or 0.165 m, T_a = -30.0 °C, T_{in} = 20.0 °C, T_{fin} = -10.0 °C.

Shape	β_1	β_2	Bi	t_{fdm}	EHTD	MCP
Slab	∞	∞	0.010	24.130	1.00	1.00
	∞	∞	0.032	7.668	1.00	1.00
	∞	∞	0.100	2.479	1.00	1.00
	∞	∞	0.316	0.833	1.00	1.00
	∞	∞	1.000	30.790	1.00	1.00
	∞	∞	3.162	13.820	1.00	1.00
	∞	∞	10.000	8.445	1.00	1.00
	∞	∞	31.620	6.866	1.00	1.00
	∞	∞	100.000	6.388	1.00	1.00
		1.000	0.010	8.043	3.00	1.00
		1.000	0.032	2.557	3.00	1.00
		1.000	0.100	0.827	3.00	1.01
		1.000	0.316	0.279	2.98	1.10
		1.000	1.000	10.942	2.81	1.33
		1.000	3.162	5.315	2.60	1.35
		1.000	10.000	3.365	2.51	1.27
		1.000	31.620	2.746	2.50	1.23
		1.000	100.000	2.555	2.50	1.21
		1.255	0.010	8.627	2.80	1.00
		1.255	0.032	2.747	2.79	1.05
		1.255	0.100	0.889	2.79	1.12
		1.255	0.316	0.302	2.76	1.18
		1.255	1.000	11.990	2.57	1.45
		1.255	3.162	5.876	2.35	1.43
		1.255	10.000	3.789	2.23	1.36
Finite		1.255	31.620	3.096	2.22	1.29
Cylinder		1.255	100.000	2.884	2.22	1.27
$D_r \leq D_y$		1.582	0.010	9.168	2.63	1.00
		1.582	0.032	2.922	2.62	1.11
		1.582	0.100	0.947	2.62	1.20
		1.582	0.316	0.324	2.57	1.35
		1.582	1.000	12.992	2.37	1.55
		1.582	3.162	6.345	2.18	1.47
		1.582	10.000	4.066	2.08	1.37
		1.582	31.620	3.312	2.07	1.30
		1.582	100.000	3.085	2.07	1.28
		2.503	0.010	10.054	2.40	1.00
		2.503	0.032	3.210	2.39	1.22
		2.503	0.100	1.045	2.37	1.48
		2.503	0.316	0.366	2.27	1.76
		2.503	1.000	14.530	2.12	1.66
		2.503	3.162	6.900	2.00	1.45
		2.503	10.000	4.218	2.00	1.28
		2.503	31.620	3.431	2.00	1.22
		2.503	100.000	3.194	2.00	1.21

Table C.1 continued...   277

Shape	β_1	β_2	Bi	t_{fdm}	EHTD	MCP
		4.000	0.010	10.739	2.25	1.54
		4.000	0.032	3.437	2.23	2.09
		4.000	0.100	1.138	2.18	2.34
		4.000	0.316	0.399	2.09	2.07
		4.000	1.000	15.182	2.03	1.55
		4.000	3.162	6.893	2.01	1.28
		4.000	10.000	4.216	2.00	1.17
		4.000	31.620	3.431	2.00	1.14
		4.000	100.000	3.194	2.00	1.13
		6.297	0.010	11.208	2.15	2.12
		6.297	0.032	3.610	2.12	3.10
		6.297	0.100	1.207	2.05	3.10
Finite		6.297	0.316	0.412	2.02	1.92
Cylinder		6.297	1.000	15.273	2.02	1.35
$D_r \leq D_y$		6.297	3.162	6.876	2.01	1.17
		6.297	10.000	4.212	2.01	1.11
		6.297	31.620	3.431	2.00	1.09
		6.297	100.000	3.194	2.00	1.08
		10.000	0.010	11.562	2.09	3.50
		10.000	0.032	3.730	2.06	3.73
		10.000	0.100	1.231	2.01	2.77
		10.000	0.316	0.410	2.03	1.47
		10.000	1.000	15.228	2.02	1.19
		10.000	3.162	6.876	2.01	1.10
		10.000	10.000	4.212	2.01	1.07
		10.000	31.620	3.431	2.00	1.06
		10.000	100.000	3.194	2.00	1.05
	1.000		0.010	8.043	3.00	1.00
	1.000		0.032	2.565	2.99	1.00
	1.000		0.100	0.829	2.99	1.04
	1.000		0.316	0.279	2.98	1.10
	1.000		1.000	10.942	2.81	1.33
	1.000		3.162	5.315	2.60	1.35
	1.000		10.000	3.365	2.51	1.27
	1.000		31.620	2.746	2.50	1.23
	1.000		100.000	2.555	2.50	1.21
	1.582		0.010	10.658	2.26	1.00
	1.582		0.032	3.371	2.28	1.14
	1.582		0.100	1.105	2.24	1.38
	1.582		0.316	0.382	2.18	1.52
	1.582		1.000	15.806	1.95	1.81
	1.582		3.162	8.182	1.69	1.77
	1.582		10.000	5.578	1.51	1.69
	1.582		31.620	4.680	1.47	1.61
Finite	1.582		100.000	4.384	1.46	1.58
Cylinder	2.503		0.010	13.428	1.80	1.45
$D_r \geq D_y$	2.503		0.032	4.301	1.78	1.73
	2.503		0.100	1.410	1.76	1.96
	2.503		0.316	0.508	1.64	2.34
	2.503		1.000	21.760	1.42	2.36
	2.503		3.162	11.384	1.21	2.09
	2.503		10.000	7.608	1.11	1.87
	2.503		31.620	6.293	1.09	1.73
	2.503		100.000	5.981	1.07	1.71
	4.000		0.010	16.119	1.50	1.80
	4.000		0.032	5.160	1.49	2.20
	4.000		0.100	1.731	1.43	2.95
	4.000		0.316	0.647	1.29	3.26
	4.000		1.000	27.393	1.12	2.67
	4.000		3.162	13.483	1.03	2.05
	4.000		10.000	8.395	1.01	1.69
	4.000		31.620	6.852	1.00	1.56
	4.000		100.000	6.388	1.00	1.52

Table C.1 continued...   278

Shape	β_1	β_2	Bi	t_{fdm}	EHTD	MCP
Finite Cylinder $D_r \geq D_y$	6.300		0.010	18.406	1.31	2.84
	6.300		0.032	5.940	1.29	3.57
	6.300		0.100	2.054	1.21	4.74
	6.300		0.316	0.767	1.09	3.92
	6.300		1.000	30.515	1.01	2.53
	6.300		3.162	13.751	1.01	1.70
	6.300		10.000	8.420	1.00	1.44
	6.300		31.620	6.859	1.00	1.36
	6.300		100.000	6.388	1.00	1.33
	10.000		0.010	20.260	1.19	4.03
	10.000		0.032	6.668	1.15	6.48
	10.000		0.100	2.336	1.06	6.37
	10.000		0.316	0.830	1.00	3.68
	10.000		1.000	30.729	1.00	1.99
	10.000		3.162	13.806	1.00	1.45
	10.000		10.000	8.445	1.00	1.28
	10.000		31.620	6.866	1.00	1.23
	10.000		100.000	6.388	1.00	1.21
Infinite Rod	1.000	∞	0.010	12.065	2.00	1.00
	1.000	∞	0.032	3.834	2.00	1.00
	1.000	∞	0.100	1.243	1.99	1.08
	1.000	∞	0.316	0.421	1.98	1.14
	1.000	∞	1.000	16.053	1.92	1.21
	1.000	∞	3.162	7.708	1.79	1.26
	1.000	∞	10.000	4.916	1.72	1.23
	1.000	∞	31.620	4.013	1.71	1.19
	1.000	∞	100.000	3.751	1.70	1.18
	1.255	∞	0.010	13.443	1.80	1.00
	1.255	∞	0.032	4.284	1.79	1.13
	1.255	∞	0.100	1.390	1.78	1.20
	1.255	∞	0.316	0.474	1.76	1.31
	1.255	∞	1.000	18.437	1.67	1.38
	1.255	∞	3.162	9.009	1.53	1.39
	1.255	∞	10.000	5.828	1.45	1.34
	1.255	∞	31.620	4.863	1.41	1.31
	1.255	∞	100.000	4.543	1.41	1.29
	1.582	∞	0.010	14.804	1.63	1.04
	1.582	∞	0.032	4.725	1.62	1.28
	1.582	∞	0.100	1.536	1.61	1.46
	1.582	∞	0.316	0.528	1.58	1.49
	1.582	∞	1.000	20.946	1.47	1.55
	1.582	∞	3.162	10.391	1.33	1.51
	1.582	∞	10.000	6.772	1.25	1.43
	1.582	∞	31.620	5.651	1.22	1.39
	1.582	∞	100.000	5.279	1.21	1.36
	2.503	∞	0.010	17.273	1.40	1.30
	2.503	∞	0.032	5.525	1.39	1.63
	2.503	∞	0.100	1.808	1.37	1.85
	2.503	∞	0.316	0.636	1.31	1.94
	2.503	∞	1.000	25.744	1.20	1.85
	2.503	∞	3.162	12.644	1.09	1.64
	2.503	∞	10.000	8.074	1.05	1.47
	2.503	∞	31.620	6.634	1.04	1.40
	2.503	∞	100.000	6.178	1.03	1.37
	4.000	∞	0.010	19.366	1.25	1.52
	4.000	∞	0.032	6.204	1.24	2.11
	4.000	∞	0.100	2.054	1.21	2.46
	4.000	∞	0.316	0.738	1.13	2.48
	4.000	∞	1.000	29.408	1.05	1.97
	4.000	∞	3.162	13.629	1.01	1.53
	4.000	∞	10.000	8.353	1.01	1.33
	4.000	∞	31.620	6.805	1.01	1.27
	4.000	∞	100.000	6.369	1.00	1.26

Table C.1 continued...   279

Shape	β_1	β_2	Bi	t_{fdm}	EHTD	MCP
Infinite Rod	6.297	∞	0.010	20.892	1.16	2.32
	6.297	∞	0.032	6.732	1.14	3.22
	6.297	∞	0.100	2.268	1.09	3.47
	6.297	∞	0.316	0.810	1.03	2.74
	6.297	∞	1.000	30.729	1.00	1.78
	6.297	∞	3.162	13.820	1.00	1.36
	6.297	∞	10.000	8.445	1.00	1.22
	6.297	∞	31.620	6.866	1.00	1.18
	6.297	∞	100.000	6.388	1.00	1.17
	10.000	∞	0.010	22.077	1.09	3.57
	10.000	∞	0.032	7.200	1.07	5.19
	10.000	∞	0.100	2.430	1.02	4.22
	10.000	∞	0.316	0.828	1.01	2.29
	10.000	∞	1.000	30.790	1.00	1.50
	10.000	∞	3.162	13.820	1.00	1.23
	10.000	∞	10.000	8.445	1.00	1.14
	10.000	∞	31.620	6.866	1.00	1.11
	10.000	∞	100.000	6.388	1.00	1.10
	1.000	1.000	0.010	8.043	3.00	1.00
	1.000	1.000	0.032	2.563	2.99	1.10
	1.000	1.000	0.100	0.830	2.99	1.18
	1.000	1.000	0.316	0.284	2.93	1.34
	1.000	1.000	1.000	11.459	2.69	1.58
	1.000	1.000	3.162	5.713	2.42	1.54
	1.000	1.000	10.000	3.745	2.26	1.46
	1.000	1.000	31.620	3.061	2.24	1.38
	1.000	1.000	100.000	2.852	2.24	1.34
	1.000	1.582	0.010	9.189	2.63	1.41
	1.000	1.582	0.032	2.930	2.62	1.48
	1.000	1.582	0.100	0.955	2.60	1.55
	1.000	1.582	0.316	0.331	2.51	1.65
	1.000	1.582	1.000	13.636	2.26	1.83
	1.000	1.582	3.162	6.938	1.99	1.73
	1.000	1.582	10.000	4.570	1.85	1.59
	1.000	1.582	31.620	3.746	1.83	1.49
	1.000	1.582	100.000	3.485	1.83	1.45
Rectangular Brick	1.000	2.503	0.010	10.071	2.40	1.59
	1.000	2.503	0.032	3.220	2.38	1.73
	1.000	2.503	0.100	1.056	2.35	1.90
	1.000	2.503	0.316	0.372	2.24	1.99
	1.000	2.503	1.000	15.273	2.02	1.95
	1.000	2.503	3.162	7.540	1.83	1.70
	1.000	2.503	10.000	4.610	1.83	1.43
	1.000	2.503	31.620	3.987	1.72	1.44
	1.000	2.503	100.000	3.714	1.72	1.41
	1.000	4.000	0.010	10.763	2.24	2.43
	1.000	4.000	0.032	3.448	2.22	2.47
	1.000	4.000	0.100	1.147	2.16	2.67
	1.000	4.000	0.316	0.408	2.04	2.39
	1.000	4.000	1.000	16.028	1.92	1.86
	1.000	4.000	3.162	7.734	1.79	1.59
	1.000	4.000	10.000	4.916	1.72	1.43
	1.000	4.000	31.620	4.008	1.71	1.35
	1.000	4.000	100.000	3.729	1.71	1.33
	1.582	1.582	0.010	10.686	2.26	1.62
	1.582	1.582	0.032	3.417	2.24	1.70
	1.582	1.582	0.100	1.117	2.22	1.82
	1.582	1.582	0.316	0.394	2.11	1.99
	1.582	1.582	1.000	16.706	1.84	2.14
	1.582	1.582	3.162	8.791	1.57	2.00
	1.582	1.582	10.000	5.960	1.42	1.84
	1.582	1.582	31.620	4.972	1.38	1.72
	1.582	1.582	100.000	4.656	1.37	1.68

Table C.1 continued...   280

Shape	β_1	β_2	Bi	t_{fdm}	EHTD	MCP
	1.582	2.503	0.010	11.922	2.02	1.73
	1.582	2.503	0.032	3.817	2.01	1.93
	1.582	2.503	0.100	1.256	1.97	2.20
	1.582	2.503	0.316	0.453	1.84	2.43
	1.582	2.503	1.000	19.280	1.60	2.36
	1.582	2.503	3.162	10.029	1.38	2.07
	1.582	2.503	10.000	6.702	1.26	1.86
	1.582	2.503	31.620	5.546	1.24	1.72
	1.582	2.503	100.000	5.181	1.23	1.67
	1.582	4.000	0.010	12.869	1.88	2.52
	1.582	4.000	0.032	4.131	1.86	2.77
	1.582	4.000	0.100	1.379	1.80	2.92
	1.582	4.000	0.316	0.501	1.66	2.82
	1.582	4.000	1.000	20.692	1.49	2.32
	1.582	4.000	3.162	10.414	1.33	1.95
	1.582	4.000	10.000	6.838	1.24	1.73
	1.582	4.000	31.620	5.632	1.22	1.61
	1.582	4.000	100.000	5.249	1.22	1.57
Rectangular Brick	2.503	2.503	0.010	13.458	1.79	2.35
	2.503	2.503	0.032	4.313	1.78	2.49
	2.503	2.503	0.100	1.426	1.74	2.65
	2.503	2.503	0.316	0.526	1.58	2.86
	2.503	2.503	1.000	22.807	1.35	2.66
	2.503	2.503	3.162	11.792	1.17	2.21
	2.503	2.503	10.000	7.560	1.12	1.85
	2.503	2.503	31.620	6.230	1.10	1.71
	2.503	2.503	100.000	5.807	1.10	1.66
	2.503	4.000	0.010	14.704	1.64	3.08
	2.503	4.000	0.032	4.728	1.62	3.14
	2.503	4.000	0.100	1.587	1.56	3.30
	2.503	4.000	0.316	0.591	1.41	3.34
	2.503	4.000	1.000	25.114	1.23	2.73
	2.503	4.000	3.162	12.621	1.10	2.15
	2.503	4.000	10.000	8.136	1.04	1.82
	2.503	4.000	31.620	6.615	1.04	1.66
	2.503	4.000	100.000	6.154	1.04	1.61
	4.000	4.000	0.010	16.173	1.49	3.15
	4.000	4.000	0.032	5.216	1.47	3.57
	4.000	4.000	0.100	1.772	1.40	3.96
	4.000	4.000	0.316	0.672	1.24	3.88
	4.000	4.000	1.000	28.274	1.09	2.89
	4.000	4.000	3.162	13.643	1.01	2.09
	4.000	4.000	10.000	8.353	1.01	1.68
	4.000	4.000	31.620	6.825	1.01	1.55
	4.000	4.000	100.000	6.350	1.01	1.51

Table C.2 <u>Results of Finite Element Method Calculations To Determine</u>
          <u>Geometric Factors For Multi-Dimensional Irregular Shapes</u>

Using Tylose thermal property data (Table 5.1), $h\to0.0$ W m^{-2} °C^{-1} or
h = 1000.0 W m^{-2} °C^{-1}, T_a = -30.0 °C, T_{in} = 20.0 °C, T_{fin} = -10.0 °C.

Shape[1] & Code	Bi	EHTD	MCP
2DI 1	0.0	2.00	1.00
	92.4	2.00	1.00
2DI 2	0.0	1.61	1.00
	67.6	1.34	1.20
2DI 3	0.0	1.84	1.00
	83.0	1.70	1.08
2DI 4	0.0	1.56	1.00
	60.0	1.24	1.27
2DI 5	0.0	2.00	1.00
	63.6	2.00	1.00
2DI 6	0.0	1.73	1.00
	51.5	1.51	1.16
2DI 7	0.0	1.82	1.00
	55.2	1.65	1.11
2DI 8	0.0	1.32	1.00
	28.8	1.05	1.30
Pyramid	0.0	2.37	1.00
	50.0	1.48	1.72
Sphere	0.0	3.00	1.00
	77.0	3.00	1.00
Egg	0.0	2.75	1.00
	103.0	2.49	1.11
Fish	0.0	2.23	1.00
	72.7	1.26	1.82

[1] 2DI = two-dimensional irregular shape, code from Table 6.6, geometry
parameters are given in Table 10.1.